

UNIVERSIDADE DE LISBOA
INSTITUTO SUPERIOR TÉCNICO

**Valorisation of pectin-rich agro-industrial residues by yeasts:
Potential and Challenges**

Luís Miguel Candeias Martins

Supervisor: Doctor Isabel Maria de Sá Correia Leite de Almeida

**Thesis approved in public session to obtain the PhD Degree in
Biotechnology and Biosciences**

Jury final classification: Pass with Distinction

2021

UNIVERSIDADE DE LISBOA
INSTITUTO SUPERIOR TÉCNICO

**Valorisation of pectin-rich agro-industrial residues by yeasts:
Potential and Challenges**

Luís Miguel Candeias Martins

Supervisor: Doctor Isabel Maria de Sá Correia Leite de Almeida

**Thesis approved in public session to obtain the PhD Degree in
Biotechnology and Biosciences**

Jury final classification: Pass with Distinction

Jury

Chairperson: Doctor Duarte Miguel de França Teixeira dos Prazeres, Instituto Superior Técnico, Universidade de Lisboa.

Members of the Committee:

Doctor Isabel Maria de Sá Correia Leite de Almeida, Instituto Superior Técnico, Universidade de Lisboa

Doctor Lucília Maria Alves Ribeiro Domingues, Escola de Engenharia, Universidade do Minho

Doctor Miguel Nobre Parreira Cacho Teixeira, Instituto Superior Técnico, Universidade de Lisboa

Doctor Elke Nevoigt, Department of Life Sciences and Chemistry, Jacobs University Bremen, Alemanha

Doctor Margarida Isabel Rosa Bento Palma, Instituto Superior Técnico, Universidade de Lisboa

Funding Institution

Portuguese Foundation for Science and Technology (FCT)

ABSTRACT

The implementation of a circular bioeconomy based on the efficient bioconversion of agro-industrial residues by selected yeasts is an important societal challenge. Agro-industrial residues are low-cost carbon sources (C-sources) for microbial growth, in particular those rich in pectin, which are generated in high amounts worldwide from the sugar industry or the industrial processing of fruits and vegetables. The hydrolysis of the pectin-rich residues, specifically of sugar beet pulp (SBP), releases neutral sugars (D-glucose, L-arabinose and D-galactose), an acidic sugar (D-galacturonic acid) and other potential C-sources which are also metabolic inhibitors such as acetic acid and methanol.

Although *Saccharomyces cerevisiae* is the most important and explored yeast cell factory in Yeast Biorefineries for the production of bioethanol, the interest in non-*S. cerevisiae* yeast species with higher catabolic and biosynthetic versatility and tolerance to bioprocess-related stresses is gaining momentum. The challenges faced in the bioconversion of pectin-rich hydrolysates by yeasts involve the search for optimized metabolic pathways for the catabolism of all the carbon sources present and the efficient biosynthesis of relevant value-added compounds and high tolerance to bioprocess-related stresses.

Methanol is a feedstock for methylotrophic yeasts, is present in SBP hydrolysates, and is a major impurity in crude glycerol, a by-product of biodiesel production. Nevertheless, methanol tolerance determinants and toxicity mechanisms are poorly known compared with ethanol. The chemogenomic analysis performed in this thesis identified tolerance genes whose expression is required for maximum methanol and/or ethanol tolerance. The clustering of the identified tolerance genes indicated an enrichment of functional categories in the methanol dataset not enriched in the ethanol dataset, such as chromatin remodeling, DNA repair and fatty acid biosynthesis. Several genes involved in DNA repair (eight *RAD* genes), identified as specific for methanol toxicity, were previously reported as tolerance determinants for formaldehyde, a methanol detoxification pathway intermediate. This study is a first step not only for toxicity/tolerance mechanistic insights but also for the rational genomic manipulation of yeasts to obtain more robust strains.

In this thesis, it was also isolated from SBP and identified, at the molecular level, several yeast isolates. Among them, *Rhodotorula mucilaginosa* IST 390 whose performance was examined and optimized, together with the performance of another oleaginous red yeast, *R. toruloides* PYCC 5615, envisaging the full utilization of the C-sources in SBP hydrolysate (at pH 5.0). The dual role of acetic acid as carbon and energy source and as a growth and metabolism inhibitor was examined. Acetic acid (30 mM at pH 5.0) prevented the catabolism of D-galacturonic acid and L-arabinose after the complete use of the other C-sources. However,

D-glucose and acetic acid were simultaneously and efficiently metabolized, followed by D-galactose. SBP hydrolysate supplementation with amino acids was crucial to allow D-galacturonic acid and L-arabinose catabolism even in the presence of acetic acid. SBP valorization through the production of lipids and carotenoids by *Rhodotorula* strains, supported by complete catabolism of the major C-sources present, looks promising for industrial implementation.

Keywords: Yeast biorefineries, pectin-rich residues, sugar beet pulp, toxicogenomics, oleaginous red yeasts

RESUMO

A implementação de uma bioeconomia circular com base na conversão eficiente de resíduos agroindustriais por leveduras é um importante desafio social. Os resíduos agroindustriais são uma fonte de carbono baixo valor comercial para o crescimento microbiano, em particular os resíduos ricos em pectina que são gerados em elevadas quantidades mundialmente pela indústria açucareira ou pela indústria processadora de fruta e vegetais. A hidrólise dos resíduos ricos em pectina, principalmente de beterraba sacarina, liberta açúcares neutros (D-glucose, L-arabinose and D-galactose) e um açúcar-ácido (ácido D-galacturónico), e outras potenciais fontes de carbono e inibidoras do metabolismo como sejam o ácido acético e metanol.

A levedura *Saccharomyces cerevisiae* é a mais importante e explorada espécie como fábrica celular para a produção de bioetanol em biorefinarias. Contudo, o interesse em espécies de levedura não-*Saccharomyces* tem ganho relevância uma vez que este grupo heterogéneo incluiu leveduras com maior versatilidade catabólica e biossintética e maior tolerância a stresses presentes nos bioprocessos. Os desafios encontrados na bioconversão dos hidrolisados ricos em pectina por leveduras incluem a otimização de vias metabólicas envolvidas no catabolismo eficiente de todas fontes de carbono presentes, a biossíntese eficiente de productos com valor acrescentado e no aumento da tolerância a stresses relacionados com o desenvolvimento de bioprocessos.

O metanol está presente em hidrolisados de beterraba sacarina, é uma matéria-prima para as leveduras metilotróficas e é a maior impureza no glicerol-bruto, um subproduto da produção de biodiesel e potencial substrato para biorrefinarias. Quando comparado com o etanol, os mecanismos de toxicidade e os determinantes de tolerância ao metanol encontram-se muito menos estudados. A análise quimiogenómica realizada nesta dissertação identificou, à escala do genoma, os genes de tolerância cuja expressão é necessária para a máxima tolerância ao metanol e ao etanol. O agrupamento dos genes de tolerância identificados indica um enriquecimento em certas categorias funcionais no conjunto dos resultados para metanol que não se encontram enriquecidos nos de etanol, como sejam: remodelação da cromatina, reparação de DNA e biossíntese de ácidos gordos. Vários genes envolvidos na reparação do DNA (oito genes *RAD*), foram identificados como específicos para o metanol e anteriormente identificados como determinantes de tolerância para o formaldeído, um intermediário da via de desintoxicação do metanol em levedura. Este estudo é um primeiro passo não só para a compreensão dos mecanismos de toxicidade/tolerância mas também para uma manipulação genómica racional para a obtenção de leveduras mais robustas.

Nesta tese foram isoladas e identificadas, ao nível molecular, leveduras de várias espécies da polpa de beterraba sacarina. Entre elas, uma estirpe de *Rhodotorula mucilaginosa* cujo desempenho foi avaliado e otimizado a par com o de uma outra levedura oleaginosa *R. toruloides* PYCC 5615, com vista à utilização total das fontes de carbono presentes no hidrolisado de polpa de beterraba sacarina a pH 5.0. Foi estudado o papel do ácido acético como fonte de carbono/energia e inibidor do metabolismo celular. O ácido acético (30 mM a pH 5.0) impediu o catabolismo do ácido D-galacturónico e da L-arabinose após o consumo das outras fontes de carbono. No entanto, a D-glucose e o ácido acético foram metabolizados simultaneamente, a que se seguiu o consumo de D-galactose. A suplementação do hidrolisado de polpa de beterraba sacarina com aminoácidos foi crucial para permitir o catabolismo do D-galacturónico ácido e da L-arabinose mesmo na presença de ácido acético. A valorização da polpa de beterraba sacarina para produção de lípidos e carotenoides por estirpes de *Rhodotorula* com utilização completa das principais fontes de carbono presentes, parece promissora com vista a implementação industrial.

Palavras-chave: Biorrefinarias de leveduras, resíduos ricos em pectina, beterraba sacarina; quimiogenómica, leveduras vermelhas oleaginosas

ACKNOWLEDGEMENTS

First, I would like to acknowledge Professor Isabel Sá-Correia, my supervisor and head of the Biological Sciences Research Group (BSRG), Institute for Bioengineering and Biosciences (iBB) for the opportunity to join her research group carry out my PhD work under her invaluable supervision. Her scientific vision and background and guidance on the experimental activities was vital for the success of the work and for my scientific formation. I am most thankful for her commitment and drive to push me to be the best PhD student I can possibly be.

I would also like to acknowledge the ERANET-IB *YEASTPEC* project partners and their research teams, Professor Elke Nevoigt (Jacobs University, Bremen), Professor Wolfgang Liebl (TUM, Munich) and Doctor Peter Richard (VTT, Espoo) for all the scientific interactions and discussions. I also acknowledge the contribution of several members of the BSRG. My thanks to the PhD student Marta Mota (iBB/IST) for her major contribution to the chemogenomic analysis and our co-authored paper and to Catarina C. Monteiro, Paula M. Semedo and Xavier Diaz for their help in some laboratory experiments. A special acknowledgement also goes to Doctor Margarida Palma for guiding me during the yeast isolation and identification and during my early steps in Isabel Sá-Correia laboratory and Doctor Cláudia Godinho for helping me with the fluorescence analysis of lipids and microscopy.

This thesis work was funded by the Portuguese Foundation for Science and Technology (FCT) in the context of the ERANET-IB project *YEASTPEC* (Engineering of the yeast *Saccharomyces cerevisiae* for bioconversion of pectin- containing agro-industrial side-streams) (ERA-IB-2/0003/2015). Funding (multiannual) received by iBB from FCT (UIDB/04565/2020) is also acknowledged. I also acknowledge my PhD fellowship (PD/BD/128035/2016) from the FCT funded Doctoral Program in “Applied and Environmental Microbiology”, that allowed me to enrol the Instituto Superior Técnico, Universidade de Lisboa, PhD Program in Biotechnology and Biosciences. I also acknowledge Professor Margarida Casal and the Directive Board of FCT- funded Doctoral Program in Applied and Environmental Microbiology for the opportunity to have joined this program. A project fellowship received in the context of the YEASTRACT+ database, a Node Service of the Portuguese distributed infrastructure for biological data BioData.pt funded by *Programa Operacional Regional de Lisboa 2020* (LISBOA-01-0145-FEDER-022231), is also acknowledged.

The following personal acknowledgements will be addressed in Portuguese:

Um agradecimento pessoal à minha orientadora, a Professora Isabel Sá-Correia, pela sua dedicação, persistência e transmissão de conhecimentos ao longo destes últimos anos. Sem dúvida, é exemplo de capacidade de trabalho e dedicação aos seus alunos e colaboradores, enaltecendo as minhas capacidades e sem ela este documento não teria sido possível.

Gostaria de agradecer à comunidade do BSRG, que todos os dias contribuiu de forma positiva para o sucesso do meu trabalho. Um obrigado aos meus colegas de laboratório (6.6.13), Cláudia Godinho, Margarida Palma, Ricardo Ribeiro, Marta Mota, Nuno Melo, Miguel Antunes e àqueles que durante estes anos também estiveram presentes no meu percurso, em especial ao Amir Hassan, Rui Pacheco, Catarina Monteiro, Paula Semedo e Xavier Diaz. Um agradecimento a todos os colegas do Programa Doutoral *Applied and Environmental Microbiology*, em particular aos que me receberam na Universidade do Minho no início deste percurso.

Um especial agradecimento à Patrícia Lindeza e à sua família, pelo amor, carinho e confiança. O mais profundo agradecimento vai para os meus pais, irmã e avós, sem vocês tudo isto não seria possível, obrigado!

TABLE OF CONTENTS

ABSTRACT-----	I
RESUMO -----	III
ACKNOWLEDGEMENTS-----	V
TABLE OF CONTENTS -----	VII
LIST OF FIGURES -----	X
LIST OF TABLES -----	XVI
LIST OF ACRONYMS -----	XVII
THESIS MOTIVATION AND OUTLINE -----	XIX
1 GENERAL INTRODUCTION-----	1
1.1 Valorization of pectin-rich agro-industrial residues by yeasts-----	4
1.1.1 Overview -----	4
1.2 Pectin-rich agro-industrial residues as feedstocks for Biotechnology -----	5
1.2.1 Pectin structure and pectin-rich biomasses-----	5
1.2.2 Pectin-rich biomass processing and composition of the resulting hydrolysates--	7
1.3 Yeast metabolism of sugar monomers present in pectin-rich hydrolysates -----	11
1.3.1 The challenges-----	11
1.3.1.1 D-Galacturonic acid pathways from fungi, expressed in <i>S. cerevisiae</i> , and from the oleaginous yeast <i>Rhodospiridium toruloides</i> -----	12
1.3.1.2 L-Arabinose metabolism -----	17
1.3.1.3 D-Xylose metabolism -----	18
1.3.1.4 D-Glucose and D-galactose metabolism -----	19
1.3.1.5 L-Rhamnose metabolism -----	20
1.4 Toxicity and possible metabolization of compounds likely present in pectin-rich biomass hydrolysates -----	20
1.4.1 Multiple chemical stresses likely affecting pectin rich biomass bioconversion -	20
1.4.1.1 Acetic acid and D-galacturonic acid as carbon sources and toxic compounds	21
1.4.1.2 Methanol as carbon source and toxic compound-----	23
1.4.1.3 Heavy metals and agricultural pesticides as toxic compounds-----	24
1.4.2 Bioconversion of carbon source mixtures: the challenges -----	24
1.5 Value-added bioproducts from pectin-rich hydrolysates by non-conventional yeasts -----	26
1.6 Metabolic engineering of non-conventional yeasts with potential for the bioconversion of pectin-rich residues-----	30
1.7 Concluding remarks -----	31

2.1	THE IDENTIFICATION OF GENETIC DETERMINANTS OF METHANOL TOLERANCE IN YEAST SUGGESTS DIFFERENCES IN METHANOL AND ETHANOL TOXICITY MECHANISMS AND CANDIDATES FOR IMPROVED METHANOL TOLERANCE ENGINEERING	35
2.2	INTRODUCTION	36
2.3	MATERIALS AND METHODS	39
2.3.1	Strains and Growth Media	39
2.3.2	Genome-Wide Search for Yeast Determinants of Methanol or Ethanol Tolerance	39
2.3.3	Growth Curves of Selected Deletion Mutants under Methanol-Induced Stress	40
2.4	RESULTS	42
2.4.1	Selection of Methanol and Ethanol Concentrations for the Chemogenomic Analysis	42
2.4.2	Identification of Genes Required for Methanol and Ethanol Tolerance at a Genome-Wide Scale	43
2.4.3	Genes Involved in DNA Repair and Mitotic Cell Cycle	44
2.4.4	Genes involved in autophagy	46
2.4.5	Genes involved in reserve polysaccharides, cell wall and membrane biosynthesis	47
2.4.6	Genes Involved in Protein Synthesis	49
2.4.7	Genes Involved in Vacuolar Function and Endosomal Transport	49
2.4.8	Transcriptional Control and Regulatory Tolerance Networks	52
2.5	DISCUSSION	59
3.1	EFFICIENT UTILIZATION OF ALL CARBON SOURCES PRESENT IN SUGAR BEET PULP HYDROLYSATES BY THE OLEAGINOUS RED YEASTS <i>RHODOTORULA TORULOIDES</i> AND <i>R. MUCILAGINOSA</i>	67
3.2	INTRODUCTION	68
3.3	MATERIALS AND METHODS	71
3.3.1	Identification Isolation and identification of <i>Rhodotorula mucilaginosa</i> IST 390 from sugar beet pulp	71
3.3.2	Yeast strains, growth media and conditions	72
3.3.3	Effect of acetic acid concentration on yeast growth and carbon source catabolism	73
3.3.4	Preparation of sugar beet pulp hydrolysate	73
3.3.5	Determination of concentrations of sugars and acetic acid	74
3.3.6	Assessment of lipid production	75
3.3.7	Assessment of carotenoid production	75
3.3.8	Statistical analysis	76
3.4	RESULTS	77

3.4.1 Isolation of <i>Rhodotorula mucilaginosa</i> IST 390 from sugar beet pulp -----	77
3.4.2 Differential utilization of the carbon sources present in SBP hydrolysate during <i>R. mucilaginosa</i> IST 390 and <i>R. toruloides</i> PYCC 5615 cultivation -----	77
3.4.3 Sugar utilization from a synthetic-SBP-hydrolysate-medium is affected by acetic acid and improved by amino acid supplementation and inoculum increase-----	78
3.4.4 Performance of <i>R. toruloides</i> PYCC 5615 in SBP hydrolysate supplemented with commercial YNB with amino acids and effect of ammonium sulphate concentration--	81
3.4.5 Preliminary assessment of lipid and carotenoid production by three oleaginous red yeast strains during SBP bioconversion. -----	84
3.5 DISCUSSION -----	89
4 GENERAL DISCUSSION-----	93
4.1 DISCUSSION -----	95
5 THESIS PUBLICATIONS -----	101
6 REFERENCES -----	129
7 SUPPLEMENTARY MATERIAL -----	141

LIST OF FIGURES

FIGURE 1.1-SCHEMATIC REPRESENTATION OF THE CHEMICAL STRUCTURE OF FOUR PECTIC POLYSACCHARIDES: HOMOGALACTURONAN (HG), SUBSTITUTED HG XYLOGALACTURONAN (XGA), RHAMNOGALACTURONAN I AND II (RG-I AND RG-II), BASED ON (MOHNEN 2008).	6
FIGURE 1. 2- DRY WEIGHT COMPOSITION OF PECTIN-RICH RESIDUES, IN PARTICULAR SUGAR BEET PULP 1 (BERLOWSKA ET AL. 2018) AND 2 (EDWARDS AND DORAN-PETERSON 2012), APPLE POMACE 1 (GROHMANN AND BOTHAST 1994) AND 2 (BHUSHAN ET AL. 2008) AND CITRUS PEEL 1 (ZHOU ET AL. 2008) AND 2 (JOHN ET AL. 2017).....	7
FIGURE 1.3- SCHEMATIC REPRESENTATION OF <i>S. CEREVISIAE</i> STRAINS (WILD TYPE AND GENETICALLY ENGINEERED WITH HETEROLOGOUS D-GALACTURONIC ACID DEGRADATION PATHWAYS. A) <i>S. CEREVISIAE</i> WILD-TYPE STRAIN SHOWING THE BASAL NATURAL UPTAKE OF D-GALACTURONIC ACID BY GAL2P TRANSPORTER AND PASSIVE DIFFUSION OF THE UNDISSOCIATED FORM THROUGH PLASMA MEMBRANE (PM). B) ENGINEERED <i>S. CEREVISIAE</i> STRAINS EXPRESSING D-GALÁ MEMBRANE TRANSPORTER GAT1 FROM <i>NEUROSPORA CRASSA</i> AND THE URONATE DEHYDROGENASE (UDH) FROM <i>AGROBACTERIUM TUMEFACIENS</i> AND D-GALACTURONIC ACID REDUCTASE (GAAA) FROM <i>ASPERGILLUS NIGER</i> TO CONVERT D-GALÁ INTO THE METABOLITES MESO-GALACTARIC ACID AND L-GALACTONATE, (BENZ ET AL., 2014). C) ENGINEERED <i>S. CEREVISIAE</i> STRAIN WITH D-GALACTURONIC ACID PLASMA MEMBRANE TRANSPORTERS FROM <i>N. CRASSA</i> (GAT1) AND ENZYMES OF THE D-GALÁ CATABOLIC PATHWAY GAAA, GAAB, GAAC AND GAAD FROM <i>A. NIGER</i> (IN GREEN) AND LGD1 FROM <i>TRICHODERMA RESEEI</i> (IN PURPLE); D-FRUCTOSE WAS USED AS CO-SUBSTRATE (BIZ ET AL., 2016). D) ENGINEERED <i>S. CEREVISIAE</i> STRAINS WITH THE NON-GLUCOSE REPRESSIBLE PLASMA MEMBRANE D-GALACTURONIC ACID TRANSPORTER GATA FROM <i>A. NIGER</i> (GATA) AND D-GALÁ CATABOLIC PATHWAY AS IN C); D-GLUCOSE WAS USED AS CO-SUBSTRATE (PROTZKO ET AL., 2018).....	14
FIGURE 1. 4- SCHEMATIC REPRESENTATION OF THE OXIDATIVE PENTOSE PHOSPHATE PATHWAY (WAMELINK ET AL., 2008).	15
FIGURE 1. 5- SCHEMATIC REPRESENTATION OF THE D-GALACTURONIC ACID CATABOLIC PATHWAY PROPOSED FOR <i>RHODOSPORIDIUM TORULOIDES</i> IFO 0880. THE GENES GUT1, GUT2, FBP AND PGI BELONG TO CENTRAL METABOLISM. TAG, TRIACYLGLYCEROL; PPP, PENTOSE PHOSPHATE PATHWAY (BASED ON (PROTZKO ET AL. 2019).	16
FIGURE 1. 6- SCHEMATIC REPRESENTATION OF THE INITIAL STEPS OF ARABINOSE METABOLISM IN FUNGI (THE OXIDOREDUCTASE PATHWAY) OR IN BACTERIA (THE ISOMERASE PATHWAY). XK, D-XYLULOSE KINASE; AI, L-ARABINOSE ISOMERASE; RK, L-RIBULOKINASE; RPE, L-RIBULOSE-5-PHOSPHATE 4-EPIMERASE; XDH, XYLITOL DEHYDROGENASE; AR, L-ARABINOSE REDUCTASE; LAD, L-ARABITOL 4-DEHYDROGENASE; LXR, L-XYLULOSE REDUCTASE (ADAPTED FROM FONSECA ET AL, 2007).....	17

FIGURE 1. 7- ACETIC ACID METABOLISM IN YEAST. THE PDH PATHWAY IS INDICATED BY BLUE ARROWS, WHILE THE PDH BYPASS IS INDICATED BY ORANGE ARROWS. PDH: PYRUVATE DEHYDROGENASE; PDC: PYRUVATE DECARBOXYLASE; ALD: ALDEHYDE DEHYDROGENASE; ACS: ACETYL-COA SYNTHETASE; ADH: ALCOHOL DEHYDROGENASE (HUANG ET AL. 2016)..... 22

FIGURE 1. 8-PHYLOGENETIC TREE OF RELEVANT YEASTS AND RELATED FILAMENTOUS FUNGI DISCUSSED IN THIS WORK. THE TREE WAS CONSTRUCTED USING THE NEIGHBOUR-JOINING METHOD BASED ON THE ALIGNMENT OF THE LARGE SUBUNIT (26S) RIBOSOMAL DNA SEQUENCE. THE SEQUENCES USED WERE OBTAINED FROM "ENSEMBLFUNGI" DATABASE. THE YEASTS COLOURED WITH BLUE (THE ASCOMYCETOUS YEASTS *KLUYVEROMYCES MARXIANUS*, *KLUYVEROMYCES LACTIS*, *MEYEROZYMA GUILLIERMODII*, *PICHIA STIPITIS*, *OGATAEA POLYMORPHA* AND *PICHIA KUDRIAVZEVII*) ARE CAPABLE OF UTILIZING D-XYLOSE AND L-ARABINOSE AS CARBON SOURCES (C-SOURCES). IN RED COLOUR ARE REPRESENTED BASIDIOMYCETOUS YEASTS (UNDERLINED), SUCH AS *RHODOSPORIDIUM TORULOIDES*, *RHODOTORULA GRAMINIS* AND *PSEUDOZYMA HUBEIENSIS* AND FILAMENTOUS FUNGI (*TRICHODERMA REESEI*, *ASPERGILLUS NIGER* AND *NEUROSPORA CRASSA*) WHICH ARE ABLE TO GROW IN D-GALACTURONIC ACID AND ALSO IN D-XYLOSE AND L-ARABINOSE. THE YEAST SPECIES *TORULASPORA DELBRUECKII* REPRESENTED IN YELLOW IS CAPABLE TO GROW IN D-GALACTURONIC ACID AND D-XYLOSE. THE PHYLOGENETIC TREE ALSO INCLUDES (BLACK COLOUR) *SACCHAROMYCES CEREVISIAE S288C*, *ZYGOSACCHAROMYCES BAILII*, *YARROWIA LIPOLYTICA* AND *KOMAGATAELLA PHAFFII*. THE YEAST SPECIES *S. CEREVISIAE K. MARXIANUS*, *M. GUILLIERMONDII*, *P. STIPITIS*, *P. KUDRIAVZEVII* AND *T. DELBRUECKII* ARE INTERESTING BIOETHANOL PRODUCTERS, WHILE *H. UVARUM* IS ALSO RESPONSIBLE FOR THE FRUITY-LIKE AROMATIC COMPOUNDS IN FERMENTED BEVERAGES. *Y. LIPOLYTICA*, *P. HUBEIENSIS*, *R. GRAMINIS* AND *R. TORULOIDES* ARE OLEAGINOUS YEASTS WHICH CAN CONVERT C-SOURCES INTO HIGH CONCENTRATIONS AND A WIDE RANGE OF LIPIDS. THE SPECIES *K. PHAFFII* IS MAINLY USED AS CELL FACTORY FOR HETEROLOGOUS PROTEIN EXPRESSION WHILE *Z. BAILII* EXHIBITS A REMARKABLE TOLERANCE TO WEAK ACIDS..... 26

FIGURE 2. 1- VISUAL DESCRIPTION OF THE CRITERIA USED TO DEFINE THE DIFFERENT LEVELS OF SUSCEPTIBILITY TO METHANOL OF THE DELETION MUTANT STRAINS TESTED. WILD-TYPE AND DELETION MUTANT STRAINS WERE SPOTTED ONTO SOLID YPD MEDIUM (PH 4.5) SUPPLEMENTED WITH 8%(V/V) OF METHANOL. THREE LEVELS OF SUSCEPTIBILITY WERE DEFINED WHEN THE GROWTH OF THE SINGLE MUTANT STRAINS WAS SLIGHTLY DIMINISHED COMPARED TO WILD TYPE (+), SIGNIFICANTLY REDUCED (++), OR ABOLISHED (+++). 40

FIGURE 2. 2- COMPARISON OF THE GROWTH CURVES OF *S. CEREVISIAE* BY4741 IN YPD MEDIUM (PH 4.5) SUPPLEMENTED OR NOT (●) WITH 5% (□), 8% (◇), 10% (◐), OR 14% (v/v) (△) OF METHANOL. GROWTH WAS FOLLOWED IN A MICROPLATE READER BY MEASURING THE OPTICAL DENSITY AT 595 NM OF A 96-WELL PLATE INCUBATED AT 35 °C WITH ORBITAL AGITATION, FOR 36 HOURS. 42

FIGURE 2. 3- EFFECT OF EQUIVALENT METHANOL AND ETHANOL CONCENTRATIONS IN THE GROWTH CURVES OF *S. CEREVISIAE* BY4741. CELLS WERE CULTIVATED IN LIQUID YPD MEDIUM (PH 4.5) SUPPLEMENTED, OR

NOT (CIRCLES), WITH 8% (V/V) METHANOL (TRIANGLES) OR 5.5% (V/V) ETHANOL (SQUARES) AT 35 °C WITH ORBITAL AGITATION (250 RPM). GROWTH WAS FOLLOWED BASED ON CULTURE OPTICAL DENSITY AT 600 NM (OD_{600NM}) AND THE GROWTH CURVES SHOWN ARE REPRESENTATIVE OF AT LEAST THREE INDEPENDENT EXPERIMENTS. 43

FIGURE 2. 4- BIOLOGICAL FUNCTIONS ENRICHED IN THE DATASETS OF GENES REQUIRED FOR YEAST TOLERANCE TO METHANOL (BLACK BARS) OR ETHANOL (WHITE BARS). GENES LISTED IN SUPPLEMENTARY MATERIAL, TABLE S1 AND S2, WERE CLUSTERED ACCORDING TO THEIR BIOLOGICAL PROCESS GO ASSIGNMENTS USING THE PANTHER CLASSIFICATION SYSTEM ([HTTP://PANTHERDB.ORG](http://pantherdb.org)), AND FUNCTIONAL CATEGORIES WERE CONSIDERED TO BE OVER-REPRESENTED IF P-VALUE < 0.05. THE FOLD ENRICHMENT IS CALCULATED BY DIVIDING THE NUMBER OF GENES PRESENT IN THE INPUT DATASET BY THE TOTAL NUMBER OF GENES OF YEAST GENOME EXPECTED TO BELONG TO SPECIFIC FUNCTIONAL CLASS. (1) INDICATES THE BIOLOGICAL FUNCTIONS THAT ARE ONLY ENRICHED IN THE METHANOL DATASET WHILE (2) INDICATES THOSE ONLY ENRICHED IN THE ETHANOL DATASET. THE BIOLOGICAL FUNCTIONS WITH NO INDICATION ARE ENRICHED IN BOTH DATASETS. 44

FIGURE 2. 5- CLUSTERING OF METHANOL-TOLERANCE GENES THAT ARE TARGETS OF TRANSCRIPTION FACTORS (TF) THAT ALSO EXERT PROTECTION AGAINST THIS ALCOHOL. (A) NUMBER OF TARGET GENES (INTO BRACKETS) FOR EACH TF THAT ARE REQUIRED FOR METHANOL TOLERANCE. (B) PERCENTAGE OF METHANOL TOLERANCE GENES REGULATED BY EACH TF RELATIVELY TO THE TOTAL NUMBER OF GENES OF EACH DESCRIBED REGULON. METHANOL TOLERANCE GENES WERE CLUSTERED IN ASSOCIATION WITH THEIR DOCUMENTED REGULATORS USING THE INFORMATION AVAILABLE IN THE YEASTRACT DATABASE (DECEMBER 2020). THE TFs FOUND TO EXERT PROTECTION ONLY AGAINST METHANOL ARE IN BOLD; THE TFs UNDERLINED AND IN BOLD ARE THOSE FOUND IN THE METHANOL AND ETHANOL DATASETS. 54

FIGURE 2. 6- EFFECT OF METHANOL IN THE GROWTH CURVES OF THE PARENTAL STRAIN BY4741 (CIRCLES), AND DERIVED IXR1 Δ (HEXAGONS) AND OPI1 Δ (SQUARES) MUTANTS IN YPD LIQUID MEDIUM, (A) OR IN THIS MEDIUM SUPPLEMENTED WITH 8%(V/V) METHANOL(B) AT 35°C WITH ORBITAL AGITATION (250 RPM). THE GROWTH CURVES ARE REPRESENTATIVE OF AT LEAST THREE INDEPENDENT EXPERIMENTS. 55

FIGURE 2. 7-SUSCEPTIBILITY TO METHANOL OF THE PARENTAL STRAIN *S. CEREVISIAE* BY4741 AND DERIVED DELETION MUTANTS YAP1 Δ , MSN4 Δ , AND MSN2 Δ BY SPOT ASSAYS. YEAST CELL SUSPENSIONS USED AS INOCULA FOR SPOT ASSAYS WERE PREPARED USING CELLS HARVESTED IN THE EXPONENTIAL PHASE OF GROWTH (CULTURE $OD_{600NM} = 0.5 \pm 0.05$). CELL SUSPENSIONS WERE DILUTED IN STERILE WATER TO AN $OD_{600NM} = 0.25 \pm 0.005$ (A) AND THIS SOLUTION WAS USED TO PREPARE 1:5 (B), 1:25 (C), 1:125 (D), AND 1:625 (E) DILUTED SUSPENSIONS. SUSCEPTIBILITY PHENOTYPES WERE REGISTERED AFTER 48 HOURS OF INCUBATION AT 35 °C. 56

FIGURE 2. 8- GENETIC INTERACTION NETWORKS BETWEEN THE TFs GLN3 (A), IXR1 (B), OPI1 (C), RPH1 (D), SOK2 (E), STB5 (F) , SFL1 (G) AND UME6 (H), REQUIRED FOR TOLERANCE TO METHANOL AND THE METHANOL TOLERANCE GENES IDENTIFIED IN THIS STUDY THAT ARE THEIR DOCUMENTED TARGETS. THE INTERACTION NETWORKS WERE OBTAINED USING THE REGULATORY INTERACTIONS AVAILABLE IN

YEASTRACT (DECEMBER 2020, [HTTP://YEASTRACT-PLUS.ORG/YEASTRACT/SCEREVISIAE/INDEX.PHP](http://yeastract-plus.org/yeastract/scerevisiae/index.php)). THE POSITIVE, NEGATIVE, AND UNSPECIFIED REGULATORY INTERACTIONS, CORRESPOND, TO GREEN, RED, AND BLACK LINES, RESPECTIVELY. THE INTERACTIONS ARE BASED IN EXPRESSION DATA (DASHED LINES) OR DNA BINDING (FULL LINES). THE COLOR OF THE BOXES REPRESENTS DIFFERENT FUNCTIONAL GROUPS AS INDICATED IN THE LEGEND..... 58

FIGURE 2. 9- GENETIC INTERACTION NETWORKS BETWEEN THE TFs GLN3 (A), Ixr1 (B), Opi1 (C), RPH1 (D), SOK2 (E), STB5 (F), SFL1 (G) AND UME6 (H), REQUIRED FOR TOLERANCE TO METHANOL AND THE METHANOL TOLERANCE GENES IDENTIFIED IN THIS STUDY THAT ARE THEIR DOCUMENTED TARGETS. THE INTERACTION NETWORKS WERE OBTAINED USING THE REGULATORY INTERACTIONS AVAILABLE IN YEASTRACT (DECEMBER 2020, [HTTP://YEASTRACT-PLUS.ORG/YEASTRACT/SCEREVISIAE/INDEX.PHP](http://yeastract-plus.org/yeastract/scerevisiae/index.php)). THE POSITIVE, NEGATIVE, AND UNSPECIFIED REGULATORY INTERACTIONS, CORRESPOND, TO GREEN, RED, AND BLACK LINES, RESPECTIVELY. THE INTERACTIONS ARE BASED IN EXPRESSION DATA (DASHED LINES) OR DNA BINDING (FULL LINES). THE COLOR OF THE BOXES REPRESENTS DIFFERENT FUNCTIONAL GROUPS AS INDICATED IN THE LEGEND. 58

FIGURE 2. 10- SCHEMATIC MODEL PROPOSED, FOR METHANOL TOXICITY, INCLUDING THE DETOXIFICATION INTERMEDIATES FORMALDEHYDE AND FORMIC ACID. (A) BIOLOGICAL FUNCTIONS FOUND TO BE ENRICHED IN THE METHANOL DATASET. THE BIOLOGICAL FUNCTIONS SHARED WITH THE ETHANOL DATASET ARE IN BLUE AND THE ENRICHED BIOLOGICAL FUNCTIONS, SPECIFIC TO THE METHANOL DATASET, ARE IN RED. (B) METHANOL DETOXIFICATION PATHWAY AND THE ANTICIPATED TOXIC EFFECTS OF EACH METABOLIC INTERMEDIATE, IN PARTICULAR HAVING DNA AS AN IMPORTANT MOLECULAR TARGET FOR THE FORMIC ACID-INDUCED ROS [86] AND FORMALDEHYDE ALKYLATING ACTIVITY. (C) TO OVERCOME THE EFFECTS OF METHANOL IN YEAST CELLS, DNA REPAIR MECHANISMS PLAY AN IMPORTANT ROLE IN PRESERVING DNA INTEGRITY AFTER METHANOL EXPOSURE; MECHANISMS FOUND TO BE RELEVANT FOR METHANOL TOLERANCE INVOLVE, AMONG OTHERS, THE RAD GENES, AND OTHER GENES INVOLVED IN DNA REPAIR AND IN THE OXIDATIVE STRESS RESPONSE. SEVERAL TFs FOUND TO CONFER METHANOL TOLERANCE ARE ADDITIONAL POTENTIAL TARGETS FOR GENETIC ENGINEERING TO OBTAIN MORE ROBUST STRAINS, ABLE TO COPE WITH DELETERIOUS CONCENTRATIONS OF METHANOL. 65

FIGURE 3. 1- GROWTH CURVES AND CARBON SOURCE UTILIZATION BY A) *RHODOTORULA MUCILAGINOSA* IST 390 AND B) *RHODOTORULA TORULOIDES* PYCC 5615 CULTIVATED IN SUGAR BEET PULP (SBP) HYDROLYSATE H11 DERIVED MEDIUM. SBP HYDROLYSATE H11 WAS SUPPLEMENTED WITH 5 G/L OF AMMONIUM SULPHATE, ADJUSTED TO PH 5.0 AND INOCULATED WITH AN INITIAL OPTICAL DENSITY AT 600NM (OD_{600nm}) OF 4. YEAST CULTIVATIONS WERE PERFORMED AT 30°C WITH ORBITAL AGITATION (250 RPM). THE DATA ARE MEANS OF TWO INDEPENDENT EXPERIMENTS AND BARS REPRESENT STANDARD DEVIATIONS. 78

FIGURE 3. 2- EFFECT OF ACETIC ACID AND/OR AMINO ACID SUPPLEMENTATION OF SYNTHETIC SBP HYDROLYSATE ON THE CATABOLISM OF DIFFERENT CARBON SOURCES BY *R. TORULOIDES* PYCC 5615.

GROWTH AND CARBON-SOURCES UTILIZATION PROFILES BY *R. TORULOIDES* PYCC 5615 WHEN CULTIVATED IN: (A) MIXED-SUGAR MEDIUM (9 G/L D-GALACTURONIC ACID, 4 G/L D-GLUCOSE, 3 G/L D-GALACTOSE, 12 G/L L-ARABINOSE) PREPARED IN YEAST NITROGEN BASE (WITH 5 G/L AMMONIUM SULPHATE);(B) THE SAME MIXED-SUGAR MEDIUM AS IN (A) SUPPLEMENTED WITH 40 MM OF ACETIC ACID (C) THE SAME MIXED-SUGAR MEDIUM AS IN (A) SUPPLEMENTED WITH AMINO ACIDS (10 MG/L OF L-HISTIDINE, 20 MG/L OF DL-METHIONINE AND 20 MG/L DL-TRYPTOPHAN); (D) THE SAME MIXED-SUGAR MEDIUM SUPPLEMENTED WITH AMINO ACIDS AS IN (C) AND WITH 40 MM OF ACETIC ACID. MEDIA WERE ADJUSTED AT PH 5.0, CULTURES WERE INOCULATED WITH AN INITIAL OD_{600NM} OF 2 AND CULTIVATION WAS CARRIED OUT AT 30°C WITH ORBITAL AGITATION (250 RPM)..... 79

FIGURE 3. 3- EFFECT OF INCREASING CONCENTRATIONS OF ACETIC ACID (0 MM (A), 20 MM (B) AND 40 MM (C)) ADDED TO THE SYNTHETIC SBP HYDROLYSATE WITH THE MIXTURE OF SUGARS IN COMMERCIAL YNB (WITH AMMONIUM SULPHATE AND AMINO ACIDS) AT PH 5.0 IN *R. TORULOIDES* PYCC 5615 GROWTH AND SUGAR UTILIZATION. ALL CULTURES WERE INOCULATED WITH AN INITIAL OD_{600NM} OF 4 AND CULTIVATION WAS CARRIED OUT AT 30°C WITH ORBITAL AGITATION (250 RPM)..... 80

FIGURE 3. 4- PERFORMANCE OF *R. TORULOIDES* PYCC 5615 IN SBP HYDROLYSATE H11 SUPPLEMENTED WITH COMMERCIAL YNB WITH AMMONIUM SULPHATE AND AMINO ACIDS. CULTIVATION WAS PERFORMED AT 30°C WITH ORBITAL AGITATION (250 RPM). THE INITIAL CULTURE OD_{600NM} WAS 8. 82

FIGURE 3. 5- PERFORMANCE OF *R. MUCILAGINOSA* IST390 IN SBP HYDROLYSATE H11 SUPPLEMENTED WITH COMMERCIAL YNB WITH AMMONIUM SULPHATE AND AMINO ACIDS. CULTIVATION WAS PERFORMED AT 30°C WITH ORBITAL AGITATION (250 RPM). THE INITIAL CULTURE OD_{600NM} WAS 8. 82

FIGURE 3. 6- EFFECT OF DIFFERENT INITIAL CONCENTRATIONS OF AMMONIUM SULPHATE (A) 5, (B) 2.5 AND (C) 1 G/L ON THE UTILIZATION OF THE DIFFERENT CARBON SOURCES PRESENT IN SBP HYDROLYSATE H13 DURING THE CULTIVATION OF *R. TORULOIDES* PYCC 5615. THE SUGAR BEET PULP HYDROLYSATE H13 MEDIUM AT PH 5.0 WAS PREPARED IN YNB SUPPLEMENTED WITH THE AMINO ACIDS PRESENT IN COMMERCIAL YNB BESIDES THE DIFFERENT AMMONIUM SULPHATE CONCENTRATIONS TO BE TESTED. CULTIVATIONS WERE PERFORMED AT 30°C, WITH ORBITAL AGITATION (250 RPM). INOCULATION WAS WITH AN INITIAL OD_{600NM} OF 4..... 83

FIGURE 3. 7- BIOCONVERSION OF SBP HYDROLYSATE H13 SUPPLEMENTED WITH 1.7 G/L OF YNB (WITHOUT AMMONIUM SULPHATE OR AMINO ACIDS) AND WITH 2.5 G/L AMMONIUM SULPHATE AND THE AMINO ACIDS PRESENT IN COMMERCIAL YNB, AT PH 5.0, BY *R. MUCILAGINOSA* IST 390 (A), *R. TORULOIDES* PYCC 5615 (B), *R. TORULOIDES* IFO 0880 (C) FOR LIPID PRODUCTION. CULTIVATIONS WERE PERFORMED AT 30°C, WITH ORBITAL INCUBATION (250 RPM). MEDIA WERE INOCULATED WITH CELLS CORRESPONDING TO AN INITIAL OPTICAL DENSITY OF 8. LIPID PRODUCTION WAS ASSESSED BY NILE RED STAINING WITH A NORMALIZED CELL SUSPENSION (OD_{600NM} = 1) AND BASED ON RELATIVE FLUORESCENCE UNITS (RFU). ORANGE BARS REPRESENT AVERAGE RFU VALUES AND STANDARD DEVIATION VALUES ARE SHOWN. ... 84

FIGURE 3. 8- MICROSCOPIC OBSERVATIONS OF *R. MUCILAGINOSA* IST 390, *R. TORULOIDES* PYCC 5615, AND *R. TORULOIDES* IFO 0880 CELLS STAINED WITH NILE RED FLUORESCENCE DYE DURING CULTIVATION IN SBP HYDROLYSATE H13 DERIVED MEDIUM AS DESCRIBED IN FIGURE 3.7 LEGEND. CELLS WERE HARVESTED DURING THE GROWTH CURVES SHOWN IN FIGURE 3.6. THE ARRANGEMENT, SIZE AND FLUORESCENCE INTENSITY OF THE LIPID DROPLETS ACCUMULATED INSIDE THE CELLS WAS EXAMINED ALONG YEASTS' CULTIVATION. ONE OF THE DIFFERENT PICTURES TAKEN AT THE SAME INCUBATION TIMES IS SHOWN AS REPRESENTATIVE EXAMPLE. 87

FIGURE 3. 9- CELL PELLETS OF *RHODOTORULA MUCILAGINOSA* IST 390 (A), *R. TORULOIDES* PYCC 5615 (B) AND *R. TORULOIDES* IFO 0880 (C) HARVESTED DURING YEAST BIOCONVERSION OF SUGAR BEET PULP HYDROLYSATE H13. SAMPLES WERE HARVESTED FROM THE CULTURES CHARACTERIZED IN FIGURE 3.7. 88

FIGURE 4. 1- PERFORMANCE OF *RHODOTORULA TORULOIDES* PYCC 5615 (A) AND OF AN ENGINEERED *S. CEREVISIAE* STRAIN DEVELOPED IN ELKE NEVOIGT LABORATORY (JACOB UNIVERSITY, BREMEN) (B), DURING THE CONVERSION OF SBP HYDROLYSATE H13 SUPPLEMENTED WITH COMMERCIAL YNB WITH AMMONIUM SULPHATE AND AMINO ACIDS. CULTIVATION WAS PERFORMED AT 30°C WITH ORBITAL AGITATION (250 RPM). THE INITIAL CULTURE OD_{600NM} WAS 4. THE CULTURE B WAS ADDITIONALLY SUPPLEMENTED WITH 15 G/L OF PURE GLYCEROL. 99

LIST OF TABLES

TABLE 1.1- COMPOSITION OF PECTIN-RICH AGRO-INDUSTRIAL RESIDUES HYDROLYSATES DEPENDING ON THEIR PRE-TREATMENT AND HYDROLYSIS.....	8
TABLE 1.2- PERCENTAGE (OF TOTAL DRY MATTER) OF ACETYLATION AND METHYLATION OF DIFFERENT PECTIN-RICH MATERIALS.	10
TABLE 1. 3- REPORTED EXAMPLES OF BIOCONVERSION OF PECTIN-RICH RESIDUES BY NON-CONVENTIONAL YEASTS.....	28
TABLE 2. 1- GENES INVOLVED IN DNA REPAIR AND MITOTIC CELL CYCLE IDENTIFIED IN THIS STUDY AS DETERMINANTS OF YEAST TOLERANCE TO METHANOL, COMPARED WITH ETHANOL. THE DESCRIPTION OF THE ENCODED PROTEIN FUNCTIONS IS BASED ON THE INFORMATION AT SGD (WWW.YEASTGENOME.ORG). THE CLASSIFICATION OF THE SUSCEPTIBILITY PHENOTYPE LEVEL IS AS DESCRIBED IN THE MATERIAL AND METHODS SECTION.	45
TABLE 2. 2-. GENES INVOLVED IN AUTOPHAGY IDENTIFIED IN THIS STUDY AS DETERMINANTS OF YEAST TOLERANCE TO METHANOL, COMPARED WITH ETHANOL. GENES IN BOLD ARE SPECIFIC TO MACROAUTOPHAGY AND THE CORRESPONDING MUTANTS EXHIBITED A STRONG SUSCEPTIBILITY PHENOTYPE, AND THE UNDERLINED GENES ARE SPECIFIC TO RETICULOPHAGY. ATG11 IS COMMON TO BOTH TYPES OF AUTOPHAGY. SYMBOLS ARE AS IN TABLE 2.1.....	46
TABLE 2. 3- GENES INVOLVED IN RESERVE CARBOHYDRATE, CELL WALL, AND MEMBRANE BIOSYNTHESIS IDENTIFIED IN THIS STUDY AS DETERMINANTS OF YEAST TOLERANCE TO METHANOL, COMPARED WITH ETHANOL. SYMBOLS ARE AS IN TABLE 2.1.	48
TABLE 2. 4- GENES INVOLVED IN VACUOLAR ORGANIZATION AND ACIDIFICATION IDENTIFIED IN THIS STUDY AS DETERMINANTS OF YEAST TOLERANCE TO METHANOL, COMPARED WITH ETHANOL. SYMBOLS ARE AS IN TABLE 2.1.	50
TABLE 2. 5- GENES INVOLVED IN VESICULAR TRANSPORT IDENTIFIED IN THIS STUDY AS DETERMINANTS OF YEAST TOLERANCE TO METHANOL, COMPARED WITH ETHANOL. SYMBOLS ARE AS IN TABLE 2.1.	51
TABLE 2. 6- TRANSCRIPTION FACTORS (TF) IDENTIFIED ONLY IN THE METHANOL DATASET ⁽¹⁾ , THE ETHANOL-SPECIFIC TFs ⁽²⁾ , AND THE TFs SHARED BETWEEN METHANOL AND ETHANOL DATASETS ^(1,2) . SYMBOLS ARE AS IN TABLE 2.1.	52
TABLE 3. 1- COMPOSITION OF THE TWO SUGAR BEET PULP HYDROLYSATE BATCHES USED IN THIS STUDY.....	74
TABLE 3. 2- SPECIFIC PRODUCTION YIELD OF CAROTENOIDS (MG / G DRY BIOMASS) AND VOLUMETRIC CAROTENOID CONCENTRATION (MG/L) PRODUCED BY THE THREE RED YEAST STRAINS AFTER 144 H OF CULTIVATION IN SUGAR BEET PULP HYDROLYSATE H13 AS DESCRIBED IN FIGURE 3.6 LEGEND.	86
TABLE S1. 1- LIST OF GENES WHOSE EXPRESSION INCREASES <i>S. CEREVISIAE</i> TOLERANCE TO 8%(v/v) METHANOL BASED ON THE SCREENING OF THE EUROSCARF DELETION MUTANT COLLECTION; THE ELIMINATION OF THE INDICATED GENES INCREASES YEAST SUSCEPTIBILITY TO METHANOL. BIOLOGICAL FUNCTIONS ARE BASED ON THE INFORMATION AVAILABLE IN SGD (WWW.YEASTGENOME.ORG). THE SYMBOLS '+++', '++' AND '+' REFER TO PHENOTYPES AS SHOWN IN FIGURE 2.1.	140
TABLE S1. 2- LIST OF GENES WHOSE EXPRESSION INCREASES <i>S. CEREVISIAE</i> TOLERANCE TO 5.5%(v/v) ETHANOL BASED ON THE SCREENING OF THE EUROSCARF DELETION MUTANT COLLECTION; THE ELIMINATION OF THE INDICATED GENES INCREASES YEAST SUSCEPTIBILITY TO ETHANOL. BIOLOGICAL FUNCTIONS ARE BASED ON THE INFORMATION AVAILABLE IN SGD (WWW.YEASTGENOME.ORG). THE SYMBOLS '+++', '++' AND '+' CORRESPOND TO PHENOTYPES AS SHOWN IN FIGURE 2.1.	167

LIST OF ACRONYMS

ATP	Adenosine TriPhosphate
BLAST	Basic Local Alignment Search Tool
CCR	Carbon Catabolite Repression
EU	European Union
EUROSCARF	European <i>Saccharomyces cerevisiae</i> archive for functional analysis
FDA	Food and Drug Administration
GO	Gene Ontology
HPLC	High Pressure Liquid Chromatography
ITS	Internal Transcribed Spacer
NAD	Nicotinamide Adenine Dinucleotide
NADP	Nicotinamide Adenine Dinucleotide Phosphate
OD_{600nm}	Optical density at 600nm
PPP	Pentose Phosphate Pathway
pKa	log(Ka), where Ka is the acid dissociation constant
ROS	Reactive Oxygen Species
SBP	Sugar beet pulp
SCP	Single Cell Protein
TCA	Tricarboxylic Acid Cycle
TF	Transcription Factor
YEAstract	Yeast Search for Transcriptional Regulators and Consensus Tracking
YNB	Yeast Nitrogen Base
YPD	Yeast extract Peptone Dextrose

THESIS MOTIVATION AND OUTLINE

Yeasts are eukaryotic unicellular fungi that are widely distributed in natural environments including terrestrial, aquatic and atmospheric environments in association with plants, animals and insects (Satyanarayana and Kunze 2009). In nature, yeasts play important roles in food chains and in carbon, nitrogen and sulphur cycles. They are also used as cell factories for the production of relevant compounds in different industrial sectors. Since 1996, following the completion of the sequencing of the entire *Saccharomyces cerevisiae* genome, this yeast species is playing a central role in the biotechnology field for the development of new approaches to biological research. The products of modern yeast biotechnologies are widely spread among different economic sectors, in particular, food and beverages, chemicals, pharmaceuticals, industrial enzymes, agriculture and environment (Satyanarayana and Kunze 2009).

The increased concern about the negative impact of fossil fuels on the environment, particularly related with greenhouse gas emissions, led society to find renewable energy supplies (Angenent et al. 2004). This societal challenge requires the development and introduction of large-scale bioprocesses for the bioconversion of biomass resources into biofuels, for instance, bioethanol (Almeida et al. 2012). Recently, the biorefinery processes have gained relevance envisaging the conversion of biomass resources, including forest and agro-industrial residues, into environmentally friendly materials, chemicals and energy, opening the opportunities for reuse, recycle, and remanufacture different feedstocks, not competing with crops, towards a circular bioeconomy (Ubando et al. 2020). The aim of circular bioeconomy is to mitigate the effects of climate change while providing renewable carbon sources (biomass) for biotechnological processes as well as for creating business and employment opportunities, especially in the rural areas. Therefore, the concept of bioeconomy is related with a biorefinery model, for instance the lignocellulosic biorefineries (Ubando et al. 2020). The lignocellulosic biomass pertains to second-generation biomass feedstocks including the fractions of lignin, hemicellulose, cellulose and pectin, to be converted by yeast strains with natural or engineered suitable catabolic and biosynthetic activities envisaging the sustainable production of bio-products from the mixed carbon sources present in biomass hydrolysates (Leong et al. 2018).

Among the most promising microbes for biofuel production are oleaginous yeasts, characterized by the copious accumulation of triglycerides, which are useful precursors for conversion to biodiesel, green diesel, and jet fuel (Spagnuolo et al. 2019). Oleaginous yeasts have other advantages including a broader metabolism of different carbon sources and considerable tolerance to inhibitors produced during biomass feedstock hydrolysis (Sitepu et al. 2014b). The neutral lipid stocks produced by oleaginous yeasts consist mostly of

triacylglycerol (TAG) in the form of intracellular lipid droplets (LD) surrounded by a monolayer of phospholipids. These lipids can be directly used as a fuel or blended with petroleum diesel and used in diesel engines with little or no modification. Currently, the majority of studies on oleaginous yeasts have dealt with several species, namely *Yarrowia lipolytica*, *Lipomyces*., *Cryptococcus* and *Rhodotorula* species (Sitepu et al. 2014b). Several *Rhodotorula* strains have gained relevance in biotechnology processes envisaging the conversion of different feedstock in several valuable compounds besides microbial lipids, such as pigments and enzymes (Lyman et al. 2019). The potential of these yeasts has been demonstrated in particular for the biodiesel industry due to the accumulation of polyunsaturated fatty acid triacylglycerol, being a suitable alternative to plant derived lipids' industry (Jones et al. 2019; Kumar et al. 2020). *Rhodotorula* species can also produce carotenoids, such as β -carotene, torulene and torularhodin, which are regarded as valuable compounds for human health. In fact, carotenoids reinforce the immune system of the body, protect the skin against harmful ultraviolet radiation, whereas the anti-oxidative properties are being explored in cancer prevention (Kot et al. 2018). In red oleaginous yeasts, the role of carotenoids is cell protection against the negative influence of reactive oxygen species and radiation. Torularhodin was reported to have higher scavenging activity toward peroxy radicals than β -carotene (Kot et al. 2018). Process parameters that significantly regulate the process of carotenoid biosynthesis are the type of carbon and nitrogen sources, the ratio C/N, although the content of individual carotenoid fractions also depends, at a large extent, on the yeast strain. Also, the culture conditions (e.g., temperature, pH, aeration) and micronutrients supplied must be optimized according to the yeast strain used, in order to achieve high yields of carotenoid biosynthesis (Kot et al. 2019; Lopes et al. 2020).

This thesis was developed in the context of the ERANET- Industrial Biotechnology (IB) II project, "YEASTPEC" (Engineering of the yeast *Saccharomyces cerevisiae* for bioconversion of pectin- containing agro-industrial side-streams). The YEASTPEC project was a collaborative research work between our group at iBB, IST/ULisboa (PI: Isabel Sá-Correia) and the groups of Elke Nevoigt (Jacobs University Bremen, Germany), Wolfgang Liebl (TUM-Technical University of Munich), Peter Richard (VTT-Technical Research Centre of Finland Ltd) and the company GlobalYeast (Heverlee, Belgium). The general objective of this project was the valorization of cheap agro-industrial residues rich in pectin that represent attractive substrates for industrial biotechnology largely unexplored, in particular sugar beet pulp (SBP) available in large amounts in Europe. Apart from D-glucose and D-galactose, SBP hydrolysates are particularly rich in D-galacturonic acid and L-arabinose. Both sugars cannot be naturally used by *Saccharomyces. cerevisiae*. The objective of YEASTPEC was to construct a robust industrial *S. cerevisiae* strain that is able to ferment all abundant monosaccharides present in SBP hydrolysates into ethanol. One major novelty of the approach was to address the inherent

redox problem of the heterologous D-galacturonic acid catabolic pathways using glycerol as co-substrate. The objective was also to engineer the industrial strain for improved process robustness towards multiple stresses occurring during industrial fermentation of sugar beet pulp hydrolysates. The contribution of our iBB, IST/ULisboa team was centered on the identification of genetic determinants of tolerance to multiple stresses of relevance in the project context and to apply the knowledge gathered to improve yeast robustness and to guide bioprocess improvement by reducing stress deleterious effects. In particular, those associated to the presence of acetic acid and methanol in pectin rich residues hydrolysates were considered since D-galacturonic acid residues are acetylated and methylated.

The first chapter of this PhD thesis provides a literature review on the opportunities and challenges posed to the bioconversion of pectin-rich residues by yeasts. This review focuses on the valorisation of pectin-rich residues by exploring the potential of non-conventional yeasts that exhibit vast metabolic versatility for the efficient use of a diversity of carbon substrates present in their hydrolysates and high robustness to cope with the multiple stresses encountered. The major challenges and the progresses made related with the isolation, selection, sugar catabolism, metabolic engineering and use of non-conventional yeasts and *S. cerevisiae*-derived strains for the bioconversion of pectin-rich residue hydrolysates are discussed. The reported examples of value-added products synthesized by different yeasts using pectin-rich residues are reviewed. This timely review was published in the journal "Applied Microbiology and Biotechnology" (Martins et al. 2020) (<https://doi.org/10.1007/s00253-020-10697-7>). The review paper was prepared by the PhD candidate under the guidance of the supervisor, Prof. Isabel Sá-Correia. The other co-authors, the MSc students Catarina C. Monteiro and Paula M. Semedo, contributed to the literature search.

The second chapter of this thesis was dedicated to the identification of genes whose expression is required for maximum methanol or ethanol tolerance to get mechanistic insights and envisaging the future rational genomic manipulation to obtain more robust yeast strains. To reach this objective, a chemogenomic analysis was performed based on the screening of the Euroscarf *Saccharomyces cerevisiae* haploid deletion mutant collection to search for susceptibility phenotypes in YPD medium supplemented with 8% (v/v) methanol, at 35 °C, compared with an equivalent ethanol concentration (5.5% (v/v)) to compare the mechanisms underlying methanol and ethanol toxicity and tolerance. This was considered essential because the various genome-wide studies available that allowed the identification of genetic determinants of ethanol tolerance were performed under different experimental conditions and the criteria used to identify genes that when deleted lead to ethanol susceptibility phenotypes, varied. The results obtained indicate that, despite the similarities identified for a vast number of genetic determinants of tolerance to these two alcohols, DNA repair and membrane

remodeling are among the more specific responses to counteract methanol toxicity. This study provides new valuable information on genes and potential regulatory networks involved in overcoming methanol and ethanol toxicity. This knowledge is an important starting point for the improvement of methanol and ethanol tolerance in yeasts capable of catabolizing promising bioeconomy feedstocks, including industrial residues. Methanol is a promising feedstock alternative to sugar-based raw materials for the bioproduction of fuels, specialty chemicals, polymers, and other value-added products due to its abundance and relatively low cost (Zhang et al. 2018; Fabarius et al. 2020). Methanol is also the major impurity in crude glycerol, reaching relatively high levels that can vary considerably from batch to batch (Chen and Liu 2016). Therefore, yeast methanol-tolerance would increase the feasibility of bioprocesses that use crude glycerol as substrate (Vartiainen et al. 2019). Since methanol toxicity can limit the productivity of bioprocesses that use crude glycerol as co-substrate, a research topic addressed by Elke Nevoigt partner laboratory, in Bremen, the development of more tolerant yeasts would increase their feasibility. Methanol is also present at relatively low concentrations in hydrolysates from pectin-rich agro-industrial residues since the D-galacturonic acid monomers are methyl-esterified in different positions. The results obtained in this work were published in the “Journal of Fungi” (Special Issue: Yeast Biorefineries), (Mota et al. 2021) (<https://doi.org/10.3390/jof7020090>). The contribution of the candidate for the article, which coincides with chapter 2, was on the screening of the yeast disruptome under ethanol stress and the analysis of the results obtained. He also contributed to the chemogenomic experiments with methanol that were mainly performed by Marta Mota who also took care of the global analyses of the results gathered.

The third chapter focuses on the role of agro-industrial residues as low-cost carbon sources (C-sources) for microbial growth and production of value-added bioproducts, in particular those rich in pectin, generated in high amounts worldwide from the sugar industry or the industrial processing of fruits and vegetables (Martins et al. 2020). Sugar beet pulp (SBP) hydrolysates contain predominantly the neutral sugars D-glucose, L-arabinose and D-galactose and the acidic sugar D-galacturonic acid. Acetic acid is also present at significant concentrations since the D-galacturonic acid residues are acetylated (Leijdekkers et al. 2013). In this thesis work, the performance of a *Rhodotorula mucilaginosa* strain, isolated from SBP and identified at the molecular level during this work was examined and optimized. This study was extended to another oleaginous red yeast species, *R. toruloides*, envisaging the full utilization of the C-sources from SBP hydrolysate (at pH 5.0). The dual role of acetic acid as carbon and energy source and as a growth and metabolism inhibitor was examined. Acetic acid was proved to inhibit or prevent the catabolism of D-galacturonic acid and L-arabinose after the complete use of the other C-sources. However, D-glucose and acetic acid were simultaneously metabolized efficiently, followed by galactose. SBP hydrolysate

supplementation with amino acids was crucial to allow D-galacturonic acid and L-arabinose catabolization. SBP valorization envisaging the production of lipids and carotenoids by *Rhodotorula spp.*, and the complete catabolism of the major C-sources present, looks promising. The results presented in this chapter are included in a manuscript entitled “*Complete Utilization of the Major Carbon Sources Present in Sugar Beet Pulp Hydrolysates by the Oleaginous Red Yeasts Rhodotorula toruloides and R. mucilaginosa*” submitted to the “Journal of Fungi” (special issue on “Yeast Biorefineries”). The candidate was the major contributor to this manuscript. SBP hydrolysates were prepared at, and obtained from, the YEASTPEC partner Wolfgang Liebl’ laboratory.

A missing chapter would include results of a collaborative work with the YEASTPEC partner Elke Nevoigt laboratory. A draft of this work is already written to be submitted for publication as soon as considered suitable. In this work an engineered *S. cerevisiae* strain was developed in the Bremen laboratory for the efficient co-utilization of D-galacturonic acid and crude glycerol in SBP hydrolysate. The major novelty of the approach was to address the inherent redox problem of the heterologous galacturonic acid catabolic pathways by co-feeding glycerol and appropriately engineering the glycerol catabolic pathway. Notably, glycerol is a major low-value by-product of current biodiesel production and thus also available in huge quantities (Chen and Liu 2016). The candidate is the second author of this manuscript having been involved in several experiments envisaging the exploration of this engineered strain in SBP hydrolysates including the effect of acetic acid. Since the manuscript is still unsubmitted and for reasons of intellectual property, this chapter is absent from this provisory version of the thesis.

The chapter four includes an integrated discussion of the results obtained and on future perspectives taking into consideration all the previous chapters in the state of the art context.

1| General Introduction

This Chapter includes a review paper published in:

Martins, L.C., Monteiro, C.C., Semedo, P.M., Sá-Correia I., (2020) *Valorisation of pectin-rich agro-industrial residues by yeasts: potential and challenges. Applied Microbiology and Biotechnology* 104, 6527–6547.

Abstract

Pectin-rich agro-industrial residues are feedstocks with potential for sustainable biorefineries. They are generated in high amounts worldwide from the industrial processing of fruits and vegetables. The challenges posed to the industrial implementation of efficient bioprocesses are however manifold and thoroughly discussed in this review paper, mainly at the biological level. The most important yeast cell-factory-platform for advanced biorefineries is currently *Saccharomyces cerevisiae* but this yeast species cannot naturally catabolise the main sugars present in pectin-rich agro-industrial residues hydrolysates, in particular D-galacturonic acid and L-arabinose. However, there are non-*Saccharomyces* species (non-conventional yeasts) considered advantageous alternatives whenever they can express highly interesting metabolic pathways, natively assimilate a wider range of carbon sources or exhibit higher tolerance to relevant bioprocess-related stresses. For this reason, the interest in non-conventional yeasts for biomass-based biorefineries is gaining momentum. This review paper focuses on the valorisation of pectin-rich residues by exploring the potential of yeasts that exhibit vast metabolic versatility for the efficient use of the carbon substrates present in their hydrolysates and high robustness to cope with the multiple stresses encountered. The major challenges and the progresses made related with the isolation, selection, sugar catabolism, metabolic engineering and use of non-conventional yeasts and *S. cerevisiae*-derived strains for the bioconversion of pectin-rich residues hydrolysates are discussed. The reported examples of value-added products synthesized by different yeasts using pectin-rich residues are reviewed.

1.1 Valorization of pectin-rich agro-industrial residues by yeasts

1.1.1 Overview

Agro-industrial residues are currently in the spotlight of research and development activities worldwide; they are raw materials for the biotechnology industry, as renewable sources of carbon, nitrogen and other nutrients for microbial growth and metabolite production (Cherubini 2010; Liguori and Faraco 2016; Liu et al. 2016; Dahiya et al. 2018). The utilization of organic waste residues as substrates to produce added-value products are environmentally friendly strategies by saving and reutilizing resources. The implementation of a circular bio-economy based on microorganisms, in particular non-conventional (non-*Saccharomyces*) yeast strains with metabolic versatility and tolerance to bioprocesses-related stresses is an important societal challenge (Leandro et al. 2006; Fletcher et al. 2016; Cristobal-Sarramian and Atzmüller 2018; Zuin et al. 2018; Rebello et al. 2018; Nielsen 2019).

Agro-industrial residues derived from sugary materials (e.g. sugar beet, sugarcane or fruits and vegetables) and starchy feedstocks (e.g. wheat, corn, rice or potatoes) and lignocellulosic substrates (e.g. wood, straw and grasses) (Balat 2011). Pectin-rich agricultural residues and agro-food industry residues are potential feedstocks for the production of biofuels and other relevant bioproducts (Schmitz et al. 2019). Currently, a large fraction of the pectin-rich residues (e.g. sugar beet pulp and citrus peel) are dried for further use as cattle feed or put in landfills for soil improvement, although it is desirable to find new ways to convert these residues into renewable chemicals using natural or engineered microbes (Richard and Hilditch 2009; Ajila et al. 2012). The residues with the highest pectin content (sugar beet pulp, citrus peels, and apple pomace) are accumulated in high amounts worldwide from the sugar industry or the industrial processing of fruits and vegetables (Peters 2006; Balat 2011). These residues are partially pre-treated during sugar (from sugar beets) and juice (from fruits) extraction and have a low lignin content which facilitates processing (Berlowska et al. 2018). Despite the difficulties inherent to the high variability of these feedstocks due to diverse geographical distribution and seasonality, they are cheap and abundant (Peters 2006; Balat 2011). However, they are interesting feedstocks for microbial fermentations, as the enzymatic hydrolysis of their component polysaccharides can be economically accomplished to yield fermentable neutral sugars (hexoses and pentoses) and D-galacturonic acid (D-GalA) (Leijdekkers et al. 2013; Cárdenas-Fernández et al. 2017; Torre et al. 2019).

Saccharomyces cerevisiae is currently, and by far, the most important yeast cell factory in the biotechnology industry and the major cell factory platform for the production of bioethanol and other biofuels and chemicals in advanced biorefineries (Satyanarayana and Kunze 2009;

de Jong et al. 2012; Hong and Nielsen 2012; Nielsen 2019). Endogenously, *S. cerevisiae* can only use a very limited range of carbon sources. For this reason, genetically modified strains have been developed to also utilize pentoses and D-galacturonic acid for synthesis of novel compounds (Hong and Nielsen 2012; Benz et al. 2014; Biz et al. 2016; Yaguchi et al. 2018; Rebello et al. 2018; Protzko et al. 2018; Nielsen 2019). However, there are non-conventional species considered advantageous alternatives to *S. cerevisiae* since they can express highly interesting metabolic pathways (Rebello et al. 2018), efficiently assimilate a wider range of carbon sources (Do et al. 2019) or exhibit higher tolerance to relevant bioprocess-related stresses, such as the presence of a wide range of inhibitory compounds and supraoptimal temperatures (Radecka et al. 2015; Kręgiel et al. 2017; Mukherjee et al. 2017). Several non-conventional yeast species are capable of producing high concentrations of sugar alcohols (namely xylitol and arabitol) (Schirmer-Michel et al. 2009; Loman et al. 2018), lipids and single cell oils for food or energy applications (Ratledge 2010; Taskin et al. 2016; Anschau 2017; Hicks et al. 2020), enzymes (Serrat et al. 2004; Saravanakumar et al. 2009; Sahota and Kaur 2015) and pigments (Buzzini and Martini 2000; Aksu and Tuğba Eren 2005) among other added-value compounds. It should be noted that different yeast species, and even strains, significantly differ in the products synthesized and in their production rates and yields (Rodríguez Madrera et al. 2015; van Dijk et al. 2019). Non-conventional yeasts have recently been in the focus of active and relevant research, their genome sequences are being released and suitable genetic engineering tools are either available or being developed for different purposes (Mira et al. 2014; Palma et al. 2017; Nambu-Nishida et al. 2017; Lee et al. 2018; Cai et al. 2019; Protzko et al. 2019; among several other examples). Thus, it is expected that, in the near future, the currently accepted designation of “non-conventional yeast” will no longer be adequate and non-*Saccharomyces* strains will successfully be used in the industry (Johnson 2013a; Radecka et al. 2015; Kręgiel et al. 2017; Siripong et al. 2018). This review paper presents relevant results and discusses the potential and the current challenges of the use of yeasts for the valorisation of pectin-rich agro-industrial residues.

1.2 Pectin-rich agro-industrial residues as feedstocks for Biotechnology

1.2.1 Pectin structure and pectin-rich biomasses

Pectin is a family of complex heteropolysaccharides and a structural component of plant cell walls (Mohnen 2008). Pectin is composed of a linear chain of α -1,4 linked D-galacturonic acid (D-GalA) molecules which represent about 70% of total weight in a homogalacturonan

polymer. There are three major pectin polymers: homogalacturonan (HG), rhamnogalacturonan I (RG-I) and rhamnogalacturonan II (RG-II) (**Figure 1.1**). More complex pectin structures, such as rhamnogalacturonan I and II, have side chains composed by neutral sugars that include L-rhamnose, L-arabinose, D-xylose, D-galactose, L-fucose and D-glucose, among others (Sakai et al. 1993) These sugars are linked to D-galacturonic acid by β -1,2 and β -1,4 glycosidic linkages (**Figure 1.1**) (Jayani et al. 2005; Mohnen 2008). Moreover, D-galacturonic acid (D-GalA) residues can be methyl-esterified at the C6 carboxyl group and/or O-acetylated at C-2 or C-3 and neutralized by ions, like sodium, calcium or ammonium (Sakai et al. 1993a; Jayani et al. 2005).

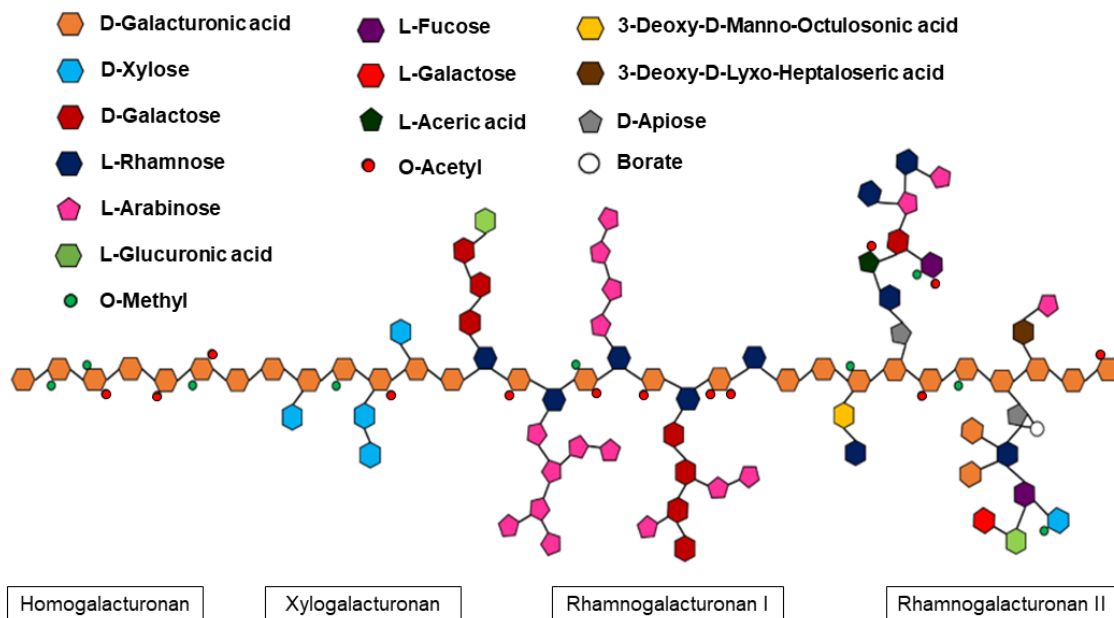


Figure 1.1-Schematic representation of the chemical structure of four pectic polysaccharides: homogalacturonan (HG), substituted HG xylogalacturonan (XGA), rhamnogalacturonan I and II (RG-I and RG-II), based on (Mohnen 2008).

Pectin-rich biomasses, in particular the agro-food residues left after fruit or vegetable processing for juice or sugar production, (e.g. apple pomace, citrus waste, and sugar beet pulp) are abundant and widely underused bioresources (Zhou et al. 2008; Mohnen 2008). Although most food waste streams contain pectin too, the residues mentioned above exhibit the highest pectin content with pectin concentrations ranging from 12% to 35% of the biomass dry weight (Müller-Maatsch et al. 2016).The low lignin content of these processed wastes is

an interesting trait because lignin can impair with the enzymatic degradation of cellulose and hemicellulose and its monomers cannot be used as carbon sources so far (Guo et al. 2009). Lignin, the most recalcitrant cell wall material, can be combusted and converted into electricity and heat (Limayem and Ricke 2012). The composition of agro-food residues and the bioavailability of their various polysaccharide fractions are highly dependent on natural variation, husbandry practices, fruit maturity and post-harvest management (Grohmann and Bothast 1994). The apparent high variability of the different pectin-rich biomasses regarding the dry-weight composition in pectin and other polysaccharides is shown in **Figure 1.2**. Determining pectin in biomass quantitatively is actually quite challenging and the differences detected may simply result from the use of different analytic methods and sub-optimal techniques (Quemener et al. 1993; Kühnel 2011; Wikiera et al. 2015).

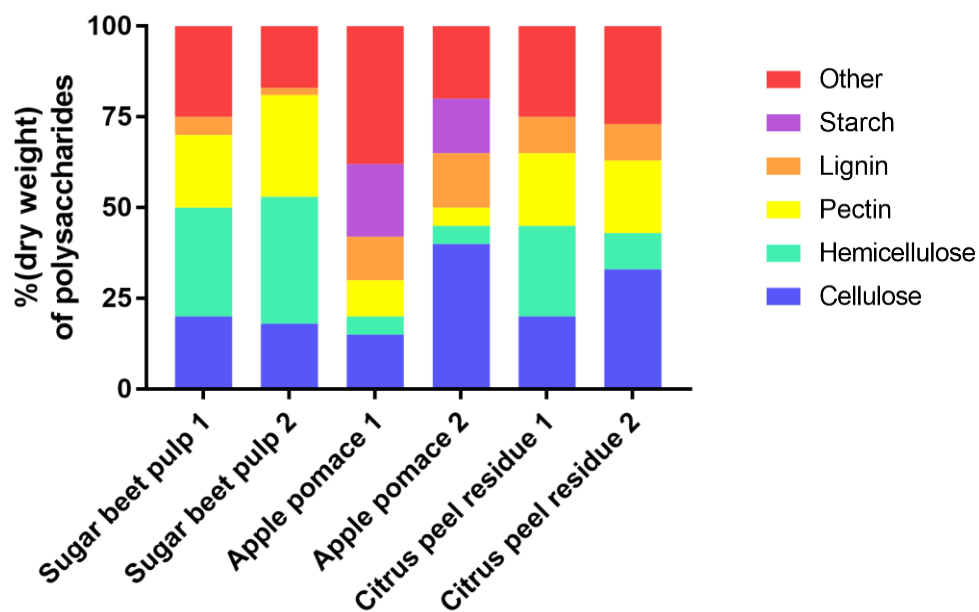


Figure 1. 2- Dry weight composition of pectin-rich residues, in particular sugar beet pulp 1 (Berlowska et al. 2018) and 2 (Edwards and Doran-Peterson 2012), apple pomace 1 (Grohmann and Bothast 1994) and 2 (Bhushan et al. 2008) and citrus peel 1 (Zhou et al. 2008) and 2 (John et al. 2017).

1.2.2 Pectin-rich biomass processing and composition of the resulting hydrolysates

The bioconversion of pectin-rich agro-industrial residues requires pre-treatment step(s) before microbial utilization in order to avoid the recalcitrant material and to increase surface area to facilitate and enhance the hydrolysis step (Limayem and Ricke 2012). After pre-treatment, the enzymatic or acidic hydrolysis of cellulose, hemicellulose and pectin structures allow the release of monomeric sugars (saccharification) that will subsequently be converted

into ethanol and/or other bioproducts by yeasts. Filamentous fungi, in particular *Aspergillus* sp., *Trichoderma reesei* and *Neurospora crassa* naturally have degrading machinery consisting in hydrolytic and oxidative enzymes which play an important role in plant biomass degradation (Schmitz et al. 2019). A recent review details the enzyme repertoire of filamentous fungi and their specific transcriptional regulation patterns for efficient biomass degradation (Benocci et al. 2017).

Remarkably, the sugar composition of the hydrolysates obtained from the same pectin-rich agro-industrial residue is highly dependent on the pre-treatment and enzyme hydrolysis conditions used (Table 1.1) reducing the reproducibility of the hydrolysis process (Merz et al. 2016).

Table 1.1- Composition of pectin-rich agro-industrial residues hydrolysates depending on their pre-treatment and hydrolysis.

Feedstock	Pre-treatment	Hydrolysis	Sugar composition after hydrolysis (g/100g matter)	Reference
Sugar beet pulp	Steam explosion at 152°C to 175.5°C and 4 to 8 bar pressure	<p>(Soluble fraction) <u>Acid hydrolysis:</u> 72% H₂SO₄ for 1 hour at 30°C and 150rpm</p> <p>(insoluble fraction) <u>Enzyme hydrolysis:</u> 0.5 mg cellulase/g glucan 50°C with shaking for 24 hrs</p>	Glucose 26 Arabinose 24 Xylose 1.6 Rhamnose 2.4 Galactose 6 Galacturonic acid 14 Glucose 10 Arabinose 0.4 Xylose 0.3 Rhamnose 0.1 Galactose 0.1 Galacturonic acid <0.1	(Hamley-Bennett et al. 2016)
		Not used	<p><u>Enzyme hydrolysis:</u> Viscozyme and Ultraflo Max (Novozymes) treatment</p> <p><u>Total of reducing sugars 6.6</u></p>	(Berlowska et al. 2017)
Apple pomace	15 g/L sulfuric acid for 16 min at 91°C with laccase 100 units/L at 30°C for 12h at 90 rpm	<p><u>Enzyme hydrolysis:</u> Viscozyme and Celluclast (0.5 µL/mL, 0.038 mg/mL) together with Novozyme 188 (0.05 µL/mL, 0.0024mg/mL)</p>	Galacturonic acid 33 Glucose 21 Arabinose 17 Galactose 5	(Gama et al. 2015)
	Not used	<p><u>Acid hydrolysis</u> 1.5 g sulfuric acid/100 mL, 91°C reaction temperature during 16 min</p>	18.2 g of glucose and fructose/100 g dry matter	(Parmar and Rupasingh 2012)
	Not used	<p><u>Acid hydrolysis</u> 72% sulfuric acid for 45 min at room temperature and diluted with distilled water to 4% sulfuric acid, followed by autoclaving for 1 h at 121 °C</p>	Galacturonic acid (<i>not quantified</i>) Glucose 25 Fructose 24 Arabinose 6 Sucrose 9 Galactose 4 Xylose 6 Rhamnose 2	(Choi et al. 2015)
	Not used	<p><u>Acid hydrolysis</u> 2 M Trifluoroacetic acid for 2 hours at 100°C with constant shaking</p>	<u>Rhamnose 0.5</u> <u>Arabinose 8</u> <u>Glucose 12</u> <u>Galactose 4</u> <u>Xylose 4</u> <u>Mannose 0.7</u>	(Wikiera et al. 2015)
	<p><u>Acid hydrolysis</u> 0.2 M Trifluoroacetic acid for 72 hours at 80°C with constant shaking</p>	<p><u>Enzyme hydrolysis:</u> Viscozyme (25µL) incubated at 50°C during 24h with constant shaking</p>	<u>Rhamnose 0.4</u> <u>Arabinose 7</u> <u>Glucose 11</u> <u>Galactose 4</u> <u>Xylose 4</u> <u>Mannose 0.3</u>	
	80% v/v ethanol for 20 min, filtered on a sintered glass, and dried at 40 °C for 72h	<p><u>Acid hydrolysis:</u> 0.05 M hydrochloric acid at 85°C</p>	Galacturonic acid 15 Arabinose 4 Galactose 1 Glucose 1 Rhamnose 0.5	(Yapo et al. 2007)
Citrus peel	Not used	<p><u>Acid hydrolysis</u> 72% sulfuric acid for 45 min at room temperature and diluted with distilled water to 4% sulfuric acid, followed by autoclaving for 1 h at 121 °C</p>	<u>Orange peel</u> Galacturonic acid (<i>not quantified</i>) Glucose 36 Fructose 12 Arabinose 6 Sucrose 5.6 Galactose 3 Xylose 2 Rhamnose 2 <u>Lemon peel</u>	(Choi et al. 2015)
		<p><u>Acid hydrolysis</u> 72% sulfuric acid for 45 min at room temperature and diluted with distilled water to 4% sulfuric acid, followed by autoclaving for 1 h at 121 °C</p>	Galacturonic acid (<i>not quantified</i>) Glucose 27 Fructose 3 Arabinose 5 Sucrose 0 Galactose 5 Xylose 3 Rhamnose 2	
	Steam explosion at 150°C for 10 min and 15 kg/cm pressure	<p>Pectinase, xylanase (5 mg/g dry matter), and β-glucosidase (2 mg/g dry matter) cocktail at 45°C for 24h</p>	Galacturonic acid (<i>not quantified</i>) Glucose 45 Fructose 18 Arabinose 3 Galactose 2	(Choi et al. 2013)

Pectin-rich biomass hydrolysates may also include growth inhibitory compounds, such as weak acids, furan derivatives and phenolic compounds generated during pre-treatment and acid hydrolysis of pectin-rich materials (Palmqvist and Hahn-Hägerdal 2000). Acetic acid and methanol are potential growth inhibitors that are likely to be present (Vendruscolo et al. 2008; Günan Yücel and Aksu 2015; Berlowska et al. 2018). These compounds have potential to affect yeast growth, fermentation kinetics and metabolite production yields, (dos Santos and Sá-Correia 2015; Cunha et al. 2019). Although, the individual toxicity of some of these compounds can be relatively low, their combined toxic effects can be additive or even synergistic (Palmqvist and Hahn-Hägerdal 2000; Teixeira et al. 2011). The average degree of methylation and acetylation of diverse pectin-rich residues is different with sugar beet exhibiting the highest acetylation degree (Table 1.2). Other potentially critical inhibitors are heavy metals and pesticides. They have also been detected in pectin-rich residues, mainly due to the geochemical cycles and human activities, such as intensive agriculture, waste treatment and disposal and transportation (Legrand 2005; Skrbic et al. 2010; Mukherjee et al. 2017).

Table 1.2- Percentage (of total dry matter) of acetylation and methylation of different pectin-rich materials.

Pectin substrate	Acetylation (%)	Methylation (%)	References
Citrus fruits (Orange, Lime, lemon)	3	60-80	(Sakai et al. 1993a; Yapo et al. 2007; Williams 2011)
Apple	4	80	(Sakai et al. 1993a; Williams 2011)
Sugar beet	10-20	Up to 60	(Sakai et al. 1993a; Yapo et al. 2007b; Williams 2011)

1.3 Yeast metabolism of sugar monomers present in pectin-rich hydrolysates

1.3.1 The challenges

The efficient utilization by yeasts of the mixtures of sugar monomers present in hydrolysates derived from pectin-rich residues is essential for their biotechnological valorization. Sugar beet pulp and citrus peel hydrolysates contain predominantly the neutral sugars L-arabinose, D-glucose and D-galactose, and the acidic sugar D-galacturonic acid (Micard et al. 1996; Berlowska et al. 2018). This means that the convenient yeast species/strains to be used should be able to rapidly and efficiently catabolize all the sugars present (Du et al. 2019).

The presence and simultaneous use of several sugars in pectin hydrolysates is an important challenge also due to carbon catabolite repression (CCR) regulation (Kayikci and Nielsen 2015; Gao et al. 2019). This regulation mechanism limits the efficient utilization of multiple carbon substrates in biotechnological processes like those developed for the valorization of pectin-rich residues. In fact, the uptake of secondary carbon sources (e.g. L-arabinose, D-galacturonic acid, D-xylose) is inhibited in the presence of the preferred substrate (D-glucose), prolonging fermentation time as the result of sequential, rather than the simultaneous, use of the carbon sources (Huisjes et al. 2012; Wu et al. 2016; Yaguchi et al. 2018; Lane et al. 2018). *S. cerevisiae* has a highly complex and still not fully understood network of signals and regulations, through (de)phosphorylation mechanisms depending on the presence of D-glucose in the medium which have been on the focus of extensive review papers (Gancedo 1992; Conrad et al. 2014; Kayikci and Nielsen 2015).

Moreover, pectin-rich hydrolysates contain a significant amount of D-galacturonic acid that is neither naturally used by *S. cerevisiae* nor by other relevant yeast species, such as *Kluyveromyces marxianus*, *Yarrowia lipolytica*, *Pichia stipitis*, among others. Recent efforts have been reported in order to genetically engineer *S. cerevisiae* to efficiently express the D-galacturonic acid catabolic pathway (Benz et al. 2014; Zhang et al. 2015; Nielsen and Keasling 2016; Matsubara et al. 2016; Biz et al. 2016; Kalia and Saini 2017; Lian et al. 2018; Protzko et al. 2018; Jeong et al. 2020). Moreover, since pectin-rich hydrolysates have significant amounts of L-arabinose, efforts have also addressed the expression of this pentose-fermentative pathway in *S. cerevisiae* strains (Wisselink et al. 2007; Ye et al. 2019). The pathways involved in the catabolism of D-galacturonic acid and L-arabinose, the main sugars released from pectin-rich feedstocks hydrolysis are detailed below (**Figure 1.3** and **1.6**). D-galacturonic acid catabolic pathway is emphasized because this acid sugar catabolism is currently the big

challenge for which there is relevant recent literature. Non-conventional yeast species/strains reported in the scientific literature as naturally capable of such catabolism are also referred.

1.3.1.1 D-Galacturonic acid pathways from fungi, expressed in *S. cerevisiae*, and from the oleaginous yeast *Rhodospidium toruloides*

D-Galacturonic acid is not catabolized by the yeast *S. cerevisiae* that misses the catabolic pathway (**Figure 1.3-A**). Moreover, as an acid sugar, D-galacturonic acid is more oxidised than the neutral hexose and pentose sugars. This means that its metabolism, is not redox neutral as D-glucose metabolism and the fermentation of D-galacturonic acid requires more NADPH cofactor molecules to produce ethanol (Richard and Hilditch 2009).

The D-galacturonic acid plasma membrane transporter Gat1 from *N. crassa* was identified, characterized and the encoding gene *GAT1* successfully expressed in *S. cerevisiae* allowing the increased uptake of D-galacturonic acid in this yeast cell factory (Benz et al. 2014) (**Figure 1.3-B**). In fact, D-galacturonic acid uptake is poorly performed when mediated by the native Gal2 or other hexose transporters (Huisjes et al. 2012; Benz et al. 2014; Biz et al. 2016), even though D-galacturonic acid was shown to be taken up rapidly by *S. cerevisiae* (Souffriau et al. 2012). With the co-expression in yeast of a D-galacturonic acid reductase (from the filamentous fungus *Aspergillus niger*) or an uronate dehydrogenase (from the bacterium *Agrobacterium tumefaciens* involved in plant infection), a transporter-dependent conversion of D-galacturonic acid towards a more reduced (L-galactonate) or oxidized (*meso*-galactaric acid) downstream metabolites, was also demonstrated (**Figure 1.3-B**) (Benz et al. 2014). This heterologous co-expression, although highly relevant as prove of concept, missed the expression of the complete D-galacturonic catabolic pathway for the full catabolisation of this acid sugar.

Therefore, several efforts have been made envisaging the development of a genetically engineered *S. cerevisiae* strain capable of efficiently use D-galacturonic acid from pectin-rich hydrolysates. For this purpose, the genes *GAAA*, *GAAC*, *GAAD* encoding D-galacturonic acid reductase, 2-keto-3-deoxy- L-galactonate aldolase respectively, from *A. niger* and the gene *LGD1* encoding D-galactonate dehydratase from *T. reesei*, were successfully expressed in *S. cerevisiae* (**Figure 1.3-C**) (Biz et al. 2016). The entire D-galacturonic acid catabolic pathway from filamentous fungi comprises two NADPH-dependent enzymes: the D-galacturonate reductase and the L-glyceraldehyde reductase, for the catabolisation of D-galacturonic acid into glycerol (Biz et al. 2016) (**Figure 1.3-C**) leading to intracellular cofactor imbalance. For the efficient functioning of D-galacturonic acid catabolic pathway from filamentous fungi in *S.*

cerevisiae, the pathway has to be coupled with NADPH regeneration steps which can be achieved through the operation of the oxidative Pentose Phosphate Pathway (PPP).

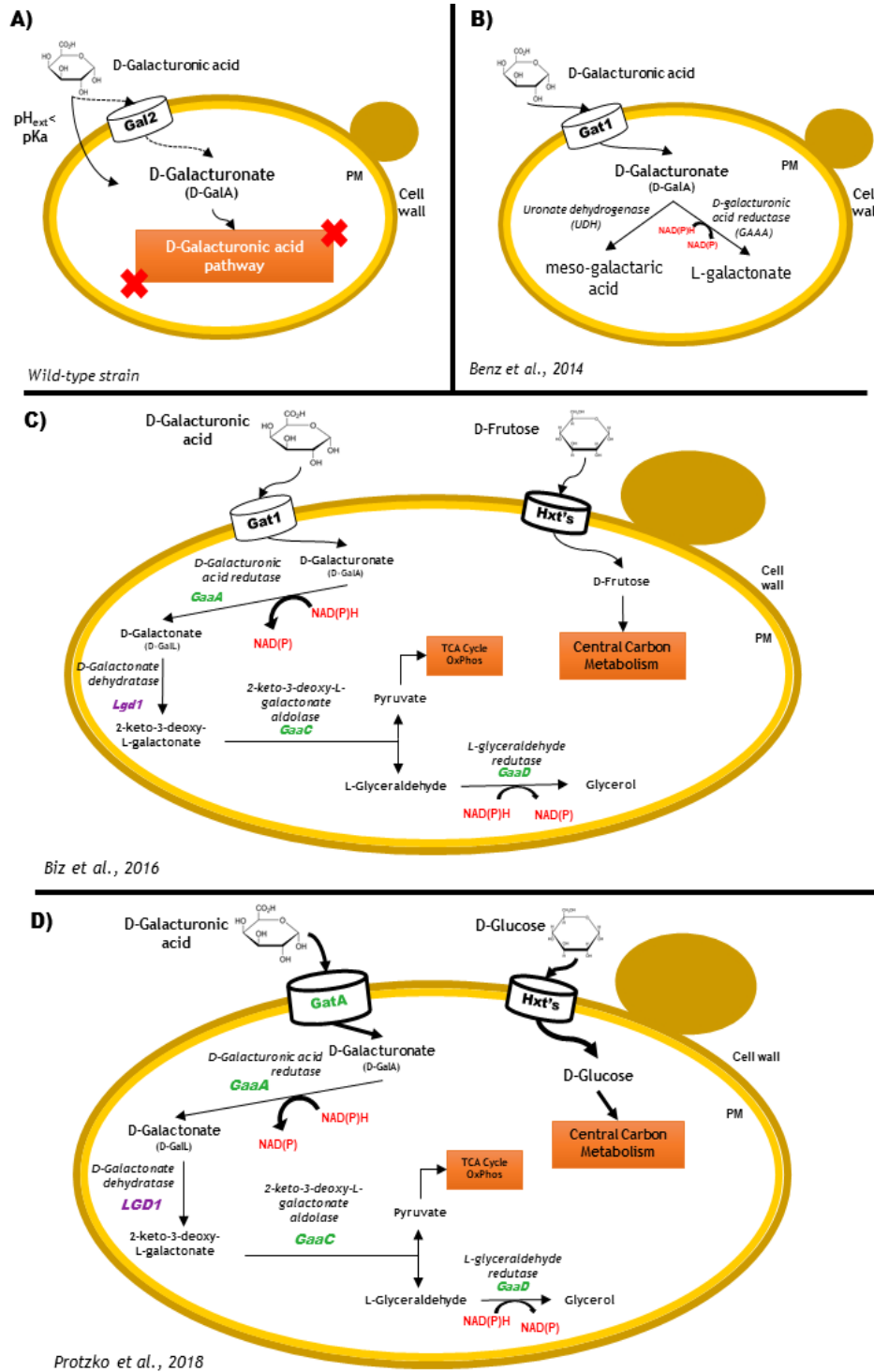


Figure 1.3- Schematic representation of *S. cerevisiae* strains (wild type and genetically engineered with heterologous *D*-galacturonic acid degradation pathways. **A)** *S. cerevisiae* wild-type strain showing the basal natural uptake of *D*-galacturonic acid by Gal2p transporter and passive diffusion of the undissociated form through plasma membrane (PM). **B)** Engineered *S. cerevisiae* strains expressing *D*-GalA membrane transporter Gat1 from *Neurospora crassa* and the uronate dehydrogenase (UDH) from *Agrobacterium tumefaciens* and *D*-galacturonic acid reductase (GAAA) from *Aspergillus niger* to convert *D*-GalA into the metabolites meso-galactaric acid and *L*-galactonate, (Benz et al., 2014). **C)** Engineered *S. cerevisiae* strain with *D*-galacturonic acid plasma membrane transporters from *N. crassa* (GAT1) and enzymes of the *D*-GalA catabolic pathway GaaA, GaaB, GaaC and GaaD from *A. niger* (in green) and LGD1 from *Trichoderma reesei* (in purple); *D*-Fructose was used as co-substrate (Biz et al., 2016). **D)** Engineered *S. cerevisiae* strains with the non-glucose repressible plasma membrane *D*-galacturonic acid transporter GatA from *A. niger* (GATA) and *D*-GalA catabolic pathway as in C); *D*-glucose was used as co-substrate (Protzko et al., 2018).

The oxidative PPP converts D-glucose-6-P into D-ribulose-5-P and CO₂ with the simultaneous reduction reaction of two molecules of NADP to NADPH (**Figure 1.4**) (Wamelink et al. 2008).

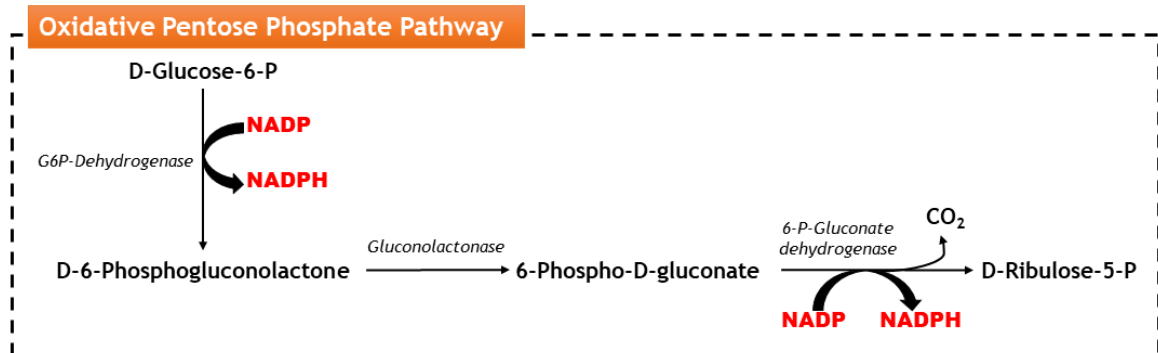


Figure 1. 4- Schematic representation of the oxidative pentose phosphate pathway (Wamelink et al., 2008).

This cofactor regeneration may enable the catabolisation of D-galacturonic acid in engineered *S. cerevisiae* strains. However, the use of co-substrates such as D-fructose or D-glucose is required although their presence leads to the delay of D-galacturonic acid catabolisation (Benz et al. 2014; Biz et al. 2016). The successful heterologous expression of the *A. niger* D-galacturonic acid transporter *GatA* in *S. cerevisiae* allowed the co-uptake of D-galacturonic acid and D-glucose which could also facilitate the regeneration of redox cofactors needed for fully conversion of D-galacturonic acid (**Figure 1.3-D**) (Protzko et al. 2018). A more recent study reported the expression of the efficient previously described fungal D-galacturonic acid catabolic pathway in a pentose-fermenting *S. cerevisiae* strain by the expression of a pentose (D-xylose and L-arabinose) catabolic pathway including genes from *Pichia stipitis* and *Ambrosiozyma monospora*, both natural pentose fermentative yeasts (Jeong et al. 2020). Additionally, the authors made a double deletion from genes *PHO13* (involved in phosphatase regulation) and *ALD6* (a cytosolic aldehyde dehydrogenase required for conversion of acetaldehyde to acetate). All these genetic modifications enabled the co-consumption of more than 10 g/L of D-galacturonic acid with L-arabinose and D-xylose (Ye et al. 2019; Jeong et al. 2020).

The genome-wide and enzymatic analysis of the basidiomycete red oleaginous yeast *Rhodospidium toruloides* (also known as *Rhodotorula toruloides*) IFO 0880, revealed an efficient D-galacturonic acid metabolism, with highly active enzymes (**Figure 1.5**), suggesting this strain as a potential industrial platform for biodiesel and carotenoid biosynthesis from pectin-rich hydrolysates (Sitepu et al. 2014a; Spagnuolo et al. 2019; Protzko et al. 2019). The D-galacturonic acid metabolic pathway of *R. toruloides* was found to be similar to the *T. reesei* pathway, being the catabolic enzymes highly induced by D-galacturonic acid (Protzko et al.

2019). Moreover, *R. toruloides* IFFO 0880 was found to co-utilize D-galacturonic acid in the presence of either D-glucose or D-xylose.

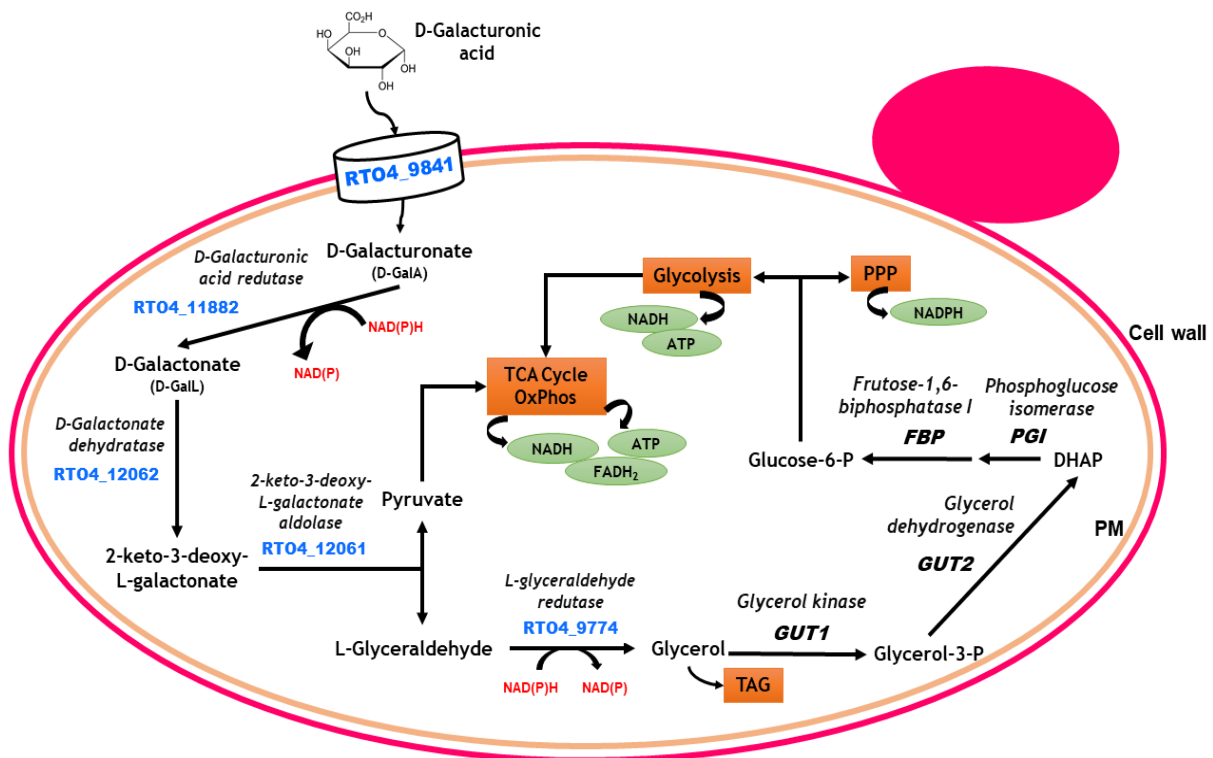


Figure 1. 5- Schematic representation of the D-galacturonic acid catabolic pathway proposed for *Rhodosporidium toruloides* IFFO0880. The genes *GUT1*, *GUT2*, *FBP* and *PGI* belong to central metabolism. *TAG*, triacylglycerol; *PPP*, Pentose Phosphate Pathway (based on (Protzko et al. 2019)).

The final product of D-galacturonic acid catabolic pathway is glycerol that has to be used for cofactor regeneration through the oxidative pentose phosphate pathway. The study performed in *R. toruloides* IFFO 0880 also showed that the genes *GUT1*, encoding a glycerol kinase, and *GUT2*, encoding a mitochondrial glycerol 3-phosphate dehydrogenase, involved in glycerol metabolism and induced in presence of D-galacturonic acid, enabled D-galacturonic acid conversion into glycerol without the need of an additional carbon source. This study proposed that the glycerol produced could be converted into glucose-6-phosphate and, through the oxidative pentose phosphate pathway, the cofactors used in D-galacturonic acid catabolisation would be regenerated (Protzko et al. 2019). Different routes of glycerol catabolic pathways have been described in yeasts, using NAD⁺- or NADP⁺-dependent enzymes, balancing the intracellular redox power and enabling growth in respirable carbon sources (Klein et al. 2017).

1.3.1.2 L-Arabinose metabolism

L-Arabinose is a five-carbon sugar and, unlike other pentoses that naturally occur in the D-form such as D-xylose, L-arabinose is more common than D-arabinose in nature. Arabinose catabolic pathways include the oxidoreductase (fungal) and the isomerase (bacterial) pathways (**Figure 1.6**). In both pathways, L-arabinose is converted into D-xylulose-5-phosphate, which is metabolized by the non-oxidative phase of the pentose phosphate pathway.

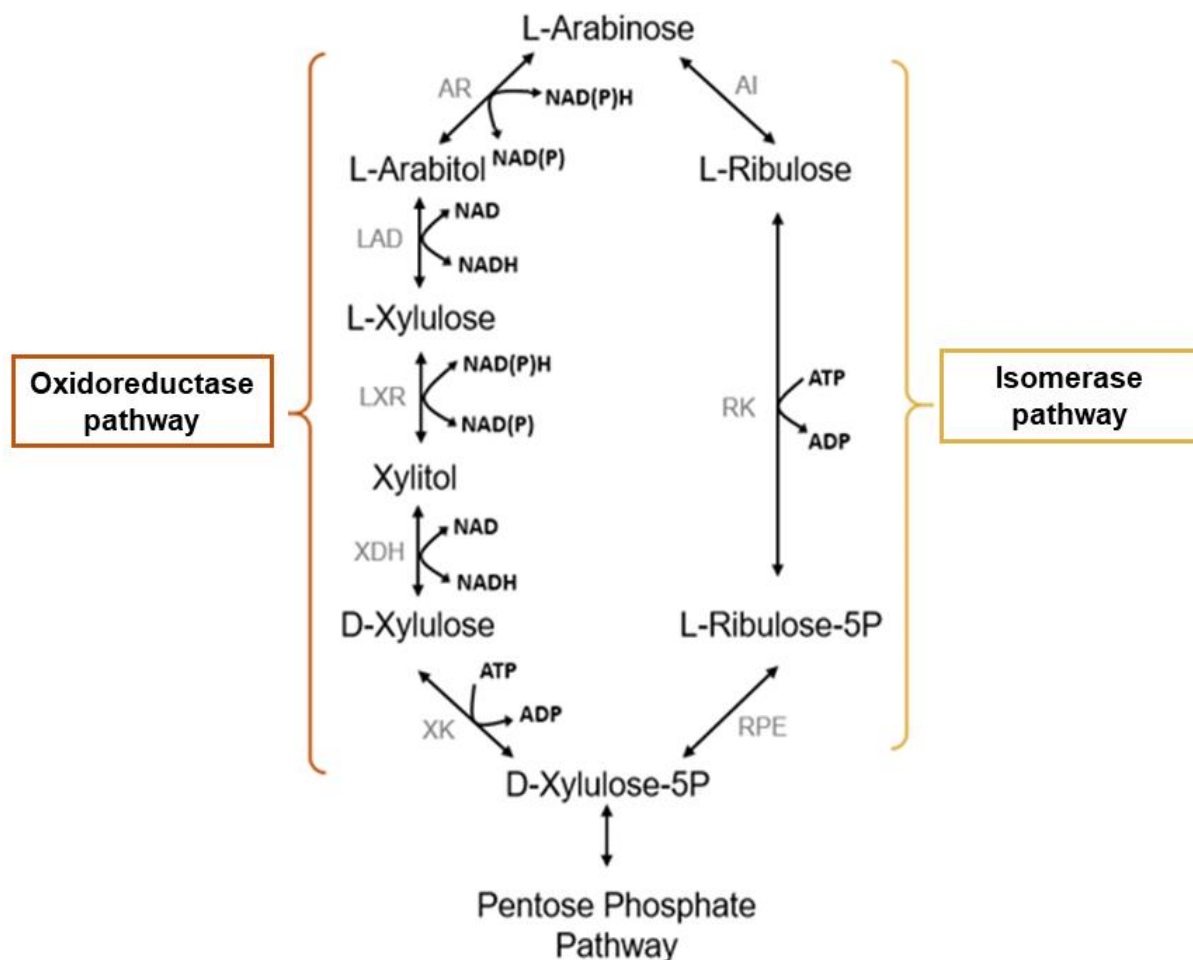


Figure 1. 6- Schematic representation of the initial steps of arabinose metabolism in fungi (the oxidoreductase pathway) or in bacteria (the isomerase pathway). XK, D-xylulose kinase; AI, L-arabinose isomerase; RK, L-ribulokinase; RPE, L-ribulose-5-phosphate 4-epimerase; XDH, xylitol dehydrogenase; AR, L-arabinose reductase; LAD, L-arabitol 4-dehydrogenase; LXR, L-xylulose reductase (adapted from Fonseca et al, 2007).

In the fungal pathway, L-arabinose reductase (AR) prefers NADPH as cofactor, whereas the sugar alcohol dehydrogenases (LAD and XDH) are strictly dependent on NAD (Seiboth and Metz 2011). Under low oxygen conditions, the availability of NAD is limited, which may

cause an accumulation of L-arabitol (Loman et al. 2018). Furthermore, L-arabinose can be converted into xylitol, the common denominator between the catabolic pathways of L-arabinose and D-xylose (**Figure 1.6**). Due to their partially overlapping pathways, there is a strong correlation between the utilization of these two pentoses in yeasts (Seiboth and Metz 2011). The introduction of a reconstructed fungal L-arabinose oxidoreductase pathway (from *T. reesei* and *A. monospora* strains) into *S. cerevisiae*, allowed L-arabinose utilization and the production of substantial amounts of L-arabitol due to the severe redox imbalance resulting from the utilization of NADPH in the reduction step catalysed by L-xylulose reductase (LXR) (Bettiga et al. 2009). In fact, L-xylulose reductase from *A. monospora* is NADH-dependent enzyme, contrarily to most fungi which are NADPH-dependent for this specific enzyme. However, NADH is produced in the oxidation reactions catalysed by L-arabitol-4-dehydrogenase (LAD) and xylitol dehydrogenase (XDH) improving intracellular redox balance (Bettiga et al. 2009).

Although L-arabinose fermentation by yeasts was thought to be unfeasible, several yeast species have been identified as capable of producing ethanol from L-arabinose, in particular *Candida aurangiensis*, *Candida succiphila*, *A. monospora*, *Candida* sp. (YB-2248) (Dien et al. 1996) and *Meyerozyma guilliermondii* (Martini et al. 2016). Moreover, the successful engineering of *S. cerevisiae* to ferment L-arabinose, by expressing the L-arabinose isomerase pathway of the bacterial species of *Lactobacillus plantarum* (**Figure 1.6**) and overexpressing the *S. cerevisiae* genes encoding the enzymes of the nonoxidative pentose phosphate pathway, along with extensive evolutionary engineering, resulted in ethanol production (0.43 g g⁻¹) from L-arabinose during anaerobic growth (Wisselink et al. 2007). To increase L-arabinose fermentation rates, potential L-arabinose transporters have been identified and overexpressed in *S. cerevisiae*. For example, the overexpression of *S. cerevisiae* Gal2 led to the increase of L-arabinose fermentation rate (Becker and Boles 2003). However, this endogenous *S. cerevisiae* hexose transporter not only exhibits very low affinities towards pentoses but is also strongly inhibited by D-glucose (Gao et al. 2019). The expression of heterologous transporters with higher affinities for L-arabinose over D-glucose, in particular of Stp2 from *Arabidopsis thaliana* and AraT from *Scheffersomyces stipitis*, led to the improvement of L-arabinose fermentation, in anaerobiosis, especially at low L-arabinose concentrations. However, L-arabinose uptake through these two transporters is also inhibited by the presence of glucose (Subtil and Boles 2011).

1.3.1.3 D-Xylose metabolism

There are two major metabolic routes to catabolize D-xylose: the oxidoreductase pathway (fungal pathway) and the xylose isomerase (bacterial pathway). D-xylose is reduced to xylitol catalysed by NAD(P)H-dependent xylose reductase. Xylitol is then either secreted from the

cell or oxidized to D-xylulose by NAD-dependent xylitol dehydrogenase. This dual cofactor preference of XR for NAD(P)H and XDH for NAD causes an imbalance of these two cofactors, representing a major bottleneck in this pathway (Agarwal and Singh, 2019; Jagtap and Rao, 2018). Although *S. cerevisiae* genome contains genes encoding D-xylose-metabolizing enzymes, their native expression level is too low to support cell growth when D-xylose is the sole carbon and energy source (Nieves et al., 2015). The overexpression of *S. cerevisiae* hexose transporters encoding genes *HXT7*, *HXT5*, and *GAL2* leads to improved D-xylose uptake (Hamacher et al., 2002). However, these endogenous hexose transporters not only exhibit very low affinities towards pentoses, but D-xylose uptake is also highly inhibited by D-glucose. Heterologous transporters with higher affinities for D-xylose over D-glucose were identified in *Candida intermedia* and *Meyerozyma guilliermondii*, (the Gxs1p and Mgt05196p respectively) and successfully expressed in *S. cerevisiae*, resulting in higher intracellular accumulation of D-xylose in an engineered *S. cerevisiae* strain (Leandro et al., 2006) (C. Wang et al., 2015).

There are non-conventional yeast species capable of fermenting D-xylose to ethanol. Although the tolerance to ethanol of *Scheffersomyces (Pichia) stipitis* is low, this species is considered one of the best D-xylose-fermenting yeast species (Shi et al., 2014). *Ogataea (Hansenula) polymorpha* is a thermotolerant methylotrophic yeast, able to produce ethanol from D-xylose, at higher temperatures (Ryabova et al., 2003). The yeast *Scheffersomyces shehatae* has also been described as a potential ethanol producer from D-xylose, even in low oxygen availability environment (Bideaux et al., 2016). Some *Candida intermedia* strains were also described as D-xylose fermenters (Moreno et al., 2019).

1.3.1.4 D-Glucose and D-galactose metabolism

In yeasts, D-glucose is initially converted through glycolysis into pyruvate, producing 2 molecules of ATP per molecule of D-glucose. Pyruvate can be degraded by either respiration or fermentation pathways. During respiration, pyruvate undergoes the oxidative decarboxylation catalyzed by pyruvate dehydrogenase and is transformed into acetyl-Coenzyme A, which is oxidized in the TCA cycle to CO₂, resulting in a net gain of 36 molecules of ATP per molecule of D-glucose. In alcoholic fermentation, pyruvate is transformed into ethanol, resulting in a net gain of 2 ATP per D-glucose.

D-Galactose is another hexose that, before entering in glycolysis has to be converted into a D-glucose derivative by the enzymes of the Leloir pathway. This pathway is ATP-dependent, and a molecule of D-galactose is converted into glucose-1-phosphate ready to be used in glycolysis (Sellick et al., 2008). D-Glucose and D-galactose are consumed sequentially by wild-

type *S. cerevisiae* strains because the Leloir pathway is repressed by D-glucose (Huisjes et al., 2012).

1.3.1.5 L-Rhamnose metabolism

L-rhamnose can also be found, in low amounts, in hydrolysates from pectin-rich residues. Several bacterial and fungal species are able to use L-rhamnose as carbon and energy source, however wild type strains of *S. cerevisiae* are not able to grow in L-rhamnose as carbon source (Sloothaak et al. 2016). L-rhamnose catabolism occurs by two different pathways: the phosphorylative pathway (present in bacteria) and the non-phosphorylative pathway (present in bacteria and yeasts). In the non-phosphorylative pathway, L-rhamnose is converted into pyruvate and L-lactaldehyde through four metabolic reactions involving L-rhamnose-1-dehydrogenase (RHA1) that catalyses the oxidation of L-rhamnose to L-rhamnono- γ -lactone, a L-rhamnono- γ -lactonase (LRA2) for the conversion of L-rhamnono- γ -lactone to L-rhamnonate, L-rhamnonate dehydratase (LRA3) for the conversion L-rhamnonate to 2-keto-3-deoxy-L-rhamnonate (L-KDR) and a 2-keto-3-deoxy-L-rhamnonate (L-KDR) aldolase (LRA4) for the conversion the 2-keto-3-deoxy intermediate to pyruvate and L-lactaldehyde (Koivistoinen et al. 2012; Khosravi et al. 2017). Genes involved in L-rhamnose catabolism are conserved in *Scheffersomyces stipitis*, *Debaromyces hansenii*, *Candida lusitanae* and *Candida guilliermondii* are arranged in a cluster being upregulated in presence of L-rhamnose (Koivistoinen et al., 2012).

1.4 Toxicity and possible metabolization of compounds likely present in pectin-rich biomass hydrolysates

1.4.1 Multiple chemical stresses likely affecting pectin rich biomass bioconversion

It is likely that pectin-rich residues may include variable levels of toxic compounds. Frequently, their concentrations are not always known or even considered, but these compounds may have a potential combined inhibitory effect for yeast growth and metabolism, acting in conjunction or synergistically. In particular, since pectin structures are acetylated and methyl-esterified in different positions of the D-galacturonic acid molecule, this biomass hydrolysis releases acetic acid and methanol that accumulate in the hydrolysate. The potential role of these compounds both as carbon sources and as toxicants with potential to inhibit yeast growth and fermentation, is discussed below. Other toxic compounds are likely present in

pectin-rich residues. This is the case for heavy metals that in small amounts are essential micronutrients for yeasts but when they reach toxic concentrations induce the generation of reactive oxygen species (ROS) leading to oxidative stress and loss of biological functions (Mukherjee et al. 2017). The pesticides (fungicides, herbicides and insecticides) used in agriculture may also be present in significant amounts, varying among countries although the maximum residual levels allowed are regulated (European Parliament 2009). Other toxic compounds, for instance phenolic compounds and furans, resulting from acid hydrolysis, may also be present (Berlowska et al. 2018). The accumulation of ethanol or other toxic metabolites are additional sources of combined chemical stresses challenging yeast performance during the bioprocess.

1.4.1.1 Acetic acid and D-galacturonic acid as carbon sources and toxic compounds

Acetic acid is present in pectin-rich residues hydrolysates at higher concentrations in sugar beet pulp hydrolysates compared with citrus peel (Grohmann et al. 1999; Günan Yücel and Aksu 2015), as discussed before. Acetic acid is also a yeast metabolite generated during growth and fermentation. Acetic acid is a source of carbon and energy for a large number of yeasts and can be converted into lipids (Huang et al. 2016) (**Figure 1.7**). Most of the yeast species capable of growing in high acetic acid concentrations are oleaginous, since acetate can be assimilated and converted into acetyl-CoA, a lipid biosynthesis precursor (Spagnuolo et al. 2019). At sub-lethal concentrations, acetic acid is catabolized by several yeast species, like *S. cerevisiae*, *Candida utilis*, *Torulaspora delbruecki* and *Dekkera anomala*, its utilization being repressed by D-glucose (Radecka et al. 2015). However, D-glucose and acetic acid are simultaneously catabolized in the highly tolerant *Zygosaccharomyces bailii* species (Rodrigues et al. 2012).

Depending on the level of acetic acid-induced stress and on the tolerance of a specific yeast strain, acetic acid can act as a growth inhibitor due to the ability of the non-dissociated form (pKa 4.7) to diffuse across plasma membrane and cause toxicity when in the cytosol (Mira et al. 2010b; Mira et al. 2011; Palma et al. 2018). The subsequent deprotonation of this acid in the cytosol, with a pH around neutrality, leads to the accumulation of the acetate counter-ion and cytosol acidification (Carmelo et al. 1997). The effect of a specific concentration of acetic acid is particularly drastic at pH below the pKa of the acid. To obtain a holistic view on the toxic effects and the adaptive responses of yeasts to acetic acid, the following review paper is suggested (Palma et al. 2018). The non-conventional food spoilage yeast species *Z. bailii* is able to thrive in acid foods and beverages due to its remarkable

tolerance to weak acids at low pH (Mira et al. 2014; Palma et al. 2017). In fact, *Z. bailii* is able to grow at concentrations of acetic acid 3-fold higher (370-555 mM) than *S. cerevisiae* (80-150 mM) (Palma et al. 2015; Palma et al. 2018). The remarkable tolerance of *Z. bailii* to weak acids has brought to light the potential of this yeast species as an alternative cell factory for the production of high levels of weak acids.

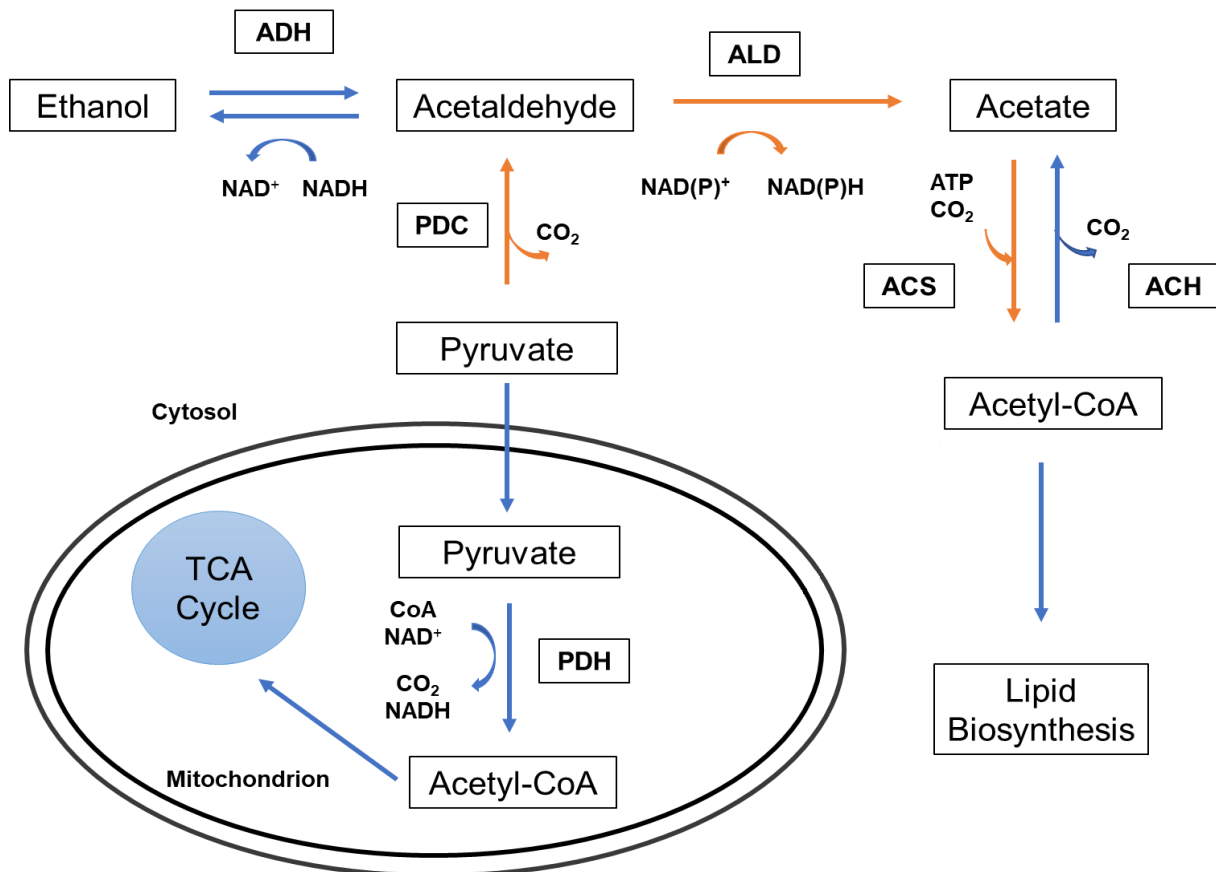


Figure 1. 7- Acetic acid metabolism in yeast. The PDH pathway is indicated by blue arrows, while the PDH bypass is indicated by orange arrows. PDH: pyruvate dehydrogenase; PDC: pyruvate decarboxylase; ALD: aldehyde dehydrogenase; ACS: acetyl-CoA synthetase; ADH: alcohol dehydrogenase (Huang et al. 2016)

Moreover, the understanding of the mechanisms underlying the tolerance to weak acids in *Z. bailii sensu lato* allows the identification of candidate molecular targets for the rational genome engineering for the construction of more robust *S. cerevisiae* strains (Mira et al. 2014; Guerreiro et al. 2016; Palma et al. 2017; Palma and Sá-Correia 2019). Other reported acetic acid tolerant yeast species are: *Pichia kudriavzevii* (Dandi et al. 2013) and *Candida glycerinogenes* (Ji et al. 2016; Zhao et al. 2019). For efficient bioconversion of pectin-rich residues hydrolysates rich in acetic acid, the use of tolerant strains and/or a pH above this weak acid's pKa is required.

The presence of D-galacturonic acid, even at low concentrations (up to 10 g/L) and pH 3.5 (below the pKa of the acid), in a cultivation medium with a mixture of D-glucose, D-galactose, D-xylose and L-arabinose, mimicking pectin-rich residues hydrolysates, was reported to affect the fermentation of most of the sugars with the exception of D-glucose by a genetically engineered pentose-fermenting strain *S. cerevisiae* CEN.PK 113-7D grown under anaerobiosis (Huisjes et al. 2012). However, at pH 5, at which the concentration of the undissociated toxic form is low, sugar fermentation performance was not affected by the presence of D-galacturonic acid (Huisjes et al. 2012).

1.4.1.2 Methanol as carbon source and toxic compound

Methanol is another toxic compound likely present in pectin-rich hydrolysates. Methanol toxicity mechanisms are poorly studied but, like ethanol and other alcohols, the cell membranes are the anticipated molecular targets (van der Klei et al. 2006). Methanol can be converted into formaldehyde which is a more toxic compound (Yasokawa et al. 2010). For *S. cerevisiae*, 1.23 M of methanol or 1.8 mM of formaldehyde, are concentrations reported to inhibit growth without causing cell death (Yasokawa et al. 2010).

Despite *S. cerevisiae* inability to grow in methanol, there are several non-conventional yeasts that can efficiently use it as the sole carbon and energy source. Since methanol is an inexpensive carbon source, methylotrophic yeasts have been examined for biotechnological applications, ranging from the production of single-cell protein (SCP) and heterologous recombinant proteins to the production of number of chemical compounds (Limtong et al. 2008; Johnson 2013b; Siripong et al. 2018). The most well-known methylotrophic yeast species are *Candida boidinii*, *Ogataea (Pichia) methanolica*, *Komagataella (formerly Pichia) pastoris*, *Ogataea minuta* and *Ogataea (formerly Hansenula) polymorpha*, as well as *Candida parapsilosis*, *Candida (formerly Torulopsis) glabrata* and *Ogataea (formerly Pichia) thermomethanolica* (Limtong et al. 2008; Kurtzman and Robnett 2010; Johnson 2013b). The successful genetic modification of *S. cerevisiae* by expressing enzymes from *Pichia pastoris* methanol catabolic pathway (AOX, encoding alcohol oxidases, CAT encoding a catalase, DAS, encoding a dihydroxyacetone synthase, and DAK, encoding a dihydroxyacetone kinase) enabled the consumption by the recombinant *S. cerevisiae* strain of 50% of initial methanol concentration (Dai et al. 2017).

1.4.1.3 Heavy metals and agricultural pesticides as toxic compounds

Heavy metals are essential micronutrients for yeasts. However, when above concentration threshold, they induce the generation of reactive oxygen species (ROS) leading to oxidative stress with the oxidation of proteins, lipids and nucleic acids, thus affecting their biological functions (Mukherjee et al. 2017). In general, pectin can bind different heavy metals depending on their structure and natural environment (following preference: $Pb^{2+} \gg Cu^{2+} > Co^{2+}$ (cobalt) $> Ni^{2+}$ (nickel) $\gg Zn^{2+} > Cd^{2+}$). Sugar beet biomass has preferential affinity for Cu^{2+} and Pb^{2+} (Schiewer and Patil 2008). The tolerance to heavy metals is strain-dependent and the variability is large among strains of the same species to different metals (Balsalobre et al. 2003; Vadkertiová and Sláviková 2006). The pesticides (fungicides, herbicides and insecticides) used in agriculture vary among countries, but the maximum residual levels allowed are regulated in the EU and by FDA. The mechanisms of toxicity and tolerance to agricultural pesticides in yeasts are more poorly studied, although the global effects of the herbicide 2,4-D and the agricultural fungicide mancozeb, among others, have been reported (Teixeira et al. 2007; Dias et al. 2010; dos Santos 2012).

1.4.2 Bioconversion of carbon source mixtures: the challenges

The hydrolysates prepared from pectin-rich residues include a wide range of different carbon-sources (C-sources) at variable concentrations, depending on the type of biomass and their processing conditions, as detailed above. The assimilation of usable C-sources by yeasts is strictly regulated and most of the catabolic pathways are subject to CCR (Simpson-Lavy and Kupiec 2019). This constitutes a major challenge for the efficient and economic utilization of complex substrates in biotechnological processes since in the presence of a preferred sugar, the uptake of secondary carbon sources is inhibited and their sequential utilization prolong the fermentation time. When D-glucose is present in the extracellular medium, the uptake and catabolism of other carbon sources is repressed in *S. cerevisiae*, (Kayikci and Nielsen 2015; Wu et al. 2016; Lane et al. 2018). Strategies for circumventing CCR are especially important when it comes to the use of inexpensive and renewable feedstocks containing mixtures of carbon sources, such as in the case of pectin-rich residues. In fact, the separation of individual substrates is costly and impractical and for this reason, the efficient utilization of substrate mixtures is a necessity that requires additional strain-improvement efforts (Gao et al. 2019). Efforts to enable C-sources co-utilization include the introduction of non-native sugar transporters or catabolic pathways that are not subject to CCR or by adaptive evolution and

targeted genome engineering (Papapetridis et al. 2018). Yeast strains are susceptible to CCR and in the specific case of pectin-rich biomass hydrolysates, the D-glucose present is used at first and D-galactose is expected to be consumed subsequently since the Leloir pathway, through which a molecule of D-galactose is converted into glucose-1-phosphate ready to be used in glycolysis (Sellick et al. 2008), is repressed by D-glucose (Huisjes et al. 2012). In the case of strains capable of using the other less easily metabolised carbon sources, they will be used sequentially. For example, the strain *M. guilliermondii* FTI 20037 was found to have a native ability to catabolise hexose and pentoses, but when cultivated in a mixed-sugars medium, L-arabinose is only consumed when D-glucose and D-xylose are complete depleted from the medium (Mussatto et al. 2006). However, the simultaneous co-consumption of D-glucose, D-xylose, and L-arabinose by *Pseudozyma hubeiensis* IPM1-10 in artificial hydrolysate of lignocellulosic biomass (mixed-sugar medium) was reported leading to the production of high amounts of lipids in less time compared with single-sugar media (Tanimura et al. 2016). Very recently, a pentose-fermenting strain *S. cerevisiae* YE9 expressing the fungal D-galacturonic acid pathway and deleted from *PHO13* and *ALD6* genes (see above), was able to co-consume D-galacturonic acid, L-arabinose and D-xylose (mixed-sugar medium), showing a low susceptibility to catabolic repression (Jeong et al. 2020).

Moreover, D-glucose affects the expression of genes related to other cellular functions such as respiration, gluconeogenesis, and the general stress response mechanisms (Lane et al. 2018). The repression of respiration in glucose-containing environments is known as the “Crabtree effect” (Pfeiffer and Morley 2014). The “Crabtree effect” is observed in *S. cerevisiae* that even under aerobic conditions undergoes alcoholic fermentation when D-glucose is present at non-limiting concentrations (Pfeiffer and Morley 2014). The fermentative, Crabtree-positive yeasts include the genera *Saccharomyces*, *Zygosaccharomyces*, *Dekkera*, and *Schizosaccharomyces* while Crabtree-negative yeasts include strains belonging to the genera *Pichia*, *Debaryomyces*, *Candida* or *Kluyveromyces* (Rozpędowska et al. 2011).

It is important to notice that the use of recombinant yeasts, constructed based on the application of metabolic engineering and synthetic biology tools, has shown that when single substrates are used several limitations to their metabolism may occur, resulting in low yield (Liu et al. 2020). For instance, when the target product has distinct chemical properties or requires long synthetic routes from starting substrates (Babel 2009). The improvement of product biosynthesis through the optimally balance of biosynthetic components can be achieved by the application of mixed substrates, changing flux distribution and cellular resources, instead of intensive genetic modifications (Liu et al. 2020).

1.5 Value-added bioproducts from pectin-rich hydrolysates by non-conventional yeasts

The interest in non-*Saccharomyces* yeasts is gaining momentum due to a variety of important features they possess that are not present in the model yeast *S. cerevisiae* making this large group of yeast species/strains desirable cell factories for the synthesis of a wide-range of added-value products (Radecka et al. 2015). These traits of metabolic versatility and yeast physiology are highly valuable for the biosynthesis of interesting added-value compounds from pectin-rich residues hydrolysates (Wagner and Alper 2016; Rebello et al. 2018). A significant genetic distance is observed in the phylogenetic tree prepared for yeasts exhibiting different capacities to catabolise pentoses (among the ascomycetous yeasts) or D-galacturonic acid (basidiomycetous yeasts, close to filamentous fungi with a similar metabolic trait) (Figure 1.8).

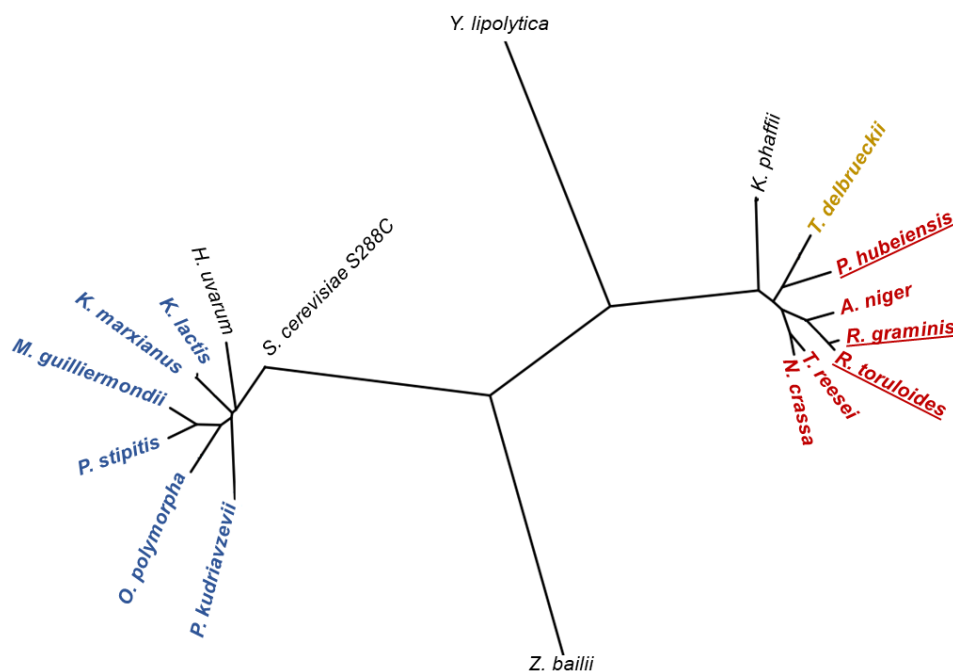


Figure 1. 8-Phylogenetic tree of relevant yeasts and related filamentous fungi discussed in this work. The tree was constructed using the neighbour-joining method based on the alignment of the large subunit (26S) ribosomal DNA sequence. The sequences used were obtained from "EnsemblFungi" database. The yeasts coloured with blue (the Ascomycetous yeasts *Kluyveromyces marxianus*, *Kluyveromyces lactis*, *Meyerozyma guilliermondii*, *Pichia stipitis*, *Ogataea polymorpha* and *Pichia kudriavzevii*) are capable of utilizing D-xylose and L-arabinose as carbon sources (C-sources). In red colour are represented basidiomycetous yeasts (underlined), such as *Rhodospordium toruloides*, *Rhodotorula graminis* and *Pseudozyma hubeiensis* and filamentous fungi (*Trichoderma reesei*, *Aspergillus niger* and *Neurospora crassa*) which are able to grow in D-galacturonic acid and also in D-xylose and L-arabinose. The yeast species *Torulasporea delbrueckii* represented in yellow is capable to grow in D-galacturonic acid and D-xylose. The phylogenetic tree also includes (black colour) *Saccharomyces cerevisiae* S288C, *Zygosaccharomyces bailii*, *Yarrowia lipolytica* and *Komagataella phaffii*. The yeast species *S. cerevisiae* *K. marxianus*, *M. guilliermondii*, *P. stipitis*, *P. kudriavzevii* and *T. delbrueckii* are interesting bioethanol producers, while *H. uvarum* is also responsible for the fruity-like aromatic compounds in fermented beverages. *Y. lipolytica*, *P. hubeiensis*, *R. graminis* and *R. toruloides* are oleaginous yeasts which can convert C-sources into high concentrations and a wide range of lipids. The species *K. phaffii* is mainly used as cell factory for heterologous protein expression while *Z. bailii* exhibits a remarkable tolerance to weak acids.

Although several non-conventional yeasts with potential for the bioconversion of pectin-rich wastes have received the “generally recognized as safe” (GRAS) label from FDA (Food and Drug Administration), there are several interesting species that are, unfortunately, reported opportunistic pathogens (Wirth and Goldani 2012; Johnson 2013a). The genera *Cryptococcus*, *Candida* and *Rhodotorula* are some of those encompassing pathogenic species, such as *Cryptococcus neoformans* and *Cryptococcus gatii* (Johnson 2013a) as well as *Rhodotorula mucilaginosa*, *Rhodotorula glutinis*, and *Rhodotorula minuta* (Wirth and Goldani 2012). However, the potential of some of them to produce interesting metabolites is high and therefore they are potential sources of genetic information for the engineering of GRAS species.

There is a wide range of products synthesized by different non-conventional yeast species using pectin-rich substrates that have been reported in the literature. A summary of these examples is shown in **Table 1.3**. Most of the bioethanol in the market is produced from hexose fermentation by the yeast *S. cerevisiae*, namely from D-glucose and D-fructose. However, several yeast species are also able to ferment other sugars present in pectin-rich residues and were reported as bioethanol producers from that biomass. This is the case for strains of *K. marxianus* (Serrat et al. 2004), *M. guilliermondii* (Schirmer-Michel et al. 2008; Schirmer-Michel et al. 2009), *Scheffersomyces (Pichia) stipitis* (Günan Yücel and Aksu 2015), *P. kudriavzevii* (Kaur Sandhu et al. 2012), *Hanseniaspora uvarum* and *Hanseniaspora valbyensis* (Rodríguez Madrera et al. 2015).

H. uvarum and *H. valbyensis* strains produce volatile fruity-like aroma compounds, with high acetic acid esters content, from apple pomace (Rodríguez Madrera et al. 2015). These volatile or non-volatile aromatic compounds are very valuable ingredients in chemical, food, cosmetic and pharmaceutical industries (Martínez et al. 2017) and comprise 25% (aroma compounds) of global market of food additives (Rodríguez Madrera et al. 2015).

Single-cell oil and lipids, namely fatty acids, are obtained from oleaginous yeasts, for utilization as substitutes for vegetable oils and animal and vegetal fats (e.g. as cocoa butter) (Wang et al. 2012). The demand for biobased-fuels to replace fossil-based-products has led to an increase of biodiesel production and other oleochemical products from oleaginous yeasts (Wang et al. 2012; Anschau 2017). Yeast species, such as, *Y. lipolytica*, *Trichosporon cutaneum*, *Trichosporon fermentans* and *Cryptococcus curvatus* were reported as yeast-platforms to produce different levels of fatty acids from pectin-residues. Remarkably, *C. curvatus* can convert acetate (5 g/L, at pH 6.0) into oils (up to 50% (w/w) of lipid accumulation in the biomass) (Christophe et al. 2012) and *Rhodospiridium toruloides* can convert 20 g/L of acetic acid (at pH 6.0) in lipids up to 48%(w/w) of the biomass (Huang et al. 2016). *R. toruloides* lipids are mainly triacylglycerols (C₁₆ and C₁₈ fatty acids) (Singh et al. 2018) and the dried cellular biomass can be directly converted into biodiesel (Guo et al. 2019). A recent study conducted with 18 strains of oleaginous yeasts also reported the accumulation of lipids in *R.*

toruloides NRRL 1091 and *Cryptococcus laurentii* UCD 68-201 (77 and 47% on a dry matter basis, respectively) from orange peel extract (Carota et al. 2020).

Table 1. 3- Reported examples of bioconversion of pectin-rich residues by non-conventional yeasts

Yeast	Pectin-rich residues	Initial sugar concentration	Bioproducts (final concentration or yield)	References
		(of total sugars in hydrolysate)		
<i>Scheffersomyces (Pichia) stipitis</i> NRRL Y-7124	Sugar beet pulp hydrolysate	75 g/L	Ethanol (37.1 g/L)	(Günan Yücel and Aksu 2015)
<i>Pichia kudriavzevii</i> KVMP10	Kinnow mandarin peels hydrolysate	79 g/L	Ethanol (34g/L)	(Kaur Sandhu et al. 2012)
	Orange peel hydrolysate	101 g/L	Ethanol (54g/L)	(Koutinas et al. 2016)
<i>Candida parapsilosis</i> IFM 48375	Orange peel hydrolysate	-	Ethanol (0.85 g EtOH/ 4.2g of dry matter of orange peel)	(Tsukamoto et al. 2013)
<i>Candida parapsilosis</i> NRRL Y-12969	Orange peel hydrolysate	-	Ethanol (0.76 g EtOH/ 4.2 of dry matter of orange peel)	(Tsukamoto et al. 2013)
<i>Hanseniaspora uvarum</i> H.u. 283	Apple pomace hydrolysate	36 g/Kg of apple pomace	Ethanol (2.8% (w/w) of reducing sugars)	(Rodríguez Madrera et al. 2015)
			Volatile fruity-like aroma compounds (esters and γ -nonalactone)	
<i>Hanseniaspora valbyensis</i> H.v. 43	Apple pomace hydrolysate	36 g/Kg of apple pomace	Ethanol (2.8% (w/w) of reducing sugars)	(Rodríguez Madrera et al. 2015)
			Volatile fruity-like aroma compounds (esters and γ -nonalactone)	
<i>Yarrowia lipolytica</i> MYA-2613	Apple pomace hydrolysate	80 g/L	Lipids (25.8 g/L) (C16:0; C18:0; C18:1 C20:0)	(Liu et al. 2019)
<i>Trichosporon cutaneum</i> AS 2.571	Beet pulp hydrolysate	52 g/L	Lipids (7.2 g/L) (Palmitic; Stearic; Oleic, Linolenic)	(Wang et al., 2015)
<i>Trichosporon fermentans</i> CICC 1368	Beet pulp hydrolysate	52 g/L	Lipids (5.8 g/L) (Palmitic; Stearic; Oleic, Linolenic)	(Wang et al., 2015)
<i>Cryptococcus curvatus</i> ATCC 20509	Beet pulp hydrolysate	52 g/L	Lipids (6.9 g/L) (Palmitic; Stearic; Oleic, Linolenic)	(Wang et al., 2015)
<i>Rhodospiridium toruloides</i> NRRL1091	Orange peel waste	18 g/L	Lipids (5.8 g/L)	(Carota et al. 2020)
			(Palmitic; Oleic)	

<i>Cryptococcus laurentii</i> UCD 68-201	Orange peel waste	18 g/L	Lipids (4.5 g/L) (Palmitic; Oleic)	
<i>Rhodotorula</i> sp.	Apple pomace hydrolysate	40 g/L	Carotenoids (16.8 mg/100 g DCW)	(Joshi et al. 2013)
<i>Trichosporon penicillatum</i> SNO-3	Citrus peel hydrolysate (Citrus unshiu)	23.2 % (w/w)	Protopectin-solubilizing enzyme	(Sakai and Okushima 1980)
<i>Torula (Candida) utilis</i> CCT3469	Apple pomace hydrolysate	15 % (w/w)	Lignocellulosic enzymes: Pectinase (25µg/mL), manganese-dependent peroxidase (2.5µg/mL), cellulase and xylanase (<1µg/mL)	(Villas-Bôas et al. 2002)
<i>Torula (Candida) utilis</i> DSM 70163		45 g/L	Single cell protein (43% g protein /g sugar consumed)	(Nigam and Vogel 1991)
<i>Candida tropicalis</i> DSM 70 15	Sugar beet pulp hydrolysate	45 g/L	Single cell protein (39% g protein /g sugar consumed)	(Nigam and Vogel 1991)
<i>Candida parapsilosis</i> DSM 70125		45 g/L	Single cell protein (34% g protein /g sugar consumed)	(Nigam and Vogel 1991)
<i>Candida solani</i> ATCC 14440		45 g/L	Single cell protein (35% g protein /g sugar consumed)	(Nigam and Vogel 1991)

A *Rhodotorula* sp. strain, isolated from spoiled sauerkraut, was reported to grow and produce carotenoids from 50 g/L apple pomace, but the addition of 0.3% (v/v) ferrous ammonium sulphate led to the highest carotenoid concentration (Joshi et al. 2013). Oleaginous yeasts were identified as capable of growing in medium containing only D-galacturonic acid as carbon source. This is the case of the species *C. laurentii*, *C. curvatus*, *Cryptococcus* cf. *aureus*, *Cryptococcus ramirezgomezianus*, *Leucosporidiella creatinivora*, *Tremella encephala*, *Geotrichum fermentans*, *R. mucilaginosa*, *Trichosporon dermatis* and *Trigonopsis variabilis* which exhibit relevant genetic information related with D-galacturonic acid metabolic pathway for alternative expression in *S. cerevisiae* (Sitepu et al. 2014a).

The production of enzymes from agro-industrial residues by yeasts is still one of the most relevant applications for these substrates, in particular for the production of pectinases (Vendruscolo et al. 2008). Single cell protein (SCP) or yeast components can easily be produced from several agro-industrial wastes, and are extremely useful for food and feed nutritional enrichment (Vendruscolo et al. 2008; Johnson and Echavarri-Erasun 2011). *Torula utilis*, *Candida tropicalis*, *Candida parapsilosis* and *Candida solani* are sources of SCP from sugar beet pulp (Nigam and Vogel 1991).

1.6 Metabolic engineering of non-conventional yeasts with potential for the bioconversion of pectin-rich residues

The application of metabolic engineering strategies to non-conventional yeasts envisages the resolution of the problems discussed in previous sections, in particular the co-utilization of different carbon sources, the enhancement of the tolerance to the inhibitors commonly present in the hydrolysates and other bioprocess-related stresses, and the improvement of, or the production of, novel bioproducts. However, the metabolic engineering of non-conventional yeasts faces several challenges such as the reduced availability of stable and high copy number plasmids and suitable approaches for foreign DNA integration into the host's genome (Löbs et al. 2017). For industrial bioprocesses, metabolic engineering requires genomic integration of genetic information for high stability of the expression cassette over extended cultivations, homogenous expression levels in cell population and the elimination of the selective marker (Löbs et al. 2017). Currently, there are several genome editing tools already available for metabolic engineering of non-conventional yeasts (Gupta and Shukla 2017). The CRISPR technology is allowing gene disruptions and integrations in several yeast species, such as *Kluyveromyces lactis*, *K. marxianus*, *S. stipitis*, *Y. lipolytica*, *Hansenula polymorpha* and *P. pastoris* (Weninger et al. 2015; Gao et al. 2016; Löbs et al. 2017; Raschmanová et al. 2018; Nurcholis et al. 2020). The perspectives of the metabolic engineering of non-conventional yeasts more suited to industrial bioprocesses are encouraging, supported by the increased availability of genome sequences obtained by next generation sequencing and the development and availability of genome editing and bioinformatic tools. Among them is the YEASTRACT+ database that also provides biological information and tools for the analysis and prediction of transcription regulatory associations at the gene and genomic levels in non-conventional yeasts of biotechnological interest, in particular *Z. baillii*, *K. lactis*, *K. marxianus*, *Y. lipolytica* and *K. phaffii* (Monteiro et al. 2020). These developments are paradigmatic examples that the exploitation of non-*Saccharomyces* yeasts is gaining momentum.

From the already significant number of examples of metabolic engineering of yeasts for biomass bioconversion, only a few examples of potential interest for the bioconversion of pectin-rich biomass were reported. Oleaginous yeasts are being intensively studied due to their native mechanisms to convert carbon sources into neutral lipids and lipid-derived compounds. For example, the triacylglyceride pathway was engineered into *Y. lipolytica* by introducing a synthetic pathway that enhances glycolysis activity with an improvement in glycolytic NADH and an increase of approximately 25% of lipid biosynthesis from D-glucose (Qiao et al. 2017). Tools for the genetic engineering of the oleaginous yeast species *R. toruloides* to improve the production of carotenoids and lipids were recently developed (Park

et al. 2018). The metabolic engineering of *K. lactis* by the construction of a null mutant in a single gene encoding a mitochondrial alternative internal dehydrogenase, led to a metabolic shift from respiration to fermentation, increasing the rate of ethanol production (González-Siso et al. 2015). In *K. marxianus*, the simultaneous knockdown of the TCA cycle and the electron transport chain genes *ACO2b*, *SDH2*, *RIP1*, and *MSS51*, resulted in a 3.8-fold increase in ethyl acetate productivity from D-glucose (Löbs et al. 2018). The examples of genetic manipulation of non-conventional yeasts for sugar transporters are not many but the heterologous integration of the xylose transporter gene *AT5G17010* from *A. thaliana* into *C. tropicalis* resulted in a 37–73% increase in xylose uptake compared to the original strain (Jeon et al. 2013). Given that synthetic biology methods and tools are being adapted to be used in non-conventional yeasts, the construction of engineered strains with specific traits for the more efficient bioconversion of pectin-rich agro-industrial residues can be anticipated.

1.7 Concluding remarks

The valorisation of pectin-rich residues resulting from the industrial processing of fruits and vegetables for the production of value-added compounds by non-conventional yeast species is gaining momentum. The challenges posed to the industrial implementation of efficient bioprocesses are however many and thoroughly discussed in this review paper. The challenges encountered, at the biological level, range from the simultaneous effective metabolisation of C-source mixtures present in pectin-rich residues hydrolysates and the required increase of yeast robustness to cope with the multiple potential stresses encountered during specific bioprocesses, to the improvement of production of interesting and novel metabolites.

2. The Identification of Genetic Determinants of Methanol Tolerance in Yeast Suggests Differences in Methanol and Ethanol Toxicity Mechanisms and Candidates for Improved Methanol Tolerance Engineering

This Chapter is published in:

Mota M.N., **Martins L.C.**, Sá-Correia I., (2021) *The Identification of Genetic Determinants of Methanol Tolerance in Yeast Suggests Differences in Methanol and Ethanol Toxicity Mechanisms and Candidates for Improved Methanol Tolerance Engineering. Journal of Fungi*; 7(2):90.

2.1 ABSTRACT

Methanol is a promising feedstock for metabolically competent yeast strains-based biorefineries. However, methanol toxicity can limit the productivity of these bioprocesses. Therefore, the identification of genes whose expression is required for maximum methanol tolerance is important for mechanistic insights and for rational genomic manipulation to obtain more robust methylotrophic yeast strains. The present chemogenomic analysis was performed with this objective based on the screening of the Euroscarf *Saccharomyces cerevisiae* haploid deletion mutant collection to search for susceptibility phenotypes in YPD medium supplemented with 8% (v/v) methanol, at 35°C, compared with an equivalent ethanol concentration [5.5% (v/v)]. Around 400 methanol tolerance determinants were identified, 81 showing a marked phenotype. The clustering of the identified tolerance genes indicates an enrichment of functional categories in the methanol dataset not enriched in the ethanol dataset, such as chromatin remodeling, DNA repair and fatty acid biosynthesis. Several genes involved in DNA repair (eight *RAD* genes), identified as specific for methanol toxicity, were previously reported as tolerance determinants for formaldehyde, a methanol detoxification pathway intermediate. This study provides new valuable information on genes and potential regulatory networks involved in overcoming methanol toxicity. This knowledge is an important starting point for the improvement of methanol tolerance in yeasts capable of catabolizing and copying with methanol concentrations present in promising bioeconomy feedstocks, including industrial residues.

2.2 INTRODUCTION

Methanol is a promising feedstock alternative to sugar-based raw materials for the bioproduction of fuels, specialty chemicals, polymers, and other value-added products due to its abundance and relatively low cost (Zhang et al. 2018; Fabarius et al. 2020; Frazão and Walther 2020; Zhu et al. 2020). Methanol is also the major impurity in crude glycerol, reaching relatively high levels that can vary considerably from batch to batch and, although it can be removed by evaporation, this process is energy demanding (Chen and Liu 2016; Vartiainen et al. 2019). Therefore, the utilization of methanol as co-substrate by methanol-tolerant methylotrophic yeasts would increase the feasibility of bioprocesses that use crude glycerol as substrate (Vartiainen et al. 2019). Methanol is also present, in relatively low concentrations, in hydrolysates from pectin-rich agro-industrial residues given that the D-galacturonic acid monomers are methyl-esterified in different positions (Yapo et al. 2007; Müller-maatsch et al. 2016; Martins et al. 2020). Differently from methylotrophic yeast species, the preferred yeast cell factory *Saccharomyces cerevisiae*, is not able to use methanol as sole carbon source but there are successful examples of *S. cerevisiae* metabolic engineering for direct methanol utilization (Dai et al. 2017b; Duan et al. 2018; Zhu et al. 2020). Although being a promising carbon source for metabolically competent yeast strains, methanol toxicity can limit the productivity of methanol-based biomanufacturing (Fabarius et al. 2020). For this reason, the identification of genes/proteins whose expression is required for maximum tolerance to methanol in the model yeast species *S. cerevisiae* is important for enlightening the mechanisms underlying methanol toxicity in methylotrophic yeasts and in other eukaryotes as well as for guiding the development of more robust yeast strains, in particular methylotrophic yeast strains (Fabarius et al. 2020). Genome-wide approaches have been enabling a holistic view and a deeper understanding of the molecular mechanisms and signaling pathways involved in the global response and adaptation of yeasts to sublethal concentrations of toxicants by allowing the identification of genes and pathways involved in the toxicological response and required for maximum tolerance (dos Santos et al. 2012; dos Santos and Sá-Correia 2015). The genome-wide identification of genes that are determinants of tolerance to methanol is a first step to allow the improvement of yeast robustness and the objective of the present study. Such chemogenomic analysis, using a *S. cerevisiae* deletion mutant collection, has been explored before to identify genes required for maximum tolerance to a variety of relevant chemical stresses including compounds of biotechnological, agronomical and pharmaceutical interest (dos Santos et al. 2012; dos Santos and Sá-Correia 2015).

The methanol detoxification pathway in *S. cerevisiae* involves two reactions: (i) the oxidation of methanol to formaldehyde carried out by alcohol dehydrogenases and (ii) the oxidation of formaldehyde to formic acid catalyzed by an aldehyde dehydrogenase (Yasokawa

et al. 2010). The genome-wide response of yeast to methanol, based on transcriptomic analyses, was reported in two studies suggesting that the major cellular targets for methanol and formaldehyde toxicity are membrane structure and proteins, respectively (Yasokawa et al. 2010) and that the response to methanol also includes the up-regulation of genes of mitochondrial and peroxisomal metabolism, alcohol and formate dehydrogenation, glutathione metabolism, at different levels, depending on yeast strain (Espinosa et al. 2019). The screening of the same yeast deletion mutant collection used in our study was carried out for the identification of formaldehyde tolerance determinants (de Graaf et al. 2009; North et al. 2016). Among them, DNA repair mechanisms were found to underlie formaldehyde tolerance, consistent with the alkylating activity of this compound (de Graaf et al. 2009; North et al. 2016). Concerning formic acid, produced in the last step of methanol detoxification in yeast (Yasokawa et al. 2010), another chemogenomic analysis performed in our lab, indicated an enrichment of tolerance genes involved in intracellular trafficking and protein synthesis, cell wall and cytoskeleton organization, carbohydrate metabolism, lipid, amino acid and vitamin metabolism, response to stress, chromatin remodeling, transcription and internal pH homeostasis (Henriques et al. 2017). This study also confirmed the involvement of the Haa1 transcription factor and the Haa1-regulon in tolerance to formic acid (Henriques et al. 2017), as described for acetic acid (Mira et al. 2010a).

Although the available studies on the determinants and signaling pathways involved in yeast tolerance to methanol are scarce, several reports on tolerance to ethanol toxicity are available, in particular at the genome-wide level (Kubota et al. 2004; van Voorst et al. 2006; Auesukaree et al. 2009; Teixeira et al. 2009; Auesukaree 2017). Due to the structural similarity of these short chain alcohols, the knowledge gathered for ethanol can be useful to understand methanol toxicity and tolerance in yeast. The screening of the yeast disruptome carried out in our laboratory for ethanol, using the same experimental methodology applied in the present work for methanol, identified, as enriched in the obtained dataset, the following genes/gene functions as required for maximum ethanol tolerance: genes associated with intracellular organization, biogenesis, and transport regarding the vacuole, the peroxisome, the endosome, and the cytoskeleton and the transcriptional machinery (Teixeira et al. 2009). The clustering of the encoded proteins, based on their known physical and genetic interactions, highlighted the importance of the vacuolar protein sorting machinery, the vacuolar H⁽⁺⁾-ATPase (V-ATPase) complex, and the peroxisome protein import machinery (Teixeira et al. 2009). Several plasma-membrane H⁽⁺⁾-ATPase and vacuolar H⁽⁺⁾-ATPase (V-ATPase) genes which are essential for maintaining the intracellular pH at physiological values (Rosa and Sá-Correia 1991; Monteiro and Sá-Correia 1998; Ogawa et al. 2000; Aguilera et al. 2006), were also found in other genome-wide screenings as ethanol tolerance determinants (Kubota et al. 2004; van Voorst et al. 2006; Auesukaree et al. 2009; Teixeira et al. 2009; Yoshikawa et al. 2009). As a lipophilic

agent, ethanol leads to the perturbation of plasma membrane lipid organization and consequently to the increase of its non-specific permeability, disrupting membrane biological function as a matrix for proteins and thus affecting their activity (Salgueiro et al. 1988; Stanley et al. 2010). Alterations of plasma membrane lipid composition is among the responses of the yeast cell considered useful to counteract those perturbations, namely at the level of the content and composition of ergosterol and unsaturated fatty acids (Chi and Arneborg 1999; You et al. 2003; Aguilera et al. 2006). Peroxisomal function is also responsible for yeast tolerance to ethanol what can be linked with phospholipid biosynthesis since cells with abnormal peroxisomal function are unable to regulate the composition of membrane phospholipids, compromising membrane remodeling to overcome ethanol-induced stress (Teixeira et al. 2009; Yoshikawa et al. 2009).

The first goal of the present study was to get insights into the global mechanisms underlying methanol toxicity through the identification of tolerance determinant genes by screening the entire Euroscarf haploid deletion mutant collection grown in YPD medium supplemented with 8% (v/v) methanol at 35°C. This chemogenomic analysis was extended to an equivalent growth inhibitory concentration of ethanol of 5.5% (v/v) performed under identical experimental conditions to compare the mechanisms underlying methanol and ethanol toxicity and tolerance. This was considered essential because the various available genome-wide studies that allowed the identification of genetic determinants of ethanol tolerance were performed under different experimental conditions: in rich medium with ethanol concentrations of 7 % (v/v) (van Voorst et al. 2006), 10 % (v/v) (Fujita et al. 2006; Auesukaree et al. 2009) and 11 % (v/v) (Kubota et al. 2004) and in minimal medium supplemented with 8 % (v/v) ethanol (Teixeira et al. 2009). Moreover, the criteria applied in those studies to identify genes that when deleted lead to an ethanol susceptibility phenotype varied. The results obtained in the present work indicate that, despite the similarities identified for a vast number of genetic determinants of tolerance to these two alcohols, DNA repair and membrane remodeling are among the more specific responses to counteract methanol toxicity. Results from this genome-wide search for genes that confer tolerance to methanol in *S. cerevisiae* can now be explored for the rational genetic manipulation of yeasts to obtain more robust strains capable to cope with stressing methanol concentrations, in particular of methylotrophic yeasts.

2.3 MATERIALS AND METHODS

2.3.1 Strains and Growth Media

The haploid parental strain *S. cerevisiae* BY4741 (MATa, his3 Δ 1, leu2 Δ 0, met15 Δ 0, ura3 Δ 0) and the collection of derived single deletion mutants were obtained from Euroscarf (Frankfurt, Germany). The screening of this collection and the growth curves shown were carried out in YPD medium containing, per liter, 2% (w/v) D-glucose (Merck, Darmstadt, Germany), 2% (w/v) yeast extract and 1% (w/v) peptone, both from BD Biosciences (Franklin Lakes, NJ, United States) acidified with HCl until pH 4.5. Solid media were prepared by addition of 2% (w/v) agar (Iberagar, Barreiro, Portugal).

2.3.2 Genome-Wide Search for Yeast Determinants of Methanol or Ethanol Tolerance

To select the alcohol concentrations to be used for the disruptome assays, the parental strain *S. cerevisiae* BY4741 was tested for susceptibility to a range of methanol or ethanol concentrations. For that, yeast cells were cultivated for 10 hours in liquid YPD medium, followed by the inoculation in fresh liquid YPD medium (pH 4.5) and growth to a standardized OD_{600nm} of 0.5 ± 0.05 . These exponentially growing culture was used to inoculate fresh liquid YPD medium (pH 4.5) supplemented with increasing alcohol concentrations (Merck, Darmstadt, Germany) at 35 °C, in 96-wells plates. Growth was followed for 36 hours using a microplate reader set at OD_{595nm} (FilterMax F5 Microplate Reader; Molecular Devices).

Based on the results of the above referred first screening, the entire BY4741 Euroscarf deletion mutant collection was screened for susceptibility to the selected concentrations of 8% (v/v) methanol or to 5.5% (v/v) ethanol, at 35 °C, in YPD medium (pH 4.5). For that, the parental and deletion mutant strains were cultivated for 16 hours in YPD medium at 30 °C with 250 rpm orbital agitation, in 96-well plates. Using a 96-pin replica platter, the cell suspensions were spotted onto the surface of YPD solid medium supplemented, or not, with 8% (v/v) methanol or 5.5% (v/v) ethanol and incubated at 35 °C. Photographs were taken after 24 hours of incubation for control plates (YPD medium) or 36–48 hours in the presence of the alcohols.

When observed, the susceptibility phenotype of each single deletion mutant was scored as (+) if the mutant strain showed, compared with the parental strain, a slight growth inhibition after the standardized incubation time, (++) if the growth was moderately inhibited compared

to the parental strain, and (+++) if no growth was observed after 48h of incubation (**Figure 2.1**).

The eventual over- or under- representation of Gene Ontology (GO) biological process terms related with the physiological function of the genes found to be required for maximum tolerance to methanol was determined using the PANTHER Classification System (<http://pantherdb.org>); over-representation of functional categories was considered significant for a p-value < 0.05 and this analysis was complemented using the information available at Saccharomyces Genome Database (SGD) (<http://www.yeastgenome.org>).

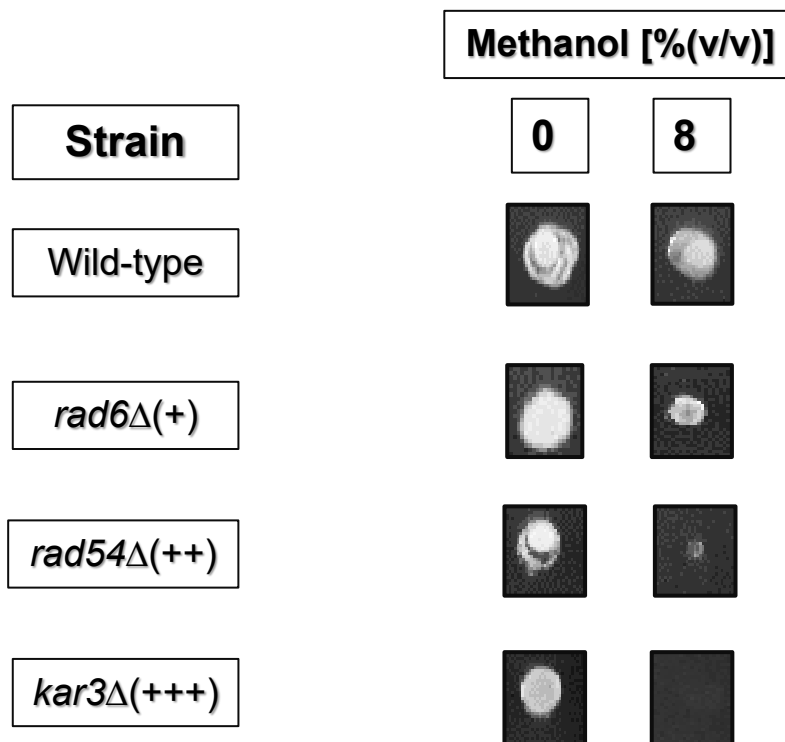


Figure 2. 1- Visual description of the criteria used to define the different levels of susceptibility to methanol of the deletion mutant strains tested. Wild-type and deletion mutant strains were spotted onto solid YPD medium (pH 4.5) supplemented with 8%(v/v) of methanol. Three levels of susceptibility were defined when the growth of the single mutant strains was slightly diminished compared to wild type (+), significantly reduced (++), or abolished (+++).

2.3.3 Growth Curves of Selected Deletion Mutants under Methanol-Induced Stress

The susceptibility of the parental strain and selected deletion mutants was compared in liquid YPD medium in Erlenmeyer flasks or onto solid YPD medium in Petri dishes, both at pH 4.5.

For the spot assays in solid YPD medium, exponentially-growing yeast cell suspensions (OD_{600nm} of 0.5 ± 0.05) were diluted to an OD_{600nm} of 0.25 ± 0.005 and this suspension was

used to prepare 1:5, 1:25, 1:125, and 1:625 serially diluted suspensions. Four microliters of each cell suspension were spotted onto YPD solid medium either or not supplemented with increasing concentrations of methanol (0, 8, 10, 12, or 14% (v/v)). Susceptibility phenotypes were observed after 48 hours of incubation at 35 °C.

For susceptibility to methanol testing by growth in liquid YPD medium, a mid-exponential cell suspension was used to inoculate 50 mL of YPD medium (pH 4.5) in 100 mL flasks, either or not supplemented with 8% (v/v) methanol, with an initial OD_{600nm} of 0.1 ± 0.05. Cell cultivation was performed at 35 °C, with orbital agitation (250 rpm) and growth followed based on culture OD_{600nm}.

2.4 RESULTS

2.4.1 Selection of Methanol and Ethanol Concentrations for the Chemogenomic Analysis

To select the appropriate methanol and ethanol concentrations to perform the planned chemogenomic analysis, the growth curves of the parental strain *Saccharomyces cerevisiae* BY4741 were compared in YPD liquid medium supplemented or not with 5%, 8%, 10% and 14% (v/v) methanol, at pH 4.5 and 35 °C during 36 hours in a 96-wells plate (**Figure 2.2**). The incubation time was fixed in 36 hours to limit alcohol evaporation. Only 8% and 10% (v/v) of methanol were considered suitable concentrations since 14% (v/v) did not allow detectable growth after 30 hours of incubation and 5% (v/v) did not significantly affect the growth profile.

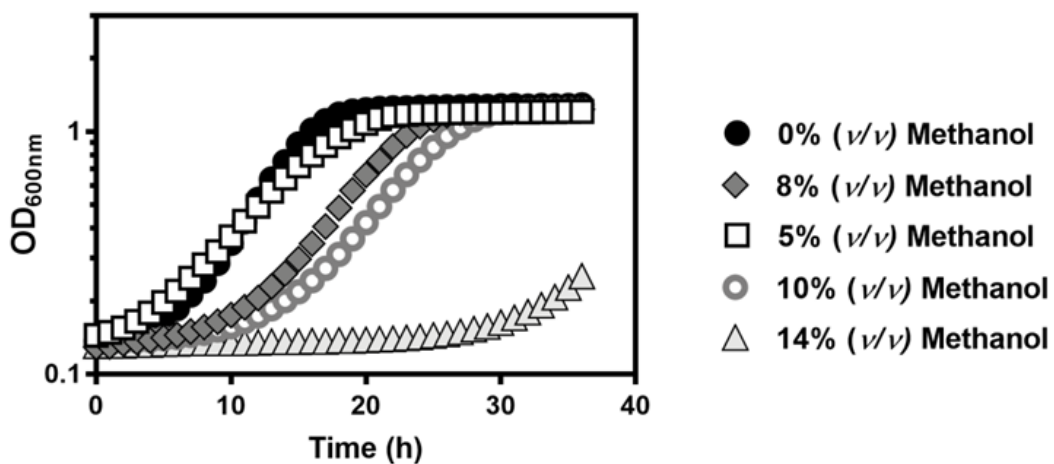


Figure 2. 2- Comparison of the growth curves of *S. cerevisiae* BY4741 in YPD medium (pH 4.5) supplemented or not (●) with 5% (□), 8% (◆), 10% (○), or 14% (v/v) (△) of methanol. Growth was followed in a microplate reader by measuring the optical density at 595 nm of a 96-well plate incubated at 35 °C with orbital agitation, for 36 hours.

An inhibitory ethanol concentration equivalent to 8% (v/v) of methanol was also selected using the same methodology and the selected value was 5.5% (v/v) (**Figure 2.3**).

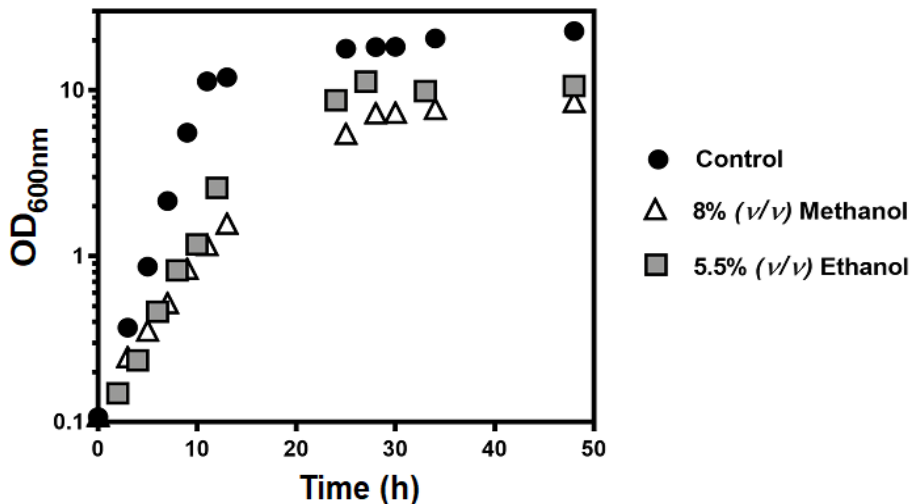


Figure 2.3- Effect of equivalent methanol and ethanol concentrations in the growth curves of *S. cerevisiae* BY4741. Cells were cultivated in liquid YPD medium (pH 4.5) supplemented, or not (circles), with 8% (v/v) methanol (triangles) or 5.5% (v/v) ethanol (squares) at 35 °C with orbital agitation (250 rpm). Growth was followed based on culture optical density at 600 nm (OD_{600nm}) and the growth curves shown are representative of at least three independent experiments.

2.4.2 Identification of Genes Required for Methanol and Ethanol Tolerance at a Genome-Wide Scale

Approximately 5100 deletion mutants were tested for susceptibility to 8% (v/v) methanol compared with the parental strain and the generated dataset compared with the dataset obtained, under the same experimental conditions, for 5.5% (v/v) of ethanol. Four hundred and two of those mutants were found to be more susceptible to methanol than the parental strain, 81 of these mutants showing full growth inhibition (+++), 170 showing a moderate growth inhibition (++) and 151 a minor growth inhibition (+). The full list of genes is available in the Supplementary Material, Table S1.1. No genes that when deleted leads to higher methanol tolerance, were detected. The full list of genes required for ethanol tolerance (Supplementary Material Table S1.2) includes 445 genes, 110 of them leading to growth abrogation when deleted under the experimental conditions tested. Based on the biological function of the genes required for maximum methanol or ethanol tolerance, they were clustered according to the PANTHER Classification System (<http://pantherdb.org>). The fold enrichment of different functional classes in the two datasets (p-value < 0.05), is shown in **Figure 2.4**. A more detailed discussion on selected methanol tolerance genes, in particular those belonging to different enriched functional classes, is described below.

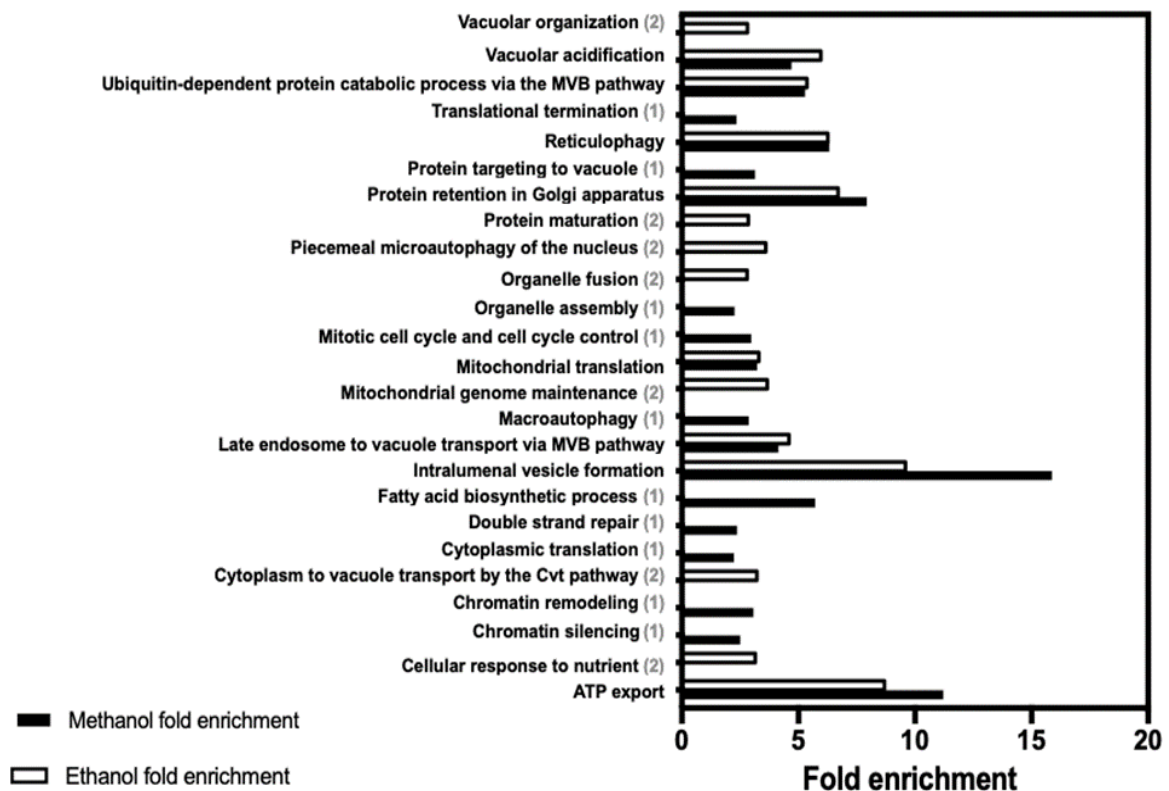


Figure 2. 4- Biological functions enriched in the datasets of genes required for yeast tolerance to methanol (black bars) or ethanol (white bars). Genes listed in Supplementary Material, Table S1 and S2, were clustered according to their biological process GO assignments using the PANTHER Classification System (<http://pantherdb.org>), and functional categories were considered to be over-represented if p -value < 0.05. The fold enrichment is calculated by dividing the number of genes present in the input dataset by the total number of genes of yeast genome expected to belong to specific functional class. (1) indicates the biological functions that are only enriched in the methanol dataset while (2) indicates those only enriched in the ethanol dataset. The biological functions with no indication are enriched in both datasets.

2.4.3 Genes Involved in DNA Repair and Mitotic Cell Cycle

Results from the performed chemogenomic analysis strongly suggest that DNA is a main specific molecular target of methanol toxicity since several genes related with DNA repair were found to be enriched in the methanol dataset but not in the ethanol dataset. Specifically, eight radiation sensitive (*RAD*) genes are relevant for overcoming methanol-induced deleterious effects given that the corresponding deletion mutants exhibited a marked susceptibility phenotype (**Table 2.1**). These genes are involved in DNA repair mechanisms, in particular in non-homologous end joining and base excision repair (*RAD27*), homologous recombination (*RAD51* and *RAD57*), post-replication repair (*RAD5*, *RAD6* and *RAD18*) and nucleotide excision repair (*RAD33*). The genes *MET18*, *MRE11*, and *SGS1*, involved in the biological functions described in **Table 2.1**, also play a role in DNA repair mechanisms. Some of the mentioned genes involved in DNA repair also participate in mitotic cell cycle (*MRE11*, *RAD6*,

and *SGS1*). The *CDC55* gene was described as involved in mitotic cell cycle, only, but the corresponding deletion mutant exhibited a strong susceptibility phenotype.

Table 2. 1- Genes involved in DNA repair and mitotic cell cycle identified in this study as determinants of yeast tolerance to methanol, compared with ethanol. The description of the encoded protein functions is based on the information at SGD (www.yeastgenome.org). The classification of the susceptibility phenotype level is as described in the Material and Methods section.

Gene/ ORF	Description of the encoded protein function	Susceptibility to methanol	Susceptibility to ethanol
<i>CDC55</i>	Regulatory subunit B of protein phosphatase 2A (PP2A), which localizes to nucleus prevents mitotic exit.	+++	No phenotype
<i>MET18</i>	Component of cytosolic iron-sulfur protein assembly (CIA) machinery. Met18 acts at a late step of Fe-S cluster assembly and it is also involved in DNA replication and repair, transcription, and telomere maintenance.	+++	+
<i>MRE11</i>	Nuclease subunit of the MRX complex with Rad50 and Xrs2; MRX complex functions in repair of DNA double-strand breaks and in telomere stability.	+++	No phenotype
<i>RAD5</i>	DNA helicase/Ubiquitin ligase; involved in error-free DNA damage tolerance (DDT), replication fork regression during post-replication repair by template switching, error-prone translesion synthesis.	++	No phenotype
<i>RAD6</i>	Ubiquitin-conjugating enzyme (E2); involved in post-replication repair as a heterodimer with Rad18, regulation of K63 polyubiquitination in response to oxidative stress, double-strand break repair and checkpoint control and as a heterodimer with Bre1.	+	No phenotype
<i>RAD18</i>	E3 ubiquitin ligase; required for post-replication repair.	++	No phenotype
<i>RAD27</i>	5' to 3' exonuclease, 5' flap endonuclease; required for Okazaki fragment processing and maturation, for long-patch base-excision repair.	+++	No phenotype
<i>RAD33</i>	Protein involved in nucleotide excision repair.	+	No phenotype
<i>RAD51</i>	Strand exchange protein involved in the recombinational repair of double-strand breaks in DNA during vegetative growth and meiosis.	+++	No phenotype
<i>RAD57</i>	Protein that stimulates strand exchange by stabilizing the binding of Rad51 to single-stranded DNA; involved in the recombinational repair of double-strand breaks in DNA during vegetative growth and meiosis.	++	No phenotype
<i>SGS1</i>	RecQ family nucleolar DNA helicase. Sgs1 play a role in genome integrity maintenance, chromosome synapsis, meiotic joint molecule/crossover formation.	++	++

2.4.4 Genes involved in autophagy

Sixteen genes involved in autophagy were found to be implicated in yeast tolerance to methanol (**Table 2.2**). Autophagy is a highly conserved eukaryotic cellular recycling process playing an important role in cell survival and maintenance, involving the formation of the autophagosome. The individual deletion of the macroautophagy genes, *AIM26*, *ATG11*, *RAS2*, *VAM7*, *VPS36*, and *YPT6* (**Table 2.2**) led to a strong methanol susceptibility phenotype. Collectively, these results suggest that methanol may have strong deleterious effects on intracellular proteins and organelles, targeting cytoplasmic contents and organelles into autophagosomes for degradation as part of the protective response.

Table 2. 2-. Genes involved in autophagy identified in this study as determinants of yeast tolerance to methanol, compared with ethanol. Genes in bold are specific to macroautophagy and the corresponding mutants exhibited a strong susceptibility phenotype, and the underlined genes are specific to reticulophagy. Atg11 is common to both types of autophagy. Symbols are as in Table 2.1.

Gene/ ORF	Description of the encoded protein function	Susceptibility to methanol	Susceptibility to ethanol
<u>AIM26</u>	Protein of unknown function. Null mutant displays elevated frequency of mitochondrial genome loss.	+++	No phenotype
<u>ATG11</u>	Adapter protein for pexophagy and the Cvt targeting pathway. Atg11 directs receptor-bound cargo to the phagophore assembly site (PAS) for packaging into vesicles.	+++	++
<u>RAS2</u>	GTP-binding protein that regulates nitrogen starvation response, sporulation, and filamentous growth.	+++	+++
<u>SNF7</u>	One of four subunits of the ESCRT-III complex. Snf1 is involved in the sorting of transmembrane proteins into the multivesicular body (MVB) pathway.	+++	+++
<u>STP22</u>	Component of the ESCRT-I complex.	++	+++
<u>VAM7</u>	Vacuolar SNARE protein.	+++	+
<u>VPS21</u>	Endosomal Rab family GTPase required for endocytic transport and sorting of vacuolar hydrolases. Vps21 is also required for endosomal localization of the CORVET complex.	++	++
<u>VPS4</u>	AAA-ATPase involved in multivesicular body (MVB) protein sorting.	++	+

VPS36	Component of the ESCRT-II complex that contains the GLUE (GRAM Like Ubiquitin binding in EAP45) domain which is involved in interactions with ESCRT-I and ubiquitin-dependent sorting of proteins into the endosome.	+++	+++
YPT6	Rab family GTPase that is required for endosome-to-Golgi, intra-Golgi retrograde, and retrograde Golgi-to-ER transport.	+++	+++

Genes involved in reticulophagy (*ATG11*, *SNF7*, *SPO7*, *STP22*, *VPS21*, *VPS4*) (**Table 2.2**), a type of selective autophagy required for the selective clearance and degradation of the endoplasmic reticulum (ER) by the cellular macroautophagy/autophagy machinery under endoplasmic reticulum stress (Reggiori and Klionsky 2013), were also found to be enriched in both methanol and ethanol datasets. The ER is the main site for cellular protein and calcium homeostasis, as well as lipid synthesis in eukaryotic cells (Delorme-Axford et al. 2019).

2.4.5 Genes involved in reserve polysaccharides, cell wall and membrane biosynthesis

Genes implicated in cell wall and membrane biosynthesis are also relevant in yeast tolerance to methanol through their function in polysaccharide metabolism and fatty acid biosynthesis (**Table 2.3**). Regarding polysaccharide metabolism, the deletion of *FKS1*, *GPH1*, *ROT2*, *SMI1*, and *TPS2* genes led to strong susceptibility phenotypes. Remarkably, genes involved in the catabolism and synthesis of the reserve carbohydrates glycogen and trehalose (*GPH1* and *TPS2* genes) and cell wall synthesis (*FKS1*, *ROT2*, and *SMI1*) are shared by the two datasets being required for maximum tolerance to both alcohols.

Genes involved in membrane synthesis relevant for methanol and ethanol tolerance, include ergosterol biosynthetic genes (*ERG2* and *ERG3*), phospholipid biosynthetic genes (*KCS1*, *LIP5*, *PDX3*), and sphingolipids biosynthetic genes (*ELO2*, *ELO3*, and *SAC1*). In particular, the deletion of the *ELO2* gene, encoding the fatty acid elongase involved in fatty acids and sphingolipids biosynthesis, led to a strong phenotype.

Table 2. 3- Genes involved in reserve carbohydrate, cell wall, and membrane biosynthesis identified in this study as determinants of yeast tolerance to methanol, compared with ethanol. Symbols are as in Table 2.1.

Gene/ ORF	Description of the encoded protein function	Susceptibility to methanol	Susceptibility to ethanol
ELO2	Fatty acid elongase, involved in sphingolipid biosynthesis; acts on fatty acids of up to 24 carbons in length.	+++	+++
ELO3	Elongase involved in fatty acid and sphingolipid biosynthesis.	++	++
ERG2	C-8 sterol isomerase; catalyses isomerization of delta-8 double bond to delta-7 position at an intermediate step in ergosterol biosynthesis.	+	+++
ERG3	C-5 sterol desaturase; glycoprotein that catalyses the introduction of a C-5(6) double bond into episterol, a precursor in ergosterol biosynthesis.	++	++
FKS1	Catalytic subunit of 1,3-beta-D-glucan synthase; binds to regulatory subunit Rho1; involved in cell wall synthesis and maintenance.	+++	+++
GPH1	Glycogen phosphorylase required for the mobilization of glycogen.	+++	++
KCS1	Inositol hexakisphosphate and inositol heptakisphosphate kinase.	++	+++
LIP5	Protein involved in biosynthesis of the coenzyme lipoic acid.	+	+
PDX3	Pyridoxine (pyridoxamine) phosphate oxidase.	++	+++
ROT2	Glucosidase II catalytic subunit; required to trim the final glucose in N-linked glycans and for normal cell wall synthesis.	+++	++
SAC1	Phosphatidylinositol phosphate (PtdInsP) phosphatase; is involved in hydrolysis of PtdIns[4]P in the early and medial Golgi.	+	++
SMI1	Protein involved in the regulation of cell wall synthesis.	+++	++
TPS2	Phosphatase subunit of the trehalose-6-P synthase/phosphatase complex that involved in synthesis of the storage carbohydrate trehalose.	+++	+

2.4.6 Genes Involved in Protein Synthesis

Methanol tolerance determinants involved in protein synthesis, through cytoplasmic and mitochondrial translation, include a large number of genes encoding (i) proteins of the large subunits of ribosomes—Ribosomal Proteins of the Large subunit, RPL genes (e.g., *RPL8A*, *RPL2B*, *RPL34B*, *RPL14A*, *RPL31B*, *RPL20A*, *RPL36B*); (ii) proteins of the small subunit of ribosomes, Ribosomal Proteins of the Small subunit, RPS genes (e.g., *RPS17A*, *RPS19A*) (Supplementary Material, Table S1.1).

The mitochondrial large subunit proteins encoded, mostly, by the family of the Mitochondrial Ribosomal Proteins of the Large subunit, MRPL genes (e.g., *MRP49*, *MRPL25*, *MRPL8*, *MRPL33*, *MRPL10*, *MRPL33*), and the mitochondrial small subunit proteins, encoded by the Mitochondrial Ribosomal Small subunit of Mitochondria (MRPS) and Ribosomal Small subunit of Mitochondria (RSM) families of genes (e.g., *MRP13*, *MRPS35*, *RSM18*, *RSM22*, *RSM23*) were required to overcome methanol-induced stress (Supplementary Material, Table S1.1).

Several other genes related with cytoplasmic translation, (*RPS16A*, *RPL20B*, *RPL21A*, *RPS24A*, *RPS27B*) and mitochondrial translation, (*GTF1*, *IFM1*, *MRF1*, *MRP7*, *MRPS12*, *MRPL20*, *MRPL22*, *MRPL24*, *MRPL7*, *MSE1*, *RSM23*, *SLM5*) were found to confer tolerance, to both methanol and ethanol (Supplementary Material, Tables S1.1 and S1.2).

2.4.7 Genes Involved in Vacuolar Function and Endosomal Transport

ATP export and intraluminal vesicle formation are the two functions with the highest level of fold enrichment in both methanol and ethanol datasets sharing 12 genes (*BRO1*, *DID4*, *DOA4*, *SNF7*, *SNF8*, *STP22*, *VPS20*, *VPS24*, *VPS25*, *VPS27*, *VPS28*, *VPS36*) with vacuolar and endosomal functions (**Figure 2.4** and **Tables 2.4** and **2.5**).

Results suggest that yeast cells exposure to methanol stress affects several transport routes such as vacuolar transport and vesicular transport. Methanol tolerance determinants related with vacuolar function include Vacuolar Membrane H⁺-ATPase (*VMA*) genes (involved in intracellular pH homeostasis (Martínez-Muñoz and Kane 2008; Charoenbhakdi et al. 2016), the Vacuolar Morphogenesis (*VAM*) genes *VMA1*, *VMA2*, *VMA7*, *VMA13*, *VAM7* (leading to a strong phenotype) and *VAM3*, *VAM6*, *VAM7*, *VAM10* (leading to a moderate phenotype) and the Vacuolar Protein Sorting (*VPS*) genes – *VPS1*, *VPS24*, *VPS25*, *VPS33*, *VPS36* (**Table 2.4**). Genes involved in vesicular transport in the datasets include those encoding the endosomal sorting complex (*BRO1*, *DID2*, *DID4*, *SNF7* and *SNF8*) (**Table 2.5**).

Table 2. 4- Genes involved in vacuolar organization and acidification identified in this study as determinants of yeast tolerance to methanol, compared with ethanol. Symbols are as in Table 2.1.

Gene/ ORF	Description of the encoded protein function	Susceptibility to methanol	Susceptibility to ethanol
VAM10	Protein involved in vacuole morphogenesis and acts at an early step of homotypic vacuole fusion that is required for vacuole tethering.	+	++
VAM3	Syntaxin-like vacuolar t-SNARE. Vam3 mediates docking/fusion of late transport intermediates with the vacuole.	+	++
VAM6	Guanine nucleotide exchange factor for the GTPase Gtr1. Vam6 is a Rab GTPase effector, interacting with both GTP- and GDP-bound conformations of Ypt7.	+	++
VAM7	Vacuolar SNARE protein; Vam7 functions with Vam3 in vacuolar protein trafficking.	+++	+
VMA1	Subunit A of the V1 peripheral membrane domain of V-ATPase.	+++	+++
VMA13	Subunit H of the V1 peripheral membrane domain of V-ATPase.	+++	+++
VMA2	Subunit B of V1 peripheral membrane domain of vacuolar H ⁺ -ATPase.	+++	No phenotype
VMA7	Subunit F of the V1 peripheral membrane domain of V-ATPase.	+++	No phenotype
VPS1	Dynammin-like GTPase required for vacuolar sorting.	+++	+++
VPS24	One of four subunits of the ESCRT-III complex. Vps24 is involved in the sorting of transmembrane proteins into the multivesicular body (MVB) pathway.	+++	+++
VPS25	Component of the ESCRT-II complex.	+++	++
VPS33	ATP-binding protein that is a subunit of the HOPS and CORVET complexes. Vps33 is essential for protein sorting, vesicle docking, and fusion at the vacuole.	+++	+++
VPS36	Component of the ESCRT-II complex.	+++	+++

Table 2. 5- Genes involved in vesicular transport identified in this study as determinants of yeast tolerance to methanol, compared with ethanol. Symbols are as in Table 2. 1.

Gene/ ORF	Description of the encoded protein function	Susceptibility to methanol	Susceptibility to ethanol
<i>BRO1</i>	Cytoplasmic class E vacuolar protein sorting (VPS) factor. Bro1 coordinates deubiquitination in the multivesicular body (MVB) pathway by recruiting Doa4 to endosomes.	++	No phenotype
<i>DID2</i>	Class E protein of the vacuolar protein-sorting (Vps) pathway. Did2 binds Vps4p and directs it to dissociate ESCRT-III complexes.	++	++
<i>DID4</i>	Class E Vps protein of the ESCRT-III complex. Did4 is required for sorting of integral membrane proteins into luminal vesicles of multivesicular bodies, and for delivery of newly synthesized vacuolar enzymes to the vacuole.	+	++
<i>SNF7</i>	One of four subunits of the ESCRT-III complex. Snf1 is involved in the sorting of transmembrane proteins into the multivesicular body (MVB) pathway.	+++	+++
<i>SNF8</i>	Component of the ESCRT-II complex.	+++	+++

2.4.8 Transcriptional Control and Regulatory Tolerance Networks

The enriched biological functions “chromatin remodeling” and “silencing” in the methanol dataset contains, among other genes, 12 transcription factors (TF) (**Table 2.6**). Five of these genes are shared with the ethanol dataset (**Table 2.6**).

Table 2. 6- Transcription factors (TF) identified only in the methanol dataset ⁽¹⁾, the ethanol-specific TFs ⁽²⁾, and the TFs shared between methanol and ethanol datasets ^(1,2). Symbols are as in Table 2.1.

Gene/ ORF	Description of the encoded protein function	Susceptibility to methanol	Susceptibility to ethanol
CBF1 ^(1,2)	Transcription factor that associates with kinetochores proteins, required for chromosome segregation.	+	++
GLN3 ⁽¹⁾	Transcriptional activator of genes regulated by nitrogen catabolite repression.	+	No phenotype
HAP5 ⁽²⁾	Transcription factor that is a subunit of the Hap2/3/4/5 CCAAT-binding complex. Hap5 is a global regulator of respiratory gene expression.	No phenotype	+
IXR1 ⁽¹⁾	Transcriptional repressor that regulates hypoxic genes during normoxia; involved in the aerobic repression of genes such as <i>COX5b</i> , <i>TIR1</i> , and <i>HEM13</i> .	+++	No phenotype
MGA2 ⁽²⁾	Transcription factor, localized in the endoplasmic reticulum membrane, involved in regulation of <i>OLE1</i> transcription.	No phenotype	++
NGG1 ⁽¹⁾	Transcriptional regulator involved in glucose repression of Gal4-regulated genes. Subunit of chromatin modifying histone acetyltransferase complexes.	++	No phenotype
OAF1 ⁽²⁾	Transcription factor that is an activator of beta-oxidation of fatty acids, peroxisome organization and biogenesis, activating transcription in the presence of oleate.	No phenotype	+
OPI1 ⁽¹⁾	Transcriptional regulator of a variety of genes. Opi1 phosphorylation by protein kinase A stimulates Opi1 function in negative regulation of phospholipid biosynthetic genes.	+++	No phenotype
RPH1 ⁽¹⁾	Transcription factor with JmjC domain-containing histone demethylase. Rph1 targets tri- and dimethylated H3K36 and associates with actively transcribed regions and promotes elongation; also involved in the repression of autophagy-related genes in nutrient-replete conditions.	+	No phenotype

<i>RPN4</i> ^(1,2)	Transcription factor that stimulates expression of proteasome encoding genes being regulated by the 26S proteasome in a negative feedback control mechanism.	+	+++
<i>RSF2</i> ⁽²⁾	Zinc-finger transcription factor that regulates both nuclear and mitochondrial genes, involved in glycerol-based growth and respiration.	No phenotype	+
<i>SFL1</i> ^(1,2)	Transcriptional repressor and activator; involved in repression of flocculation-related genes.	++	++
<i>SFP1</i> ^(1,2)	Transcription factor that regulates ribosomal protein and biogenesis genes; also involved in the regulation of the response to nutrients and stress, G2/M transitions during mitotic cell cycle and DNA-damage response and modulates cell size.	++	+++
<i>STP1</i> ⁽²⁾	Transcription factor that activates transcription of amino acid permease genes and may have a role in tRNA processing.	No phenotype	+
<i>SOK2</i> ⁽¹⁾	Transcription factor that negatively regulates pseudohyphal differentiation; also involved in the regulation of cyclic AMP (cAMP)-dependent protein kinase signal transduction pathway.	++	No phenotype
<i>STB5</i> ⁽¹⁾	Transcription factor involved in the regulation multidrug resistance and oxidative stress response.	++	No phenotype
<i>SWI6</i> ⁽²⁾	Transcription cofactor involved in meiotic gene expression. Swi6 is also required for the unfolded protein response.	No phenotype	++
<i>TUP1</i> ⁽²⁾	General repressor of transcription, through interactions with histones H3 and H4 and stabilization of nucleosomes over promoters.	No phenotype	+
<i>UME6</i> ^(1,2)	Transcriptional regulator of early meiotic genes; involved in chromatin remodelling and transcriptional repression via DNA looping.	++	+++
<i>UPC2</i> ⁽²⁾	Transcription factor that induces sterol biosynthetic genes, upon sterol depletion. Upc2 acts as a sterol sensor, binding ergosterol in sterol rich conditions.	No phenotype	+
<i>URE2</i> ⁽²⁾	Transcription factor involved in the regulation of nitrogen catabolite repression.	No phenotype	+

Using the YEASTRACT database (Monteiro et al. 2020), it was found that the number of genes in the methanol dataset described as being regulated by the identified TFs is variable (numbers indicated in **Figure 2.5, A**), ranging from 2 (*NGG1*) to 374 (*RPN4*). However, the described regulons corresponding to the TFs required for methanol tolerance also include a highly variable number of target genes (from 69 to 5834 genes, **Figure 2.5, B**).

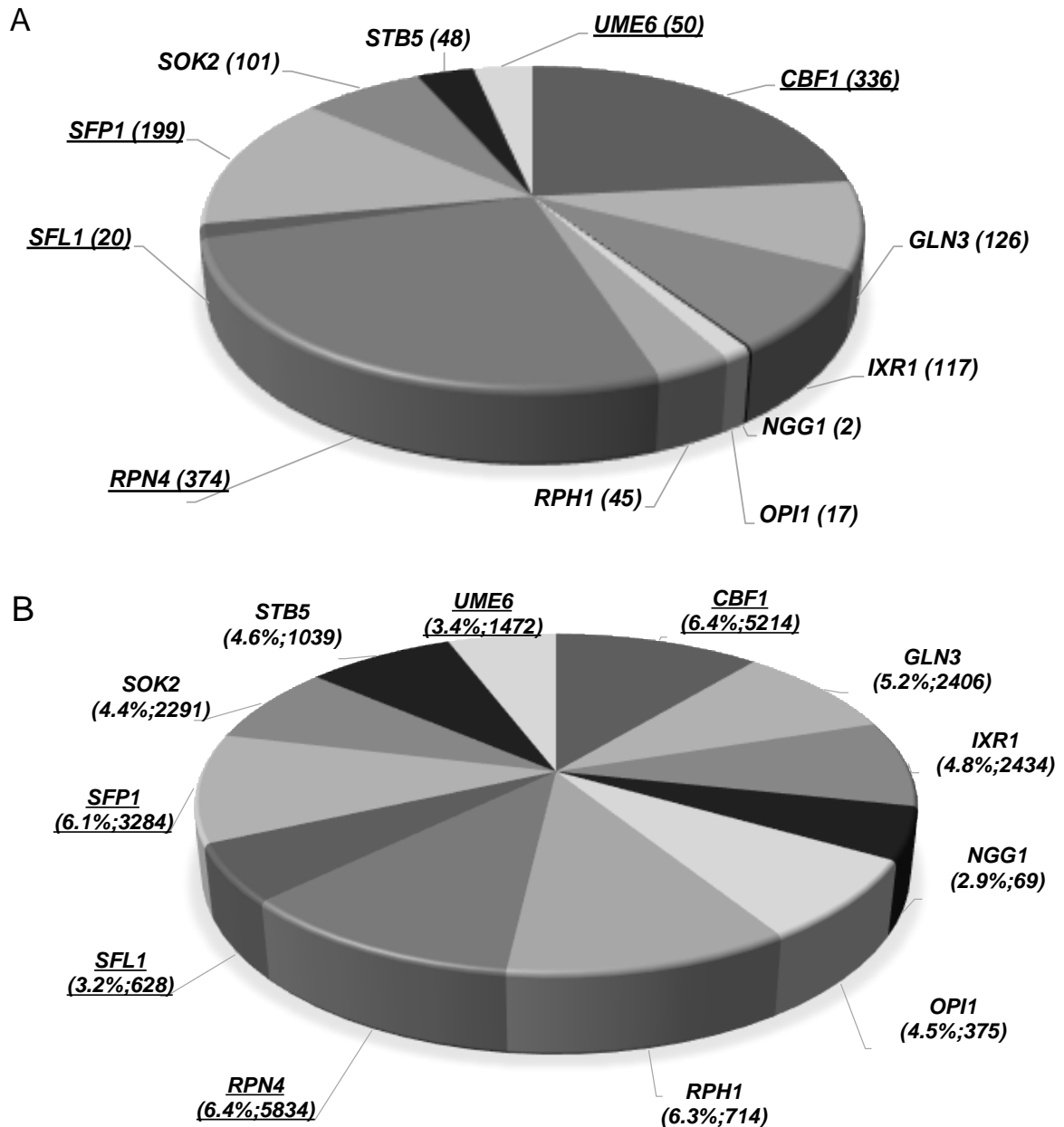


Figure 2. 5- Clustering of methanol-tolerance genes that are targets of transcription factors (TF) that also exert protection against this alcohol. **(A)** Number of target genes (into brackets) for each TF that are required for methanol tolerance. **(B)** Percentage of methanol tolerance genes regulated by each TF relative to the total number of genes of each described regulon. Methanol tolerance genes were clustered in association with their documented regulators using the information available in the Yeastract database (December 2020). The TFs found to exert protection only against methanol are in bold; the TFs underlined and in bold are those found in the methanol and ethanol datasets.

For this reason, the percentage of methanol tolerance genes among the various regulons was calculated and the methanol tolerance genes were found to represent between 3-6.4% of the described TF target genes, reaching values above 6% for the TFs Cbf1, Sfp1, Rpn4 and Rph1. Based on the levels of the methanol susceptibility phenotypes of the corresponding deletion mutants estimated under the conditions of this study and the percentage of genes of the described regulons identified as methanol determinants, the TFs Cbf1, Sfp1, Rpn4, Ixr1, Opi1, Sfl1, Sok2, Stb5, and Ume6 are suggested to have an important role and more specific role in methanol tolerance in *S. cerevisiae*, with Cbf1, Sfl1, Sfp1, Rpn4 and Ume6, also being relevant determinants of ethanol tolerance.

The methanol susceptibility phenotypes observed during the high throughput analysis were confirmed by growth in shake flasks (**Figure 2.6**).

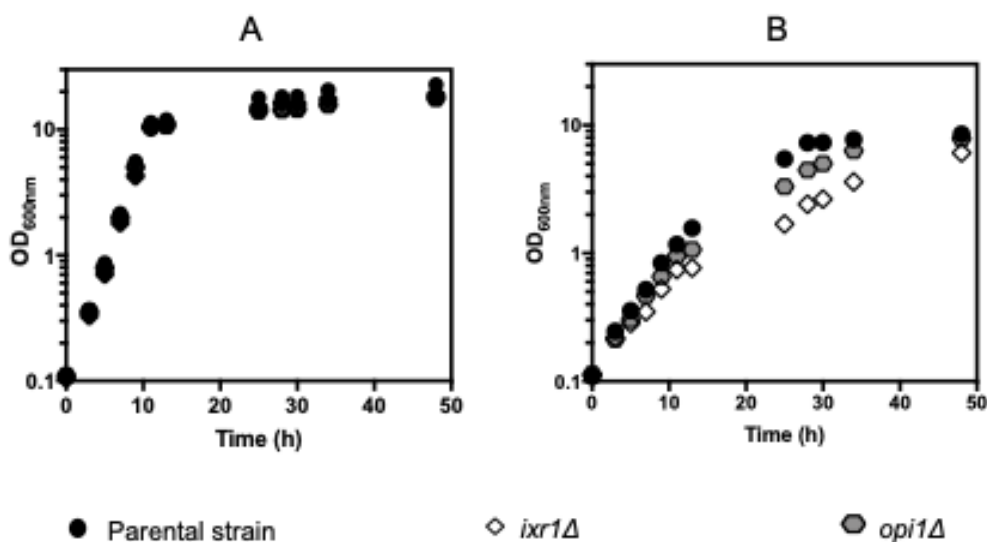


Figure 2. 6- Effect of methanol in the growth curves of the parental strain BY4741 (circles), and derived *ixr1Δ* (hexagons) and *opi1Δ* (squares) mutants in YPD liquid medium, (A) or in this medium supplemented with 8%(v/v) methanol(B) at 35°C with orbital agitation (250 rpm). The growth curves are representative of at least three independent experiments.

Considering that methanol oxidation leads to the formation of formaldehyde and formate, as intermediate metabolites and is accompanied by the production of free radicals (Skrzydłowska 2003), oxidative stress being confirmed as a major consequence of methanol-induced stress in *S. cerevisiae* (Yasokawa et al. 2010), it was intriguing that we failed to identify in the chemogenomic analysis the well-known transcriptional regulators (TR) of the general stress response, Msn2 and Msn4, and of the oxidative stress response, Yap1 (Estruch 2000; Gasch et al. 2000). To test the hypothesis put forward that the concentration of methanol used for screening the disruptome was below the threshold level for rendering those TR active, the effect of their expression at higher concentrations of methanol [10 %, 12 % and 14 % (v/v)]

were examined by spot assays in YPD solid medium (**Figure 2.7**). When YPD medium was supplemented with 8 % (v/v) methanol (the conditions used for the disruptome screening), the lack of phenotype for *msn2* Δ , *msn4* Δ and *yap1* Δ mutants was confirmed. However, at methanol concentrations in the range 10-14 % (v/v), the *yap1* Δ exhibited a marked methanol susceptibility phenotype, confirming the importance of Yap1-dependent transcription activation of oxidative-stress responsive genes above the threshold level of the inducing agent (Morano et al. 2012). Nevertheless, the growth inhibition of the single Msn2 and Msn4 deletion mutants by methanol was minor, if any. This result is consistent with the observation that the susceptibility of the single deletion mutants *msn2* Δ and *msn4* Δ under different stresses, in particular under oxidative stress, is moderate and only the phenotype of the double deletion mutant is marked (Estruch 2000).

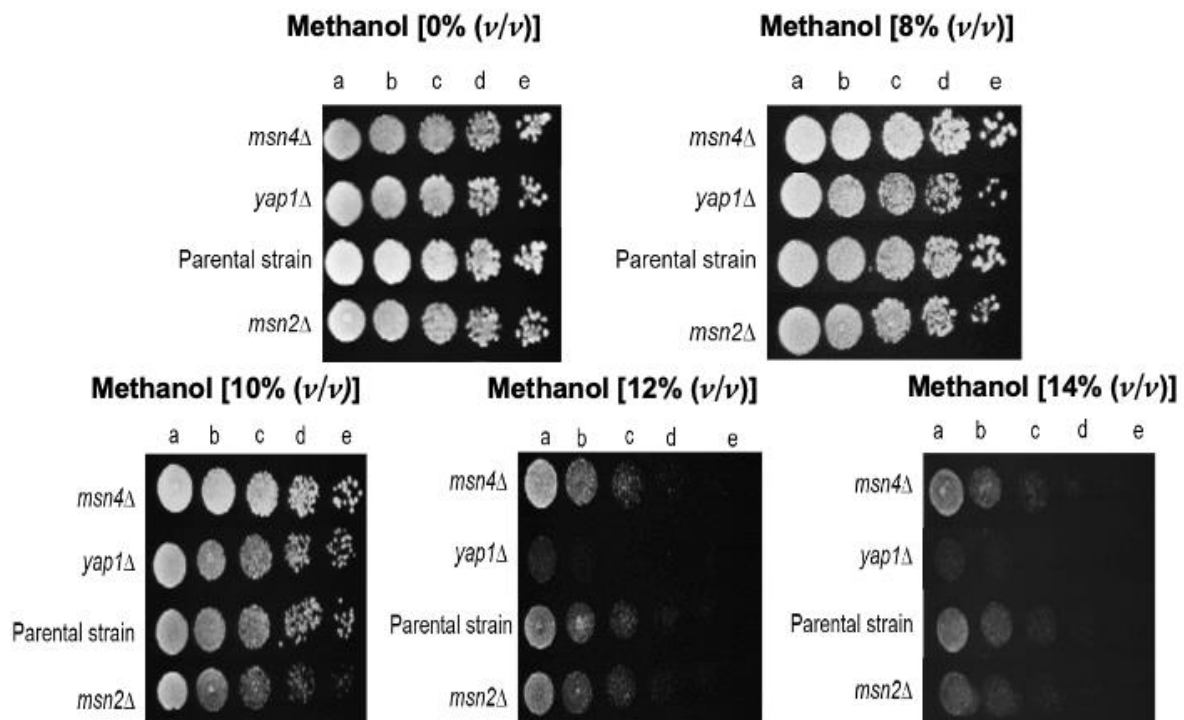


Figure 2. Susceptibility to methanol of the parental strain *S. cerevisiae* BY4741 and derived deletion mutants *yap1* Δ , *msn4* Δ , and *msn2* Δ by spot assays. Yeast cell suspensions used as inocula for spot assays were prepared using cells harvested in the exponential phase of growth (culture $OD_{600nm} = 0.5 \pm 0.05$). Cell suspensions were diluted in sterile water to an $OD_{600nm} = 0.25 \pm 0.005$ (a) and this solution was used to prepare 1:5 (b), 1:25 (c), 1:125 (d), and 1:625 (e) diluted suspensions. Susceptibility phenotypes were registered after 48 hours of incubation at 35 °C.

Based on the documented interactions (DNA binding evidences or DNA expression data) deposited in the Yeastract database (Monteiro et al. 2020), the complex regulatory networks describing the interactions between the main TFs found to be specifically required

for methanol tolerance (Gln3, Ixr1, Opi1, Rph1, Sok2, Stb5) and their target genes in the methanol dataset is shown in **Figure 2.8**, panels A to F, respectively. These methanol-specific TFs control a considerable number of the genes with strong phenotype that participate in methanol enriched biological functions discussed previously, such as DNA repair (e.g., *MET18*, *RAD27*, *RAD5*, *RAD51*, *RAD54*, *RAD57*), cell wall biosynthesis (e.g., *FKS1* and *SMI1*), membrane biosynthesis (e.g., *ELO2*, *ELO3*, *ERG2*, *ERG3*, *ROT2*), oxidative-stress responsive genes (e.g., *FEN2*, *GSH1*, *MCH5*, *PRX1*, *SOD1*) and protein synthesis (e.g., *MRPL*, *MRPS*, *RPL* and *RPS*) families of genes. The transcriptional network controlled by the TF Ixr1, that regulates hypoxic genes during normoxia, is highly complex since it controls, the highest number of genes (6) encoding other transcription factors of the methanol dataset: Gln3, Opi1, Rph1, Sok2, Stb5 and Ume6 (Chua et al. 2006; Reimand et al. 2010; Vizoso-Vázquez et al. 2012; Vizoso-Vázquez et al. 2018). Ngg1 was not included in this analysis due to the low number of regulatory interactions available at Yeasttract database. The regulatory interaction networks for the TFs that are shared between methanol and ethanol datasets, Sfl1 and Ume6, with the genes that confer methanol tolerance are presented in **Figure 2.8**, panels G and H, respectively. The regulatory networks for Cbf1, Rpn4 and Sfp1 are not shown because, due to the high density of the regulated methanol tolerance genes, they do not provide useful information.

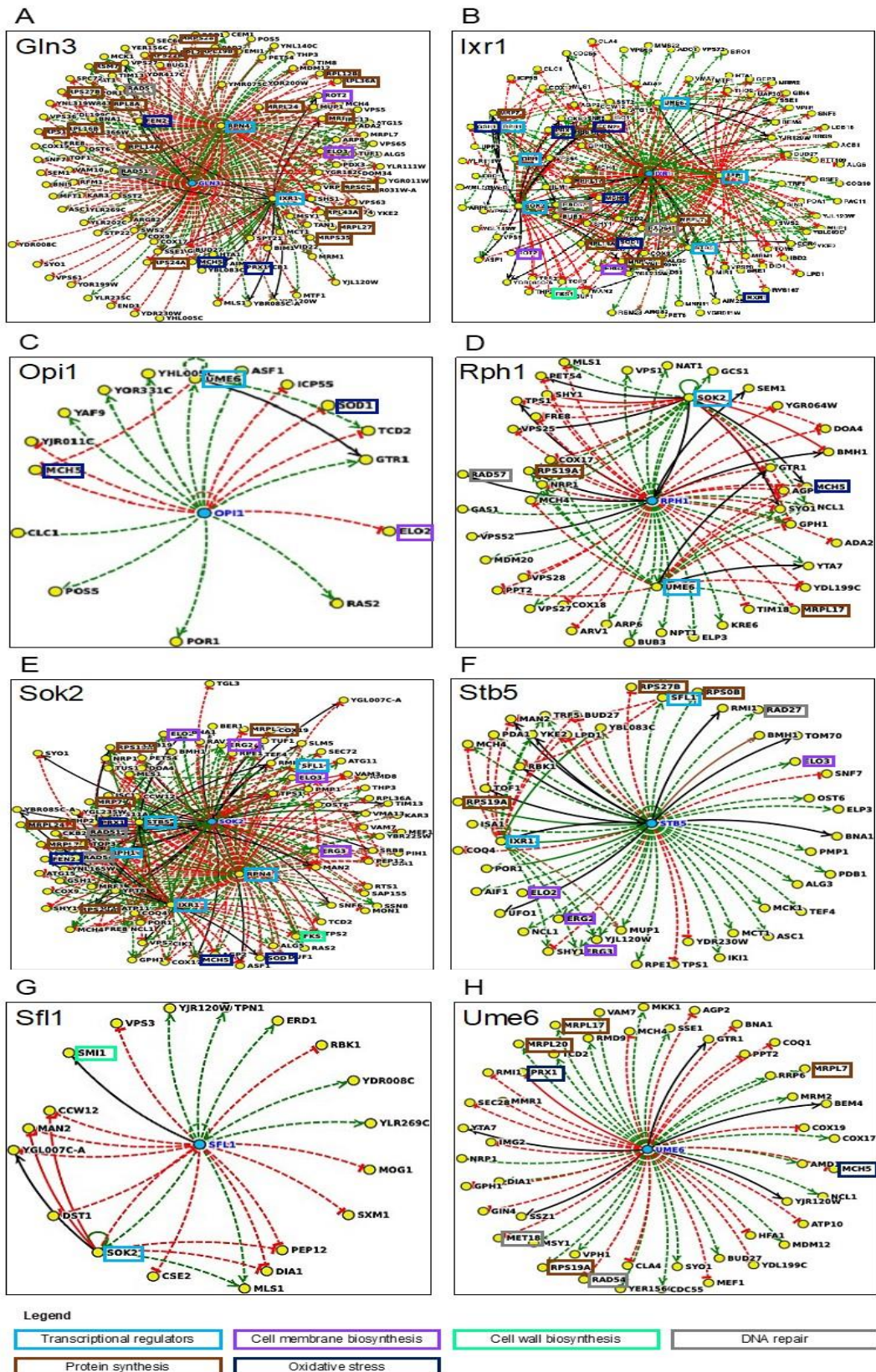


Figure 2. 8- Genetic interaction networks between the TFs *Gln3* (A), *Ixr1* (B), *Opi1* (C), *Rph1* (D), *Sok2* (E), *Stb5* (F), *Sfl1* (G) and *Ume6* (H), required for tolerance to methanol and the methanol tolerance genes identified in this study that are their documented targets. The interaction networks were obtained using the regulatory interactions available in Yeastract (December 2020, <http://yeastract-plus.org/yeastract/scerevisiae/index.php>). The positive, negative, and unspecified regulatory interactions, correspond, to green, red, and black lines, respectively. The interactions are based in expression data (dashed lines) or DNA binding (full lines). The color of the boxes represents different functional groups as indicated in the legend.

2.5 DISCUSSION

The chemogenomics analysis performed in this work provides new information on methanol toxicity and tolerance mechanisms in yeast, being the first disruptome study conducted to unveil methanol tolerance determinants at a genome-wide scale. Although the identification of methanol tolerance determinants in yeast was the main objective of this study, we also intended to compare the major determinants of tolerance to methanol *versus* ethanol to get clues on more specific methanol toxicity mechanisms and to identify relevant tolerance determinants common to both alcohols to guide future efforts concerning yeast robustness engineering. The yeast disruptome was previously screened for susceptibility to ethanol stress in several studies (Kubota et al. 2004; Fujita et al. 2006; van Voorst et al. 2006; Auesukaree et al. 2009; Teixeira et al. 2009; Yoshikawa et al. 2009). However, differences registered between the data obtained in the various experimental analyses suggest that the genetic background, growth media, level of stress and other environmental conditions influence the effect of gene expression in yeast tolerance (Teixeira et al. 2009). To address that issue, two datasets were obtained in this work by testing equivalent sub-lethal inhibitory concentrations of methanol and ethanol under the same experimental conditions. Among the 402 determinants of tolerance to methanol-induced stress, identified in YPD growth medium supplemented with 8% (v/v) at 35°C, 235 were specific to methanol, thus not shared with the ethanol dataset obtained for 5.5% (v/v) ethanol. The main feature that clearly distinguishes methanol from ethanol tolerance determinants relates with DNA repair mechanisms presumably required for overcoming methanol-induced stress. Among the 8 *RAD* genes (a designation due to the sensitivity of the corresponding mutants to exposure to X-rays (Game and Mortimer 1974)) present exclusively in methanol dataset and involved in several mechanisms of DNA repair, such as recombinational repair and double-strand break repair (Lewis et al. 2002; Symington 2002), the *RAD18*, *RAD27*, *RAD5*, *RAD51* and *RAD57* genes were previously identified as formaldehyde tolerance determinants (North et al. 2016). The mechanisms required for formaldehyde tolerance involve homologous recombination and nucleotide excision repair; homologous recombination is considered the preferred mechanism to repair damage due to chronic exposure to formaldehyde while nucleotide excision repair is the preferred mechanism to repair acute exposure (de Graaf et al. 2009). The identification of genes involved in homologous recombination (*Rad51*, *Rad54*, *Rad57*) and in nucleotide excision repair (*Rad33*) indicates that both mechanisms are important for methanol tolerance.

Although there are differences between the major methanol or ethanol tolerance determinants, there are tolerance mechanisms in common. Since straight-chain alcohols toxicity can be related with the octanol-water partition coefficient $\log P_{ow}$ value (Salter and Kell 1995), and $\log P_{ow}$ values for methanol and ethanol are -0.74 and -0.30, respectively (Sangster

1989), compared with methanol, ethanol is more lipophilic and therefore, expectably, more toxic as the result of membrane targeting (Sikkema et al. 1995; Weber and De Bont 1996). Consistent with the concept that membranes are molecular targets for methanol and ethanol toxic effects, genes required for membrane composition control were identified as required for alcohol tolerance, in particular genes involved in the biosynthesis of ergosterol, phospholipids and sphingolipids (Kubota et al. 2004; Fujita et al. 2006; van Voorst et al. 2006; Auesukaree et al. 2009; Teixeira et al. 2009; Yoshikawa et al. 2009). In this context, the TF Ume6, an important ethanol tolerance determinant (Kubota et al. 2004; Fujita et al. 2006; Auesukaree et al. 2009; Teixeira et al. 2009) that is known to regulate phospholipid biosynthetic gene expression (Jackson and Lopes 1996), was found in methanol and ethanol datasets. Together with other tolerance genes involved in the establishment of membrane composition, those genes reinforce the idea of the importance of membrane remodeling to counteract alcohol stress. Alcohol-induced permeabilization of plasma membrane leads to the increased passive influx of ions, in particular protons, across plasma membrane, contributing to cytosolic acidification and the dissipation of the electrochemical membrane potential (Leão and Van Uden 1984; Martínez-Muñoz and Kane 2008; Charoenbhakdi et al. 2016). Since the H⁺-ATPase, present at the vacuolar membrane (V-ATPase), is involved in the regulation of intracellular pH homeostasis (Martínez-Muñoz and Kane 2008) it is understandable that several subunits of this multimeric protein were identified as required for methanol and ethanol tolerance. Methanol is likely an inducer of intracellular and vacuolar acidification, as described for ethanol (Rosa and Sá-Correia 1996; Carmelo et al. 1997; Teixeira et al. 2009) and the maintenance of intracellular pH (pH_i) homeostasis is affected by V-ATPase defects, emphasizing the importance of this function in tolerance to various straight-chain alcohols (Fujita et al. 2006). The biosynthesis of the reserve polysaccharides, glycogen and trehalose also appears to be relevant for yeast tolerance to methanol and ethanol, as suggested by the identification of two genes involved in the synthesis of trehalose (*TPS1* and *TPS2*) and one gene required for glycogen degradation (*GPH1*) in the datasets. Trehalose and glycogen accumulate under stress conditions and are important in carbon storage and as compatible solutes (Welsh 2000) and trehalose exerts a protective effect on biomembranes, avoiding desiccation and protein denaturation (Wiemken 1990). *TPS1* and *GPH1* were also found in other chemogenomic studies as ethanol tolerance determinants (Kubota et al. 2004; van Voorst et al. 2006; Teixeira et al. 2009; Yoshikawa et al. 2009).

The importance of autophagic processes in methanol and ethanol tolerance is also suggested by our study, a role that can be related with cell protection against DNA and other macromolecules and organelle damaging (Kroemer et al. 2010; Reggiori and Klionsky 2013). In fact, autophagy is considered a central component of the integrated stress response (Kroemer et al. 2010). Reticulophagy, a type of selective autophagy (Reggiori and Klionsky

2013), is an enriched biological function in both datasets. These results are consistent with previous studies reporting that ethanol exposure can lead to endoplasmic reticulum stress, contributing to impaired protein folding and inducing the unfolded protein response (Miyagawa et al. 2014). Methanol also decreases the level of hydration of proteins, leading to tertiary structure modifications, in which polar groups are exposed and can interact mutually (Chen et al. 1995; Skrzydlewska 2003). Formaldehyde, due to reaction with the amino- and sulfhydryl-groups in small molecules, peptides, proteins and nucleic acids, contributes to the formation of inter- and intramolecular bridges (Bolt 1987; Skrzydlewska 2003). These conformational changes, caused by methanol or formaldehyde, are comparable to the effect of ethanol inducing endoplasmic reticulum stress, consistent with a common cellular response to these alcohols. The *de novo* synthesized proteins from the endoplasmic reticulum, destined for secretion from the cell, endocytic processes or to the plasma membrane are delivered to the Golgi apparatus (Banfield 2011). The retention of proteins in the Golgi apparatus, suggested by specific methanol and ethanol tolerance determinants obtained in the two datasets of this study, in particular *DID4*, *VPS1*, *VPS27*, *VPS36*, *VPS4*, *VPS5* genes, corroborates the occurrence of changes in protein structure induced by the alcohols linking protein defects due to alcohol exposure to protein sequestration in the Golgi. Furthermore, the processes of intracellular trafficking, including vacuolar protein targeting, endosome transport, and transport mediated by the endosomal sorting complexes needed for transport (ESCRT-I, -II, and -III), as well as ubiquitin-dependent protein sorting to the vacuole, were found to confer methanol tolerance, similarly to what was described for ethanol (Kubota et al. 2004; Fujita et al. 2006; van Voorst et al. 2006; Auesukaree et al. 2009; Teixeira et al. 2009). The endosomal sorting complexes, as well as ubiquitin-dependent sorting to the vacuole, are important for degradation of methanol/formaldehyde and ethanol induced misfolded proteins that likely suffer damage due to alcohol toxicity.

Concerning the putative regulatory networks involved in methanol tolerance, twelve TFs were identified in our chemogenomic analysis. Five of them are relevant to overcome the stress induced by either methanol or ethanol: Cbf1, Rpn4, Sfl1, Sfp1 and Ume6. Regarding Rpn4 and Sfp1, these TFs reportedly confer tolerance to a wide variety of environmental stresses (Dohmen et al. 2007; Ma and Liu 2010; Chen et al. 2016). The regulation data available in Yeastract pointed out Rpn4 as a major regulator: 5834 genes of yeast genome are under Rpn4 control and above 90 % of the alcohol tolerance genes present in both datasets are known to be under Rpn4 regulation. This TF was previously reported to be activated by ethanol shock (Alexandre et al. 2001) or short exposure to this alcohol (Bubis et al. 2020). Rpn4 stimulates the expression of proteasome subunit genes as well as of genes involved DNA repair (Dohmen et al. 2007), which are enriched biological functions in the methanol dataset. The regulation of the DNA-damage response is also dependent on Sfp1 (Marion et al.

2004), that was previously identified as an ethanol tolerance determinant (Teixeira et al. 2009). Cbf1 regulates around 80% of methanol and ethanol datasets, being the second major regulator of alcohol tolerance genes. The Yeastract tool “Rank by TF”, enabling automatic selection and ranking of transcription factors potentially involved in the regulation of the genes of methanol and ethanol datasets, attributed a significant p-value to Cbf1 and Rpn4 (<0.05 in both datasets) and for Sfp1 (<0.06 and 0.08, in methanol and ethanol datasets, respectively). These results emphasize the importance of these TFs in the regulation of methanol and ethanol tolerance genes and its potential as candidates for alcohol tolerance engineering. The genetic engineering of TFs has been proposed as an important approach for improvement of yeast tolerance to several toxicants. Successful approaches using this strategy includes Haa1 engineering to increase *S. cerevisiae* acetic acid tolerance (Swinnen et al. 2017) or the tolerance to a mixture of acetic acid and furfural by the increased co-expression of Haa1 and Tye7 (Li et al. 2020) or Ace2 and Sfp1 (Chen et al. 2016). To improve methanol and ethanol tolerance, Cbf1, Rpn4 and Sfp1 are promising molecular targets of genetic engineering. Recently, the heterologous expression of IrrE, a global regulatory protein from the prokaryotic organism *Deinococcus radiodurans*, was engineered to improve yeast tolerance to inhibitors present in lignocellulose hydrolysates or to high temperatures (Wang et al. 2020a).

Concerning the TFs encoded by genes only found in the methanol dataset, *GLN3*, *IXR1*, *NGG1*, *OPI1*, *RPH1*, *SOK2* and *STB5*, they are involved in several bioprocesses, such as nitrogen catabolism (Scherens et al. 2006), oxygen sensing (Vizoso-Vázquez et al. 2012), histone acetylation and demethylation (Eberharter et al. 1999; Klose et al. 2007), lipid biosynthesis (Sreenivas and Carman 2003), autophagy (Bernard et al. 2015), pseudohyphal growth (Pan and Heitman 2000) and oxidative stress response (Larochelle et al. 2006).

Ixr1 and Opi1 are suggested to play a significant role in methanol tolerance since the corresponding deletion mutants exhibited a marked methanol susceptibility phenotype. Ixr1 is a transcriptional repressor of hypoxic genes' transcription during normoxia (Vizoso-Vázquez et al. 2012) and in the corresponding deletion mutant, *ixr1Δ*, the expression of genes related to ribosomal genes are downregulated (Vizoso-Vázquez et al. 2018). Ixr1 also controls the levels of dNTPs in the cell required for DNA synthesis and repair (Tsaponina and Chabes 2013). Also, *IXR1* may be involved in the oxidative stress response, since the mutant *ixr1Δ* is more susceptible to peroxides (Castro-Prego et al. 2010) and its promoter region has a binding site for *STB5*, a regulator of the oxidative stress response (Vizoso-Vázquez et al. 2018). Opi1 is a transcriptional repressor involved in the regulation of phospholipid synthesis in response to inositol availability (Sreenivas and Carman 2003). The deletion of the *OPI1* gene was found to jeopardize mitochondrial metabolism, by decreasing the levels of cardiolipin by 50%, resulting in low cytochrome content and high mitochondrial DNA instability (Luévano-Martínez et al. 2013). Our results suggest, for the first time, the importance of mitochondrial genome in

methanol tolerance, similarly to what has been proposed for ethanol (Jiménez and Benítez 1988; Teixeira et al. 2009). Given that *IXR1* is involved in the regulation of around 30% of the genes in the methanol dataset, including other transcription factors encoding genes (*OPI1*, *RPH1*, *SFP1*, *SOK2*, *STB5* and *UME6*) (Chua et al. 2006; Reimand et al. 2010; Vizoso-Vázquez et al. 2012; Vizoso-Vázquez et al. 2018) and the deletion mutant exhibits a strong methanol susceptibility phenotype, this regulator, together with Opi1 can be considered promising candidate for TF engineering in *S. cerevisiae*.

Methanol oxidation is accompanied with the production of free radicals in complex eukaryotes (Skrzydłowska 2003) and, in yeast, oxidative stress was pointed out as a major consequence of exposure to methanol (Yasokawa et al. 2010). Formic acid is also an oxidative stress inducer and, in mammals, formate binds to cytochrome c, inhibiting the last step of the electron transport chain in mitochondria (Iwaki and Rich 2004) and to the disruption of the proton gradient and the consequent decrease of ATP synthesis (Nicholls 1975). In yeast, formic acid can lead to the rapid burst of intracellular reactive oxygen species (Lin 2012) and, consequently, to oxidative stress (Guo and Olsson 2016). Besides *IXR1* and *STB5*, other oxidative stress responsive genes were found to be determinants of methanol tolerance, including genes encoding antioxidant enzymes such as superoxide dismutase (Sod1), methionine- S-sulfoxide reductase (Mrx2), peroxiredoxin (Prx1) as well as Gsh1, a gamma glutamylcysteine synthetase involved in the first step of glutathione biosynthesis. Also, two transporters, Fen2 and Mch5 involved in overcoming oxidative stress (Wojtczak and Slyshenkov 2003; Ashoori and Saedisomeolia 2014) are relevant due to the inability of the corresponding deletion mutants to grow in methanol. Fen2 is a H⁺-pantothenate (vitamin B5) symporter (Stolz et al. 1999) and mutations in *FEN2* lead to reduced biosynthesis of ergosterol and fatty acids (Stolz et al. 1999), which emphasizes the importance of membrane composition and properties in methanol tolerance. In addition, the *Corynebacterium glutamicum* Cgl0833, a Na⁺/pantothenate symporter, is required for methanol tolerance (Wang et al. 2020b). Mch5 is a transporter from the major facilitator superfamily that proceeds to the uptake of riboflavin (Reihl and Stolz 2005), a vitamin that is required for the activity of glutathione reductase in the FAD coenzyme form (Ashoori and Saedisomeolia 2014). Although many important TFs for methanol tolerance were identified in this genome-wide study, the major regulator of the response to oxidative stress, Yap1 were not identified but, for higher levels of methanol stress, *YAP1* expression was confirmed as a critical methanol tolerance determinant.

Despite the potential of methanol as a (co)substrate for the biotechnology industry, the global mechanisms by which this alcohol exerts its toxicity are still unclear. Based on the results from this study and on the above referred discussion, a schematic model on the hypothesized methanol toxicity and tolerance mechanisms are presented, specifying the more specific mechanisms and those shared with ethanol (Figure 2.9, A). The reported toxicity

mechanisms of the detoxification intermediates formaldehyde and formic acid are also included (Figure 2.9, B).

Results from this genome-wide search for methanol tolerance genes can also be explored for the rational genomic manipulation of the yeast cell to obtain more robust strains capable of coping with high methanol or high methanol and ethanol concentrations by exploring information on a cumulative inhibitor tolerance phenotype, as recently reported for *S. cerevisiae* engineering towards improved tolerance to for the multiple inhibitors present in lignocellulosic-based fermentations (Brandt et al. 2020). Since TFs engineering is an emerging strategy to increase yeast tolerance to different biotechnological relevant stresses (Chen et al. 2016; Swinnen et al. 2017; Li et al. 2020), it would be interesting to explore the modulation of the expression or the alteration of the amino acid sequence of the TFs here identified as promising (Figure 2.9, C). Among them are Cbf1, Rpn4 and Sfp1, for alcohol tolerance, and Ixr1 and Opi1, specifically for methanol tolerance. The knowledge here obtained, and the list of genes provided in this study can be considered an important starting point for the improvement of yeast tolerance to methanol or to methanol and ethanol in biotechnologically relevant yeast species for which the necessary genome sequence and editing tools are currently available or could be developed. The exploitation of the bioinformatics tool NCYeast database (Non- Conventional Yeast; <http://yeastract-plus.org/ncyeastract/>) (Monteiro et al. 2020) will facilitate the identification of orthologous genes in the yeast species currently included in the database as well as the regulatory associations already described for other yeast species, especially for *S. cerevisiae* in the sister database Yeast (http://yeastract-plus.org/yeastract/scerevisiae/index.php), using the new tools for cross-species transcription regulation comparison (Monteiro et al. 2020). In particular, this is currently an useful resource to guide the genetic engineering of biotechnologically relevant yeasts, such as the methylotrophic yeast species *Komagataella phaffii* and the oleaginous yeast species *Yarrowia lipolytica* (Monteiro et al. 2020).

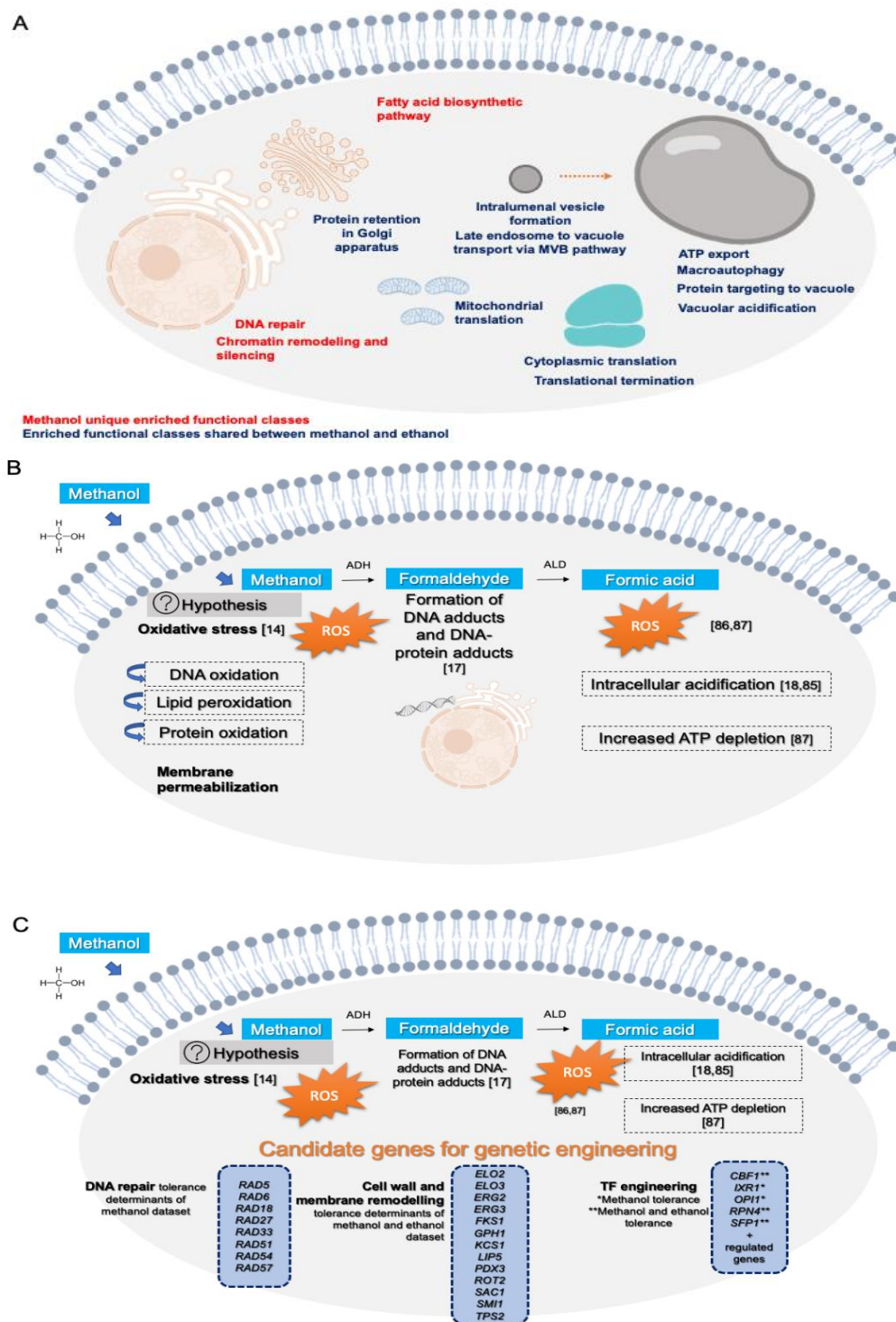


Figure 2. 9- Schematic model proposed, for methanol toxicity, including the detoxification intermediates formaldehyde and formic acid. (A) Biological functions found to be enriched in the methanol dataset. The biological functions shared with the ethanol dataset are in blue and the enriched biological functions, specific to the methanol dataset, are in red. (B) Methanol detoxification pathway and the anticipated toxic effects of each metabolic intermediate, in particular having DNA as an important molecular target for the formic acid-induced ROS [86] and formaldehyde alkylating activity. (C) To overcome the effects of methanol in yeast cells, DNA repair mechanisms play an important role in preserving DNA integrity after methanol exposure; mechanisms found to be relevant for methanol tolerance involve, among others, the RAD genes, and other genes involved in DNA repair and in the oxidative stress response. Several TFs found to confer methanol tolerance are additional potential targets for genetic engineering to obtain more robust strains, able to cope with deleterious concentrations of methanol.

3. Efficient utilization of all carbon sources present in sugar beet pulp hydrolysates by the oleaginous red yeasts *Rhodotorula toruloides* and *R. mucilaginosa*

This Chapter was submitted to the Journal of Fungi (for the Yeast Biorefineries special issue):

Martins, L.C., Palma, M., Angelov, A., Nevoigt, E., Liebl., W., Sá-Correia, I., (2021) *Efficient utilization of all carbon sources present in sugar beet pulp hydrolysates by the oleaginous red yeasts *Rhodotorula toruloides* and *R. mucilaginosa*. Journal of Fungi. (under revision)*

3.1 ABSTRACT

Agro-industrial residues are low-cost carbon sources (C-sources) for microbial growth and production of value-added bioproducts. Among the agro-industrial residues available, those rich in pectin are generated in high amounts worldwide from the sugar industry or the industrial processing of fruits and vegetables. Sugar beet pulp (SBP) hydrolysates contain predominantly the neutral sugars D-glucose, L-arabinose and D-galactose and the acidic sugar D-galacturonic acid. Acetic acid is also present at significant concentrations since the D-galacturonic acid residues are acetylated. In this study, we have examined and optimized the performance of a *Rhodotorula mucilaginosa* strain, isolated from SBP and identified at the molecular level during this work. This study was extended to another oleaginous red yeast species, *R. toruloides*, envisaging the full utilization of the C-sources from SBP hydrolysate (at pH 5.0). The dual role of acetic acid as carbon and energy source and as a growth and metabolism inhibitor was examined. Acetic acid prevented the catabolism of D-galacturonic acid and L-arabinose after the complete use of the other C-sources. However, D-glucose and acetic acid were simultaneously and efficiently metabolized, followed by D-galactose. SBP hydrolysate supplementation with amino acids was crucial to allow D-galacturonic acid and L-arabinose catabolism. SBP valorization through the production of lipids and carotenoids by *Rhodotorula* strains, supported by complete catabolism of the major C-sources present, looks promising for industrial implementation.

3.2 INTRODUCTION

The implementation of a circular bio-economy based on the efficient bioconversion of agro-industrial residues by selected yeast species/strains is an important societal challenge (Zuin et al. 2018; Rebello et al. 2018; Martins et al. 2020). Agro-industrial residues can serve as low-cost raw material for the biotechnology industry; these organic wastes are sources of carbon, nitrogen and other nutrients for microbial growth and metabolite production while decreasing their negative effects as environmental pollutants (Cherubini 2010; Dahiya et al. 2018). Among the agro-industrial residues available, those rich in pectin (e.g. sugar beet pulp, citrus peels, apple pomace) have potential as feedstocks for the production of biofuels and other industrial bioproducts (Martani et al. 2020; Martins et al. 2020). They are generated in high amounts worldwide from the sugar industry or the industrial processing of fruits and vegetables (Peters 2006). Moreover, they are partially pre-treated and have a low lignin content thus facilitating biomass processing for saccharification and fermentation (Berlowska et al. 2018).

Pectin substances are complex heteropolysaccharides and structural components of plant cell walls, having backbone chains of partially methylated α -1,4 linked D-galacturonic acid (homogalacturonan, rhamnogalacturonan II, xylogalacturonan) or D-galacturonic acid and rhamnose (rhamnogalacturonan I), with sugar beet pectin consisting mainly of homogalacturonan, rhamnogalacturonan I and rhamnogalacturonan II (Mohnen 2008; Leijdekkers et al. 2013). The pectin structure complexity depends on variations in methylesterification and acetylation as well as the variety of glycosidic side chains attached to the backbone. These glycosidic side chains are composed of neutral sugars that include L-arabinose, D-xylose, D-galactose, L-rhamnose, L-fucose and D-glucose, among others, linked to D-galacturonic acid and rhamnose units. In particular arabinose from the branched pectic arabinan side chains of rhamnogalacturonan-I represents a significant percentage of the sugar beet pulp dry matter (Mohnen 2008; Leijdekkers et al. 2013). After the pre-treatment of pectin-rich agro-industrial residues, the enzymatic or acidic hydrolysis of cellulose, hemicellulose and pectin structures allow the release of monomeric sugars that can subsequently be converted by yeasts into a wide range of bioproducts (Hamley-Bennett et al. 2016; Berlowska et al. 2017). The D-galacturonic acid residues can be methyl-esterified at the C-6 carboxyl group and/or acetylated at C-2 or C-3, and neutralized by ions, like sodium, calcium or ammonium (Sakai et al. 1993b). Therefore, after the hydrolysis of pectin-rich residues, the acetate and methanol generated in the process are present in the hydrolysates and, depending on the concentrations reached, these toxic compounds can inhibit yeast growth and biosynthetic activity (Martins et al. 2020). The hydrolysates made from pectin-rich biomass may also contain additional inhibitory compounds such as other weak acids, furan derivatives and phenolic compounds,

at different concentrations, depending on the way of processing (Palmqvist and Hahn-Hägerdal 2000). Heavy metals and pesticides (fungicides, herbicides and insecticides) used in agriculture are other potential inhibitors of yeast metabolism often present in the hydrolysates (Martins et al. 2020). Although the toxicity of some of these compounds at the concentrations present in hydrolysates of pectin-rich residues can be relatively low individually, their toxic effects can be additive or even synergistic, and in combination they may therefore seriously compromise bioprocesses utilizing this feedstock (Palmqvist and Hahn-Hägerdal 2000; Teixeira et al. 2011; dos Santos and Sá-Correia 2015).

Although *Saccharomyces cerevisiae* is the most important yeast cell factory in the biotechnology industry and the major cell factory platform for the production of bioethanol and other biofuels and chemicals in advanced biorefineries (Satyanarayana and Kunze 2009b; Nielsen 2019), the interest in non-*S. cerevisiae* yeast species with higher catabolic and biosynthetic versatility and tolerance to bioprocess-related stresses is gaining momentum (Rebello et al. 2018). The large and heterogeneous group of nonconventional yeasts includes species/strains with desirable properties for their utilization as cell factories for the synthesis of a wide range of added-value products from a range of carbon sources present in biomass hydrolysates (Radecka et al. 2015; Diaz et al. 2018). In the case of pectin-rich residues, the efficient and complete utilization by the selected yeast species of the whole mixture of sugar monomers present in the hydrolysates is essential for their economical valorization in industrial biotechnology. Sugar beet pulp hydrolysates contain predominantly the neutral sugars D-glucose, L-arabinose and D-galactose and the acidic sugar D-galacturonic acid (Micard et al. 1996; Berłowska et al. 2018). Due to carbon catabolite repression (CCR) (Kayikci and Nielsen 2015), these sugars are not simultaneously utilized, which presents another challenge. In fact, CCR leads to inhibition of the uptake and catabolism of the secondary carbon sources, i.e. L-arabinose, D-galacturonic acid, D-xylose, in the presence of the preferred substrate, i.e. D-glucose, prolonging the fermentation time due to the sequential, rather than simultaneous use of all the carbon sources (Huisjes et al. 2012; Wu et al. 2016).

Pectin-rich hydrolysates contain a significant amount of D-galacturonic acid that is neither naturally used by *S. cerevisiae*, nor by other yeast species used in biotechnology, such as *Kluyveromyces marxianus*, *Yarrowia lipolytica* or *Scheffersomyces (Pichia) stipitis*. D-Galacturonic acid is the most challenging sugar to be catabolized, followed by L-arabinose. Several efforts have been dedicated to the development of genetically engineered *S. cerevisiae* strains able to use D-galacturonic acid (Benz et al. 2014; Matsubara et al. 2016; Biz et al. 2016; Protzko et al. 2018; Jeong et al. 2020) and L-arabinose (Wisselink et al. 2007; Ye et al. 2019) by expression of their catabolic pathways. L-Arabinose is a neutral sugar that is also present in significant amounts in pectin-rich hydrolysates. However, since D-galacturonic acid is more oxidised than the neutral hexose and pentose sugars, the

fermentation of D-galacturonic acid to ethanol and CO₂ is not redox neutral, as opposed to that of D-glucose and related sugars. D-Galacturonic acid thus requires more NAD(P)H for its catabolism than generated in its fermentation (Richard and Hilditch 2009). Therefore, despite the successful expression in *S. cerevisiae* of enzymes and a membrane transporter comprising a heterologous D-galacturonic acid catabolic pathway using genes from the filamentous fungi *Aspergillus niger* and *Trichoderma reesei*, sufficient regeneration of NADPH has remained a challenge (Biz et al. 2016; Protzko et al. 2018). An interesting alternative to *S. cerevisiae* metabolic engineering is the exploitation of nonconventional yeasts for pectin-rich residues' bioconversion especially if they are intrinsically able to efficiently use all the carbon sources present in the hydrolysates and to produce relevant added-value compounds (Rebello et al. 2018). Among those promising yeasts, is the basidiomycete red yeast *Rhodotorula toruloides* (formerly known as *Rhodospiridium toruloides*), which has an efficient D-galacturonic acid catabolism (Protzko et al. 2019) and is a potential industrial platform organism for biodiesel and carotenoid production (Park et al. 2018). Industrial production of lipids by oleaginous red yeasts has been considered competitive with plant oil-derived products (e.g. biodiesel), since their production is cleaner and more sustainable (Cárdenas-Fernández et al. 2017; Jones et al. 2019). *Rhodotorula* strains are also producers of carotenoids used in the food, pharmaceutical and cosmetics industries (e.g. β-carotene, torulene and torularhodin) (Kot et al. 2018).

In this study, we have examined and optimized the performance of a *Rhodotorula mucilaginosa* strain, isolated from sugar beet pulp and identified at the molecular level during this work, envisaging the full utilization of the carbon sources present in SBP hydrolysate. The study was extended to two promising *Rhodotorula toruloides* strains for bioproduction of lipids and carotenoids (Park et al. 2018; Protzko et al. 2019). SBP hydrolysate supplementation with amino acids was found to be crucial for the efficient catabolism of both D-galacturonic acid and L-arabinose. The dual role of the acetic acid present in SBP hydrolysates as i) an additional source of carbon and energy for growth and ii) an inhibitor for growth and metabolism, was also examined. This study provides strong evidence that the concept of SBP valorization through the production of lipids and carotenoids by *Rhodotorula* spp. from the complete catabolism of all major C-sources present in SBP hydrolysates, is promising for implementation in an economical biotechnological process.

3.3 MATERIALS AND METHODS

3.3.1 Identification Isolation and identification of *Rhodotorula mucilaginosa* IST 390 from sugar beet pulp

The strain *Rhodotorula mucilaginosa* IST 390 used in this study was isolated from a sample of sugar beet pulp (SBP), a kind gift from the Belgian sugar company Tiense Suikerraffinadarij N.V. Raffinerie Tirlémontoise S.A., obtained in the context of the YEASTPEC EraNet IB Project. This SBP sample was kept frozen at -20°C until use. For yeast isolation, 50 g of SBP were mixed with 500 mL of sterile water and chloramphenicol (100 µg/mL) to prevent bacterial growth. This mixture was incubated at 30°C, with orbital agitation (250 rpm) for one week. After this period, the mixture was serially diluted and plated on YPD agar (Yeast extract 1 % (Difco), Peptone 2 % (Difco), D-Glucose 2 % (Merck), Agar 2 % (Merck)) supplemented with chloramphenicol (100 µg/mL). Plates were incubated for 2-4 days at 30°C. A pink colony identified on the surface of the YPD agar plate was streaked onto a fresh YPD agar plate and incubated under the same conditions to confirm its purity. This yeast isolate IST 390 was maintained at 4°C until DNA extraction was performed. For long-term storage, the isolate was preserved at -80 °C in YPD medium containing 15% (v/v) glycerol.

For the molecular identification of IST 390 isolate, genomic DNA was extracted using the phenol:chloroform:isoamyl alcohol method (Hoffman 1997) and used as a template for the amplification of the D1/D2 domain sequence of the 26S ribosomal DNA (rDNA) and the internal transcribed spacer (ITS) region of rDNA. Polymerase Chain Reaction (PCR) was performed, respectively, using primer pairs NL-1 (5'-GCATATCAATAAGCGGAGGAAAAG-3') and NL-4 (5'-GGTCCGTGTTTCAAGACGG-3'), and ITS1 (5'-TCCGTAGGTGAACCTGCGG-3') and ITS4 (5'-TCCTCCGCTTATTGATATGC-3') shown to be effective for the taxonomic identification of yeasts (Kurtzman and Robnett 1998). The two DNA fragments were purified using NZYGel pure (NZYtech, Portugal) and Sanger-sequenced (Stabvida Portugal) using each corresponding primer. Isolate IST 390 was identified by comparing its D1/D2 and ITS sequences with those deposited in GenBank using the BLAST algorithm from the National Center for Biotechnology Information (NCBI) (<http://www.ncbi.nlm.nih.gov/blast>). The consensus sequences from D1/D2 and ITS rDNA regions were deposited in GenBank under the accession numbers MW547775 and MW547772, respectively.

3.3.2 Yeast strains, growth media and conditions

The yeast strains *Rhodotorula mucilaginosa* IST 390, *Rhodospiridium toruloides* PYCC 5615, a conjugated strain derived from IFO 0559 x IFO 0880 (Banno 1967) and obtained from the Portuguese Yeast Culture Collection, and *R. toruloides* IFO 0880, a robust host for lipid overproduction and genome-scale metabolic model (Banno 1967; Dinh et al. 2019) obtained from Belgian Coordinated Collections of Microorganisms, were used in this study.

A growth medium mimicking sugar beet pulp (SBP) hydrolysate was prepared adding either i) 6.7 g/L of Yeast Nitrogen Base (YNB; including 5 g/L ammonium sulphate and amino acids 10 mg/L of L-histidine, 20 mg/L DL-methionine and 20 mg/L DL-tryptophan) (Fisher Scientific), or ii) 1.7 g/L Yeast Nitrogen Base (without ammonium sulphate and amino acids) (Fisher Scientific) supplemented with 5 g/L of ammonium sulphate or iii) 1.7 g/L of Yeast Nitrogen Base (without ammonium sulphate and amino acids) (Fisher Scientific) supplemented with 5 g/L of ammonium sulphate and the amino acids in i). The three media were used to allow different manipulations of the components. They were supplemented with a mixture of carbon sources composed of D-glucose (10 g/L), L-arabinose (12 g/L), D-galactose (3 g/L), D-galacturonic acid (10 g/L) and acetic acid (35 mM, equivalent to 2.1 g/L when the objective was to mimic SBP hydrolysate). The concentration of each carbon source was defined based on its concentration in SBP hydrolysates H11 and H13 (Table 3.1) and in other batches prepared as described below. Initial medium pH was adjusted to 5.0 using a solution of 10M NaOH and sterilized by filtration using a 0.2 µm filter (Whatman® Puradisc).

The SBP hydrolysate-based media were prepared using the SBP hydrolysates H11 or H13 prepared as described below and filter-sterilized using a 0.2 µm flow bottle top filter. These media consisted of either: i) SBP hydrolysate at pH 5.0 (adjusted using 10M NaOH) supplemented with 5 g/L of ammonium sulphate; or ii) SBP hydrolysate supplemented with 6.7 g/L of Yeast Nitrogen Base (Fisher Scientific) containing, among other components, 5 g/L of ammonium sulphate and 10 mg/L of L-histidine, 20 mg/L DL-methionine and 20 mg/L DL-tryptophan; iii) or SBP hydrolysate supplemented with 1.7 g/L of Yeast Nitrogen Base (without ammonium sulphate or amino acids), supplemented with different concentrations of ammonium sulphate (1, 2.5 or 5 g/L), and the amino acids present in ii). These compounds were added to iii) from stock solutions at the indicated final concentrations, depending on the objective.

For yeast cultivation in SPB hydrolysate-based media (using batches H11 or H13), yeast strains were pre-cultured for 12 h in YPD liquid medium (Yeast extract 1 % (Difco), Peptone 2 % (Difco), D-Glucose 2 % (Merck)) at pH 5.0) (50 mL of medium in 100 mL shake flasks) at 30°C with orbital shaking (250 rpm). After pre-cultivation, yeast cells were grown in the same medium and conditions and harvested in the mid-exponential phase of growth by

centrifugation (5000 g, 10 min), washed twice with sterile water and inoculated at an $OD_{600nm}=4\pm 0.1$ or $OD_{600nm}=8\pm 0.1$, in 25 mL SBP hydrolysate (pH 5.0), with or without supplementation with Yeast Nitrogen Base (Fisher Scientific), and with or without ammonium sulphate or amino acids, depending on the experiment. Cultivations were performed in cotton-plugged 50 mL flasks with 25 mL of medium, at 30°C with orbital shaking (250 rpm). Yeast growth was followed by periodically measuring the optical density during 120-150 h. Culture samples were collected at different time points to determine the extracellular concentration of carbon sources and metabolites.

3.3.3 Effect of acetic acid concentration on yeast growth and carbon source catabolism

The effect of acetic acid on the growth profile and carbon source catabolism by *Rhodotorula mucilaginosa* IST 390 and *Rhodospiridium toruloides* PYCC 5615 was tested using the mixed-sugar medium (in YNB with ammonium and amino acids) mimicking SBP hydrolysate but supplemented with increasing concentrations of acetic acid (0, 20 and 40 mM), adjusted to pH 5.0 with 10M NaOH. Cell inocula with exponentially growing cells were prepared as described above and cells were inoculated at an initial $OD_{600nm}=4\pm 0.1$. Cultivation and sampling were performed as described above.

3.3.4 Preparation of sugar beet pulp hydrolysate

For the preparation of the SBP hydrolysate H13, a 10 L fermenter reaction vessel was filled with 2.67 kg (wet weight) of pressed SBP from the 2017 sugar beet campaign received from Raffinerie Tirlémontoise, and water was added to a volume of 9 L. The mixture in the fermenter was autoclaved (20 min, 121 °C) and connected to the controller of a Biostat B fermenter (Sartorius, Göttingen, Germany). For enzymatic hydrolysis, 5 mL of Viscozyme L and 5 mL Celluclast (Sigma-Aldrich, Missouri, USA) were added and the mixture was continuously stirred (4000 rpm) at 40 °C. Prior to use, the commercial enzyme preparations were deprived of low molecular mass solutes by gel filtration chromatography with a PD-10 desalting column (GE Healthcare, Chicago, USA) using 25 mM sodium phosphate buffer pH 6.0 as the eluent, resulting in a 1.4-fold dilution of the original enzyme cocktails, and were filtered with a FiltropurS PES 0.45 µm syringe filter (Sarstedt, Nümbrecht, Germany). After 24 h, another 5 mL of each of the Viscozyme L and Celluclast preparations was added followed by further incubation (40°C, 4000 rpm, 24 h) after which most of the particulate material was

degraded. After centrifugation (20 min, 5400 g) the supernatant was filtered using Whatman Folded Filters 597½ (GE Healthcare, Chicago, USA) followed by filter-sterilization with a 0.2 µm Flow Bottle Top Filter (Thermo Fisher Scientific, Massachusetts, USA). The SBP hydrolysate H11 was generated as described for H13 but on 1/10 the scale in a volume of 1 L.

The composition of the different hydrolysates obtained exhibited some variation. The composition of the two different batches (H11 and H13) used in this study is shown in **Table 3.1**. These hydrolysates were prepared at the Technical University of Munich laboratory.

Table 3. 1- Composition of the two Sugar Beet Pulp hydrolysate batches used in this study

SBP hydrolysate	D-Glucose g/L	D-Galactose g/L	L-Arabinose g/L	D-Galacturonic acid g/L	Acetic Acid mM (g/L)
H11	9.4	4.8	13.1	11.3	33.5 (2.0)
H13	6.7	2.2	9.3	9.4	32.0 (1.9)

3.3.5 Determination of concentrations of sugars and acetic acid

Culture samples periodically collected were centrifuged (9700 g, 3 min) in a microcentrifuge MiniSpin Plus (Eppendorf) and 100 µL of the supernatant was pipetted into high-performance liquid chromatography (HPLC) vials and diluted with 900 µL of 50 mM H₂SO₄. The concentration of carbon sources present in each sample was determined by HPLC (Hitachi LaChrom Elite), using a column Aminex HPX-87H (Bio-Rad) coupled with UV/visible detector (for D-galacturonic acid and acetic acid detection) and refractive index detector (for D-glucose, L-arabinose and D-galactose detection). Ten microliter of each sample was loaded on the column and eluted with 5 mM H₂SO₄ as mobile phase at a flow rate of 0.6 mL/min for 30 min. The column and refractive index detector temperature was set at 65°C and 40°C, respectively. The concentration of each sugar and of acetic acid was calculated using calibration curves prepared for each compound.

3.3.6 Assessment of lipid production

The production of lipids was assessed by Nile Red staining as previously described (Kumar et al. 2020) with minor modifications. Yeast cells cultivated in 25 mL of SBP hydrolysate supplemented with 1.7 g/L of YNB (without ammonium sulphate and amino acids), 2.5 g/L of ammonium sulphate and 10 mg/L of L-histidine, 20 mg/L DL-methionine and 20 mg/L DL-tryptophan in 50 mL shake flasks were collected by centrifugation (9700 g for 3 min), washed twice with 10 mM potassium phosphate buffer (PBS) (pH 7.0), and the cells were resuspended in 1 mL of PBS with OD_{600nm} adjusted to 1.0. This cell suspension (with $OD_{600nm} = 1$) was mixed with Nile Red (Sigma-Aldrich) solution (2.5 $\mu\text{g/mL}$) (stock solution prepared in dimethyl sulphoxide (DMSO) and acetone (1:1)) followed by microwave treatment (1150 watts power, 30 s). A total of 100 μL , of each cell suspension normalized to $OD_{600nm} = 1$ and containing the Nile Red fluorescence dye, was transferred to a black 96-well optical plate (Thermo Fisher Scientific, NY, USA) and relative fluorescence units (RFU) were measured using a FilterMax F5 Multi-Mode Microplate Reader (Molecular Devices) using the excitation and emission wavelengths of 535 and ~ 625 nm, respectively. Relative neutral lipid content was represented as RFU. Fluorescence measurements were performed for two biological replicates and three technical replicates.

For microscopic observation of lipid droplets inside the yeast cells, 5 μL of the cell suspension previously stained with Nile Red was examined with a Zeiss Axioplan microscope equipped with adequate epifluorescence interface filters. Fluorescence emission was collected with a coupled device camera (AxioCam 503 colour; Zeiss), and the images were analysed with ZEN 2 Microscope Software (Zeiss). The exposure time was kept constant among microscopic analyses and intensity measurements were background-corrected.

3.3.7 Assessment of carotenoid production

Carotenoid production was assessed after 144 h of yeast cultivation in SBP hydrolysate H13. Cells were collected by centrifugation (5000 g, 15 min) and the pellet was lyophilized during 48 h using a freeze dryer (CoolSafe 55-4 – ScanVac). The dried pellets were weighed, as dry cell weight (*dcw*, grams) for total carotenoid content calculation. For carotenoid pigment extraction, disruption of yeast cells was performed by adding 10 mL of acetone and 2 mL of zirconium beads (Sigma-Aldrich; $d = 0.5$ mm) to lyophilized cell pellets, followed by vigorous mixing during 20 min in a vortex (VWR). The suspension was centrifuged (~ 8000 g, 15 min) and the liquid fraction transferred to a clean 15 mL falcon tube, for acetone evaporation. The carotenoid pellet was dissolved in 1 mL of acetone and the concentration determined by optical

absorbance spectroscopy. The absorbance of the coloured suspension was measured at $\lambda = 450$ nm and the carotenoid content determined using the formula:

$$\text{Total carotenoid content } (\mu\text{g} \cdot \text{g}^{-1}) = \frac{A_{total} \times \text{Volume (mL)} \times 10^4}{A_{1cm}^{1\%} \times \text{sample weight(g)}}$$

where A_{total} = Absorbance; Volume = total volume of extract (1 mL); $A_{1cm}^{1\%} = 2500$, which is the absorption coefficient recommended for mixtures of carotenoids (Rodriguez-Amaya, Delia Kimura 2004).

3.3.8 Statistical analysis

All experiments were performed at least twice and results from a representative experiment are shown.

3.4 RESULTS

3.4.1 Isolation of *Rhodotorula mucilaginosa* IST 390 from sugar beet pulp

Sugar beet pulp (SBP) is likely an interesting material for the isolation of different microorganisms since at room temperature SBP can be degraded by the exo- and endopolygalacturonases as well as pectin and pectate lyases produced by filamentous fungi such as *Aspergillus niger* or *Trichoderma reesei* that hydrolyse the pectin backbone (Martens-Uzunova and Schaap 2008). Moreover, the sugars present in the side chains of the pectin backbone and in pectin-derived oligosaccharides are also released by the action of different glycoside hydrolases and lyases (Leijdekkers et al. 2013). In this work, a SBP sample suspended in water with chloramphenicol was used as growth medium for the isolation of yeast strains envisaging the full catabolism of the sugars present in pectin, in particular the more challenging sugars D-galacturonic acid and L-arabinose. Among others, strain IST 390 was isolated, identified and used in this study. The comparison of its D1/D2 and ITS sequences with the sequences deposited in the NCBI database showed that these sequences share 100% identity with the corresponding sequences from *R. mucilaginosa* strains, indicating that strain IST 390 belongs to the *R. mucilaginosa* species. Recent literature has described the potential of *Rhodotorula* sp. for the biosynthesis of lipids and carotenoids from biomass feedstocks (Taskin et al. 2016; Carota et al. 2020). Moreover, *R. toruloides* was demonstrated to have an efficient metabolism for D-galacturonic acid and the underlying molecular basis was elucidated (Protzko et al. 2019). Since D-galacturonic acid is the major and most challenging sugar present in pectin substances, the isolated *R. mucilaginosa* strain IST 390 was selected for further studies involving the bioconversion of sugar beet pulp hydrolysates.

3.4.2 Differential utilization of the carbon sources present in SBP hydrolysate during *R. mucilaginosa* IST 390 and *R. toruloides* PYCC 5615 cultivation

The SBP hydrolysate H11 includes several carbon sources at different concentrations (Table 3.1). Since SBP is a not fully defined rich medium, in the first experiments *R. toruloides* PYCC 5615 and *R. mucilaginosa* IST 390 were cultivated at 30°C in shake flasks with orbital agitation in hydrolysate H11 without extra nutrient supplementation, but with the pH adjusted from pH 3.1 to pH 5.0 to reduce the toxic effect of the acetic acid (Table 3.1). Contrary to our

expectations, neither D-galacturonic acid nor L-arabinose was used after more than 100 h of cultivation even though the other carbon sources were all fully used (results not shown). This result led us to supplement the H11 with ammonium sulphate (5 g/L) to avoid a possible nitrogen limitation. However, as with the unsupplemented hydrolysate, the two strains cultivated in the ammonium sulphate supplemented hydrolysate H11, at 30°C and inoculated at an initial OD_{600nm} of 4, were not able to catabolize most of the D-galacturonic acid and L-arabinose during 120 h of cultivation (**Figure 3.1**).

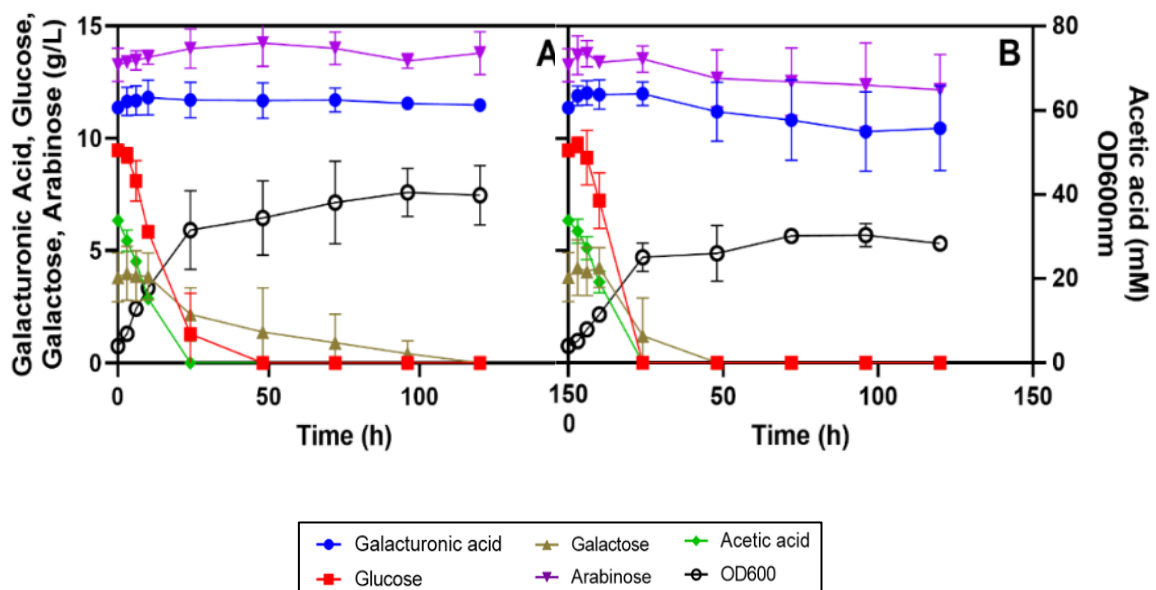


Figure 3. 1- Growth curves and carbon source utilization by A) *Rhodotorula mucilaginosa* IST 390 and B) *Rhodotorula toruloides* PYCC 5615 cultivated in Sugar Beet Pulp (SBP) hydrolysate H11 derived medium. SBP hydrolysate H11 was supplemented with 5 g/L of ammonium sulphate, adjusted to pH 5.0 and inoculated with an initial optical density at 600nm (OD_{600nm}) of 4. Yeast cultivations were performed at 30°C with orbital agitation (250 rpm). The data are means of two independent experiments and bars represent standard deviations.

3.4.3 Sugar utilization from a synthetic-SBP-hydrolysate-medium is affected by acetic acid and improved by amino acid supplementation and inoculum increase

Considering the relatively high levels of acetic acid present in SBP hydrolysates, ranging from 30 to 40 mM (or 1.8 to 2.4 g/L), the possibility that its presence could be interfering with the utilization of D-galacturonic acid and L-arabinose was considered. In fact, this carbon source can also be a strong metabolic inhibitor, depending on its concentration, medium pH and the tolerance of the yeast strain. To test this hypothesis, a synthetic SBP medium was prepared in YNB, with 5 g/L of ammonium and supplemented with representative

concentrations of the sugars present in the SPB hydrolysates obtained in different batches. Interestingly, the absence of acetic acid from this medium allowed the utilization of D-galacturonic acid and of a significant percentage of the L-arabinose (**Figure 3.2-A**). Confirming previous results obtained in SBP hydrolysate, when 40 mM of acetic acid were added to the synthetic medium, the utilization of both sugars was abrogated. This response is consistent with the idea that acetic acid affects not only growth kinetics and D-glucose and D-galactose utilization rates, but hinders the capacity of *R. toruloides* PYCC 5615 to catabolize D-galacturonic acid and L-arabinose (**Figure 3.2-B**).

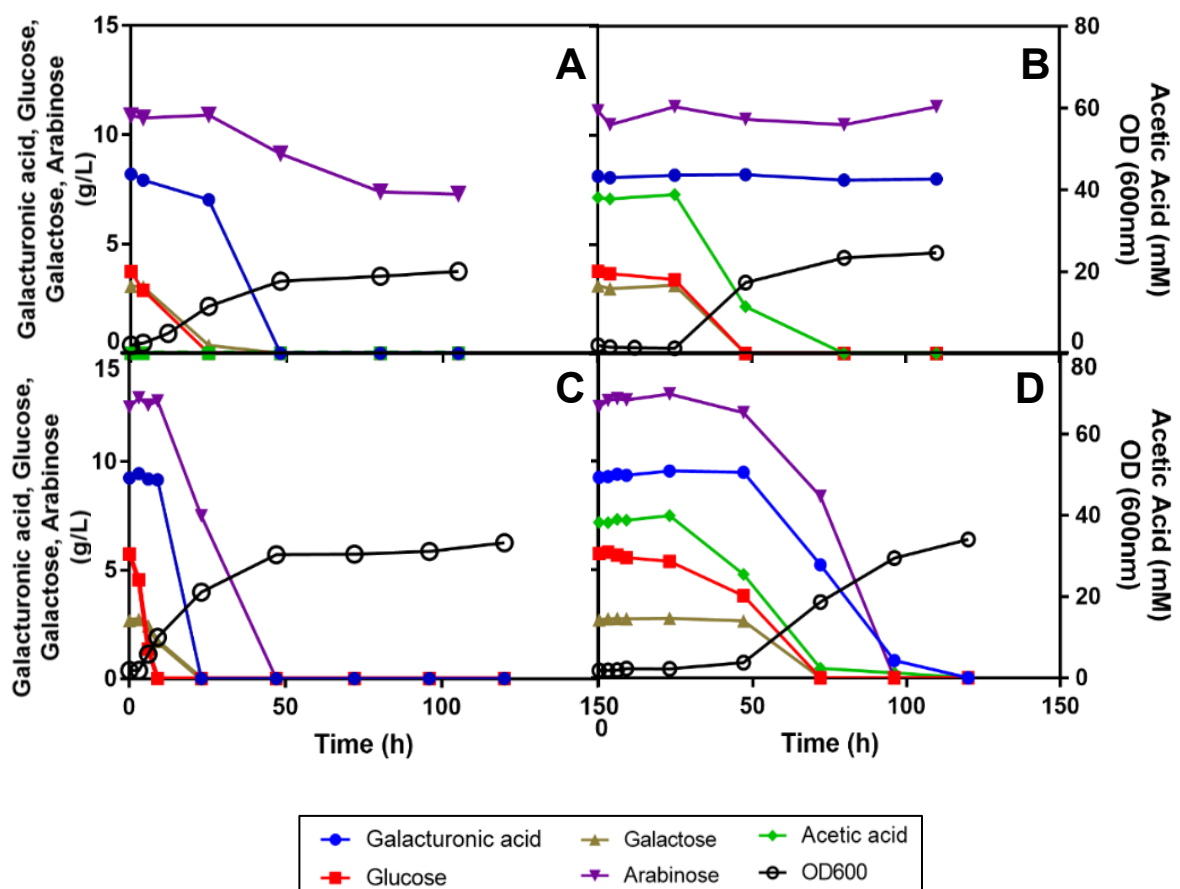


Figure 3. 2- Effect of acetic acid and/or amino acid supplementation of synthetic SPB hydrolysate on the catabolism of different carbon sources by *R. toruloides* PYCC 5615. Growth and carbon-sources utilization profiles by *R. toruloides* PYCC 5615 when cultivated in: (A) mixed-sugar medium (9 g/L D-galacturonic acid, 4 g/L D-glucose, 3 g/L D-galactose, 12 g/L L-arabinose) prepared in Yeast Nitrogen Base (with 5 g/L ammonium sulphate); (B) the same mixed-sugar medium as in (A) supplemented with 40 mM of acetic acid (C) the same mixed-sugar medium as in (A) supplemented with amino acids (10 mg/L of L-histidine, 20 mg/L of DL-methionine and 20 mg/L DL-tryptophan); (D) the same mixed-sugar medium supplemented with amino acids as in (C) and with 40 mM of acetic acid. Media were adjusted at pH 5.0, cultures were inoculated with an initial OD_{600nm} of 2 and cultivation was carried out at 30°C with orbital agitation (250 rpm).

Given that non-conventional yeasts may require nutrient adjustments to enable the catabolism and conversion of different carbon and nitrogen sources into the desired products, a number of nutrient supplementations were considered. When the commercial YNB (with ammonium sulphate and the amino acids L-histidine (10 mg/L), DL-methionine (20 mg/L) and DL-tryptophan (20 mg/L)) was used all the above referred sugars were consumed after 50 h of cultivation (**Figure 3.2-C**). Moreover, when this medium was supplemented with 40 mM of acetic acid, all the sugars were fully consumed after 120 h of cultivation even though at a lower rate, accompanying acetic acid-induced growth inhibition and the induction of 50 h latency (Figure 3.2-D).

To assess the effect of increasing concentrations of acetic acid in growth performance and sugars' catabolism capacity of *R. toruloides* PYCC 5615, this strain was grown in the same synthetic SBP hydrolysate medium in complete commercial YNB (with ammonium and amino acids) supplemented with increasing concentrations (0, 20 and 40 mM) of acetic acid, at pH 5.0. An initial OD_{600nm} of 4 was used to additionally assess the role of this parameter (**Figure 3.3-A, B, C**).

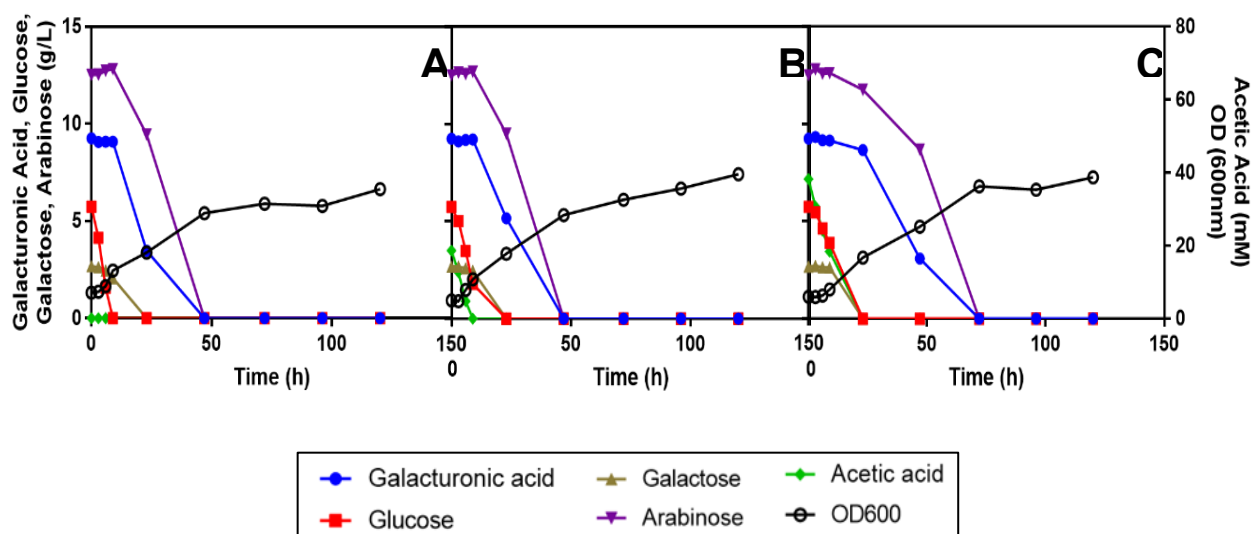


Figure 3.3- Effect of increasing concentrations of acetic acid (0 mM (A), 20 mM (B) and 40 mM (C)) added to the synthetic SBP hydrolysate with the mixture of sugars in commercial YNB (with ammonium sulphate and amino acids) at pH 5.0 in *R. toruloides* PYCC 5615 growth and sugar utilization. All cultures were inoculated with an initial OD_{600nm} of 4 and cultivation was carried out at 30°C with orbital agitation (250 rpm).

Results indicate that in YNB medium with amino acids and when a higher inoculum concentration was used (initial OD_{600nm} of 4.0) the negative impact of acetic acid concentrations below 20 mM at pH 5.0 in *R. toruloides* PYCC 5615 growth performance was negligible (**Figures 3.3-A and 3.3-B**). Moreover, the use of acetic acid as carbon source led to a higher

final biomass concentration. The increase of acetic acid concentration to 40 mM at pH 5.0 led to a slight extension of lag phase up to 6 hours, and to a decrease in yeast growth rate and in the D-galacturonic acid and L-arabinose consumption rates, when compared to growth in the absence of acetic acid (**Figure 3.3-C**). Remarkably, the increase of the concentration of the inoculum had a marked positive impact in the yeast performance compared with the results obtained when, under the same conditions, the initial cell concentration was one half (**Figure 3.2-D** and **Figure 3.3-C**). In fact, the duration of the lag phase was significantly reduced (from 48 to 8 h) and the utilization of all C-sources was possible after 75 h compared with 100 h of cultivation.

Collectively, these results obtained with media derived from synthetic SBP hydrolysate indicate that the performance of *R. toruloides* PYCC 5615 in SBP hydrolysate is significantly affected by the acetic acid concentration present and that amino acid supplementation and the increase of the inoculum concentration are important manipulations to be implemented for the bioprocess improvement.

3.4.4 Performance of *R. toruloides* PYCC 5615 in SBP hydrolysate supplemented with commercial YNB with amino acids and effect of ammonium sulphate concentration

Having demonstrated the effect of the presence of amino acids on the catabolism of all the major carbon sources present in synthetic SBP hydrolysate medium, the performance of *R. toruloides* PYCC 5615 was tested in real SBP hydrolysate H11 at pH 5.0 with addition of commercial YNB with amino acids and use of a high inoculum concentration (corresponding to OD_{600nm} of 8.0) (**Figure 3.4**). Results confirm the capacity of this strain to fully use all the carbon sources present after less than 100 h of cultivation, contrasting with the results obtained when amino acids were not supplemented to the hydrolysate and a lower concentration of inoculum was used (**Figure 3.4** compared with **Figure 3.1-B**). A similar result was observed for *R. mucilaginosa* IST 390 (**Figure 3.5**), confirming the beneficial effect of amino acids for the utilization of all carbon sources present in SBP hydrolysates in *Rhodotorula* strains.

Given that the nitrogen demand is determined by the yeast strain used and concentration of C-sources available, and that the carbon-to-nitrogen (C/N) ratio is crucial for the accumulation of lipids in oleaginous yeasts (Lopes et al. 2020; Maza et al. 2020) and that it was intended to assess the potential of these oleaginous yeasts for SBP valorization, the effect of the concentration of ammonium sulphate supplementation was examined.

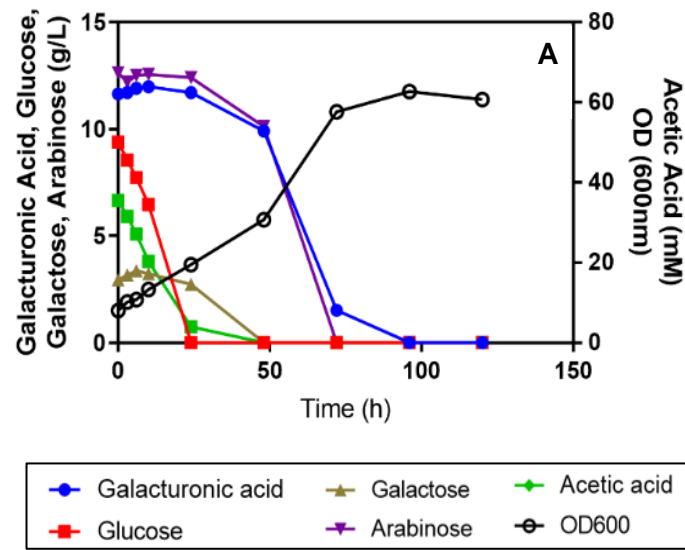


Figure 3. 4- **Performance of *R. toruloides* PYCC 5615 in SBP hydrolysate H11 supplemented with commercial YNB with ammonium sulphate and amino acids.** Cultivation was performed at 30°C with orbital agitation (250 rpm). The initial culture OD_{600nm} was 8.

Although SBP hydrolysates include natural nitrogen sources, in particular primary amino acids and free ammonia (Martani et al. 2020), the catabolism by *R. toruloides* PYCC 5615 of all C-sources available was not possible in the absence of amino acid supplementation, as shown before.

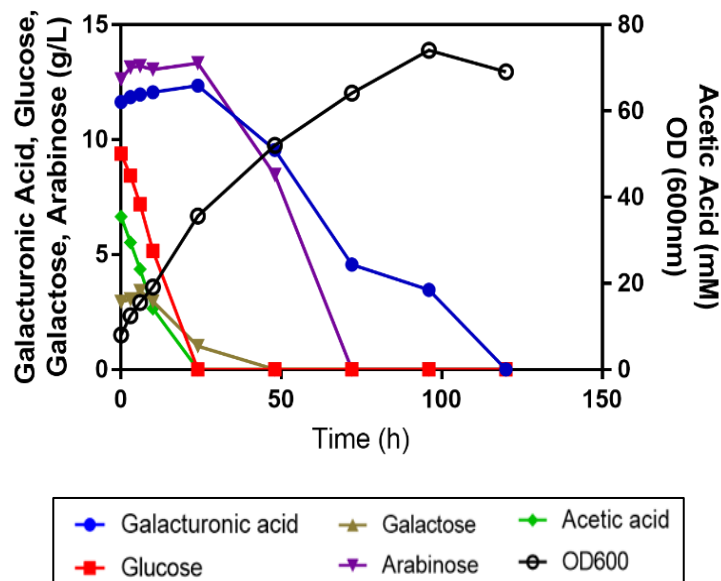


Figure 3. 5- **Performance of *R. mucilaginosa* IST390 in SBP hydrolysate H11 supplemented with commercial YNB with ammonium sulphate and amino acids.** Cultivation was performed at 30°C with orbital agitation (250 rpm). The initial culture OD_{600nm} was 8.

Since the concentration of ammonium sulphate added in former experiments was the one present in commercial YNB (5 g/L) and such a relatively high concentration can affect lipid production yield, the supplementation of SBP hydrolysate H13 with YNB (without ammonium sulphate or amino acids, but supplemented with the amino acids present in the commercial medium) and different concentrations of ammonium sulphate (5, 2.5 and 1 g/L) was tested (**Figure 3.6**). The results indicate that different initial concentrations of ammonium sulphate may also affect the percentage of consumption of the C-sources available (**Figure 3.6**). The batch of SBP hydrolysate used here, H13, has a lower concentration of all the sugars and of acetic acid compared with H11 (**Table 3.1**). This alters the apparent yeast performance compared with other cultivations performed in H11, in which it was easier to complete the use of all the major carbon sources. Apparently, the reduction of ammonium concentration from 5 g/L to 2.5 g/L did not significantly affect the consumption rate or percentage for all the C-sources (**Figure 3.6-A and 3.6-B**).

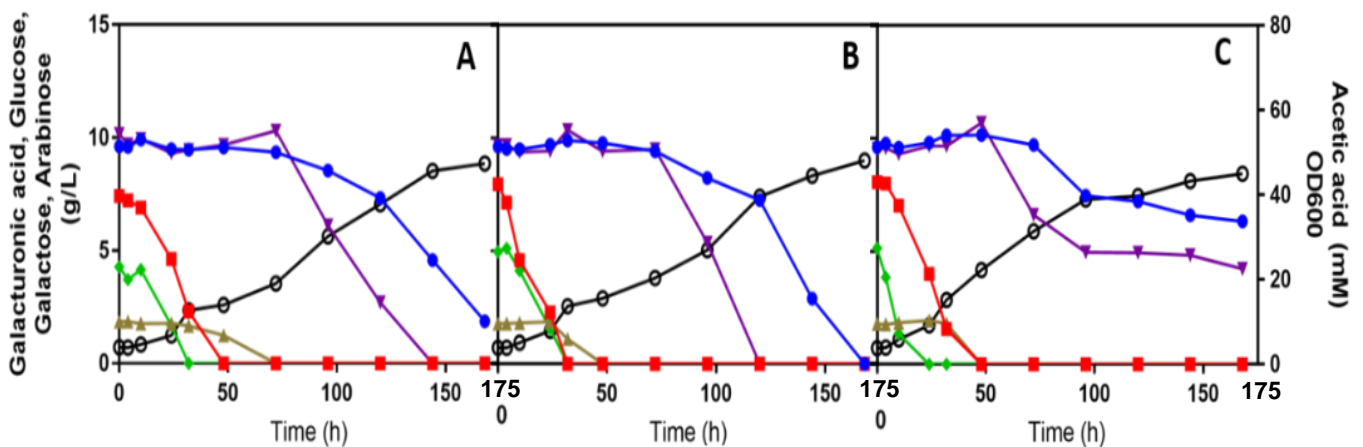


Figure 3. 6- Effect of different initial concentrations of ammonium sulphate (A) 5, (B) 2.5 and (C) 1 g/L on the utilization of the different carbon sources present in SBP hydrolysate H13 during the cultivation of *R. toruloides* PYCC 5615. The sugar beet pulp hydrolysate H13 medium at pH 5.0 was prepared in YNB supplemented with the amino acids present in commercial YNB besides the different ammonium sulphate concentrations to be tested. Cultivations were performed at 30°C, with orbital agitation (250 rpm). Inoculation was with an initial OD_{600nm} of 4.

However, the addition of only 1 g/L ammonium sulphate limited the percentage of the D-galacturonic acid and L-arabinose sugars used after the consumption of the more easily used C-sources (D-glucose, D-galactose and acetic acid) (**Figure 3.6-C**). Both D-galacturonic acid and L-arabinose were not fully used. The final biomass concentration attained in the cultivation with 1 g/L ammonium sulphate was slightly lower suggesting that the lower performance can be, at least partially, attributed to nitrogen limitation.

3.4.5 Preliminary assessment of lipid and carotenoid production by three oleaginous red yeast strains during SBP bioconversion.

The data obtained during this work allowed the identification of a set of experimental conditions leading to the efficient catabolism of the different C-sources present in SBP hydrolysates by *R. toruloides* PYCC 5615. In the last part of the work, the performance of growth, C-sources catabolism, lipid accumulation, and carotenoid biosynthesis was also assessed for two other oleaginous red yeast strains (**Figure 3.7**). Given that *R. toruloides* PYCC 5615 was derived from *R. toruloides* strains IFO 0559 and IFO 0880 (Banno 1967), and *R. toruloides* IFO 0880 is considered a robust host for lipid overproduction and genome-scale metabolic model (Banno 1967; Dinh et al. 2019), this strain was also included in this study as well as *R. mucilaginosa* IST 390 isolated herein (**Figure 3.7**).

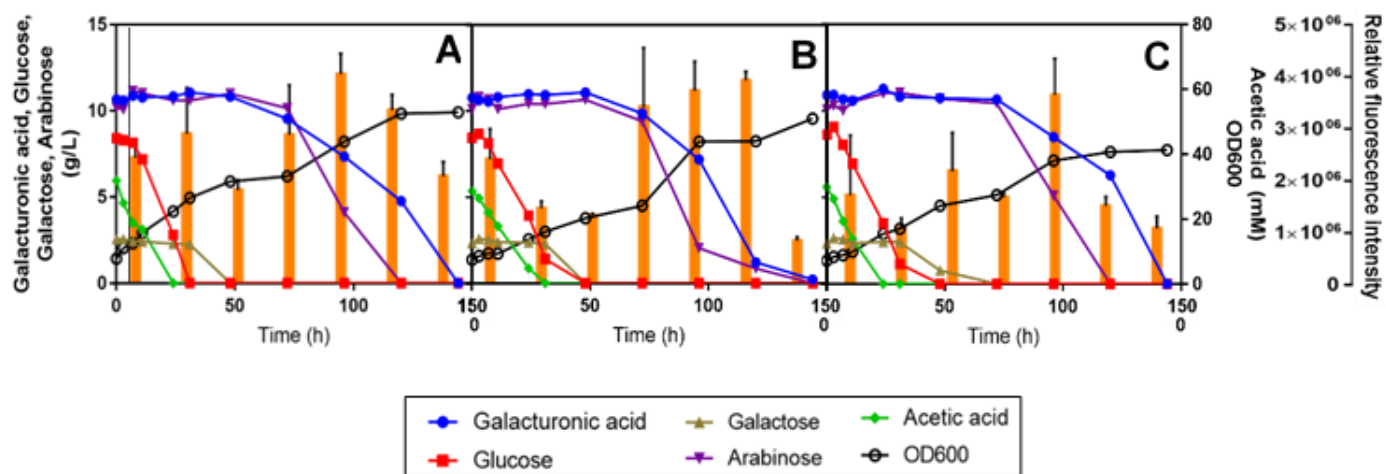


Figure 3. 7- Bioconversion of SBP hydrolysate H13 supplemented with 1.7 g/L of YNB (without ammonium sulphate or amino acids) and with 2.5 g/L ammonium sulphate and the amino acids present in commercial YNB, at pH 5.0, by *R. mucilaginosa* IST 390 (A), *R. toruloides* PYCC 5615 (B), *R. toruloides* IFO 0880 (C) for lipid production. Cultivations were performed at 30°C, with orbital incubation (250 rpm). Media were inoculated with cells corresponding to an initial optical density of 8. Lipid production was assessed by Nile Red staining with a normalized cell suspension ($OD_{600nm} = 1$) and based on relative fluorescence units (RFU). Orange bars represent average RFU values and standard deviation values are shown.

The assays were carried out in sugar beet pulp hydrolysate H13 supplemented with 1.7 g/L of YNB (without ammonium sulphate or amino acids) and 2.5 g/L of ammonium sulphate

(based on the results presented in **Figure 3.6**) and the above described amino acids used to supplement YNB. Among the three oleaginous yeast strains tested, *R. mucilaginosa* IST 390 showed the highest consumption rate of D-glucose, acetic acid and galactose but all the strains used these C-sources efficiently. The three *Rhodotorula* sp. strains were able to co-consume D-glucose and acetic acid, which is an important advantage in industrial settings when feedstocks containing both carbon sources are used. However, *R. toruloides* PYCC 5615 was the most efficient strain to fully use D-galacturonic acid, with L-arabinose being consumed faster by all three strains. Lipid accumulation in these oleaginous yeast strains was also preliminarily assessed under conditions leading to the full and more rapid utilization of all the C-sources present in SPB hydrolysates (**Figure 3.7-A, B and C**). Results suggest that lipids were accumulated in lipid droplets especially in the *R. toruloides* strains after 48 h of cultivation when D-glucose, D-galactose and acetic acid were exhausted and continued during the second phase of growth during which L-arabinose and D-galacturonic acid were co-consumed (**Figure 3.7** and **Figure 3.8**). The fluorescence microscopy observations appear to suggest that *R. toruloides* IFO 0880 was the strain that under identical conditions was able to accumulate lipids in larger lipid droplets, while *R. mucilaginosa* IST 390 was less promising in that respect (**Figure 3.8**). The cell morphology, as well as the arrangement and size of the lipid droplets was found to change during yeast cultivation (**Figure 3.8**). After 120 h and up to 144 h of cultivation, an intensification of the orange/red colour of the yeast cells, presumably related with the increase in carotenoid biosynthesis and associated with lipid droplet turnover, was observed (**Figure 3.8** and **Figure 3.9**). In *S. cerevisiae*, the lipid droplet turnover is an intricate process, depending, among others, on phosphorylation events that stimulate lipolytic activity (Koch et al. 2014). Under nutrient starvation, lipolytic breakdown is triggered leading to lipid oxidation to generate cellular energy and channel different metabolites towards synthesis of carotenoids, that are useful to protect the cells from oxidative damage (Mata-Gómez et al. 2014; Van Zutphen et al. 2014).

The content in carotenoids is known to depend on the yeast strain, culture medium composition, and external physical factors (e.g. light, temperature, aeration, osmotic stress, etc) (Kot et al. 2018; Pham et al. 2020). The total concentration of carotenoids produced by the three red yeast strains after 144 h of cultivation was assessed. *Rhodotorula mucilaginosa* IST 390 produced the lowest amount of total carotenoids (81 µg/g dcw) (**Table 3.2**) while the highest total carotenoid content was observed for *R. toruloides* PYCC 5615 (255 µg/g dry weight).

Table 3. 2- Specific production yield of carotenoids ($\mu\text{g} / \text{g}$ dry biomass) and volumetric carotenoid concentration (mg/L) produced by the three red yeast strains after 144 h of cultivation in sugar beet pulp hydrolysate H13 as described in figure 3.6 legend.

Yeast strain	Total carotenoids	
	($\mu\text{g/g}$ dry biomass)	(mg/L)
R. mucilaginos a IST 390	81	1,4
R. toruloides PYCC 5615	255	5,4
R. toruloides IFO 0880	158	2,8

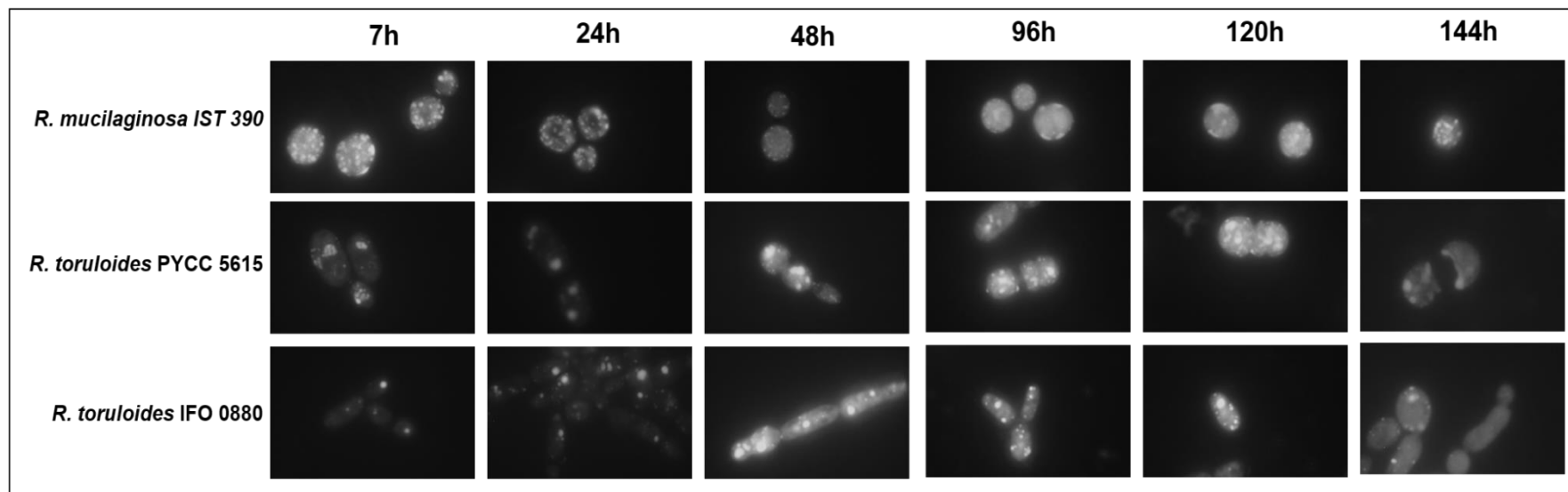


Figure 3. 8- Microscopic observations of *R. mucilaginosa* IST 390, *R. toruloides* PYCC 5615, and *R. toruloides* IFO 0880 cells stained with Nile red fluorescence dye during cultivation in SBP hydrolysate H13 derived medium as described in Figure 3.7 legend. Cells were harvested during the growth curves shown in Figure 3.6. The arrangement, size and fluorescence intensity of the lipid droplets accumulated inside the cells was examined along yeasts' cultivation. One of the different pictures taken at the same incubation times is shown as representative example.

Although *R. toruloides* IFO 0880 produced lower levels of total carotenoids (158 µg/g dry weight) than *R. toruloides* PYCC 5615 after 144 h of cultivation, this might be because it took more time to use up the total amount of the C-sources. Visual observation of the cell pellets obtained is consistent with this hypothesis since the colour intensification in strain IFO 0880 was observed later (after 120 h). This hypothesis may also partially apply to the poorer performance of the *R. mucilaginosa* strain. It has also to be said that the nature of the mixtures of carotenoids produced by *R. mucilaginosa* and *R. toruloides* strains was different as suggested by the colour of the cell pellets: pink-coloured pellets for *R. mucilaginosa* IST 390 confirming the high percentage of torulene/torularhodin (pink colour) pigment (Kot et al. 2018), whereas *R. toruloides* PYCC 5615 and *R. toruloides* IFO 0880 had a red-orange colour suggesting similar percentages of β-carotene (orange) and torulene/torularhodin carotenoids (Qi et al. 2020) (**Figure 3.9**).

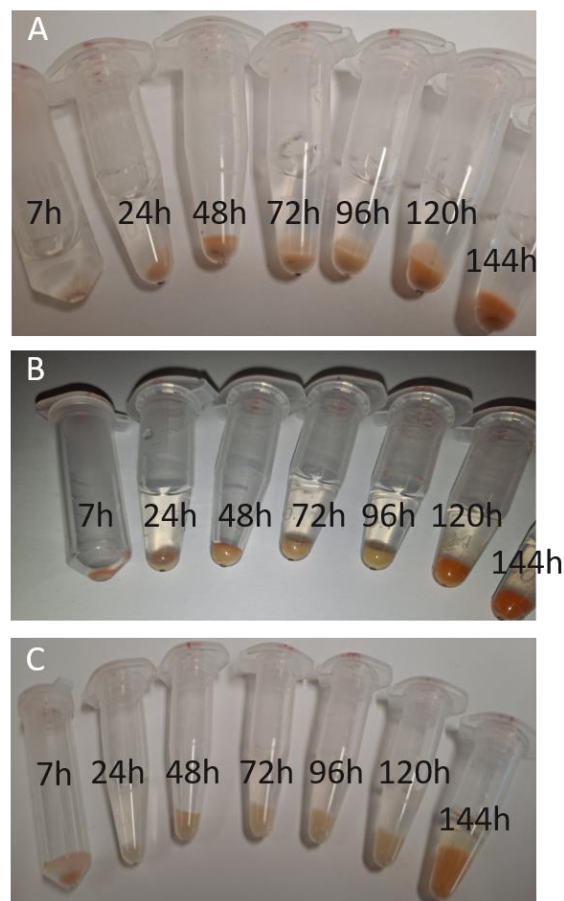


Figure 3. 9- Cell pellets of *Rhodotorula mucilaginosa* IST 390 (A), *R. toruloides* PYCC 5615 (B) and *R. toruloides* IFO 0880 (C) harvested during yeast bioconversion of sugar beet pulp hydrolysate H13. Samples were harvested from the cultures characterized in Figure 3.7.

3.5 DISCUSSION

Pectin-rich agricultural residues are potential feedstocks for the microbial production of biofuels, bulk chemicals and other added value compounds. Among them, sugar beet pulp (SBP) and citrus peel waste (CPW) represent a large fraction of those pectin-rich residues (Martins et al. 2020; Jeong et al. 2021). Although these residues are currently used for cattle feeding or landfill soil improvement, they are considered interesting alternative feedstocks for biorefineries because they are partially pre-treated and have a low lignin content which facilitates processing to yield a number of potentially metabolizable carbon sources (Leijdekkers et al. 2013; Martins et al. 2020). Depending on the concentrations present in the hydrolysates due to the release of acetyl and methyl groups from pectin (Müller-Maatsch et al. 2016), acetic acid and methanol are potential inhibitors of yeast growth and metabolism although methanol is not expected to reach concentrations that are inhibitory (Mota et al. 2021). Considering the presence of D-galacturonic acid and L-arabinose at very significant amounts in pectin-rich residues hydrolysates, the complete utilization of the complex mixture of carbon sources requires yeast strains with a broad intrinsic catabolic capacity. In recent years, a number of non-conventional yeast species have gained significant attention as promising cell factories for the production of biofuels and added-value compounds based on agro-industrial feedstocks in environmentally-friendly bioprocesses (Rebello et al. 2018). Among them, *Rhodotorula* species/strains have emerged as promising for the natural catabolism of the highly challenging oxidized sugar D-galacturonic acid (Protzko et al. 2019). However, their performance when cultivated in media with multiple C-sources as those present in pectin-rich residues hydrolysates has not been studied in depth and is the focus of this study.

In order to find novel yeast isolates with desirable traits to efficiently use the mixture of carbon-sources present in SBP hydrolysates, we explored yeast diversity associated with SBP samples. Even though the SBP sample received was kept frozen, it was possible to successfully isolate and identify different yeast species (e.g., *Rhodotorula mucilaginosa*, *Kluyveromyces marxianus*, *Clavispora lusitanea*, *Cryptococcus laurentii*) from this sample (unpublished results). In this work, only the isolated *R. mucilaginosa* strain was tested. However, interestingly, a *C. laurentii* strain was recently successfully used for lipid production from orange peel waste medium (Sitepu et al. 2014a; Carota et al. 2020). *K. marxianus* is also an interesting species due to its thermotolerance and ability to assimilate a wide range of sugars, in particular L-arabinose (but not D-galacturonic acid) and its capacity to efficiently produce bioethanol (Lane and Morrissey 2010). For these reasons, future exploration of these other strains obtained from SBP is considered of interest. The potential of the strain *R. mucilaginosa* IST 390 isolated from SBP and of *R. toruloides* PYCC 5615 for the efficient catabolism of the main C-sources present in SBP hydrolysate (D-glucose, D-galactose, acetic

acid, D-galacturonic acid, and L-arabinose) was examined. The presence of acetic acid in the hydrolysates (30-40 mM or 1.8-2.1 g/L) adjusted at pH 5.0 did not limit the rapid and full utilization of D-glucose, D-galactose and of acetic acid itself from SPB but, at pH 3.5, growth was abrogated. Independently of the reported capacity of *R. toruloides* for catabolizing D-galacturonic acid (Protzko et al. 2019), the catabolization of this acidic sugar and of L-arabinose was dramatically affected by the presence of acetic acid. This was demonstrated based on the comparison of the consumption profiles of the major C-sources by both species from a synthetic media mimicking SBP hydrolysates either or not supplemented with acetic acid. At higher or lower concentrations, acetic acid is expected to be always present in SBP hydrolysates, therefore limits the full use of all the C-sources. In fact, since pectin is acetylated in different positions of the D-galacturonic acid molecule, SBP hydrolysis releases acetic acid that accumulates in the hydrolysate and this is particularly problematic for sugar beet pulp hydrolysates compared with citrus peel hydrolysates (Martins et al. 2020).

The rapid co-consumption of the D-glucose and acetic acid present in SBP hydrolysates (only supplemented with ammonium sulphate and set up at pH 5.0), by *R. mucilaginosa* and *R. toruloides*, was another interesting observation. This is a much-appreciated trait in industrial bioprocesses because it can lead to the decrease of the production time and energy costs and enhance bioproduct productivity. D-glucose and acetic acid co-consumption is not observed in *S. cerevisiae* wild-type strains because glucose represses acetate metabolism but was also described in the nonconventional food spoilage yeast *Zygosaccharomyces bailii* (Palma et al. 2018). The ability to co-consume D-glucose and acetic acid is an additional important trait of *Rhodotorula* species as promising cell factories for lipid and carotenoid production for the valorisation of agro-food and forestry residues in which these two C-sources are present. The consumption of D-galactose was found to occur only after D-glucose consumption, suggesting that its catabolism is subject to catabolite repression in *Rhodotorula* species, as in *S. cerevisiae* (Sellick et al. 2008).

In this study it was also found, using a synthetic SPB medium, that even in the absence of acetic acid the efficient full consumption of D-galacturonic acid and L-arabinose by both *R. mucilaginosa* IST 390 and *R. toruloides* PYCC 5615 was only achieved when amino acids (10 mg/L of L-histidine, 20 mg/L of DL-methionine and 20 mg/L DL-tryptophan) were added to the medium or to the real SBP hydrolysate. Our results indicate that amino acid supplementation also enhances the consumption of D-glucose, D-galactose, acetic acid, but, more importantly, may allow the complete use of D-galacturonic acid and L-arabinose. The catabolic pathway for D-galacturonic acid utilization in *R. toruloides* was recently characterized including enzymes similar to those described in the ascomycetous filamentous fungi *Aspergillus niger* and *Trichoderma reesei* (Protzko et al. 2019). The pathway that converts D-galacturonate into glycerol in filamentous fungi comprises four different cytosolic enzymes and two of them (D-

galacturonic acid reductase and L-glyceraldehyde reductase) are NADPH-dependent (Martens-Uzunova and Schaap 2008). Therefore, the efficiency of the D-galacturonic acid catabolic pathway in yeasts and filamentous fungi relies on the regeneration of the redox cofactor NADPH, which can occur through the oxidative phase of the pentose phosphate pathway (PPP) (Wamelink et al. 2008). Moreover, in yeasts and filamentous fungi, the pentoses arabinose and xylose are also catabolized through the oxidoreductase pathway which also requires the redox co-factors NADPH and NADH (Fonseca et al. 2007; Xu et al. 2011). Redox homeostasis is an essential requirement for metabolism maintenance and energy generation due to the involvement of NAD(H) and NADP(H) redox cofactors in several metabolic networks and in particular for both D-galacturonic acid and L-arabinose utilization. Therefore, we hypothesize that the supplemented amino acids might be required to counteract the deleterious effects of acetic acid, including on metabolic pathways involved in NADH and NADPH regeneration thus guaranteeing enough redox potential for the catabolism of D-galacturonic acid and L-arabinose present in SBP hydrolysates by red oleaginous yeasts. Consistent with our hypothesis, it was reported, based on transcriptomic and metabolomic analyses, that the expression of 24 genes involved in NAD(P)/NAD(P)H homeostasis was greatly reduced in acetic acid stressed cells; these genes being mainly correlated to NAD⁺ synthesis and redox transformation from NAD(P) to NAD(P)H (Dong et al. 2017). Acetic acid-induced intracellular acidification (Palma et al. 2018) was found to have a crucial influence on the oxidation-reduction potential of specific reductases and dehydrogenases (Orij et al. 2011) and the redox homeostasis between NAD(P)H and NAD(P) plays a major role in the modification of the metabolic flux in yeast (Croft et al. 2020). Additionally, it was found that acetic acid severely reduced ATP levels and the gene expression of some nutrient transporters (Nielsen 2003; Dong et al. 2017; Croft et al. 2020). Based on transcriptomic and metabolomic analyses it was also found that acetic acid-induced stress has varying impacts on amino acid metabolism, carbohydrate metabolism, and lipid metabolism (Dong et al. 2017). Compared with untreated cells, the concentration of all detected amino acids was found to be dramatically reduced in the yeast cells treated with acetic acid at more than one time point and the uptake and biosynthesis of amino acids from glycolysis, TCA cycle and other pathways were suppressed upon acetic acid stress (Dong et al. 2017). In summary, considering the deleterious effects of acetic acid in maintaining intracellular pH and redox homeostasis and in affecting nutrient uptake, this stress greatly affects the global metabolism, in particular the biosynthesis of amino acids and related carbohydrate metabolism. It is therefore likely that amino acid supplementation may help to counteract its negative effects. Interestingly, in *S. cerevisiae*, there is strong evidence for an altered activity in the oxidative branch of the PPP after methionine supplementation with detection of elevated levels of PPP metabolites and increased abundance of the NADPH producing enzyme 6-phosphogluconate dehydrogenase

(Campbell et al. 2016). Evidence was also provided supporting the idea that in stress situations methionine causes an altered activity of the NADPH producing oxidative part of the pentose phosphate pathway, suggesting that the effects of methionine on stress response is related with an altered activity of this NADP reducing pathway (Campbell et al. 2016). In the particular case of our study, amino acid supplementation is, apparently, counteracting the negative effect of acetic acid stress in D-galacturonic acid and L-arabinose catabolism as well as speeding up the utilization of these sugars even in the absence of acetic acid.

Oleaginous yeasts trigger lipid accumulation when there is excess of carbon source and other nutrients, particularly nitrogen, are limiting growth, achieving more than 20% of their dry biomass as lipids (Ratledge and Wynn 2002). In this work, a preliminary evaluation of the potential of three *Rhodotorula* strains to produce lipids and carotenoids from SBP hydrolysates under conditions leading to the full utilization of the major C-sources present was conducted. For the total utilization of the C-sources present, the ratio C/N in the hydrolysates was relatively low (approximately 12), compared with values reported in the literature (above 50) (Braunwald et al. 2013; Lopes et al. 2020). For this reason, it is anticipated that there is still room for further optimization of all the process parameters. It should be referred that acetic acid also alters lipid metabolism: long-chain fatty acids were found to accumulate, but the key genes in fatty acid biosynthesis and most of the differently expressed genes involved in lipid metabolism were down-regulated (Dong et al. 2017). Therefore, this is another issue deserving further studies. At this phase it is not easy to compare, in the context of this study, the natural tolerance to acetic acid stress of the *Rhodotorula* species examined here with *S. cerevisiae* because natural *S. cerevisiae* strains are not capable of using D-galacturonic and L-arabinose and of lipid overproduction. Remarkably, the time-course microscopic observation of the lipid droplets in the yeast cells indicates that lipid accumulation occurs during the later stages of cultivation when D-galacturonic acid L-arabinose are still present and acetic acid was fully catabolized. Although no systematic and complete optimization of the process was in the focus of this work, collectively, the results obtained strongly support the idea that SBP and *Rhototorula* strains, in particular from the species *R. toruloides*, are promising feedstocks and cell factory platforms for the production of single-cell oils and pigments for energy and food applications in the context of a circular bioeconomy.

4| General Discussion

4.1 DISCUSSION

A circular economy demands for renewable or recyclable resources and reduce the consumption of raw materials and energy in the economy while protecting the environment through cutting emissions and minimising material losses (Carus and Dammer 2018). Since the biological resources are embedded in the natural biological cycle, the use of biomaterials is viewed as contributing to the circular economy, recently stated as circular bioeconomy (Carus and Dammer 2018). A main technological innovation within the biological and chemical industry is the refining of biomass into feedstock chemicals as renewable alternatives to fossil-based materials and energy (Naik et al. 2010; Leong et al. 2018). So far, biorefining is an established system for producing products such as beer, sugar, vegetable oils and wine. Currently, advanced biorefineries are being developed to process more diverse biological resources, including whole crops, forest-based resources and even marine algae, into a wide range of platform chemicals that can be further processed into energy or food (Liguori and Faraco 2016; Ubando et al. 2020). Therefore, the global market for advanced biorefineries is growing, since almost all current global investment is focused on increasing advanced biorefinery capacity and value chains (Lundmark et al. 2018; Zetterholm et al. 2020).

In the last years, lignocellulosic-based feedstocks, including residues from forestry- and agro-industries have gained more relevance, linking the lignocellulosic-based value chain, to other sectors involved in advanced biofuels production. Agro-industrial residues, in particular pectin-rich agricultural residues and agro-food industry residues, are potential feedstocks for the production of biofuels and other relevant bioproducts (Shrestha et al. 2020), instead of being used as low-value products such as for animal feed or land fertilizer. The results obtained during this thesis highlight the potential for valorisation of sugar beet pulp, a pectin-rich residue. This is an important crop in north-west Europe being the EU the world's largest producer (Berlowska et al. 2018). For pectin-rich biomass utilization, pre-treatment and hydrolysis reactions are needed to release metabolizable sugar monomers. As a consequence of those treatments, the hydrolysates accumulate microbial inhibitory compounds, such as acetic acid, methanol, furan derivatives and phenolic compounds, depending on the conditions used for hydrolysis (Martins et al. 2020). In sugar beet pulp hydrolysates, compared with citrus peel hydrolysates, acetic acid is at relatively high concentrations (1.8-2.4 g/L) being a major inhibitory compound due to the high acetylation degree of D-galacturonic acid molecules in the pectin backbone, but methanol is also present (Martins 2020). Both, acetic acid and methanol, are recognized as potential growth inhibitors for yeast growth, fermentation kinetics and metabolite production yields (Mira et al. 2010b; Palma et al. 2018; Mota et al. 2021).

This thesis work addresses a wide spectrum of challenges faced by the conversion of sugar beet pulp hydrolysates by yeasts. The presence of multiple carbon sources is known to

trigger carbon catabolite repression regulation thus limiting the efficient utilization of all the C-sources and prolonging the bioprocess duration (Gao et al. 2019; Simpson-Lavy and Kupiec 2019). SBP hydrolysates include neutral sugars and an acidic sugar (D-galacturonic acid) that is neither naturally used by *S. cerevisiae* nor by several others relevant yeast species (Martins et al. 2020). Recently, scientific efforts have addressed the expression of fungal D-galacturonic acid catabolic pathway in *S. cerevisiae* strains (Jeong et al. 2020) to efficiently produce ethanol from this acid sugar. However, the D-galacturonic acid catabolism is not redox neutral and it requires two NADPH cofactor molecules to produce pyruvate/glycerol, therefore additional genetic modifications are needed to cope with redox power homeostasis (Richard and Hilditch 2009). There are non-conventional yeast strains that are reliable alternatives to the engineering of *S. cerevisiae* to convert the sugars present in pectin-rich hydrolysates, since this large and heterogeneous group of non-conventional yeasts include species/strains with natural metabolic traits desirable for the synthesis of a wide-range of added-value products through the utilization of a wide range of carbon-sources (hexoses, pentoses, D-galacturonic acid and acetic acid) (Radecka et al. 2015; Rebello et al. 2018). The oleaginous red yeast species, for instance *Rhodotorula* strains, were reported as suitable cell factories to produce lipids and carotenoids from agro-industrial residues (Lyman et al. 2019; Carota et al. 2020). However, the challenges encountered are several and this thesis work was developed to contribute to clearly identify and surpass some of them at the biological level. In particular, it was possible to reach the complete use of all the major carbon sources present in SBP hydrolysates by *Rhodotorula* strains capable of producing lipids and carotenoids and to characterize the dual role of acetic acid as a carbon-source and an inhibitor of yeast metabolism, in particular by affecting D-galacturonic acid and arabinose utilization.

Through the chemogenomics analysis performed, new information on methanol toxicity and tolerance mechanisms, compared with ethanol, in yeast was gathered (Mota et al. 2021). Results suggest that methanol, at the concentrations predicted to be present in SBP hydrolysates (about 0.1 % (v/v)) does not represent a significant growth inhibitory issue since the *S. cerevisiae* strain used can grow with no detectable inhibition with until 10 % (v/v) of methanol (Mota et al. 2021). Among the differences between methanol and ethanol tolerance determinants, the genes involved in DNA repair mechanisms appeared as a distinguished function enriched in methanol-growing cells, similar to formaldehyde tolerance determinants (*RAD* genes) previously identified by others (North et al. 2016). Formaldehyde is formed in the detoxification pathway in *S. cerevisiae* by the oxidation of methanol to formaldehyde carried out by alcohol dehydrogenases (Yasokawa et al. 2010; Mota et al. 2021). Other more common molecular targets and tolerance genes identified in this work are related with important molecular targets for those alcohols. As lipophilic compounds, these alcohols induce plasma membrane permeabilization increasing the passive influx of ions (e.g., protons) across plasma

membrane thus contributing to cytosolic acidification and dissipation of the electrochemical membrane potential (Martínez-Muñoz and Kane 2008; Charoenbhakdi et al. 2016; Palma et al. 2018). This deleterious effect is expectably higher in the presence of ethanol since this alcohol is more lipophilic compared with methanol. Due to intracellular and vacuolar acidification, caused by alcohol stress, the maintenance of intracellular pH homeostasis is also dependent on the activity of vacuolar H⁺-ATPase (V-ATPase), highlighting the importance of its cellular function in alcohol tolerance (Rosa and Sá-Correia 1996; Carmelo et al. 1997; Teixeira et al. 2009). Also, autophagic processes have an essential role in methanol and ethanol tolerance considering their involvement in cell protection against DNA and other macromolecules and organelle damage (Kroemer et al. 2010; Reggiori and Klionsky 2013). In particular, reticulophagy (a selective autophagy required for the selective clearance and degradation of the endoplasmic reticulum (ER) by the cellular macroautophagy/autophagy machinery under endoplasmic reticulum stress) was an enriched biological function in the chemogenomic analysis for both methanol and ethanol (Kroemer et al. 2010). Endosomal sorting complexes, including the ubiquitin-dependent sorting to the vacuole, were also suggested to be involved in the degradation of methanol/formaldehyde- and ethanol-induced misfolded proteins, enabling yeast cells to recycle macromolecules that were damaged due to alcohol toxicity. A wide range of metabolic pathways are modulated by the activity of transcription factors. The stress induced by either methanol or ethanol identified common transcription factors, including Cbf1, Rpn4, Sfl1, Sfp1, and Ume6, as relevant to overcome the deleterious effect caused by these alcohols. In case of methanol exposure, Ixr1 and Opi1 are suggested to play a significant role in tolerance since the corresponding deletion mutants exhibited a marked methanol susceptibility phenotype. The IXR1 was reported to be involved in the oxidative stress response, since the mutant *ixr1Δ* is more susceptible to peroxides (Castro-Prego et al. 2010) and its promoter region has a binding site for STB5, a regulator of the oxidative stress response (Vizoso-Vázquez et al. 2018). The Opi1 is a transcriptional repressor involved in the regulation of phospholipid synthesis in response to inositol availability, compromising the lipid content of plasma membrane and the signaling of different pathways. Methanol complete oxidation produces formic acid which is a potent oxidative stress inducer that dramatically increases the level of intracellular reactive oxygen species (Lin 2012). Besides this deleterious effect, formate also binds to cytochrome c, inhibiting the last step of the electron transport chain in mitochondria and leading to the disruption of the proton gradient and the consequent decrease of ATP synthesis (Iwaki and Rich 2004). The global mechanisms underlying the toxic effects of methanol have been overlooked in the context of yeast biorefineries. This study confirmed mechanisms similar to those involved in ethanol toxicity and tolerance and identified others more specific. The genome-wide analysis performed is a first step for the rational genomic manipulation of the yeast cell to obtain more robust strains

capable of coping with high methanol or high methanol and ethanol concentrations by exploring the resulting information. Results obtained in the model yeast are likely useful for the engineering of methylotrophic yeasts to increase their robustness and consequently the productivity of methanol-based processes or of processes that use as feedstocks crude industrial residues contaminated with methanol (e.g., crude glycerol).

The exploration of yeast diversity associated with diverse environments is an important strategy to find out the most suitable strains to be used with or without subsequent metabolic engineering. The performance of a *Rhodotorula mucilaginosa* strain, isolated from SBP and identified at the molecular level during this study is an interesting example of such successful strategy since it was found to have the potential to completely use all the carbon sources present in SBP hydrolysates. Even though the SBP sample received was kept frozen, it was possible to successfully isolate other promising yeast species for pectin-rich-hydrolysates, such as *Kluyveromyces marxianus*, *Clavispora lusitanea* and *Cryptococcus laurentii*. These results are not shown in this dissertation because they were not further explored. However, their future exploration is considered of interest. In fact, a *C. laurentii* strain was recently successfully used for lipid production from orange peel waste medium (Carota et al. 2020). *K. marxianus* is also an interesting species due to its thermotolerance and ability to assimilate a wide range of sugars, in particular L-arabinose (but not D-galacturonic acid) and its capacity to efficiently produce bioethanol (Lane and Morrissey 2010).

Two other *R. toruloides* strains were examined during the thesis envisaging the full utilization of the C-sources present in SBP hydrolysates. The potential of these other oleaginous red yeasts for conversion of pectin-rich biomass hydrolysates was confirmed and it was highlighted the dual role of acetic acid (carbon source and inhibitor) in SBP hydrolysates. Acetic acid prevented the catabolism of D-galacturonic acid and L-arabinose after the complete use of the other C-sources, confirming not only the existence of carbon catabolite repression regulation in these oleaginous yeasts (Simpson-Lavy and Kupiec 2019) but also a dramatic effect in the metabolism of those more challenging secondary carbon sources. However, the metabolism of all the carbon sources in *Rhodotorula* strains were significantly improved in presence of amino acids in both synthetic SBP and SBP hydrolysates. After the addition of L-histidine, DL-methionine and DL-tryptophan (the amino acids present in commercial YNB with amino acids), the catabolism of L-arabinose and D-galacturonic acid only occurred after the depletion of D-glucose and acetic acid. It was found that acetic acid severely reduced ATP levels and the gene expression of some nutrient transporters (Nielsen 2003; Dong et al. 2017; Croft et al. 2020). Based on transcriptomic and metabolomic analyses it was also found that acetic acid-induced stress has various impacts on amino acid metabolism, carbohydrate metabolism, and lipid metabolism (Dong et al. 2017). The expression of several genes involved in NAD(P)/NAD(P)H homeostasis was greatly reduced in acetic acid stressed cells; these

genes being mainly correlated to NAD⁺ synthesis and redox transformation from NAD(P) to NAD(P)H (Dong et al. 2017). Compared with untreated cells, the concentration of all detected amino acids was found to be dramatically reduced in the yeast cells treated with acetic acid and the uptake and biosynthesis of amino acids from glycolysis, TCA cycle and other pathways were suppressed upon acetic acid stress (Dong et al. 2017). Considering the deleterious effects of acetic acid in maintaining intracellular pH and redox homeostasis and in affecting nutrient uptake, this stress greatly affects the global metabolism, in particular the biosynthesis of amino acids and related carbohydrate metabolism. However, amino acid supplementation apparently counteracts the negative effect of acetic acid stress in D-galacturonic acid and L-arabinose catabolism as well as speeds up the utilization of these sugars even in the absence of acetic acid. The information gathered in this work strongly support the idea that *Rhodotorula* strains, in particular from the species *R. toruloides*, are promising cell factory platforms for the production of single-cell oils and pigments for energy and food applications through the conversion of pectin-rich biomass hydrolysates enrolled the circular bioeconomy concept.

This thesis work was performed in the framework of the ERANET-IB project YEASTPEC. Results from the collaborative work developed with Elke Nevoigt' group are neither present in this PhD thesis nor discussed herein. In this joint work an engineered *S. cerevisiae* strain was developed in Nevoigt's laboratory for the efficient co-utilization of D-galacturonic acid and crude glycerol in SBP hydrolysate which includes acetic acid. The performance of this strain was compared in the same conditions (SBP hydrolysate H13 at pH 5.0, 30°C) with the performance of *R. toruloides* PYCC 5615 (Figure 4.1).

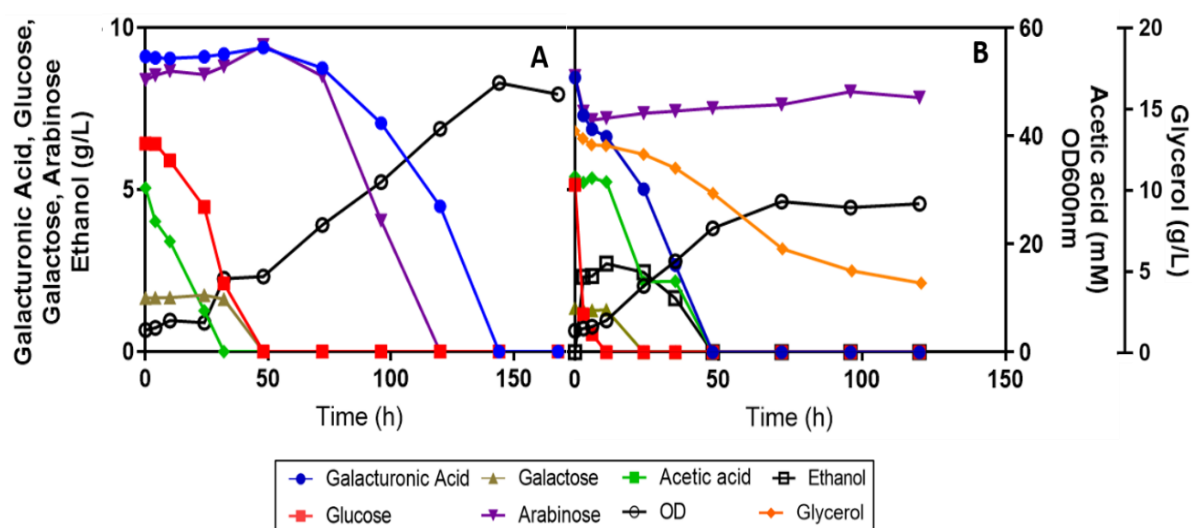


Figure 4. 1- Performance of *Rhodotorula toruloides* PYCC 5615 (A) and of an engineered *S. cerevisiae* strain developed in Elke Nevoigt Laboratory (Jacob University, Bremen) (B), during the conversion of SBP hydrolysate H13 supplemented with commercial YNB with ammonium sulphate and amino acids. Cultivation was performed at 30°C with orbital agitation (250 rpm). The initial culture OD_{600nm} was 4. The culture B was additionally supplemented with 15 g/L of pure glycerol.

In this same SPB hydrolysate, the engineered *S. cerevisiae* strain consumed D-glucose first, then D-galactose, both sugars at a higher consumption rate compared with *R. toruloides* PYCC 5615. Acetic acid was consumed after the neutral sugars but, at 50 h of cultivation, those three C-sources were completely used by both strains. D-Galacturonic acid consumption rate by the engineered *S. cerevisiae* strain was very rapid compared with *R. toruloides* PYCC 5615 being this acid sugar co-utilized with acetic acid, differently from the consumption profile in *R. toruloides* PYCC 5615 that co-consumed D-glucose and acetic acid, but only after acetic acid exhaustion D-galacturonic acid was used. (Figure 4.1) However, to support the process involving the engineered *S. cerevisiae* strain, it is mandatory to provide glycerol as co-substrate for redox cofactors regeneration during D-galacturonic catabolism and L-arabinose cannot be used because a heterologous pentose catabolic pathway is still lacking (Figure 4.1-B). A maximal concentration up to 2.8 g/L of ethanol was produced from the bioconversion of SBP H13 by the *S. cerevisiae* engineered strain while the *R. toruloides* strain produces lipids and carotenoids. The results obtained during this collaborative work were very important to uncover differences in the metabolic mechanisms involved in D-galacturonic acid catabolism in the engineered *S. cerevisiae* strain and in natural *Rhodotorula* strains. The manuscript is still unsubmitted and for reasons of intellectual property, this chapter is absent from this provisory version of the thesis.

5| Thesis publications

Peer-reviewed scientific publications directly related to this thesis:

Martins, L.C., Monteiro, C.C., Semedo, P.M., Sá-Correia I., *Valorisation of pectin-rich agro-industrial residues by yeasts: potential and challenges*. Applied Microbiology and Biotechnology 104, 6527–6547 (2020).

Mota M.N., **Martins L.C.**, Sá-Correia I., *The Identification of Genetic Determinants of Methanol Tolerance in Yeast Suggests Differences in Methanol and Ethanol Toxicity Mechanisms and Candidates for Improved Methanol Tolerance Engineering*. Journal of Fungi. 2021; 7(2):90.

Martins, L.C., Palma, M., Angelov, A., Nevoigt, E., Liebl., W., Sá-Correia, I., *Efficient utilization of all carbon sources present in sugar beet pulp hydrolysates by the oleaginous red yeasts *Rhodotorula toruloides* and *R. mucilaginosa**. Journal of Fungi. 2021. (**under review**)

Oral and poster presentation in international scientific meetings:

Martins. L.C., Mota, M.N., Sá-Correia, I., *Saccharomyces cerevisiae genes required for growth in the presence of multiple stresses of relevance in lignocellulosic bioethanol production*; 7th Conference on Physiology of Yeasts and Filamentous Fungi (PYFF), University of Milano-Bicocca, Junho 2019 (**Flash-talk presentation**)

Martins. L.C., Mota, M.N., Sá-Correia, I., *Saccharomyces cerevisiae genes required for growth in the presence of multiple stresses of relevance in lignocellulosic bioethanol production*; 7th Conference on Physiology of Yeasts and Filamentous Fungi (PYFF), University of Milano-Bicocca, Junho 2019 (**Poster presentation**)

Oral and poster presentation in national scientific meetings:

Martins, L.C., Mota, M.N., Sá-Correia, I., *Genome-wide identification of Saccharomyces cerevisiae genes involved in the modulation of tolerance to the conjugated effect of ethanol and acetic acid at low pH and high temperature*. Microbiotec'17- Universidade Católica Portuguesa do Porto, Dezembro 2017 (**Poster presentation**)

Martins, L.C., Monteiro, C., Semedo, P., Sá-Correia, I., *Isolation and potential of non-conventional yeasts for the production of added-value compounds from pectin-rich residues, in particular sugar beet pulp*. Microbiotec'19, Universidade de Coimbra, Dezembro 2019 (**Oral presentation**)

Mota, M.N., **Martins, L.C.**, Sá-Correia, I. *Genome-wide identification of genes required for methanol tolerance in Saccharomyces cerevisiae*, Microbiotec'19, Universidade de Coimbra, Dezembro 2019 (**Poster presentation**)

Peer-reviewed scientific publications not included in this thesis:

Monteiro PT, Oliveira J, Pais P, Antunes M, Palma M, Cavalheiro M, Galocha M, Godinho CP, **Martins LC**, Bourbon N, Mota MN, Ribeiro RA, Viana R, Sá-Correia I, Teixeira MC (2020) YEASTRACT+: a portal for cross-species comparative genomics of transcription regulation in yeasts. *Nucleic Acids Res* 48:642–649

6| References

6. References

- Aguilera F, Peinado RA, Millán C, Ortega JM, Mauricio JC (2006) Relationship between ethanol tolerance, H⁺-ATPase activity and the lipid composition of the plasma membrane in different wine yeast strains. *Int J Food Microbiol* 110:34–42 . <https://doi.org/10.1016/j.ijfoodmicro.2006.02.002>
- Ajila CM, Brar SK, Verma M, Tyagi RD, Godbout S, Valéro JR (2012) Bio-processing of agro-byproducts to animal feed. *Crit Rev Biotechnol* 32:382–400 . <https://doi.org/10.3109/07388551.2012.659172>
- Aksu Z, Tuğba Eren A (2005) Carotenoids production by the yeast *Rhodotorula mucilaginosa*: Use of agricultural wastes as a carbon source. *Process Biochem* 40:2985–2991 . <https://doi.org/10.1016/j.procbio.2005.01.011>
- Alexandre H, Ansanay-Galeote V, Dequin S, Blondin B (2001) Global gene expression during short-term ethanol stress in *Saccharomyces cerevisiae*. *FEBS Lett* 498:98–103 . [https://doi.org/10.1016/S0014-5793\(01\)02503-0](https://doi.org/10.1016/S0014-5793(01)02503-0)
- Almeida JRM, Fávaro LCL, Quirino BF (2012) Biodiesel biorefinery: Opportunities and challenges for microbial production of fuels and chemicals from glycerol waste. *Biotechnol Biofuels* 5:1–16 . <https://doi.org/10.1186/1754-6834-5-48>
- Angenent LT, Karim K, Al-Dahhan MH, Wrenn B a, Domínguez-Espinosa R (2004) Production of bioenergy and biochemicals from industrial and agricultural wastewater. *Trends Biotechnol* 22:477–85 . <https://doi.org/10.1016/j.tibtech.2004.07.001>
- Anschau A (2017) Lipids from oleaginous yeasts: production and encapsulation. In: *Nutrient Delivery*. Elsevier, pp 749–794
- Ashoori M, Saedisomeolia A (2014) Riboflavin (vitamin B2) and oxidative stress: A review. *Br J Nutr* 111:1985–1991 . <https://doi.org/10.1017/S0007114514000178>
- Auesukaree C (2017) Molecular mechanisms of the yeast adaptive response and tolerance to stresses encountered during ethanol fermentation. *J Biosci Bioeng* 124:133–142 . <https://doi.org/10.1016/j.jbiosc.2017.03.009>
- Auesukaree C, Damnernsawad a, Kruatrachue M, Pokethitiyook P, Boonchird C, Kaneko Y, Harashima S (2009) Genome-wide identification of genes involved in tolerance to various environmental stresses in *Saccharomyces cerevisiae*. *J Appl Genet* 50:301–310 . <https://doi.org/10.1007/BF03195688>

- Babel W (2009) The Auxiliary Substrate Concept: From simple considerations to heuristically valuable knowledge. *Eng Life Sci* 9:285–290 . <https://doi.org/10.1002/elsc.200900027>
- Balat M (2011) Production of bioethanol from lignocellulosic materials via the biochemical pathway: A review. *Energy Convers Manag* 52:858–875 . <https://doi.org/10.1016/j.enconman.2010.08.013>
- Balsalobre L, De Silóniz M-I, Valderrama M-J, Benito T, Larrea M-T, Peinado J-M (2003) Occurrence of yeasts in municipal wastes and their behaviour in presence of cadmium, copper and zinc. *J Basic Microbiol* 43:185–193 . <https://doi.org/10.1002/jobm.200390021>
- Banfield DK (2011) Mechanisms of protein retention in the Golgi. *Cold Spring Harb Perspect Biol* 3:1–14 . <https://doi.org/10.1101/cshperspect.a005264>
- Banno I (1967) Studies on the sexuality of rhodotorula. *J Gen Appl Microbiol* 13:167–196 . <https://doi.org/10.2323/jgam.13.167>
- Becker J, Boles E (2003) A Modified *Saccharomyces cerevisiae* Strain That Consumes L-Arabinose and Produces Ethanol. *Appl Environ Microbiol* 69:4144–4150 . <https://doi.org/10.1128/AEM.69.7.4144-4150.2003>
- Benocci T, Victoria M, Pontes A, Zhou M, Seiboth B, Vries RP De (2017) Biotechnology for Biofuels Regulators of plant biomass degradation in ascomycetous fungi. *Biotechnol Biofuels* 1–25 . <https://doi.org/10.1186/s13068-017-0841-x>
- Benz J, Protzko RJ, Andrich JM, Bauer S, Dueber JE, Somerville CR (2014) Identification and characterization of a galacturonic acid transporter from *Neurospora crassa* and its application for *Saccharomyces cerevisiae* fermentation processes. *Biotechnol Biofuels* 7:20 . <https://doi.org/10.1186/1754-6834-7-20>
- Berlowska J, Binczarski M, Dziugan P, Wilkowska A, Kregiel D, Witonska I (2018) Sugar Beet Pulp as a Source of Valuable Biotechnological Products. In: *Advances in Biotechnology for Food Industry*. Elsevier, pp 359–392
- Berlowska J, Pielech-Przybylska K, Balcerek M, Cieciora W, Borowski S, Kregiel D (2017) Integrated bioethanol fermentation/anaerobic digestion for valorization of sugar beet pulp. *Energies* 10: . <https://doi.org/10.3390/en10091255>
- Bernard A, Jin M, González-Rodríguez P, Füllgrabe J, Backues SK, Joseph B, Klionsky DJ (2015) Rph1/KDM4 mediates nutrient-limitation signaling that leads to the transcriptional induction of autophagy. *Curr Biol* 25:546–555 . <https://doi.org/10.1016/j.cub.2014.12.049.Rph1/KDM4>

- Bettiga M, Bengtsson O, Hahn-Hägerdal B, Gorwa-Grauslund MF (2009) Arabinose and xylose fermentation by recombinant *Saccharomyces cerevisiae* expressing a fungal pentose utilization pathway. *Microb Cell Fact* 8:40 . <https://doi.org/10.1186/1475-2859-8-40>
- Bhushan S, Kalia K, Sharma M, Singh B, Ahuja PS (2008) Processing of Apple Pomace for Bioactive Molecules. *Crit Rev Biotechnol* 28:285–296 . <https://doi.org/10.1080/07388550802368895>
- Biz A, Sugai-Guérios MH, Kuivanen J, Maaheimo H, Krieger N, Mitchell DA, Richard P (2016) The introduction of the fungal d-galacturonate pathway enables the consumption of d-galacturonic acid by *Saccharomyces cerevisiae*. *Microb Cell Fact* 15:144 . <https://doi.org/10.1186/s12934-016-0544-1>
- Bolt HM (1987) Experimental toxicology of formaldehyde. *J Cancer Res Clin Oncol* 113:305–309 . <https://doi.org/10.1007/BF00397713>
- Brandt BA, Garcia-Aparicio M, Mokomele T, Gorgens JF, van Zyl WH (2020) Rational engineering of *Saccharomyces cerevisiae* towards improved tolerance to multiple inhibitors in lignocellulose fermentations. *Biotechnol Biofuels*
- Braunwald T, Schwemmlin L, Graeff-Hönninger S, French WT, Hernandez R, Holmes WE, Claupein W (2013) Effect of different C/N ratios on carotenoid and lipid production by *Rhodotorula glutinis*. *Appl Microbiol Biotechnol* 97:6581–6588 . <https://doi.org/10.1007/s00253-013-5005-8>
- Bubis JA, Spasskaya DS, Gorshkov VA, Kjeldsen F, Kofanova AM, Lekanov DS, Gorshkov M V., Karpov VL, Tarasova IA, Karpov DS (2020) Rpn4 and proteasome-mediated yeast resistance to ethanol includes regulation of autophagy. *Appl Microbiol Biotechnol*. <https://doi.org/10.1007/s00253-020-10518-x>
- Buzzini P, Martini A (2000) Production of carotenoids by strains of *Rhodotorula glutinis* cultured in raw materials of agro-industrial origin. *Bioresour Technol* 71:41–44 . [https://doi.org/10.1016/S0960-8524\(99\)00056-5](https://doi.org/10.1016/S0960-8524(99)00056-5)
- Cai P, Gao J, Zhou Y (2019) CRISPR-mediated genome editing in non-conventional yeasts for biotechnological applications. *Microb Cell Fact* 18:63 . <https://doi.org/10.1186/s12934-019-1112-2>
- Campbell K, Vowinckel J, Keller MA, Ralser M (2016) Methionine Metabolism Alters Oxidative Stress Resistance via the Pentose Phosphate Pathway. *Antioxidants Redox Signal* 24:543–547 . <https://doi.org/10.1089/ars.2015.6516>

- Cárdenas-Fernández M, Bawn M, Hamley-Bennett C, Bharat PKV, Subrizi F, Suhaili N, Ward DP, Bourdin S, Dalby PA, Hailes HC, Hewitson P, Ignatova S, Kontoravdi C, Leak DJ, Shah N, Sheppard TD, Ward JM, Lye GJ (2017) An integrated biorefinery concept for conversion of sugar beet pulp into value-added chemicals and pharmaceutical intermediates. *Faraday Discuss* 202:415–431 . <https://doi.org/10.1039/c7fd00094d>
- Carmelo V, Santos H, Sá-Correia I (1997) Effect of extracellular acidification on the activity of plasma membrane ATPase and on the cytosolic and vacuolar pH of *Saccharomyces cerevisiae*. *Biochim Biophys Acta - Biomembr* 1325:63–70 . [https://doi.org/10.1016/S0005-2736\(96\)00245-3](https://doi.org/10.1016/S0005-2736(96)00245-3)
- Carota E, Petruccioli M, D'Annibale A, Gallo AM, Crognale S (2020) Orange peel waste-based liquid medium for biodiesel production by oleaginous yeasts. *Appl Microbiol Biotechnol* 4617–4628 . <https://doi.org/10.1007/s00253-020-10579-y>
- Carus M, Dammer L (2018) The Circular Bioeconomy - Concepts, Opportunities, and Limitations. *Ind Biotechnol* 14:83–91 . <https://doi.org/10.1089/ind.2018.29121.mca>
- Castro-Prego R, Lamas-Maceiras M, Soengas P, Carneiro I, González-Siso I, Cerdán ME (2010a) Regulatory factors controlling transcription of *Saccharomyces cerevisiae* *IXR1* by oxygen levels: A model of transcriptional adaptation from aerobiosis to hypoxia implicating *ROX1* and *IXR1* cross-regulation. *Biochem J* 425:235–243 . <https://doi.org/10.1042/BJ20091500>
- Charoenbhakdi S, Dokpikul T, Burphan T, Techo T, Auesukaree C (2016a) Vacuolar H⁺-ATPase protects *Saccharomyces cerevisiae* cells against ethanol induced oxidative and cell wall stresses. *Appl Environ Microbiol* 82:3121–3130 . <https://doi.org/10.1128/AEM.00376-16>
- Charoenbhakdi S, Dokpikul T, Burphan T, Techo T, Auesukaree C (2016b) Vacuolar H⁺-ATPase Protects *Saccharomyces cerevisiae* Cells against Ethanol-Induced Oxidative and Cell Wall Stresses. *Appl Environ Microbiol* 82:3121–3130 . <https://doi.org/10.1128/AEM.00376-16>
- Chen ST, Chen SY, Tu CC, Chiou SH, Wang KT (1995) Physicochemical properties of alkaline serine proteases in alcohol. *J Protein Chem* 14:205–215 . <https://doi.org/10.1007/BF01886761>
- Chen Y, Sheng J, Jiang T, Stevens J, Feng X, Wei N (2016) Transcriptional profiling reveals molecular basis and novel genetic targets for improved resistance to multiple fermentation inhibitors in *Saccharomyces cerevisiae*. *Biotechnol Biofuels* 9:1–18 .

<https://doi.org/10.1186/s13068-015-0418-5>

Chen Z, Liu D (2016) Toward glycerol biorefinery: metabolic engineering for the production of biofuels and chemicals from glycerol. *Biotechnol Biofuels* 9:1–15 . <https://doi.org/10.1186/s13068-016-0625-8>

Cherubini F (2010) The biorefinery concept: Using biomass instead of oil for producing energy and chemicals. *Energy Convers Manag* 51:1412–1421 . <https://doi.org/10.1016/j.enconman.2010.01.015>

Chi Z, Arneborg N (1999) Relationship between lipid composition, frequency of ethanol-induced respiratory deficient mutants, and ethanol tolerance in *Saccharomyces cerevisiae*. *J Appl Microbiol* 86:1047–1052 . <https://doi.org/10.1046/j.1365-2672.1999.00793.x>

Choi IS, Kim J-H, Wi SG, Kim KH, Bae H-J (2013) Bioethanol production from mandarin (Citrus unshiu) peel waste using popping pretreatment. *Appl Energy* 102:204–210 . <https://doi.org/10.1016/j.apenergy.2012.03.066>

Choi IS, Lee YG, Khanal SK, Park BJ, Bae H-J (2015) A low-energy, cost-effective approach to fruit and citrus peel waste processing for bioethanol production. *Appl Energy* 140:65–74 . <https://doi.org/10.1016/j.apenergy.2014.11.070>

Christophe G, Deo JL, Kumar V, Nouaille R, Fontanille P, Larroche C (2012) Production of Oils from Acetic Acid by the Oleaginous Yeast *Cryptococcus curvatus*. *Appl Biochem Biotechnol* 167:1270–1279 . <https://doi.org/10.1007/s12010-011-9507-5>

Chua G, Morris QD, Sopko R, Robinson MD, Ryan O, Chan ET, Frey BJ, Andrews BJ, Boone C, Hughes TR (2006) Identifying transcription factor functions and targets by phenotypic activation. *Proc Natl Acad Sci U S A* 103:12045–12050 . <https://doi.org/10.1073/pnas.0605140103>

Conrad M, Schothorst J, Kankipati HN, Van Zeebroeck G, Rubio-Teixeira M, Thevelein JM (2014) Nutrient sensing and signaling in the yeast *Saccharomyces cerevisiae*. *FEMS Microbiol Rev* 38:254–299 . <https://doi.org/10.1111/1574-6976.12065>

Cristobal-Sarramian A, Atzmüller D (2018) Yeast as a production platform in biorefineries: Conversion of agricultural residues into value-added products. *Agron Res* 16:377–388 . <https://doi.org/10.15159/AR.18.066>

Croft T, Venkatakrishnan P, Lin S-J (2020) NAD⁺ Metabolism and Regulation: Lessons From Yeast. *Biomolecules* 10:330 . <https://doi.org/10.3390/biom10020330>

- Cunha JT, Romani A, Costa CE, Sá-Correia I, Domingues L (2019) Molecular and physiological basis of *Saccharomyces cerevisiae* tolerance to adverse lignocellulose-based process conditions. *Appl Microbiol Biotechnol* 103:159–175 . <https://doi.org/10.1007/s00253-018-9478-3>
- Dahiya S, Kumar AN, Shanthi Sravan J, Chatterjee S, Sarkar O, Mohan SV (2018) Food waste biorefinery: Sustainable strategy for circular bioeconomy. *Bioresour Technol* 248:2–12 . <https://doi.org/10.1016/j.biortech.2017.07.176>
- Dai Z, Gu H, Zhang S, Xin F, Zhang W, Dong W, Ma J, Jia H, Jiang M (2017a) Metabolic construction strategies for direct methanol utilization in *Saccharomyces cerevisiae*. *Bioresour Technol* 245:1407–1412 . <https://doi.org/10.1016/j.biortech.2017.05.100>
- Dai Z, Gu H, Zhang S, Xin F, Zhang W, Dong W, Ma J, Jia H, Jiang M (2017b) Metabolic construction strategies for direct methanol utilization in *Saccharomyces cerevisiae*. *Bioresour Technol* 245:1407–1412 . <https://doi.org/10.1016/j.biortech.2017.05.100>
- Dandi ND, Dandi BN, Chaudhari AB (2013) Bioprospecting of thermo- and osmo-tolerant fungi from mango pulp–peel compost for bioethanol production. *Antonie Van Leeuwenhoek* 103:723–736 . <https://doi.org/10.1007/s10482-012-9854-4>
- de Graaf B, Clore A, McCullough AK (2009) Cellular pathways for DNA repair and damage tolerance of formaldehyde-induced DNA-protein crosslinks. *DNA Repair (Amst)* 8:1207–1214 . <https://doi.org/10.1016/j.dnarep.2009.06.007>
- de Jong B, Siewers V, Nielsen J (2012) Systems biology of yeast: enabling technology for development of cell factories for production of advanced biofuels. *Curr Opin Biotechnol* 23:624–630 . <https://doi.org/10.1016/j.copbio.2011.11.021>
- Delorme-Axford E, Popelka H, Klionsky DJ (2019) TEX264 is a major receptor for mammalian reticulophagy. *Autophagy* 15:1677–1681 . <https://doi.org/10.1080/15548627.2019.1646540>
- Dias PJ, Teixeira MC, Telo JP, Sá-Correia I (2010) Insights into the Mechanisms of Toxicity and Tolerance to the Agricultural Fungicide Mancozeb in Yeast, as Suggested by a Chemogenomic Approach. *Omi A J Integr Biol* 14:211–227 . <https://doi.org/10.1089/omi.2009.0134>
- Diaz AB, Blandino A, Caro I (2018) Value added products from fermentation of sugars derived from agro-food residues. *Trends Food Sci Technol* 71:52–64 . <https://doi.org/10.1016/j.tifs.2017.10.016>
- Dien BS, Kurtzman CP, Saha BC, Bothast RJ (1996) Screening for arabinose fermenting

- yeasts. *Appl Biochem Biotechnol* 57–58:233–242 . <https://doi.org/10.1007/BF02941704>
- Dinh H V., Suthers PF, Chan SHJ, Shen Y, Xiao T, Deewan A, Jagtap SS, Zhao H, Rao C V., Rabinowitz JD, Maranas CD (2019) A comprehensive genome-scale model for *Rhodospiridium toruloides* IFO0880 accounting for functional genomics and phenotypic data. *Metab Eng Commun* 9:e00101 . <https://doi.org/10.1016/j.mec.2019.e00101>
- Do DTH, Theron CW, Fickers P (2019) Organic wastes as feedstocks for non-conventional yeast-based bioprocesses. *Microorganisms* 7:1–22 . <https://doi.org/10.3390/microorganisms7080229>
- Dohmen RJ, Willers I, Marques AJ (2007) Biting the hand that feeds: Rpn4-dependent feedback regulation of proteasome function. *Biochim Biophys Acta - Mol Cell Res* 1773:1599–1604 . <https://doi.org/10.1016/j.bbamcr.2007.04.012>
- Dong Y, Hu J, Fan L, Chen Q (2017) RNA-Seq-based transcriptomic and metabolomic analysis reveal stress responses and programmed cell death induced by acetic acid in *Saccharomyces cerevisiae*. *Sci Rep* 7:1–16 . <https://doi.org/10.1038/srep42659>
- dos Santos SC (2012) Yeast toxicogenomics: genome-wide responses to chemical stresses with impact in environmental health, pharmacology, and biotechnology. *Front Genet* 3:1–17 . <https://doi.org/10.3389/fgene.2012.00063>
- dos Santos SC, Sá-Correia I (2015) Yeast toxicogenomics: lessons from a eukaryotic cell model and cell factory. *Curr Opin Biotechnol* 33:183–191 . <https://doi.org/10.1016/j.copbio.2015.03.001>
- dos Santos SC, Teixeira MC, Cabrito TR, Sá-Correia I (2012) Yeast toxicogenomics: Genome-wide responses to chemical stresses with impact in environmental health, pharmacology, and biotechnology. *Front Genet* 3:1–17 . <https://doi.org/10.3389/fgene.2012.00063>
- Du C, Li Y, Zhao X, Pei X, Yuan W, Bai F, Jiang Y (2019) The production of ethanol from lignocellulosic biomass by *Kluyveromyces marxianus* CICC 1727-5 and *Spathaspora passalidarum* ATCC MYA-4345. *Appl Microbiol Biotechnol* 103:2845–2855 . <https://doi.org/10.1007/s00253-019-09625-1>
- Duan X, Gao J, Zhou YJ (2018) Advances in engineering methylotrophic yeast for biosynthesis of valuable chemicals from methanol. *Chinese Chem Lett* 29:681–686 . <https://doi.org/10.1016/j.ccllet.2017.11.015>
- Eberharter A, Sterner DE, Schieltz D, Hassan A, Yates JR, Berger SL, Workman JL (1999) The ADA Complex Is a Distinct Histone Acetyltransferase Complex in *Saccharomyces cerevisiae*. *Mol Cell Biol* 19:6621–6631 . <https://doi.org/10.1128/mcb.19.10.6621>

- Edwards MC, Doran-Peterson J (2012) Pectin-rich biomass as feedstock for fuel ethanol production. *Appl Microbiol Biotechnol* 95:565–575 . <https://doi.org/10.1007/s00253-012-4173-2>
- Espinosa MI, Williams TC, Pretorius IS, Paulsen IT (2019) Benchmarking two *Saccharomyces cerevisiae* laboratory strains for growth and transcriptional response to methanol. *Synth Syst Biotechnol* 4:180–188 . <https://doi.org/10.1016/j.synbio.2019.10.001>
- Estruch F (2000) Stress-controlled transcription factors, stress-induced genes and stress tolerance in budding yeast. *FEMS Microbiol Rev* 24:469–486 . [https://doi.org/10.1016/S0168-6445\(00\)00035-8](https://doi.org/10.1016/S0168-6445(00)00035-8)
- European Commission Pesticides
- European Parliament (2009) Directive 2009/128/EC of the European Parliament and the Council of 21 October 2009 establishing a framework for Community action to achieve the sustainable use of pesticides. *October* 309:71–86 . https://doi.org/10.3000/17252555.L_2009.309
- Fabarius JT, Wegat V, Roth A, Sieber V (2020) Synthetic Methylophony in Yeasts: Towards a Circular Bioeconomy. *Trends Biotechnol* 1–11 . <https://doi.org/10.1016/j.tibtech.2020.08.008>
- Fletcher E, Krivoruchko A, Nielsen J (2016) Industrial systems biology and its impact on synthetic biology of yeast cell factories. *Biotechnol Bioeng* 113:1164–1170 . <https://doi.org/10.1002/bit.25870>
- Fonseca C, Romão R, Rodrigues de Sousa H, Hahn-Hägerdal B, Spencer-Martins I (2007) Arabinose transport and catabolism in yeast. *FEBS J* 274:3589–3600 . <https://doi.org/10.1111/j.1742-4658.2007.05892.x>
- Frazão CJR, Walther T (2020) Syngas and Methanol-Based Biorefinery Concepts. *Chemie-Ingenieur-Technik* 92:1680–1699 . <https://doi.org/10.1002/cite.202000108>
- Fujita K, Matsuyama A, Kobayashi Y, Iwahashi H (2006) The genome-wide screening of yeast deletion mutants to identify the genes required for tolerance to ethanol and other alcohols. *FEMS Yeast Res* 6:744–750 . <https://doi.org/10.1111/j.1567-1364.2006.00040.x>
- Gama R, Van Dyk JS, Pletschke BI (2015) Optimisation of enzymatic hydrolysis of apple pomace for production of biofuel and biorefinery chemicals using commercial enzymes. *3 Biotech* 5:1075–1087 . <https://doi.org/10.1007/s13205-015-0312-7>
- Game JC, Mortimer RK (1974) A Genetic Study of X-Ray Sensitive Mutants in Yeast. *Mutat*

Res 24:281–292

- Gancedo JM (1992) Carbon catabolite repression in yeast. *Eur J Biochem* 206:297–313 . <https://doi.org/10.1111/j.1432-1033.1992.tb16928.x>
- Gao M, Ploessl D, Shao Z (2019) Enhancing the Co-utilization of Biomass-Derived Mixed Sugars by Yeasts. *Front Microbiol* 9:1–21 . <https://doi.org/10.3389/fmicb.2018.03264>
- Gao S, Tong Y, Wen Z, Zhu L, Ge M, Chen D, Jiang Y, Yang S (2016) Multiplex gene editing of the *Yarrowia lipolytica* genome using the CRISPR-Cas9 system. *J Ind Microbiol Biotechnol* 43:1085–1093 . <https://doi.org/10.1007/s10295-016-1789-8>
- Gasch AP, Spellman PT, Kao CM, Carmel-Harel O, Eisen MB, Storz G, Botstein D, Brown PO (2000) Genomic Expression Programs in the Response of Yeast Cells to Environmental Changes. *Mol Biol Cell* 11:4241–4257 . <https://doi.org/10.1091/mbc.11.12.4241>
- González-Siso MI, Touriño A, Vizoso Á, Pereira-Rodríguez Á, Rodríguez-Belmonte E, Becerra M, Cerdán ME (2015) Improved bioethanol production in an engineered *Kluyveromyces lactis* strain shifted from respiratory to fermentative metabolism by deletion of NDI 1. *Microb Biotechnol* 8:319–330 . <https://doi.org/10.1111/1751-7915.12160>
- Grohmann K, Bothast RJ (1994) Pectin-Rich Residues Generated by Processing of Citrus Fruits, Apples, and Sugar Beets. In: *Enzymatic Conversion of Biomass for Fuels Production*. pp 372–390
- Grohmann K, Manthey JA, Cameron RG, Buslig BS (1999) Purification of Citrus Peel Juice and Molasses. *J Agric Food Chem* 47:4859–4867 . <https://doi.org/10.1021/jf9903049>
- Guerreiro J, Sampaio-Marques B, Soares R, Coelho A, Leao C, Ludovico P, Sa-Correia I (2016) Mitochondrial proteomics of the acetic acid - induced programmed cell death response in a highly tolerant *Zygosaccharomyces bailii* - derived hybrid strain. *Microb Cell* 3:65–78 . <https://doi.org/10.15698/mic2016.02.477>
- Günan Yücel H, Aksu Z (2015) Ethanol fermentation characteristics of *Pichia stipitis* yeast from sugar beet pulp hydrolysate: Use of new detoxification methods. *Fuel* 158:793–799 . <https://doi.org/10.1016/j.fuel.2015.06.016>
- Guo G, Hsu D, Chen W-H, Chen W, Hwang W (2009) Characterization of enzymatic saccharification for acid-pretreated lignocellulosic materials with different lignin composition. *Enzyme Microb Technol* 45:80–87 . <https://doi.org/10.1016/j.enzmictec.2009.05.012>
- Guo M, Cheng S, Chen G, Chen J (2019) Improvement of lipid production in oleaginous yeast

- Rhodospiridium toruloides by ultraviolet mutagenesis. *Eng Life Sci* 19:548–556 .
<https://doi.org/10.1002/elsc.201800203>
- Guo ZP, Olsson L (2016) Physiological responses to acid stress by *Saccharomyces cerevisiae* when applying high initial cell density. *FEMS Yeast Res* 16:1–11 .
<https://doi.org/10.1093/femsyr/fow072>
- Gupta SK, Shukla P (2017) Gene editing for cell engineering: trends and applications. *Crit Rev Biotechnol* 37:672–684 . <https://doi.org/10.1080/07388551.2016.1214557>
- Hamley-Bennett C, Lye GJ, Leak DJ (2016) Selective fractionation of Sugar Beet Pulp for release of fermentation and chemical feedstocks; optimisation of thermo-chemical pre-treatment. *Bioresour Technol* 209:259–264 .
<https://doi.org/10.1016/j.biortech.2016.02.131>
- Henriques SF, Mira NP, Sá-Correia I (2017) Genome-wide search for candidate genes for yeast robustness improvement against formic acid reveals novel susceptibility (Trk1 and positive regulators) and resistance (Haa1-regulon) determinants. *Biotechnol Biofuels* 10:1–11 . <https://doi.org/10.1186/s13068-017-0781-5>
- Hicks RH, Sze Y, Chuck CJ, Henk DA (2020) Enhanced inhibitor tolerance and increased lipid productivity through adaptive laboratory evolution in the oleaginous yeast *Metshnikowia pulcherrima*. *bioRxiv* 2020.02.17.952291 . <https://doi.org/10.1101/2020.02.17.952291>
- Hoffman CS (1997) Preparation of Yeast DNA . *Curr Protoc Mol Biol* 39:11–14 .
<https://doi.org/10.1002/0471142727.mb1311s39>
- Hong K-K, Nielsen J (2012) Metabolic engineering of *Saccharomyces cerevisiae*: a key cell factory platform for future biorefineries. *Cell Mol Life Sci* 69:2671–2690 .
<https://doi.org/10.1007/s00018-012-0945-1>
- Huang X-F, Liu J-N, Lu L-J, Peng K-M, Yang G-X, Liu J (2016) Culture strategies for lipid production using acetic acid as sole carbon source by *Rhodospiridium toruloides*. *Bioresour Technol* 206:141–149 . <https://doi.org/10.1016/j.biortech.2016.01.073>
- Huisjes EH, de Hulster E, van Dam JC, Pronk JT, van Maris AJA (2012) Galacturonic Acid Inhibits the Growth of *Saccharomyces cerevisiae* on Galactose, Xylose, and Arabinose. *Appl Environ Microbiol* 78:5052–5059 . <https://doi.org/10.1128/AEM.07617-11>
- Iwaki M, Rich PR (2004) Direct Detection of Formate Ligation in Cytochrome c Oxidase by ATR-FTIR Spectroscopy. *J Am Chem Soc* 126:2386–2389 .
<https://doi.org/10.1021/ja039320j>

- Jackson JC, Lopes JM (1996) The yeast *UME6* gene is required for both negative and positive transcriptional regulation of phospholipid biosynthetic gene expression. *Nucleic Acids Res* 24:1322–1329 . <https://doi.org/10.1093/nar/24.7.1322>
- Jayani RS, Saxena S, Gupta R (2005) Microbial pectinolytic enzymes: A review. *Process Biochem* 40:2931–2944 . <https://doi.org/10.1016/j.procbio.2005.03.026>
- Jeon WY, Shim WY, Lee SH, Choi JH, Kim JH (2013) Effect of heterologous xylose transporter expression in *Candida tropicalis* on xylitol production rate. *Bioprocess Biosyst Eng* 36:809–817 . <https://doi.org/10.1007/s00449-013-0907-5>
- Jeong D, Park H, Jang B-K, Ju Y, Shin MH, Oh EJ, Lee EJ, Kim SR (2021) Recent advances in the biological valorization of citrus peel waste into fuels and chemicals. *Bioresour Technol* 323:124603 . <https://doi.org/10.1016/j.biortech.2020.124603>
- Jeong D, Ye S, Park H, Kim SR (2020) Simultaneous fermentation of galacturonic acid and five-carbon sugars by engineered *Saccharomyces cerevisiae*. *Bioresour Technol* 295:122259 . <https://doi.org/10.1016/j.biortech.2019.122259>
- Ji H, Zhuge B, Zong H, Lu X, Fang H, Zhuge J (2016) Role of CgHOG1 in Stress Responses and Glycerol Overproduction of *Candida glycerinogenes*. *Curr Microbiol* 73:827–833 . <https://doi.org/10.1007/s00284-016-1132-7>
- Jiménez J, Benítez T (1988) Yeast cell viability under conditions of high temperature and ethanol concentrations depends on the mitochondrial genome. *Curr Genet* 13:461–469 . https://doi.org/10.1007/7854_2014_336
- John I, Muthukumar K, Arunagiri A (2017) A review on the potential of citrus waste for D-Limonene, pectin, and bioethanol production. *Int J Green Energy* 14:599–612 . <https://doi.org/10.1080/15435075.2017.1307753>
- Johnson EA (2013a) Biotechnology of non-*Saccharomyces* yeasts—the basidiomycetes. *Appl Microbiol Biotechnol* 97:7563–7577 . <https://doi.org/10.1007/s00253-013-5046-z>
- Johnson EA (2013b) Biotechnology of non-*Saccharomyces* yeasts—the ascomycetes. *Appl Microbiol Biotechnol* 97:503–517 . <https://doi.org/10.1007/s00253-012-4497-y>
- Johnson EA, Echavarri-Erasun C (2011) Yeast Biotechnology. In: *The Yeasts*. Elsevier, pp 21–44
- Jones AD, Boundy-Mills KL, Barla GF, Kumar S, Ubanwa B, Balan V (2019) Microbial lipid alternatives to plant lipids
- Joshi VK, Sharma R, Girdher A (2013) Production and Evaluation of Biocolour (carotenoids)

- from *Rhodotorula* using Apple Pomace: Effect of Composition of different Nitrogen Sources and Methods of Cell Disruption. *Int J Food Ferment Technol* 3:127 . <https://doi.org/10.5958/2277-9396.2014.00340.7>
- Kalia VC, Saini AK (2017) *Metabolic Engineering for Bioactive Compounds*. Springer Singapore, Singapore
- Kaur Sandhu S, Singh Oberoi H, Singh Dhaliwal S, Babbar N, Kaur U, Nanda D, Kumar D (2012) Ethanol production from Kinnow mandarin (*Citrus reticulata*) peels via simultaneous saccharification and fermentation using crude enzyme produced by *Aspergillus oryzae* and the thermotolerant *Pichia kudriavzevii* strain. *Ann Microbiol* 62:655–666 . <https://doi.org/10.1007/s13213-011-0302-x>
- Kayikci Ö, Nielsen J (2015) Glucose repression in *Saccharomyces cerevisiae*. *FEMS Yeast Res* 15:fov068 . <https://doi.org/10.1093/femsyr/fov068>
- Khosravi C, Kun RS, Visser J, Aguilar-Pontes MV, de Vries RP, Battaglia E (2017) In vivo functional analysis of L-rhamnose metabolic pathway in *Aspergillus niger*: a tool to identify the potential inducer of RhaR. *BMC Microbiol* 17:214 . <https://doi.org/10.1186/s12866-017-1118-z>
- Klein M, Swinnen S, Thevelein JM, Nevoigt E (2017) Glycerol metabolism and transport in yeast and fungi: established knowledge and ambiguities. *Environ Microbiol* 19:878–893 . <https://doi.org/10.1111/1462-2920.13617>
- Klose RJ, Gardner KE, Liang G, Erdjument-Bromage H, Tempst P, Zhang Y (2007) Demethylation of Histone H3K36 and H3K9 by Rph1: a Vestige of an H3K9 Methylation System in *Saccharomyces cerevisiae*? *Mol Cell Biol* 27:3951–3961 . <https://doi.org/10.1128/mcb.02180-06>
- Koch B, Schmidt C, Daum G (2014) Storage lipids of yeasts: A survey of nonpolar lipid metabolism in *Saccharomyces cerevisiae*, *Pichia pastoris*, and *Yarrowia lipolytica*. *FEMS Microbiol Rev* 38:892–915 . <https://doi.org/10.1111/1574-6976.12069>
- Koivistoinen OM, Arvas M, Headman JR, Andberg M, Penttilä M, Jeffries TW, Richard P (2012) Characterisation of the gene cluster for l-rhamnose catabolism in the yeast *Scheffersomyces (Pichia) stipitis*. *Gene* 492:177–185 . <https://doi.org/10.1016/j.gene.2011.10.031>
- Kot AM, Błażej S, Gientka I, Kieliszek M, Bryś J (2018) Torulene and torularhodin: “New” fungal carotenoids for industry? *Microb. Cell Fact.* 17:49
- Kot AM, Błażej S, Kieliszek M, Gientka I, Bryś J, Reczek L, Pobiega K (2019) Effect of

- exogenous stress factors on the biosynthesis of carotenoids and lipids by *Rhodotorula* yeast strains in media containing agro-industrial waste. *World J Microbiol Biotechnol* 35:1–10 . <https://doi.org/10.1007/s11274-019-2732-8>
- Kręgiel D, Pawlikowska E, Antolak H (2017) Non-Conventional Yeasts in Fermentation Processes: Potentialities and Limitations. *Old Yeasts - New Quest*. <https://doi.org/10.5772/intechopen.70404>
- Kroemer G, Mariño G, Levine B (2010) Autophagy and the Integrated Stress Response. *Mol Cell* 40:280–293 . <https://doi.org/10.1016/j.molcel.2010.09.023>
- Kubota S, Takeo I, Kume K, Kanai M, Shitamukai A, MIZUNUMA M, MIYAKAWA T, Shimoi H, Iefuji H, HIRATA D (2004) Effect of Ethanol on Cell Growth of Budding Yeast: Genes That Are Important for Cell Growth in the Presence of Ethanol. *Biosci Biotechnol Biochem* 68:968–972 . <https://doi.org/10.1271/bbb.68.968>
- Kühnel S (2011) Characterization of cell wall degrading enzymes from *Chrysosporium lucknowense* C1 and their use to degrade sugar beet pulp. Wageningen University, NL
- Kumar KK, Deeba F, Sauraj, Negi YS, Gaur NA (2020) Harnessing pongamia shell hydrolysate for triacylglycerol agglomeration by novel oleaginous yeast *Rhodotorula pacifica* INDKK. *Biotechnol Biofuels* 13:175 . <https://doi.org/10.1186/s13068-020-01814-9>
- Kurtzman CP, Robnett CJ (2010) Systematics of methanol assimilating yeasts and neighboring taxa from multigene sequence analysis and the proposal of *Peterozyma* gen. nov., a new member of the Saccharomycetales. *FEMS Yeast Res* 10:353–361 . <https://doi.org/10.1111/j.1567-1364.2010.00625.x>
- Kurtzman CP, Robnett CJ (1998) Identification and phylogeny of ascomycetous yeasts from analysis of nuclear large subunit (26S) ribosomal DNA partial sequences. *Antonie van Leeuwenhoek, Int J Gen Mol Microbiol* 73:331–371 . <https://doi.org/10.1023/A:1001761008817>
- Lane MM, Morrissey JP (2010) *Kluyveromyces marxianus*: A yeast emerging from its sister's shadow. *Fungal Biol Rev* 24:17–26 . <https://doi.org/10.1016/j.fbr.2010.01.001>
- Lane S, Xu H, Oh EJ, Kim H, Lesmana A, Jeong D, Zhang G, Tsai C-S, Jin Y-S, Kim SR (2018) Glucose repression can be alleviated by reducing glucose phosphorylation rate in *Saccharomyces cerevisiae*. *Sci Rep* 8:2613 . <https://doi.org/10.1038/s41598-018-20804-4>
- Larochelle M, Drouin S, Robert F, Turcotte B (2006) Oxidative Stress-Activated Zinc Cluster Protein Stb5 Has Dual Activator/Repressor Functions Required for Pentose Phosphate

- Pathway Regulation and NADPH Production. *Mol Cell Biol* 26:6690–6701 .
<https://doi.org/10.1128/mcb.02450-05>
- Leandro MJ, Gonçalves P, Spencer-Martins I (2006) Two glucose/xylose transporter genes from the yeast *Candida intermedia*: first molecular characterization of a yeast xylose–H⁺ symporter. *Biochem J* 395:543–549 . <https://doi.org/10.1042/BJ20051465>
- Leão C, Van Uden N (1984) Effects of ethanol and other alkanols on passive proton influx in the yeast *Saccharomyces cerevisiae*. *BBA - Biomembr* 774:43–48 .
[https://doi.org/10.1016/0005-2736\(84\)90272-4](https://doi.org/10.1016/0005-2736(84)90272-4)
- Lee M-H, Lin J-J, Lin Y-J, Chang J-J, Ke H-M, Fan W-L, Wang T-Y, Li W-H (2018) Genome-wide prediction of CRISPR/Cas9 targets in *Kluyveromyces marxianus* and its application to obtain a stable haploid strain. *Sci Rep* 8:7305 . <https://doi.org/10.1038/s41598-018-25366-z>
- Legrand G (2005) The correct use of pressed beet pulp. Collect “Guides Tech Irbab/Kbivb 46
- Leijdekkers AGM, Bink JPM, Geutjes S, Schols HA, Gruppen H (2013) Enzymatic saccharification of sugar beet pulp for the production of galacturonic acid and arabinose; a study on the impact of the formation of recalcitrant oligosaccharides. *Bioresour Technol* 128:518–525 . <https://doi.org/10.1016/j.biortech.2012.10.126>
- Leong WH, Lim JW, Lam MK, Uemura Y, Ho YC (2018) Third generation biofuels: A nutritional perspective in enhancing microbial lipid production. *Renew Sustain Energy Rev* 91:950–961 . <https://doi.org/10.1016/j.rser.2018.04.066>
- Lewis KL, Karthikeyan G, Westmoreland JW, Resnick MA (2002) Differential suppression of DNA repair deficiencies of yeast rad50 , mre11 and xrs2 mutants by EXO1 and TLC1 (the RNA component of telomerase). *Genetics* 160:49–62
- Li B, Wang L, Wu Y, Xia Z, Yang B (2020) Improving acetic acid and furfural resistance of *Saccharomyces cerevisiae* by regulating novel transcriptional factors revealed via comparative transcriptome. 1–11
- Lian J, Mishra S, Zhao H (2018) Recent advances in metabolic engineering of *Saccharomyces cerevisiae*: New tools and their applications. *Metab Eng* 50:85–108 .
<https://doi.org/10.1016/j.ymben.2018.04.011>
- Liguori R, Faraco V (2016) Biological processes for advancing lignocellulosic waste biorefinery by advocating circular economy. *Bioresour Technol* 215:13–20 .
<https://doi.org/10.1016/j.biortech.2016.04.054>

- Limayem A, Ricke SC (2012) Lignocellulosic biomass for bioethanol production: Current perspectives, potential issues and future prospects. *Prog Energy Combust Sci* 38:449–467 . <https://doi.org/10.1016/j.pecs.2012.03.002>
- Limtong S, Srisuk N, Yongmanitchai W, Yurimoto H, Nakase T (2008) *Ogataea chonburiensis* sp. nov. and *Ogataea nakhonphanomensis* sp. nov., thermotolerant, methylotrophic yeast species isolated in Thailand, and transfer of *Pichia siamensis* and *Pichia thermomethanolica* to the genus *Ogataea*. *Int J Syst Evol Microbiol* 58:302–307 . <https://doi.org/10.1099/ijs.0.65380-0>
- Lin D (2012) Toxicity mechanism of formic acid is directly linked to ROS burst and oxidative damage in yeast *Saccharomyces cerevisiae*. *Adv Mater Res* 550–553:1060–1065 . <https://doi.org/10.4028/www.scientific.net/AMR.550-553.1060>
- Liu N, Santala S, Stephanopoulos G (2020) Mixed carbon substrates: a necessary nuisance or a missed opportunity? *Curr Opin Biotechnol* 62:15–21 . <https://doi.org/10.1016/j.copbio.2019.07.003>
- Liu Z, Ho S-H, Hasunuma T, Chang J-S, Ren N-Q, Kondo A (2016) Recent advances in yeast cell-surface display technologies for waste biorefineries. *Bioresour Technol* 215:324–333 . <https://doi.org/10.1016/j.biortech.2016.03.132>
- Löbs A-K, Schwartz C, Wheeldon I (2017) Genome and metabolic engineering in non-conventional yeasts: Current advances and applications. *Synth Syst Biotechnol* 2:198–207 . <https://doi.org/10.1016/j.synbio.2017.08.002>
- Löbs AK, Schwartz C, Thorwall S, Wheeldon I (2018) Highly Multiplexed CRISPRi Repression of Respiratory Functions Enhances Mitochondrial Localized Ethyl Acetate Biosynthesis in *Kluyveromyces marxianus*. *ACS Synth Biol* 7:2647–2655 . <https://doi.org/10.1021/acssynbio.8b00331>
- Loman AA, Islam SMM, Ju L-K (2018) Production of arabinol from enzymatic hydrolysate of soybean flour by *Debaryomyces hansenii* fermentation. *Appl Microbiol Biotechnol* 102:641–653 . <https://doi.org/10.1007/s00253-017-8626-5>
- Lopes HJS, Bonturi N, Kerkhoven EJ, Miranda EA, Lahtvee PJ (2020) C/N ratio and carbon source-dependent lipid production profiling in *Rhodotorula toruloides*. *Appl Microbiol Biotechnol* 104:2639–2649 . <https://doi.org/10.1007/s00253-020-10386-5>
- Luévano-Martínez LA, Appolinario P, Miyamoto S, Uribe-carvajal S, Kowaltowski AJ (2013) Deletion of the transcriptional regulator *opi1p* decreases cardiolipin content and disrupts mitochondrial metabolism in *Saccharomyces cerevisiae*. *Fungal Genet Biol* 60:150–158 .

<https://doi.org/10.1016/j.fgb.2013.03.005>

- Lundmark R, Forsell N, Leduc S, Lundgren J, Ouraich I, Pettersson K, Wetterlund E (2018) Large-scale implementation of biorefineries
- Lyman M, Urbin S, Strout C, Rubinfeld B (2019) The Oleaginous Red Yeast *Rhodotorula/Rhodospiridium*: A Factory for Industrial Bioproducts . Yeasts Biotechnol. <https://doi.org/10.5772/intechopen.84129>
- Ma M, Liu ZL (2010) Comparative transcriptome profiling analyses during the lag phase uncover YAP1, PDR1, PDR3, RPN4 and HSF1 as key regulatory genes in genomic adaptation to the lignocellulose derived inhibitor HMF for *Saccharomyces cerevisiae*. BMC Genomics 11:660 . <https://doi.org/10.1186/1471-2164-11-660>
- Marion RM, Regev A, Segal E, Barash Y, Koller D, Friedman N, O’Shea EK (2004) Sfp1 is a stress- and nutrient-sensitive regulator of ribosomal protein gene expression. Proc Natl Acad Sci U S A 101:14315–22 . <https://doi.org/10.1073/pnas.0405353101>
- Martani F, Maestroni L, Torchio M, Ami D, Natalello A, Lotti M, Porro D, Branduardi P (2020) Conversion of sugar beet residues into lipids by *Lipomyces starkeyi* for biodiesel production. Microb Cell Fact 19:1–13 . <https://doi.org/10.1186/s12934-020-01467-1>
- Martens-Uzunova ES, Schaap PJ (2008) An evolutionary conserved d-galacturonic acid metabolic pathway operates across filamentous fungi capable of pectin degradation. Fungal Genet Biol 45:1449–1457 . <https://doi.org/10.1016/j.fgb.2008.08.002>
- Martínez-Muñoz GA, Kane P (2008) Vacuolar and plasma membrane proton pumps collaborate to achieve cytosolic pH homeostasis in yeast. J Biol Chem 283:20309–20319 . <https://doi.org/10.1074/jbc.M710470200>
- Martínez O, Sánchez A, Font X, Barrena R (2017) Valorization of sugarcane bagasse and sugar beet molasses using *Kluyveromyces marxianus* for producing value-added aroma compounds via solid-state fermentation. J Clean Prod 158:8–17 . <https://doi.org/10.1016/j.jclepro.2017.04.155>
- Martini C, Tauk-Tornisiello SM, Codato CB, Bastos RG, Ceccato-Antonini SR (2016) A strain of *Meyerozyma guilliermondii* isolated from sugarcane juice is able to grow and ferment pentoses in synthetic and bagasse hydrolysate media. World J Microbiol Biotechnol 32:80 . <https://doi.org/10.1007/s11274-016-2036-1>
- Martins LC, Monteiro CC, Semedo PM, Sá-correia I (2020) Valorisation of pectin-rich agro-industrial residues by yeasts : potential and challenges. <https://doi.org/10.1007/s00253-020-10697-7>

- Mata-Gómez LC, Montañez JC, Méndez-Zavala A, Aguilar CN (2014) Biotechnological production of carotenoids by yeasts: An overview. *Microb Cell Fact* 13:1–11 . <https://doi.org/10.1186/1475-2859-13-12>
- Matsubara T, Hamada S, Wakabayashi A, Kishida M (2016) Fermentative production of l-galactonate by using recombinant *Saccharomyces cerevisiae* containing the endogenous galacturonate reductase gene from *Cryptococcus diffluens*. *J Biosci Bioeng* 122:639–644 . <https://doi.org/10.1016/j.jbiosc.2016.05.002>
- Maza DD, Viñarta SC, Su Y, Guillamón JM, Aybar MJ (2020) Growth and lipid production of *Rhodotorula glutinis* R4, in comparison to other oleaginous yeasts. *J Biotechnol* 310:21–31 . <https://doi.org/10.1016/j.jbiotec.2020.01.012>
- Merz M, Appel D, Berends P, Rabe S, Blank I, Stressler T, Fischer L (2016) Batch-to-batch variation and storage stability of the commercial peptidase preparation Flavourzyme in respect of key enzyme activities and its influence on process reproducibility. *Eur Food Res Technol* 242:1005–1012 . <https://doi.org/10.1007/s00217-015-2606-8>
- Micard V, Renard CMGC, Thibault J-F (1996) Enzymatic saccharification of sugar-beet pulp. *Enzyme Microb Technol* 19:162–170 . [https://doi.org/10.1016/0141-0229\(95\)00224-3](https://doi.org/10.1016/0141-0229(95)00224-3)
- Mira NP, Becker JD, Sá-Correia I (2010a) Genomic expression program involving the Haa1p-regulon in *Saccharomyces cerevisiae* response to acetic acid. *OMICS* 14:587–601 . <https://doi.org/10.1089/omi.2010.0048>
- Mira NP, Henriques SF, Keller G, Teixeira MC, Matos RG, Arraiano CM, Winge DR, Sá-Correia I (2011) Identification of a DNA-binding site for the transcription factor Haa1, required for *Saccharomyces cerevisiae* response to acetic acid stress. *Nucleic Acids Res* 39:6896–6907 . <https://doi.org/10.1093/nar/gkr228>
- Mira NP, Munsterkötter M, Dias-Valada F, Santos J, Palma M, Roque FC, Guerreiro JF, Rodrigues F, Sousa MJ, Leao C, Guldener U, Sa-Correia I (2014) The Genome Sequence of the Highly Acetic Acid-Tolerant *Zygosaccharomyces bailii*-Derived Interspecies Hybrid Strain ISA1307, Isolated From a Sparkling Wine Plant. *DNA Res* 21:299–313 . <https://doi.org/10.1093/dnares/dst058>
- Mira NP, Palma M, Guerreiro JF, Sá-Correia I (2010b) Genome-wide identification of *Saccharomyces cerevisiae* genes required for tolerance to acetic acid. *Microb Cell Fact* 9:79 . <https://doi.org/10.1186/1475-2859-9-79>
- Mira NP, Teixeira MC, Sá-Correia I (2010c) Adaptive Response and Tolerance to Weak Acids in *Saccharomyces cerevisiae*: A Genome-Wide View. *Omi A J Integr Biol* 14:525–540 .

<https://doi.org/10.1089/omi.2010.0072>

- Miyagawa KI, Ishiwata-Kimata Y, Kohno K, Kimata Y (2014) Ethanol stress impairs protein folding in the endoplasmic reticulum and activates Ire1 in *Saccharomyces cerevisiae*. *Biosci Biotechnol Biochem* 78:1389–1391 .
<https://doi.org/10.1080/09168451.2014.921561>
- Mohnen D (2008) Pectin structure and biosynthesis. *Curr Opin Plant Biol* 11:266–277 .
<https://doi.org/10.1016/j.pbi.2008.03.006>
- Monteiro GA, Sá-Correia I (1998) *In vivo* activation of yeast plasma membrane H⁺-ATPase by ethanol: Effect on the kinetic parameters and involvement of the carboxyl-terminus regulatory domain. *Biochim Biophys Acta - Biomembr* 1370:310–316 .
[https://doi.org/10.1016/S0005-2736\(97\)00281-2](https://doi.org/10.1016/S0005-2736(97)00281-2)
- Monteiro PT, Oliveira J, Pais P, Antunes M, Palma M, Cavalheiro M, Galocha M, Godinho CP, Martins LC, Bourbon N, Mota MN, Ribeiro RA, Viana R, Sá-Correia I, Teixeira MC (2020) YEASTRACT+: a portal for cross-species comparative genomics of transcription regulation in yeasts. *Nucleic Acids Res* 48:642–649 . <https://doi.org/10.1093/nar/gkz859>
- Morano KA, Grant CM, Moyer-Rowley WS (2012) The response to heat shock and oxidative stress in *Saccharomyces cerevisiae*. *Genetics* 190:1157–1195 .
<https://doi.org/10.1534/genetics.111.128033>
- Mota MN, Martins LC, Sá-Correia I (2021) The Identification of Genetic Determinants of Methanol Tolerance in Yeast Suggests Differences in Methanol and Ethanol Toxicity Mechanisms and Candidates for Improved Methanol Tolerance Engineering. *J Fungi* 7:90 .
<https://doi.org/10.3390/jof7020090>
- Mukherjee V, Radecka D, Aerts G, Verstrepen KJ, Lievens B, Thevelein JM (2017) Phenotypic landscape of non-conventional yeast species for different stress tolerance traits desirable in bioethanol fermentation. *Biotechnol Biofuels* 10:216 . <https://doi.org/10.1186/s13068-017-0899-5>
- Müller-maatsch J, Bencivenni M, Caligiani A, Tedeschi T, Bruggeman G, Bosch M, Petrusan J, Droogenbroeck B Van, Elst K, Sforza S (2016) Pectin content and composition from different food waste streams. 201:37–45 .
<https://doi.org/10.1016/j.foodchem.2016.01.012>
- Müller-Maatsch J, Bencivenni M, Caligiani A, Tedeschi T, Bruggeman G, Bosch M, Petrusan J, Van Droogenbroeck B, Elst K, Sforza S (2016) Pectin content and composition from different food waste streams. *Food Chem* 201:37–45 .

<https://doi.org/10.1016/j.foodchem.2016.01.012>

- Mussatto SI, Silva CJS, Roberto IC (2006) Fermentation performance of *Candida guilliermondii* for xylitol production on single and mixed substrate media. *Appl Microbiol Biotechnol* 72:681–686 . <https://doi.org/10.1007/s00253-006-0372-z>
- Naik SN, Goud V V., Rout PK, Dalai AK (2010) Production of first and second generation biofuels: A comprehensive review. *Renew Sustain Energy Rev* 14:578–597 . <https://doi.org/10.1016/j.rser.2009.10.003>
- Nambu-Nishida Y, Nishida K, Hasunuma T, Kondo A (2017) Development of a comprehensive set of tools for genome engineering in a cold- and thermo-tolerant *Kluyveromyces marxianus* yeast strain. *Sci Rep* 7:8993 . <https://doi.org/10.1038/s41598-017-08356-5>
- Nicholls P (1975) Formate as an inhibitor of cytochrome c oxidase. *Biochem Biophys Res Commun* 67:610–616 . [https://doi.org/10.1016/0006-291X\(75\)90856-6](https://doi.org/10.1016/0006-291X(75)90856-6)
- Nielsen J (2019) Yeast Systems Biology: Model Organism and Cell Factory. *Biotechnol J* 14:1800421 . <https://doi.org/10.1002/biot.201800421>
- Nielsen J (2003) It Is All about Metabolic Fluxes. *J Bacteriol* 185:7031–7035 . <https://doi.org/10.1128/JB.185.24.7031-7035.2003>
- Nielsen J, Keasling JD (2016) Engineering Cellular Metabolism. *Cell* 164:1185–1197 . <https://doi.org/10.1016/j.cell.2016.02.004>
- Nigam P, Vogel M (1991) Bioconversion of sugar industry by-products—molasses and sugar beet pulp for single cell protein production by yeasts. *Biomass and Bioenergy* 1:339–345 . [https://doi.org/10.1016/0961-9534\(91\)90014-4](https://doi.org/10.1016/0961-9534(91)90014-4)
- North M, Gaytán BD, Romero C, De La Rosa VY, Loguinov A, Smith MT, Zhang L, Vulpe CD (2016) Functional toxicogenomic profiling expands insight into modulators of formaldehyde toxicity in yeast. *Front Genet* 7:1–11 . <https://doi.org/10.3389/fgene.2016.00200>
- Nurcholis M, Lertwattanasakul N, Rodrussamee N, Kosaka T, Murata M, Yamada M (2020) Integration of comprehensive data and biotechnological tools for industrial applications of *Kluyveromyces marxianus*. *Appl Microbiol Biotechnol* 104:475–488 . <https://doi.org/10.1007/s00253-019-10224-3>
- Ogawa Y, Nitta A, Uchiyama H, Imamura T, Shimoi H, Ito K (2000) Tolerance mechanism of the ethanol-tolerant mutant of sake yeast. *J Biosci Bioeng* 90:313–320 . [https://doi.org/10.1016/S1389-1723\(00\)80087-0](https://doi.org/10.1016/S1389-1723(00)80087-0)

- Orij R, Brul S, Smits GJ (2011) Intracellular pH is a tightly controlled signal in yeast. *Biochim Biophys Acta - Gen Subj* 1810:933–944 . <https://doi.org/10.1016/j.bbagen.2011.03.011>
- Palma M, Dias PJ, Roque F de C, Luzia L, Guerreiro JF, Sá-Correia I (2017) The *Zygosaccharomyces bailii* transcription factor Haa1 is required for acetic acid and copper stress responses suggesting subfunctionalization of the ancestral bifunctional protein Haa1/Cup2. *BMC Genomics* 18:75 . <https://doi.org/10.1186/s12864-016-3443-2>
- Palma M, Guerreiro JF, Sá-Correia I (2018) Adaptive Response and Tolerance to Acetic Acid in *Saccharomyces cerevisiae* and *Zygosaccharomyces bailii*: A Physiological Genomics Perspective. *Front Microbiol* 9:1–16 . <https://doi.org/10.3389/fmicb.2018.00274>
- Palma M, Roque F de C, Guerreiro JF, Mira NP, Queiroz L, Sá-Correia I (2015) Search for genes responsible for the remarkably high acetic acid tolerance of a *Zygosaccharomyces bailii*-derived interspecies hybrid strain. *BMC Genomics* 16:1070 . <https://doi.org/10.1186/s12864-015-2278-6>
- Palma M, Sá-Correia I (2019) Physiological Genomics of the Highly Weak-Acid-Tolerant Food Spoilage Yeasts of *Zygosaccharomyces bailii* sensu lato. *Prog. Mol. Subcell. Biol.* 58:85–109
- Palmqvist E, Hahn-Hägerdal B (2000) Fermentation of lignocellulosic hydrolysates. II: inhibitors and mechanisms of inhibition. *Bioresour Technol* 74:25–33 . [https://doi.org/10.1016/S0960-8524\(99\)00161-3](https://doi.org/10.1016/S0960-8524(99)00161-3)
- Pan X, Heitman J (2000) Sok2 Regulates Yeast Pseudohyphal Differentiation via a Transcription Factor Cascade That Regulates Cell-Cell Adhesion. *Mol Cell Biol* 20:8364–8372 . <https://doi.org/10.1128/mcb.20.22.8364-8372.2000>
- Papapetridis I, Verhoeven MD, Wiersma SJ, Goudriaan M, van Maris AJA, Pronk JT (2018) Laboratory evolution for forced glucose-xylose co-consumption enables identification of mutations that improve mixed-sugar fermentation by xylose-fermenting *Saccharomyces cerevisiae*. *FEMS Yeast Res* 18:1–17 . <https://doi.org/10.1093/femsyr/foy056>
- Park Y-K, Nicaud J-M, Ledesma-Amaro R (2018) The Engineering Potential of *Rhodospiridium toruloides* as a Workhorse for Biotechnological Applications. *Trends Biotechnol* 36:304–317 . <https://doi.org/10.1016/j.tibtech.2017.10.013>
- Parmar I, Rupasinghe HPV (2012) Optimization of dilute acid-based pretreatment and application of laccase on apple pomace. *Bioresour Technol* 124:433–439 . <https://doi.org/10.1016/j.biortech.2012.07.030>
- Peters D (2006) Raw materials. *Adv. Biochem. Eng. Biotechnol.* 105:1–30

- Pfeiffer T, Morley A (2014) An evolutionary perspective on the Crabtree effect. *Front Mol Biosci* 1:1–6 . <https://doi.org/10.3389/fmolb.2014.00017>
- Pham KD, Shida Y, Miyata A, Takamizawa T, Suzuki Y, Ara S, Yamazaki H, Masaki K, Mori K, Aburatani S, Hirakawa H, Tashiro K, Kuhara S, Takaku H, Ogasawara W (2020) Effect of light on carotenoid and lipid production in the oleaginous yeast *Rhodospiridium toruloides*. *Biosci Biotechnol Biochem* 84:1501–1512 . <https://doi.org/10.1080/09168451.2020.1740581>
- Protzko RJ, Hach CA, Coradetti ST, Hackhofer MA, Magosch S, Thieme N, Geiselman GM, Arkin AP, Skerker JM, Dueber JE, Benz JP (2019) Genomewide and Enzymatic Analysis Reveals Efficient D-Galacturonic Acid Metabolism in the Basidiomycete Yeast *Rhodospiridium toruloides*. *mSystems* 4: . <https://doi.org/10.1128/mSystems.00389-19>
- Protzko RJ, Latimer LN, Martinho Z, de Reus E, Seibert T, Benz JP, Dueber JE (2018) Engineering *Saccharomyces cerevisiae* for co-utilization of d-galacturonic acid and d-glucose from citrus peel waste. *Nat Commun* 9:5059 . <https://doi.org/10.1038/s41467-018-07589-w>
- Qi F, Shen P, Hu R, Xue T, Jiang X, Qin L, Chen Y, Huang J (2020) Carotenoids and lipid production from *Rhodospiridium toruloides* cultured in tea waste hydrolysate. *Biotechnol Biofuels* 13:1–12 . <https://doi.org/10.1186/s13068-020-01712-0>
- Qiao K, Wasylenko TM, Zhou K, Xu P, Stephanopoulos G (2017) Lipid production in *Yarrowia lipolytica* is maximized by engineering cytosolic redox metabolism. *Nat Biotechnol* 35:173–177 . <https://doi.org/10.1038/nbt.3763>
- Quemener B, Lahaye M, Thibault JF (1993) Studies on the simultaneous determination of acidic and neutral sugars of plant cell wall materials by HPLC of their methyl glycosides after combined methanolysis and enzymic prehydrolysis. *Carbohydr Polym* 20:87–94 . [https://doi.org/10.1016/0144-8617\(93\)90082-F](https://doi.org/10.1016/0144-8617(93)90082-F)
- Radecka D, Mukherjee V, Mateo RQ, Stojiljkovic M, Foulquié-Moreno MR, Thevelein JM (2015) Looking beyond *Saccharomyces*: The potential of non-conventional yeast species for desirable traits in bioethanol fermentation. *FEMS Yeast Res*. 15:53
- Raschmanová H, Weninger A, Glieder A, Kovar K, Vogl T (2018) Implementing CRISPR-Cas technologies in conventional and non-conventional yeasts: Current state and future prospects. *Biotechnol Adv* 36:641–665 . <https://doi.org/10.1016/j.biotechadv.2018.01.006>
- Ratledge C (2010) Single Cell Oils for the 21st Century. In: *Single Cell Oils*, Second Edi. Elsevier, pp 3–26

- Ratledge C, Wynn JP (2002) The biochemistry and molecular biology of lipid accumulation in oleaginous microorganisms. *Adv Appl Microbiol* 51:1–52 . [https://doi.org/10.1016/S0065-2164\(02\)51000-5](https://doi.org/10.1016/S0065-2164(02)51000-5)
- Rebello S, Abraham A, Madhavan A, Sindhu R, Binod P, Babu AK, Aneesh EM, Pandey A (2018) Non-conventional Yeast cell factories for sustainable bioprocesses. *FEMS Microbiol Lett* 365:1–10 . <https://doi.org/10.1093/femsle/fny222>
- Reggiori F, Klionsky DJ (2013) Autophagic processes in yeast: Mechanism, machinery and regulation. *Genetics* 194:341–361 . <https://doi.org/10.1534/genetics.112.149013>
- Reihl P, Stolz J (2005) The Monocarboxylate Transporter Homolog Mch5p Catalyzes Riboflavin (Vitamin B2) Uptake in *Saccharomyces cerevisiae* . *J Biol Chem* 280:39809–39817 . <https://doi.org/10.1074/jbc.M505002200>
- Reimand J, Vaquerizas JM, Todd AE, Vilo J, Luscombe NM (2010) Comprehensive reanalysis of transcription factor knockout expression data in *Saccharomyces cerevisiae* reveals many new targets. *Nucleic Acids Res* 38:4768–4777 . <https://doi.org/10.1093/nar/gkq232>
- Richard P, Hilditch S (2009) d-Galacturonic acid catabolism in microorganisms and its biotechnological relevance. *Appl Microbiol Biotechnol* 82:597–604 . <https://doi.org/10.1007/s00253-009-1870-6>
- Rodrigues F, Sousa MJ, Ludovico P, Santos H, Côrte-Real M, Leão C (2012) The Fate of Acetic Acid during Glucose Co-Metabolism by the Spoilage Yeast *Zygosaccharomyces bailii*. *PLoS One* 7:e52402 . <https://doi.org/10.1371/journal.pone.0052402>
- Rodriguez-Amaya, Delia Kimura M (2004) *HarvestPlus Handbook for Carotenoid Analysis*. HarvestPlus
- Rodríguez Madrera R, Pando Bedriñana R, Suárez Valles B (2015) Production and characterization of aroma compounds from apple pomace by solid-state fermentation with selected yeasts. *LWT - Food Sci Technol* 64:1342–1353 . <https://doi.org/10.1016/j.lwt.2015.07.056>
- Rosa M, Sá-Correia I (1991) *In vivo* activation by ethanol of plasma membrane ATPase of *Saccharomyces cerevisiae*. *Appl Environ Microbiol* 57:830–835
- Rosa MF, Sá-Correia I (1996) Intracellular acidification does not account for inhibition of *Saccharomyces cerevisiae* growth in the presence of ethanol. *FEMS Microbiol Lett* 135:271–274 . [https://doi.org/10.1016/0378-1097\(95\)00465-3](https://doi.org/10.1016/0378-1097(95)00465-3)
- Rozpędowska E, Hellborg L, Ishchuk OP, Orhan F, Galafassi S, Merico A, Woolfit M,

- Compagno C, Piškur J (2011) Parallel evolution of the make–accumulate–consume strategy in *Saccharomyces* and *Dekkera* yeasts. *Nat Commun* 2:302 . <https://doi.org/10.1038/ncomms1305>
- Sahm H (1977) Metabolism of methanol by yeasts. pp 77–103
- Sahota PP, Kaur N (2015) Characterization of enzyme naringinase and the production of debittered low alcoholic kinnow (*Citrus raticulata blanco*) beverage. *Int J Adv Res* 3:1220–1233
- Sakai T, Sakamoto T, Hallaert J, Vandamme EJ (1993a) [Pectin, Pectinase, and Protopectinase: Production,] Properties, and Applications. In: *Advances in Applied Microbiology*. pp 213–294
- Salgueiro SP, Sá-Correia I, Novais JM (1988) Ethanol-Induced Leakage in *Saccharomyces cerevisiae*: Kinetics and Relationship to Yeast Ethanol Tolerance and Alcohol Fermentation Productivity. *Appl Environ Microbiol* 54:903–9
- Salter GJ, Kell DB (1995) Solvent Selection for Whole Cell Biotransformations in Organic Media. *Crit Rev Biotechnol* 15:139–177
- Sangster J (1989) Octanol-water partition coefficients of simple organic compounds. *J Phys Chem* 18:1111–1227 . <https://doi.org/http://dx.doi.org/10.1063/1.555833>
- Saravanakumar D, Spadaro D, Garibaldi A, Gullino ML (2009) Detection of enzymatic activity and partial sequence of a chitinase gene in *Metschnikowia pulcherrima* strain MACH1 used as post-harvest biocontrol agent. *Eur J Plant Pathol* 123:183–193 . <https://doi.org/10.1007/s10658-008-9355-5>
- Satyanarayana T, Kunze G (2009a) *Yeast biotechnology: Diversity and applications*. Springer Netherlands, Dordrecht
- Satyanarayana T, Kunze G (eds) (2009b) *Yeast Biotechnology: Diversity and Applications*. Springer Netherlands, Dordrecht
- Scherens B, Feller A, Vierendeels F, Messenguy F, Dubois E (2006) Identification of direct and indirect targets of the Gln3 and Gat1 activators by transcriptional profiling in response to nitrogen availability in the short and long term. *FEMS Yeast Res* 6:777–791 . <https://doi.org/10.1111/j.1567-1364.2006.00060.x>
- Schiewer S, Patil SB (2008) Pectin-rich fruit wastes as biosorbents for heavy metal removal: Equilibrium and kinetics. *Bioresour Technol* 99:1896–1903 . <https://doi.org/10.1016/j.biortech.2007.03.060>

- Schirmer-Michel ÂC, Flôres SH, Hertz PF, Ayub MAZ (2009) Effect of oxygen transfer rates on alcohols production by *Candida guilliermondii* cultivated on soybean hull hydrolysate. J Chem Technol Biotechnol 84:223–228 . <https://doi.org/10.1002/jctb.2028>
- Schirmer-Michel ÂC, Flôres SH, Hertz PF, Matos GS, Ayub MAZ (2008) Production of ethanol from soybean hull hydrolysate by osmotolerant *Candida guilliermondii* NRRL Y-2075. Bioresour Technol 99:2898–2904 . <https://doi.org/10.1016/j.biortech.2007.06.042>
- Schmitz K, Protzko R, Zhang L, Benz JP (2019) Spotlight on fungal pectin utilization—from phytopathogenicity to molecular recognition and industrial applications. Appl Microbiol Biotechnol 2507–2524 . <https://doi.org/10.1007/s00253-019-09622-4>
- Seiboth B, Metz B (2011) Fungal arabinan and L-arabinose metabolism. Appl Microbiol Biotechnol 89:1665–1673 . <https://doi.org/10.1007/s00253-010-3071-8>
- Sellick CA, Campbell RN, Reece RJ (2008) Galactose Metabolism in Yeast—Structure and Regulation of the Leloir Pathway Enzymes and the Genes Encoding Them. In: International Review of Cell and Molecular Biology. pp 111–150
- Serrat M, Bermúdez RC, Villa TG (2004) Polygalacturonase and ethanol production in *Kluyveromyces marxianus*: Potential use of polygalacturonase in foodstuffs. Appl Biochem Biotechnol - Part A Enzym Eng Biotechnol 117:49–64 . <https://doi.org/10.1385/ABAB:117:1:49>
- Shrestha S, Kognou ALM, Zhang J, Qin W (2020) Different Facets of Lignocellulosic Biomass Including Pectin and Its Perspectives. Waste and Biomass Valorization. <https://doi.org/10.1007/s12649-020-01305-w>
- Sikkema J, De Bont JAM, Poolman B (1995) Mechanisms of membrane toxicity of hydrocarbons. Microbiol Rev 59:201–222 . <https://doi.org/10.1128/membr.59.2.201-222.1995>
- Simpson-Lavy K, Kupiec M (2019) Carbon Catabolite Repression in Yeast is Not Limited to Glucose. Sci Rep 9:6491 . <https://doi.org/10.1038/s41598-019-43032-w>
- Singh G, Sinha S, Bandyopadhyay KK, Lawrence M, Paul D (2018) Triauxic growth of an oleaginous red yeast *Rhodospiridium toruloides* on waste 'extract' for enhanced and concomitant lipid and β -carotene production. Microb Cell Fact 17:182 . <https://doi.org/10.1186/s12934-018-1026-4>
- Siripong W, Wolf P, Kusumoputri TP, Downes JJ, Kocharin K, Tanapongpipat S, Runguphan W (2018) Metabolic engineering of *Pichia pastoris* for production of isobutanol and isobutyl acetate. Biotechnol Biofuels 11:1 . <https://doi.org/10.1186/s13068-017-1003-x>

- Sitepu I, Selby T, Lin T, Zhu S, Boundy-Mills K (2014a) Carbon source utilization and inhibitor tolerance of 45 oleaginous yeast species. *J Ind Microbiol Biotechnol* 41:1061–1070 . <https://doi.org/10.1007/s10295-014-1447-y>
- Sitepu IR, Garay LA, Sestric R, Levin D, Block DE, German JB, Boundy-Mills KL (2014b) Oleaginous yeasts for biodiesel: Current and future trends in biology and production. *Biotechnol Adv* 32:1336–1360 . <https://doi.org/10.1016/j.biotechadv.2014.08.003>
- Skrbic B, Durisic-Mladenovic N, Macvanin N (2010) Determination of Metal Contents in Sugar Beet (*Beta vulgaris*) and Its Products: Empirical and Chemometrical Approach. *Food Sci Technol Res* 16:123–134 . <https://doi.org/10.3136/fstr.16.123>
- Skrzydowska E (2003) Toxicological and Metabolic Consequences of Methanol Poisoning. *Toxicol Mech Methods* 11:277–293 . <https://doi.org/10.1080/15376520390243523>
- Sloothaak J, Odoni DI, Martins dos Santos VAP, Schaap PJ, Tamayo-Ramos JA (2016) Identification of a Novel L-rhamnose Uptake Transporter in the Filamentous Fungus *Aspergillus niger*. *PLOS Genet* 12:e1006468 . <https://doi.org/10.1371/journal.pgen.1006468>
- Souffriau B, Den Abt T, Thevelein JM (2012) Evidence for rapid uptake of d-galacturonic acid in the yeast *Saccharomyces cerevisiae* by a channel-type transport system. *FEBS Lett* 586:2494–2499 . <https://doi.org/10.1016/j.febslet.2012.06.012>
- Spagnuolo M, Yaguchi A, Blenner M (2019) Oleaginous yeast for biofuel and oleochemical production. *Curr Opin Biotechnol* 57:73–81 . <https://doi.org/10.1016/j.copbio.2019.02.011>
- Sreenivas A, Carman GM (2003) Phosphorylation of the yeast phospholipid synthesis regulatory protein Opi1p by Protein Kinase A. *J Biol Chem* 278:20673–20680 . <https://doi.org/10.1074/jbc.M300132200>
- Stanley D, Bandara A, Fraser S, Chambers PJ, Stanley GA (2010) The ethanol stress response and ethanol tolerance of *Saccharomyces cerevisiae*. *J Appl Microbiol* 109:13–24 . <https://doi.org/10.1111/j.1365-2672.2009.04657.x>
- Stolz J, Hoja U, Meier S, Sauer N, Schweizer E (1999) Identification of the Plasma Membrane H⁺-Biotin Symporter of *Saccharomyces cerevisiae* by Rescue of a Fatty Acid-auxotrophic Mutant. *J Biol Chem* 274:18741–18746 . <https://doi.org/10.1074/jbc.274.26.18741>
- Subtil T, Boles E (2011) Improving L-arabinose utilization of pentose fermenting *Saccharomyces cerevisiae* cells by heterologous expression of L-arabinose transporting sugar transporters. *Biotechnol Biofuels* 4:38 . <https://doi.org/10.1186/1754-6834-4-38>

- Swinnen S, Henriques SF, Shrestha R, Ho P-W, Sá-Correia I, Nevoigt E (2017) Improvement of yeast tolerance to acetic acid through Haa1 transcription factor engineering: towards the underlying mechanisms. *Microb Cell Fact* 16:7 . <https://doi.org/10.1186/s12934-016-0621-5>
- Symington LS (2002) Role of *RAD52* epistasis group genes in homologous recombination and double-strand break repair. *Microbiol Mol Biol Rev* 66:630–670 . <https://doi.org/10.1128/MMBR.66.4.630>
- Tanimura A, Takashima M, Sugita T, Endoh R, Ohkuma M, Kishino S, Ogawa J, Shima J (2016) Lipid production through simultaneous utilization of glucose, xylose, and l-arabinose by *Pseudozyma hubeiensis*: a comparative screening study. *AMB Express* 6:58 . <https://doi.org/10.1186/s13568-016-0236-6>
- Taskin M, Ortucu S, Aydogan MN, Arslan NP (2016) Lipid production from sugar beet molasses under non-aseptic culture conditions using the oleaginous yeast *Rhodotorula glutinis* TR29. *Renew Energy* 99:198–204 . <https://doi.org/10.1016/j.renene.2016.06.060>
- Teixeira MC, Duque P, Sá-Correia I (2007) Environmental genomics: mechanistic insights into toxicity of and resistance to the herbicide 2,4-D. *Trends Biotechnol* 25:363–370 . <https://doi.org/10.1016/j.tibtech.2007.06.002>
- Teixeira MC, Mira NP, Sá-Correia I (2011) A genome-wide perspective on the response and tolerance to food-relevant stresses in *Saccharomyces cerevisiae*. *Curr Opin Biotechnol* 22:150–156 . <https://doi.org/10.1016/j.copbio.2010.10.011>
- Teixeira MC, Raposo LR, Mira NP, Lourenço AB, Sá-Correia I (2009) Genome-wide identification of *Saccharomyces cerevisiae* genes required for maximal tolerance to ethanol. *Appl Environ Microbiol* 75:5761–5772 . <https://doi.org/10.1128/AEM.00845-09>
- Torre I De, Acedos MG, Esteban J, Santos VE, Ladero M (2019) Utilisation / upgrading of orange peel waste from a biological biorefinery perspective. 5975–5991
- Tsaponina O, Chabes A (2013) Pre-activation of the genome integrity checkpoint increases DNA damage tolerance. *Nucleic Acids Res* 41:10371–10378 . <https://doi.org/10.1093/nar/gkt820>
- Ubando AT, Felix CB, Chen W-H (2020) Biorefineries in circular bioeconomy: A comprehensive review. *Bioresour Technol* 299:122585 . <https://doi.org/10.1016/j.biortech.2019.122585>
- Vadkertiová R, Sláviková E (2006) Metal tolerance of yeasts isolated from water, soil and plant environments. *J Basic Microbiol* 46:145–152 . <https://doi.org/10.1002/jobm.200510609>

- van der Klei IJ, Yurimoto H, Sakai Y, Veenhuis M (2006) The significance of peroxisomes in methanol metabolism in methylotrophic yeast. *Biochim Biophys Acta - Mol Cell Res* 1763:1453–1462 . <https://doi.org/10.1016/j.bbamcr.2006.07.016>
- van Dijk M, Erdei B, Galbe M, Nygård Y, Olsson L (2019) Strain-dependent variance in short-term adaptation effects of two xylose-fermenting strains of *Saccharomyces cerevisiae*. *Bioresour Technol* 292:121922 . <https://doi.org/10.1016/j.biortech.2019.121922>
- van Voorst F, Houghton-Larsen J, Jønson L, Kielland-Brandt MC, Brandt A (2006) Genome-wide identification of genes required for growth of *Saccharomyces cerevisiae* under ethanol stress. *Yeast* 23:351–359 . <https://doi.org/10.1002/yea.1359>
- Van Zutphen T, Todde V, De Boer R, Kreim M, Hofbauer HF, Wolinski H, Veenhuis M, Van Der Klei IJ, Kohlwein SD (2014) Lipid droplet autophagy in the yeast *Saccharomyces cerevisiae*. *Mol Biol Cell* 25:290–301 . <https://doi.org/10.1091/mbc.E13-08-0448>
- Vartiainen E, Blomberg P, Ilmén M, Andberg M, Toivari M, Penttilä M (2019a) Evaluation of synthetic formaldehyde and methanol assimilation pathways in *Yarrowia lipolytica*. *Fungal Biol Biotechnol* 6:1–13 . <https://doi.org/10.1186/s40694-019-0090-9>
- Vendruscolo F, Albuquerque PM, Streit F, Esposito E, Ninow JL (2008) Apple Pomace: A Versatile Substrate for Biotechnological Applications. *Crit Rev Biotechnol* 28:1–12 . <https://doi.org/10.1080/07388550801913840>
- Vizoso-Vázquez Á, Lamas-Maceiras M, Becerra M, González-Siso MI, Rodríguez-Belmonte E, Cerdán ME (2012) Ixr1p and the control of the *Saccharomyces cerevisiae* hypoxic response. *Appl Microbiol Biotechnol* 94:173–184 . <https://doi.org/10.1007/s00253-011-3785-2>
- Vizoso-Vázquez Á, Lamas-Maceiras M, González-Siso MI, Cerdán ME (2018) Ixr1 Regulates Ribosomal Gene Transcription and Yeast Response to Cisplatin. *Sci Rep* 8:1–14 . <https://doi.org/10.1038/s41598-018-21439-1>
- Wagner JM, Alper HS (2016) Synthetic biology and molecular genetics in non-conventional yeasts: Current tools and future advances. *Fungal Genet Biol* 89:126–136 . <https://doi.org/10.1016/j.fgb.2015.12.001>
- Wamelink MMC, Struys EA, Jakobs C (2008) The biochemistry, metabolism and inherited defects of the pentose phosphate pathway: A review. *J Inherit Metab Dis* 31:703–717 . <https://doi.org/10.1007/s10545-008-1015-6>
- Wang G-Y, Chi Z, Song B, Wang Z-P, Chi Z-M (2012) High level lipid production by a novel inulinase-producing yeast *Pichia guilliermondii* Pcla22. *Bioresour Technol* 124:77–82 .

- <https://doi.org/10.1016/j.biortech.2012.08.024>
- Wang L, Wang X, He ZQ, Zhou SJ, Xu L, Tan XY, Xu T, Li BZ (2020a) Engineering prokaryotic regulator IrrE to enhance stress tolerance in budding yeast. *Biotechnol Biofuels* 13:1–18 . <https://doi.org/10.1186/s13068-020-01833-6>
- Wang Y, Fan L, Tuyishime P, Liu J, Zhang K, Gao N, Zhang Z, Ni X, Feng J, Yuan Q, Ma H, Zheng P, Sun J, Ma Y (2020b) Adaptive laboratory evolution enhances methanol tolerance and conversion in engineered *Corynebacterium glutamicum*. *Commun Biol* 3: . <https://doi.org/10.1038/s42003-020-0954-9>
- Weber FJ, De Bont JAM (1996) Adaptation mechanisms of microorganisms to the toxic effects of organic solvents on membranes. *Biochim Biophys Acta* 1286:225–245 . [https://doi.org/10.1016/S0304-4157\(96\)00010-X](https://doi.org/10.1016/S0304-4157(96)00010-X)
- Welsh DT (2000) Ecological significance of compatible solute accumulation by microorganisms: From single cells to global climate. *FEMS Microbiol Rev* 24:263–290 . [https://doi.org/10.1016/S0168-6445\(99\)00038-8](https://doi.org/10.1016/S0168-6445(99)00038-8)
- Weninger A, Glieder A, Vogl T (2015) A toolbox of endogenous and heterologous nuclear localization sequences for the methylotrophic yeast *Pichia pastoris*. *FEMS Yeast Res* 15:fov082 . <https://doi.org/10.1093/femsyr/fov082>
- Wiemken A (1990) Trehalose in yeast, stress protectant rather than reserve carbohydrate. *Antonie Van Leeuwenhoek* 58:209–217
- Wikiera A, Mika M, Starzyńska-Janiszewska A, Stodolak B (2015) Development of complete hydrolysis of pectins from apple pomace. *Food Chem* 172:675–680 . <https://doi.org/10.1016/j.foodchem.2014.09.132>
- Williams PA (2011) Natural Polymers: Introduction and Overview. In: RSC Polymer Chemistry Series. pp 1–14
- Wirth F, Goldani LZ (2012) Epidemiology of *Rhodotorula* : An Emerging Pathogen. *Interdiscip Perspect Infect Dis* 2012:1–7 . <https://doi.org/10.1155/2012/465717>
- Wisselink HW, Toirkens MJ, del Rosario Franco Berriel M, Winkler AA, van Dijken JP, Pronk JT, van Maris AJA (2007) Engineering of *Saccharomyces cerevisiae* for Efficient Anaerobic Alcoholic Fermentation of L-Arabinose. *Appl Environ Microbiol* 73:4881–4891 . <https://doi.org/10.1128/AEM.00177-07>
- Wojtczak L, Slyshenkov VS (2003) Protection by pantothenic acid against apoptosis and cell damage by oxygen free radicals – The role of glutathione. *BioFactors* 17:61–73 .

<https://doi.org/10.1007/s10549-010-0835-x>

- Wu Y, Shen X, Yuan Q, Yan Y (2016) Metabolic Engineering Strategies for Co-Utilization of Carbon Sources in Microbes. *Bioengineering* 3:10 .
<https://doi.org/10.3390/bioengineering3010010>
- Xu P, Bura R, Doty SL (2011) Genetic analysis of D-xylose metabolism by endophytic yeast strains of *rhodotorula graminis* and *rhodotorula mucilaginosa*. *Genet Mol Biol* 34:471–478 .
<https://doi.org/10.1590/S1415-47572011000300018>
- Yaguchi A, Spagnuolo M, Blenner M (2018) Engineering yeast for utilization of alternative feedstocks. *Curr Opin Biotechnol* 53:122–129 .
<https://doi.org/10.1016/j.copbio.2017.12.003>
- Yapo BM, Lerouge P, Thibault J-F, Ralet M-C (2007) Pectins from citrus peel cell walls contain homogalacturonans homogenous with respect to molar mass, rhamnogalacturonan I and rhamnogalacturonan II. *Carbohydr Polym* 69:426–435 .
<https://doi.org/10.1016/j.carbpol.2006.12.024>
- Yapo BM, Robert C, Etienne I, Wathelet B, Paquot M (2007b) Effect of extraction conditions on the yield, purity and surface properties of sugar beet pulp pectin extracts. *Food Chem* 100:1356–1364 . <https://doi.org/10.1016/j.foodchem.2005.12.012>
- Yasokawa D, Murata S, Iwahashi Y, Kitagawa E, Nakagawa R, Hashido T, Iwahashi H (2010) Toxicity of methanol and formaldehyde towards *Saccharomyces cerevisiae* as assessed by DNA microarray analysis. *Appl Biochem Biotechnol* 160:1685–1698 .
<https://doi.org/10.1007/s12010-009-8684-y>
- Ye S, Jeong D, Shon JC, Liu KH, Kim KH, Shin M, Kim SR (2019) Deletion of PHO13 improves aerobic l-arabinose fermentation in engineered *Saccharomyces cerevisiae*. *J Ind Microbiol Biotechnol* 46:1725–1731 . <https://doi.org/10.1007/s10295-019-02233-y>
- Yoshikawa K, Tanaka T, Furusawa C, Nagahisa K, Hirasawa T, Shimizu H (2009) Comprehensive phenotypic analysis for identification of genes affecting growth under ethanol stress in *Saccharomyces cerevisiae*. *FEMS Yeast Res* 9:32–44 .
<https://doi.org/10.1111/j.1567-1364.2008.00456.x>
- You KM, Rosenfield C, Knipple DC (2003) Ethanol tolerance in the yeast *Saccharomyces cerevisiae* is dependent on cellular oleic acid content. *Appl Environ Microbiol* 69:1499–1503 . <https://doi.org/10.1128/AEM.69.3.1499>
- Zetterholm J, Bryngemark E, Ahlström J, Söderholm P, Harvey S, Wetterlund E (2020) Economic Evaluation of Large-Scale Biorefinery Deployment: A Framework Integrating

- Dynamic Biomass Market and Techno-Economic Models. *Sustainability* 12:7126 .
<https://doi.org/10.3390/su12177126>
- Zhang GC, Liu JJ, Kong II, Kwak S, Jin YS (2015) Combining C6 and C5 sugar metabolism for enhancing microbial bioconversion. *Curr. Opin. Chem. Biol.* 29:49–57
- Zhang W, Song M, Yang Q, Dai Z, Zhang S, Xin F, Dong W, Ma J, Jiang M (2018) Current advance in bioconversion of methanol to chemicals. *Biotechnol Biofuels* 11:1–11 .
<https://doi.org/10.1186/s13068-018-1265-y>
- Zhao M, Shi D, Lu X, Zong H, Zhuge B, Ji H (2019) Ethanol fermentation from non-detoxified lignocellulose hydrolysate by a multi-stress tolerant yeast *Candida glycerinogenes* mutant. *Bioresour Technol* 273:634–640 . <https://doi.org/10.1016/j.biortech.2018.11.053>
- Zhou W, Widmer W, Grohmann K (2008) Developments in Ethanol Production from Citrus Peel Waste. *Proc Fla State Hort Soc* 307–310
- Zhu T, Zhao T, Bankefa OE, Li Y (2020) Engineering unnatural methylotrophic cell factories for methanol-based biomanufacturing: Challenges and opportunities. *Biotechnol Adv* 39:107467 . <https://doi.org/10.1016/j.biotechadv.2019.107467>
- Zuin VG, Segatto ML, Ramin LZ (2018) Plants as resources for organic molecules: Facing the green and sustainable future today. *Curr Opin Green Sustain Chem* 9:1–7 .
<https://doi.org/10.1016/j.cogsc.2017.10.001>

7| Supplementary Material

7. Supplementary Tables

Table S1. 1- List of genes whose expression increases *S. cerevisiae* tolerance to 8%(v/v) methanol based on the screening of the Euroscarf deletion mutant collection; the elimination of the indicated genes increases yeast susceptibility to methanol. Biological functions are based on the information available in SGD (www.yeastgenome.org). The symbols '+++', '++' and '+' refer to phenotypes as shown in Figure 2.1.

Ammonium and vitamin metabolism

Genes	Function	Susceptibility to methanol
BNA1	3-hydroxyanthranilic acid dioxygenase. Bna1 is required for the <i>de novo</i> biosynthesis of NAD from tryptophan via kynurenine.	++
ADO1	Adenosine kinase. Ado1 is required for the utilization of S-adenosylmethionine.	+++
MET7	Folypolyglutamate synthetase. Met7 catalyses extension of the glutamate chains of the folate coenzymes, required for methionine synthesis and for maintenance of mitochondrial DNA.	+
NPR3	Subunit of the Iml1/SEACIT complex; SEACIT (Iml1-Npr2-Npr3) that is required for non-nitrogen-starvation-induced autophagy.	+
PDX3	Pyridoxine (pyridoxamine) phosphate oxidase.	++

Autophagy

Genes	Function	Susceptibility to methanol
ATG11	Adapter protein for pexophagy and the Cvt targeting pathway.	+++
ATG15	Phospholipase; Atg15 is required for lysis of autophagic and CVT bodies.	++
MON1	Subunit of a heterodimeric guanine nucleotide exchange factor (GEF). Mon1 is a subunit of the Mon1-Ccz1 GEF complex which stimulates nucleotide exchange and activation of Ypt7, a Rab family GTPase involved in membrane tethering and fusion events at the late endosome and vacuole.	++

Carbohydrate metabolism

Genes	Function	Susceptibility to methanol
<i>GPH1</i>	Glycogen phosphorylase required for the mobilization of glycogen.	+++
<i>LPD1</i>	Lipoamide dehydrogenase component (E3) of the pyruvate dehydrogenase and 2-oxoglutarate dehydrogenase multi-enzyme complexes.	+++
<i>MAN2</i>	Mannitol dehydrogenase.	+
<i>MLS1</i>	Malate synthase.	+
<i>PDA1</i>	E1 alpha subunit of the pyruvate dehydrogenase (PDH) complex.	+
<i>PDB1</i>	E1 beta subunit of the pyruvate dehydrogenase (PDH) complex.	+
<i>RPE1</i>	D-ribulose-5-phosphate 3-epimerase.	++
<i>TPS1</i>	Synthase subunit of trehalose-6-P synthase/phosphatase complex.	++
<i>TPS2</i>	Phosphatase subunit of the trehalose-6-P synthase/phosphatase complex.	+++

Cell cycle

Genes	Function	Susceptibility to methanol
<i>BNI5</i>	Linker protein responsible for recruitment of myosin to the bud neck.	+
<i>BUB3</i>	Kinetochore checkpoint WD40 repeat protein.	++
<i>CDC55</i>	Regulatory subunit B of protein phosphatase 2A (PP2A).	+++
<i>CIK1</i>	Kinesin-associated protein. Cik1 is required for both karyogamy and mitotic spindle organization.	+++
<i>CIN8</i>	Kinesin motor protein involved in mitotic spindle assembly and chromosome segregation.	++
<i>IBD2</i>	Component of the BUB2-dependent spindle checkpoint pathway.	+
<i>RTS1</i>	B-type regulatory subunit of protein phosphatase 2A (PP2A).	+
<i>SHS1</i>	Component of the septin ring that is required for cytokinesis.	+++

<i>SWM1</i>	Subunit of the anaphase-promoting complex (APC); APC is an E3 ubiquitin ligase that regulates the metaphase-anaphase transition and exit from mitosis.	+++
--------------------	--	-----

Cell wall function

Genes	Function	Susceptibility to methanol
<i>CCW12</i>	Cell wall mannoprotein. Ccw12 plays a role in maintenance of newly synthesized areas of cell wall.	++
<i>CWH41</i>	Processing alpha glucosidase I and ER type II integral membrane N-glycoprotein involved in assembly of cell wall beta 1,6 glucan and asparagine-linked protein glycosylation.	+
<i>FKS1</i>	Catalytic subunit of 1,3-beta-D-glucan synthase. Fks1 is involved in cell wall synthesis and maintenance.	+++
<i>GAS1</i>	Beta-1,3-glucanosyltransferase. Gas1 is required for cell wall assembly and also has a role in transcriptional silencing.	++
<i>KRE6</i>	Type II integral membrane protein. Kre6 is required for beta-1,6 glucan biosynthesis.	++
<i>MNN11</i>	Subunit of a Golgi mannosyltransferase complex that mediates elongation of the polysaccharide mannan backbone.	+++
<i>PEF1</i>	Penta-EF-hand protein, required for polar bud growth and cell wall abscission.	++
<i>ROT2</i>	Glucosidase II catalytic subunit. Rot2 is required to trim the final glucose in N-linked glycans and for normal cell wall synthesis.	+++
<i>SLG1</i>	Sensor-transducer of the stress-activated PKC1-MPK1 kinase pathway. Slg1 is involved in maintenance of cell wall integrity.	++
<i>SMI1</i>	Protein involved in the regulation of cell wall synthesis.	+++

Cellular signalling

Genes	Function	Susceptibility to methanol
--------------	-----------------	-----------------------------------

ASC1	G-protein beta subunit and guanine dissociation inhibitor for Gpa2 required to prevent frameshifting at ribosomes stalled at repeated CGA codons.	+
BCK1	MAPKKK acting in the protein kinase C signalling pathway, controlling cell integrity.	++
CLA4	Cdc42-activated signal transducing kinase. Cla4 is involved in septin ring assembly, vacuole inheritance, cytokinesis, sterol uptake regulation.	++
ELM1	Serine/threonine protein kinase. Elm1 regulates the orientation checkpoint, the morphogenesis checkpoint and the metabolic switch from fermentative to oxidative metabolism.	++
MKK1	MAPKK involved in the protein kinase C signalling pathway, controlling of cell integrity.	+
NBP2	Protein involved in the HOG (high osmolarity glycerol) pathway; negatively regulates Hog1 by recruitment of phosphatase Ptc1 to the Pbs2-Hog1 complex.	++
PCL6	Pho85p cyclin of the Pho80p subfamily. Pcl6 is involved in the control of glycogen storage by Pho85.	+
RAS2	GTP-binding protein that regulates nitrogen starvation response, sporulation, and filamentous growth.	+++
ROM2	Guanine nucleotide exchange factor (GEF) for Rho1 and Rho2.	+
SNF4	Activating gamma subunit of the AMP-activated Snf1 kinase complex; activates glucose-repressed genes, represses glucose-induced genes; role in sporulation, and peroxisome biogenesis.	++
SST2	GTPase-activating protein for Gpa1. Sst2 regulates desensitization to alpha factor pheromone.	++
TUS1	Guanine nucleotide exchange factor (GEF) that modulates Rho1 activity. Tus1 is involved in the cell integrity signalling pathway.	++
YPT7	Rab family GTPase; GTP-binding protein of the rab family. Ypt7 is required for homotypic fusion event in vacuole inheritance, for endosome-endosome fusion.	++

Chromatin remodelling, nucleic acid metabolism and transcription

Genes	Function	Susceptibility to methanol
ADA2	Transcription coactivator; component of the ADA and SAGA transcriptional adaptor/HAT (histone acetyltransferase) complexes.	++
AMD1	AMP deaminase that catalyses the deamination of AMP to form IMP and ammonia.	+
ARP8	Nuclear actin-related protein involved in chromatin remodelling.	+
ASF1	Nucleosome assembly factor. Asf1 is involved in chromatin assembly, disassembly and in the recovery after DSB repair.	++
BRE1	E3 ubiquitin ligase. Bre1 forms heterodimer with Rad6 to regulate K63 polyubiquitination in response to oxidative stress and to monoubiquitinate histone H2B-K123, which is required for the subsequent methylation of histone H3-K4 and H3-K79.	++
CBP2	Required for splicing of the group I intron bI5 of the COB pre-mRNA;	+
CDC73	Component of the Paf1 complex. Cdc73 binds to and modulates the activity of RNA polymerases I and II. Cdc73 is also involved in transcription elongation.	++
CHZ1	Histone chaperone for Htz1/H2A-H2B dimer.	+
CSE2	Subunit of the RNA polymerase II mediator complex.	++
CSM1	Nucleolar protein that mediates homolog segregation during meiosis I.	+++
DIA2	Origin-binding F-box protein that functions in ubiquitination of silent chromatin structural protein Sir4. Dia2 is required to target Cdc6 for destruction during G1 phase and is also required for deactivation of Rad53 checkpoint kinase, completion of DNA replication during recovery from DNA damage, assembly of RSC complex, RSC-mediated transcription regulation, and nucleosome positioning.	++
DST1	General transcription elongation factor TFIIIS. Dst1 enables RNA polymerase II to read through blocks to elongation by stimulating cleavage of nascent transcripts stalled at transcription arrest sites.	+
ELP3	Subunit of Elongator complex; Elongator is required for modification of wobble nucleosides in tRNA.	+

GCN5	Catalytic subunit of ADA and SAGA histone acetyltransferase complexes.	+
GTF1	Subunit of the trimeric GatFAB AmidoTransferase(AdT) complex. Gtf1 is involved in the formation of Q-tRNAQ.	+
HIR3	Subunit of the HIR complex, Hir3 is involved in regulation of histone gene transcription,	+
HTA1	Histone H2A. Hta1 is required for chromatin assembly and chromosome function.	++
HTZ1	Histone variant H2AZ. Htz1 is involved in transcriptional regulation through prevention of the spread of silent heterochromatin.	++
IKI1	Subunit of hexameric RecA-like ATPase Elp456 Elongator subcomplex. Iki1 is required for modification of wobble nucleosides in tRNA.	++
LSM6	Lsm (Like Sm) protein. Lsm6 is part of heteroheptameric complexes and it is involved in RNA decay.	+
MAF1	Negative regulator of RNA polymerase III that is involved in tRNA processing and stability.	++
MED1	Subunit of the RNA polymerase II mediator complex. Med1 is essential for transcriptional regulation.	++
MED2	Subunit of the RNA polymerase II mediator complex. Med2 is essential for transcriptional regulation.	++
MFT1	Subunit of the THO complex that is involved in transcription elongation and mitotic recombination.	++
MOG1	Nuclear protein that interacts with GTP-Gsp1, Mog1 stimulates nucleotide release from Gsp1 and is also involved in nuclear protein import.	+++
NCL1	S-adenosyl- L-methionine-dependent tRNA.	++
NPP1	Nucleotide pyrophosphatase/phosphodiesterase; Npp1 mediates extracellular nucleotide phosphate hydrolysis along with Npp2 and Pho5.	++
NPT1	Nicotinate phosphoribosyltransferase. Npt1 is required for silencing at rDNA and telomeres and has a role in silencing at mating-type loci.	++
NUT1	Component of the RNA polymerase II mediator complex that is required for transcriptional activation and also has a role in basal transcription.	++

PAP2	Non-canonical poly(A) polymerase. Pap2 is involved in nuclear RNA degradation as a component of TRAMP.	+
PAT1	Deadenylation-dependent mRNA-decapping factor.	+
POL32	Third subunit of DNA polymerase delta; Pol32 is involved in chromosomal DNA replication.	+
RCO1	Essential component of the Rpd3S histone deacetylase complex.	++
RFM1	Component of the Sum1-Rfm1-Hst1 complex. Rfm1 is involved in transcriptional repression of middle sporulation genes and in initiation of DNA replication.	+
RMI1	Subunit of the RecQ (Sgs1) - Top3 complex Rmi1 stimulates superhelical relaxing, DNA catenation/decatenation and ssDNA binding activities of Top3. Rmi1 is also involved in response to DNA damage;	++
RRN10	Protein involved in promoting high level transcription of rDNA; subunit of UAF (upstream activation factor) for RNA polymerase I.	++
RRP6	Nuclear exosome exonuclease component that has 3'-5' exonuclease activity that is regulated by Lrp1.	+
RSC1	Component of the RSC chromatin remodelling complex. Rsc1 is required for expression of mid-late sporulation-specific genes.	++
RTT101	Cullin subunit of a Roc1-dependent E3 ubiquitin ligase complex. Rtt101 plays a role in anaphase progression and is required for recovery after DSB repair.	++
RTT109	Histone acetyltransferase. Acetylates H3K56, H3K9.	+
SGS1	RecQ family nucleolar DNA helicase. Sgs1 play a role in genome integrity maintenance, chromosome synapsis, meiotic joint molecule/crossover formation.	++
SIN3	Component of both the Rpd3S and Rpd3L histone deacetylase complexes. Sin3 is involved in transcriptional repression and activation of diverse processes, including mating-type switching and meiosis.	+
SIR3	Silencing protein. Sir3 is required for spreading of silenced chromatin.	++
SNF6	Subunit of the SWI/SNF chromatin remodelling complex. Snf6 is involved in transcriptional regulation,	++
SPT21	Protein with a role in transcriptional silencing.	++

SPT3	Subunit of the SAGA and SAGA-like transcriptional regulatory complexes.	+
SPT4	Spt4/5 (DSIF) transcription elongation factor complex subunit; the Spt4/5 complex binds to ssRNA in a sequence-specific manner, and along with RNAP I and II has multiple roles regulating transcriptional elongation, RNA processing, quality control, and transcription-coupled repair.	+
SRB8	Subunit of the RNA polymerase II mediator complex. Srb8 is essential for transcriptional regulation and is involved in glucose repression.	+
SSN8	Cyclin-like component of the RNA polymerase II holoenzyme. Ssn8 is involved in phosphorylation of the RNA polymerase II C-terminal domain.	+++
TCD2	tRNA threonylcarbamoyladenosine dehydratase.	+
THO2	Subunit of the THO complex.	+++
THP2	Subunit of the THO and TREX complexes.	+++
THP3	Protein that may have a role in transcription elongation.	+
TOP1	Topoisomerase I; relieves torsional strain in DNA by cleaving and re-sealing the phosphodiester backbone. Top1 relaxes both positively and negatively supercoiled DNA.	++
TOP3	DNA Topoisomerase III that relax single-stranded negatively-supercoiled DNA preferentially.	++
TRF5	Non-canonical poly(A) polymerase. Trf5 is involved in nuclear RNA degradation as a component of the TRAMP complex.	+
UAF30	Subunit of UAF (upstream activation factor) complex.	+++
UBP8	Ubiquitin-specific protease component of the SAGA acetylation complex; Ubp8 is required for SAGA (Spt-Ada-Gcn5-Acetyltransferase)-mediated deubiquitination of histone H2B.	+
UPF3	Component of the nonsense-mediated mRNA decay (NMD) pathway. Upf3 is involved in decay of mRNA containing nonsense codon.	+
YAF9	Subunit of NuA4 histone H4 acetyltransferase and SWR1 complexes.	+

YNG2	Subunit of NuA4, an essential histone acetyltransferase complex.	+++
YTA7	Protein that localizes to chromatin that plays a role in regulation of histone gene expression.	++

Cytoskeleton

Genes	Functions	Susceptibility to methanol
ARP6	Actin-related protein that binds nucleosomes.	+++
BEM2	Rho GTPase activating protein (RhoGAP) that involved in the control of cytoskeleton organization and cellular morphogenesis.	+++
BEM4	Protein involved in establishment of cell polarity and bud emergence.	++
BER1	Protein involved in microtubule-related processes.	++
BIK1	Microtubule-associated protein. Bik1 is a component of the interface between microtubules and kinetochore and is involved in sister chromatid separation.	+
BIM1	Microtubule plus end-tracking protein.	++
BNI1	Formin; polarisome component; nucleates the formation of linear actin filaments, involved in cell processes such as budding and mitotic spindle orientation which require the formation of polarized actin cables.	++
GIN4	Protein kinase involved in bud growth and assembly of the septin ring.	+
HOF1	Protein that regulates actin cytoskeleton organization.	+
KAR3	Minus-end-directed microtubule motor.	+++
LDB18	Component of the dynactin complex; dynactin is required for dynein activity.	++
PAC11	Dynein intermediate chain, microtubule motor protein.	++
SLA1	Cytoskeletal protein binding protein.	+++
SPC72	Gamma-tubulin small complex (gamma-TuSC) receptor.	++
VRP1	Verprolin, proline-rich actin-associated protein; involved in cytoskeletal organization and cytokinesis.	++
YKE2	Subunit of the heterohexameric Gim/prefoldin protein complex; involved in the folding of alpha-tubulin, beta-tubulin, and actin.	+++

DNA repair

Genes	Function	Susceptibility to methanol
<i>MET18</i>	Component of cytosolic iron-sulfur protein assembly (CIA) machinery. Met18 acts at a late step of Fe-S cluster assembly and it is also involved in DNA replication and repair, transcription, and telomere maintenance.	+++
<i>MMS22</i>	Subunit of E3 ubiquitin ligase complex involved in replication repair.	+++
<i>MRE11</i>	Nuclease subunit of the MRX complex with Rad50 and Xrs2; MRX complex functions in repair of DNA double-strand breaks and in telomere stability.	+++
<i>MTF1</i>	Mitochondrial RNA polymerase specificity factor.	++
<i>RAD18</i>	E3 ubiquitin ligase; forms heterodimer with Rad6 to monoubiquitinate PCNA-K164; Rad18 is required for postreplication repair.	++
<i>RAD27</i>	5' to 3' exonuclease, 5' flap endonuclease. Rad27 is required for Okazaki fragment processing and maturation, for long-patch base-excision repair.	+++
<i>RAD33</i>	Protein involved in nucleotide excision repair.	+
<i>RAD5</i>	DNA helicase/Ubiquitin ligase. Rad5 is involved in error-free DNA damage tolerance (DDT), replication fork regression during postreplication repair by template switching, error-prone translesion synthesis.	++
<i>RAD51</i>	Strand exchange protein. Rad51 is involved in the recombinational repair of double-strand breaks in DNA during vegetative growth and meiosis.	+++
<i>RAD54</i>	DNA-dependent ATPase that stimulates strand exchange. Rad54 is involved in the recombinational repair of double-strand breaks in DNA during vegetative growth and meiosis.	++
<i>RAD57</i>	Protein that stimulates strand exchange by stabilizing the binding of Rad51 to single-stranded DNA. Rad57 is involved in the recombinational repair of double-strand breaks in DNA during vegetative growth and meiosis.	++
<i>RAD6</i>	Ubiquitin-conjugating enzyme (E2). Rad6 is involved in postreplication repair as a heterodimer with Rad18,	+

	regulation of K63 polyubiquitination in response to oxidative stress, DSBR and checkpoint control and as a heterodimer with Bre1.	
TOF1	Subunit of a replication-pausing checkpoint complex. Tof1-Mrc1-Csm3 complex acts at the stalled replication fork to promote sister chromatid cohesion after DNA damage, facilitating gap repair of damaged DNA.	+

Internal pH homeostasis

Genes	Function	Susceptibility to methanol
PMP1	Regulatory subunit for the plasma membrane H ⁽⁺⁾ -ATPase Pma1.	++
VMA1	Subunit A of the V1 peripheral membrane domain of V-ATPase.	+++
VMA13	Subunit H of the V1 peripheral membrane domain of V-ATPase.	+++
VMA2	Subunit B of V1 peripheral membrane domain of vacuolar H ⁺ -ATPase.	+++
VMA7	Subunit F of the V1 peripheral membrane domain of V-ATPase.	+++
VPH1	Subunit a of vacuolar-ATPase V0 domain.	+
VPH2	Integral membrane protein required for V-ATPase function.	++

Intracellular trafficking and protein sorting

Genes	Function	Susceptibility to methanol
ACB1	Acyl-CoA-binding protein that transports newly synthesized acyl-CoA esters from fatty acid synthetase (Fas1-Fas2) to acyl-CoA-consuming processes.	+
ARF1	ADP-ribosylation factor; GTPase of the Ras superfamily involved in regulation of coated vesicle formation in intracellular trafficking within the Golgi.	++
ARV1	Cortical ER protein. Arv1 is implicated in the membrane insertion of tail-anchored C-terminal single transmembrane domain proteins.	+++

BMH1	14-3-3 protein, major isoform. Bmh1 controls proteome at post-transcriptional level, binds proteins and DNA and it is involved in regulation of exocytosis, vesicle transport, Ras/MAPK and rapamycin-sensitive signalling, aggresome formation, spindle position checkpoint.	+
BRO1	Cytoplasmic class E vacuolar protein sorting (VPS) factor. Bro1 coordinates deubiquitination in the multivesicular body (MVB) pathway by recruiting Doa4 to endosomes.	++
BUG1	Cis-Golgi localized protein involved in ER to Golgi transport.	++
CCR4	Component of the CCR4-NOT transcriptional complex. CCR4-NOT is involved in regulation of gene expression.	++
CLC1	Clathrin light chain and a subunit of the major coat protein involved in intracellular protein transport and endocytosis. Clc1 regulates endocytic progression.	+++
DID2	Class E protein of the vacuolar protein-sorting (Vps) pathway. Did2 binds Vps4p and directs it to dissociate ESCRT-III complexes.	++
DID4	Class E Vps protein of the ESCRT-III complex. Did4 is required for sorting of integral membrane proteins into luminal vesicles of multivesicular bodies, and for delivery of newly synthesized vacuolar enzymes to the vacuole.	+
DOA4	Ubiquitin hydrolase. Doa4 deubiquitinates intraluminal vesicle (ILVs) cargo proteins and is required for recycling ubiquitin from proteasome-bound ubiquitinated intermediates.	++
END3	EH domain-containing protein involved in endocytosis.	+
GCS1	ADP-ribosylation factor GTPase activating protein (ARF GAP); involved in ER-Golgi transport.	+++
GLO3	ADP-ribosylation factor GTPase activating protein (ARF GAP) that is involved in ER-Golgi transport.	+
GSF2	Endoplasmic reticulum (ER) localized integral membrane protein that may promote secretion of certain hexose transporters.	++
GTR1	Subunit of a TORC1-stimulating GTPase and the EGO/GSE complex. Gtr1 is also a subunit of Gtr1-Gtr2,	+

	a GTPase that activates TORC1 in response to amino acid stimulation.	
LDB19	Alpha-arrestin involved in ubiquitin-dependent endocytosis.	++
PEP12	Target membrane receptor (t-SNARE); for vesicular intermediates traveling between the Golgi apparatus and the vacuole; controls entry of biosynthetic, endocytic, and retrograde traffic into the prevacuolar compartment.	++
RAV1	Subunit of RAVE complex (Rav1, Rav2, Skp1). The RAVE complex promotes assembly of the V-ATPase holoenzyme.	+++
RCY1	F-box protein involved in recycling endocytosed proteins.	++
RRT2	Methylesterase performing penultimate step of diphthamide biosynthesis; Rrt2 is involved in endosomal recycling; forms complex with Rtt10p that functions in retromer-mediated pathway for recycling internalized cell-surface proteins.	++
RVS167	Calmodulin-binding actin-associated protein with roles in endocytic membrane tabulation and constriction, and exocytosis.	+
SEC28	Epsilon-COP subunit of the coatomer. Sec28 regulates retrograde Golgi-to-ER protein traffic.	++
SEC66	Non-essential subunit of Sec63 complex.	+++
SEC72	Non-essential subunit of Sec63 complex.	+++
SNF7	One of four subunits of the ESCRT-III complex. Snf1 is involved in the sorting of transmembrane proteins into the multivesicular body (MVB) pathway.	+++
SNF8	Component of the ESCRT-II complex.	+++
STP22	Component of the ESCRT-I complex.	++
SXM1	Nuclear transport factor (karyopherin) that is involved in protein transport between the cytoplasm and nucleoplasm.	+
SYO1	Transport adaptor or symportin that facilitates synchronized nuclear coimport of the two 5S-rRNA binding proteins Rpl5 and Rpl11. Syo1 is required for biogenesis of the large ribosomal subunit.	++
TIM18	Component of the mitochondrial TIM22 complex that is involved in insertion of polytopic proteins into the inner membrane.	+

TRS65	Component of transport protein particle (TRAPP) complex II; TRAPP II is a multimeric guanine nucleotide-exchange factor for the GTPase Ypt1, regulating intra-Golgi and endosome-Golgi traffic.	+++
VAM10	Protein involved in vacuole morphogenesis and acts at an early step of homotypic vacuole fusion that is required for vacuole tethering.	+
VAM3	Syntaxin-like vacuolar t-SNARE. Vam3 mediates docking/fusion of late transport intermediates with the vacuole.	+
VAM6	Guanine nucleotide exchange factor for the GTPase Gtr1. Vam6 is a Rab GTPase effector, interacting with both GTP- and GDP-bound conformations of Ypt7.	+
VAM7	Vacuolar SNARE protein; Vam7 functions with Vam3 in vacuolar protein trafficking.	+++
VPS1	Dynamin-like GTPase required for vacuolar sorting.	+++
VPS20	Myristoylated subunit of the ESCRT-III complex.	++
VPS21	Endosomal Rab family GTPase required for endocytic transport and sorting of vacuolar hydrolases. Vps21 is also required for endosomal localization of the CORVET complex.	++
VPS24	One of four subunits of the ESCRT-III complex. Vps24 is involved in the sorting of transmembrane proteins into the multivesicular body (MVB) pathway.	+++
VPS25	Component of the ESCRT-II complex.	+++
VPS27	Endosomal protein that forms a complex with Hse1. Vps27 is required for recycling Golgi proteins, forming luminal membranes and sorting ubiquitinated proteins destined for degradation.	+++
VPS28	Component of the ESCRT-I complex.	++
VPS3	Component of CORVET membrane tethering complex. VPS is required for the sorting and processing of soluble vacuolar proteins, acidification of the vacuolar lumen, and assembly of the vacuolar H ⁺ -ATPase.	+++
VPS33	ATP-binding protein that is a subunit of the HOPS and CORVET complexes. Vps33 is essential for protein sorting, vesicle docking, and fusion at the vacuole.	+++
VPS36	Component of the ESCRT-II complex.	+++

VPS4	AAA-ATPase involved in multivesicular body (MVB) protein sorting.	++
VPS5	Nexin-1 homolog required for localizing membrane proteins from a prevacuolar/late endosomal compartment back to late Golgi.	+
VPS52	Component of the GARP (Golgi-associated retrograde protein) complex. GARP is required for the recycling of proteins from endosomes to the late Golgi, and for mitosis after DNA damage induced checkpoint arrest.	++
VPS64	Protein required for cytoplasm to vacuole targeting of proteins.	++
VPS72	Htz1-binding component of the SWR1 complex. Vps72 is required for vacuolar protein sorting.	+
VPS74	Golgi phosphatidylinositol-4-kinase effector and PtdIns4P sensor. Vps74 interacts with the cytosolic domains of cis and medial glycosyltransferases, and in the PtdIns4P-bound state mediates the targeting of these enzymes to the Golgi.	+
YPT6	Rab family GTPase required for endosome-to-Golgi, intra-Golgi retrograde, and retrograde Golgi-to-ER transport.	+++

Ion homeostasis

Genes	Function	Susceptibility to methanol
FRE8	Protein with sequence similarity to iron/copper reductases; involved in iron homeostasis.	++

Lipid synthesis

Genes	Function	Susceptibility to methanol
ELO2	Fatty acid elongase, involved in sphingolipid biosynthesis.	+++
ELO3	Elongase involved in fatty acid and sphingolipid biosynthesis.	++
ERG2	C-8 sterol isomerase; catalyses isomerization of delta-8 double bond to delta-7 position at an intermediate step in ergosterol biosynthesis.	+

ERG3	C-5 sterol desaturase. Erg3 is glycoprotein that catalyses the introduction of a C-5(6) double bond into episterol, a precursor in ergosterol biosynthesis.	++
ISC1	Inositol phosphosphingolipid phospholipase C. Isc1 hydrolyzes complex sphingolipids to produce ceramide.	+
KCS1	Inositol hexakisphosphate and inositol heptakisphosphate kinase.	++
LIP5	Protein involved in biosynthesis of the coenzyme lipoic acid.	+
SAC1	Phosphatidylinositol phosphate (PtdInsP) phosphatase. Sac1 is involved in hydrolysis of PtdIns[4]P in the early and medial Golgi.	+
SPO7	Putative regulatory subunit of Nem1-Spo7 phosphatase holoenzyme. Spo7 regulates nuclear growth by controlling phospholipid biosynthesis.	++
TGL3	Bifunctional triacylglycerol lipase and LPE acyltransferase; major lipid particle-localized triacylglycerol (TAG) lipase; catalyses acylation of lysophosphatidylethanolamine (LPE), a function which is essential for sporulation.	+

Mitochondrial function

Genes	Function	Susceptibility to methanol
AIF1	Mitochondrial cell death effector.	+
ATP10	Mitochondrial inner membrane protein that is an assembly factor for the F0 sector of mitochondrial F1F0 ATP synthase	++
ATP11	Molecular chaperone that is required for the assembly of alpha and beta subunits into the F1 sector of mitochondrial F1F0 ATP synthase.	+
CEM1	Mitochondrial beta-keto-acyl synthase required for mitochondrial respiration.	++
COA3	Mitochondrial protein required for cytochrome c oxidase assembly.	+
COQ1	Hexaprenyl pyrophosphate synthetase. Coq1 catalyses the first step in ubiquinone (coenzyme Q) biosynthesis.	+

COQ10	Coenzyme Q (ubiquinone) binding protein that functions in the delivery of Q6 to its proper location for electron transport during respiration.	+
COQ4	Protein with a role in ubiquinone (Coenzyme Q) biosynthesis.	+
COX17	Copper metallochaperone that transfers copper to Sco1 and Cox11.	+
COX18	Mitochondrial integral inner membrane protein required for membrane insertion of C-terminus of Cox2,	++
COX19	Protein required for cytochrome c oxidase assembly.	+
COX9	Subunit VIIa of cytochrome c oxidase (Complex IV).	++
GEP4	Mitochondrial phosphatidylglycerophosphatase (PGP phosphatase). Gep4 dephosphorylates phosphatidylglycerolphosphate to generate phosphatidylglycerol, an essential step during cardiolipin biosynthesis.	++
HFA1	Mitochondrial acetyl-coenzyme A carboxylase that catalyses the production of malonyl-CoA in mitochondrial fatty acid biosynthesis.	+
ICP55	Mitochondrial aminopeptidase. Icp55 cleaves the N termini of at least 38 imported proteins after cleavage by the mitochondrial processing peptidase (MPP), thereby increasing their stability.	++
IMP1	Catalytic subunit of mitochondrial inner membrane peptidase complex; required for maturation of mitochondrial proteins of the intermembrane space	+
ISA1	Protein required for maturation of mitochondrial [4Fe-4S] proteins.	+
MDM12	Mitochondrial outer membrane protein, required for transmission of mitochondria to daughter cells and for mitophagy.	+
MDM20	Non-catalytic subunit of the NatB N-terminal acetyltransferase. Mdm20 is involved in mitochondrial inheritance and actin assembly.	++
MEF1	Mitochondrial elongation factor involved in translational elongation.	+
MGM1	Mitochondrial GTPase required for mitochondrial morphology, fusion, and genome maintenance.	++
MIR1	Mitochondrial phosphate carrier that imports inorganic phosphate into mitochondria.	+++

MMR1	Phosphorylated protein of the mitochondrial outer membrane.	++
MRF1	Mitochondrial translation release factor that is involved in stop codon recognition and hydrolysis of the peptidyl-tRNA bond during mitochondrial translation.	+
MRM1	Ribose methyltransferase that modifies a functionally critical, conserved nucleotide in mitochondrial 21S rRNA	+
MRM2	Mitochondrial 2' O-ribose methyltransferase that is required for methylation of U(2791) in 21S rRNA.	+
MSE1	Mitochondrial glutamyl-tRNA synthetase.	+
MSY1	Mitochondrial tyrosyl-tRNA synthetase.	+
PET54	Mitochondrial inner membrane protein that binds to the 5' UTR of the COX3 mRNA to activate its translation together with Pet122 and Pet494.	+++
POR1	Mitochondrial porin (voltage-dependent anion channel) required for maintenance of mitochondrial osmotic stability and mitochondrial membrane permeability.	+
POS5	Mitochondrial NADH kinase that phosphorylates NADH.	+
PRX1	Mitochondrial peroxiredoxin with thioredoxin peroxidase activity. Prx1 has a role in reduction of hydroperoxides.	++
RMD9	Mitochondrial protein required for respiratory growth.	+
SHE9	Mitochondrial inner membrane protein required for normal mitochondrial morphology.	+
SHY1	Mitochondrial inner membrane protein required for complex IV assembly,	+
SLM5	Mitochondrial asparaginyl-tRNA synthetase.	+++
TIM13	Mitochondrial intermembrane space protein that forms a complex with Tim8 that delivers a subset of hydrophobic proteins to the TIM22 complex for insertion into the inner membrane.	+++
TIM8	Mitochondrial intermembrane space protein. Tim8 forms a complex with Tim13 that delivers a subset of hydrophobic proteins to the TIM22 complex for inner membrane insertion.	+
TOM6	Component of the TOM (translocase of outer membrane) complex. Tom6 is responsible for recognition and initial import steps for all mitochondrially directed proteins.	+

<i>TOM70</i>	Component of the TOM (translocase of outer membrane) complex that is involved in the recognition and initial import steps for all mitochondrially directed proteins.	++
<i>TUF1</i>	Mitochondrial translation elongation factor Tu (EF-Tu). Tuf1 is involved in fundamental pathway of mtDNA homeostasis.	+

Protein folding

Genes	Function	Susceptibility to methanol
<i>BUD27</i>	Unconventional prefoldin protein involved in translation initiation; required for correct assembly of RNAP I, II, and III in an Rpb5-dependent manner.	++
<i>GIM3</i>	Subunit of the heterohexameric cochaperone prefoldin complex; prefoldin binds specifically to cytosolic chaperonin and transfers target proteins to it.	+++
<i>IRC25</i>	Component of a heterodimeric Poc4-Irc25 chaperone. Irc25 is involved in assembly of alpha subunits into the 20S proteasome.	+
<i>PAC10</i>	Part of the heteromeric co-chaperone GimC/prefoldin complex - promotes efficient protein folding.	++
<i>PIH1</i>	Component of the conserved R2TP complex (Rvb1-Rvb2-Tah1-Pih1). The R2TP complex interacts with Hsp90 (Hsp82 and Hsc82) to mediate assembly large protein complexes such as box C/D snoRNPs and RNA polymerase II.	+++
<i>SSE1</i>	ATPase component of heat shock protein Hsp90 chaperone complex. Sse1 binds unfolded proteins.	+
<i>SSZ1</i>	Hsp70 protein that interacts with Zuo1. Ssz1 is also involved in pleiotropic drug resistance via sequential activation of <i>PDR1</i> and <i>PDR5</i> .	++
<i>UMP1</i>	Chaperone required for correct maturation of the 20S proteasome.	++
<i>VPS75</i>	NAP family histone chaperone. Vps75 binds to histones and Rtt109, stimulating histone acetyltransferase activity	++

Protein modification

Genes	Functions	Susceptibility to methanol
AKR1	Palmitoyl transferase involved in protein palmitoylation.	+++
ALG3	Dolichol-P-Man dependent alpha (1-3) mannosyltransferase that is involved in synthesis of dolichol-linked oligosaccharide donor for N-linked glycosylation of proteins.	++
ALG5	UDP-glucose:dolichyl-phosphate glucosyltransferase that is involved in asparagine-linked glycosylation in the endoplasmic reticulum.	++
ALG6	Alpha 1,3 glucosyltransferase that is involved in transfer of oligosaccharides from dolichyl pyrophosphate to asparagine residues of proteins during N-linked protein glycosylation.	+
ALG8	Glucosyl transferase that is involved in N-linked glycosylation.	++
ARG82	Inositol polyphosphate multikinase (IPMK); sequentially phosphorylates Ins(1,4,5)P3 to form Ins(1,3,4,5,6)P5.	++
CKB2	Beta' regulatory subunit of casein kinase 2 (CK2). Ckb2 is a Ser/Thr protein kinase with roles in cell growth and proliferation.	+
DUF1	Ubiquitin-binding protein of unknown function.	+
MCK1	Dual-specificity Ser/Thr and tyrosine protein kinase. Mck1 participates in chromosome segregation, meiotic entry, genome stability.	+
MTQ2	Adenosylmethionine-dependent methyltransferase.	+
NAT1	Subunit of protein N-terminal acetyltransferase NatA.	++
OST6	Subunit of the oligosaccharyltransferase complex of the ER lumen complex. This complex catalyses asparagine-linked glycosylation of newly synthesized proteins.	+
PER1	Protein of the endoplasmic reticulum required for GPI-phospholipase A2 activity that remodels the GPI anchor as a prerequisite for association of GPI-anchored proteins with lipid rafts.	++
PPT2	Phosphopantetheine:protein transferase (PPTase). Ppt2 activates mitochondrial acyl carrier protein (Acp1).	++
SAP155	Protein required for function of the Sit4 protein phosphatase.	++

SEM1	19S proteasome regulatory particle lid subcomplex component.	++
SLX8	Subunit of Slx5-Slx8 SUMO-targeted ubiquitin ligase (STUbL) complex. Slx plays a role in proteolysis of spindle positioning protein Kar9, DNA repair proteins Rad52 and Rad57.	++
UFO1	F-box receptor protein; subunit of the Skp1-Cdc53-F-box receptor (SCF) E3 ubiquitin ligase complex.	++
VID22	Glycosylated integral membrane protein that plays a role in fructose-1,6-bisphosphatase degradation.	++
YME1	Catalytic subunit of i-AAA protease complex. Yme1 is responsible for degradation of unfolded or misfolded mitochondrial gene products.	++

Protein synthesis

Genes	Function	Susceptibility to methanol
DOM34	Protein that facilitates ribosomal subunit dissociation.	+
GEP3	Protein required for mitochondrial ribosome small subunit biogenesis.	+
IMG2	Mitochondrial ribosomal protein of the large subunit.	+++
MRP7	Mitochondrial ribosomal protein of the large subunit.	++
MRPL10	Mitochondrial ribosomal protein of the large subunit.	+
MRPL17	Mitochondrial ribosomal protein of the large subunit.	+
MRPL20	Mitochondrial ribosomal protein of the large subunit.	++
MRPL22	Mitochondrial ribosomal protein of the large subunit.	+
MRPL24	Mitochondrial ribosomal protein of the large subunit.	+
MRPL25	Mitochondrial ribosomal protein of the large subunit.	+
MRPL27	Mitochondrial ribosomal protein of the large subunit.	+
MRPL7	Mitochondrial ribosomal protein of the large subunit.	++
MRPS28	Mitochondrial ribosomal protein of the small subunit.	+
MRPS35	Mitochondrial ribosomal protein of the small subunit.	++
RPL12B	Ribosomal 60S subunit protein L12B.	+
RPL14A	Ribosomal 60S subunit protein L14A	++
RPL16B	Ribosomal 60S subunit protein L16B.	+
RPL19B	Ribosomal 60S subunit protein L19B.	++
RPL21A	Ribosomal 60S subunit protein L21A.	++

RPL36A	Ribosomal 60S subunit protein L36A.	+++
RPL43A	Ribosomal 60S subunit protein L43A.	++
RPL8A	Ribosomal 60S subunit protein L8A.	+
RPS0B	Protein component of the small (40S) ribosomal subunit.	++
RPS11A	Protein component of the small (40S) ribosomal subunit.	+
RPS17A	Ribosomal protein 51 (rp51) of the small (40s) subunit.	+
RPS19A	Protein component of the small (40S) ribosomal subunit.	+
RPS22B	Protein component of the small (40S) ribosomal subunit.	++
RPS24A	Protein component of the small (40S) ribosomal subunit.	+
RPS27B	Protein component of the small (40S) ribosomal subunit.	+
RSM18	Mitochondrial ribosomal protein of the small subunit.	+
RSM23	Mitochondrial ribosomal protein of the small subunit.	+
RSM7	Mitochondrial ribosomal protein of the small subunit.	+++
TEF4	Gamma subunit of translational elongation factor eEF1B.	+++
IFM1	Mitochondrial translation initiation factor 2.	++

Response to stress

Genes	Function	Susceptibility to methanol
GSH1	Gamma glutamylcysteine synthetase. Gsh1 catalyses the first step in glutathione (GSH) biosynthesis.	++
MXR1	Methionine-S-sulfoxide reductase that is involved in the response to oxidative stress, Mxr1 also protects iron-sulfur clusters from oxidative inactivation along with <i>MXR2</i> .	+
RMD8	Cytosolic protein required for sporulation.	++
SOD1	Cytosolic copper-zinc superoxide dismutase; detoxifies superoxide.	+++

Transcription factors

Gene	Function	Susceptibility to methanol
CBF1	Transcription factor that associates with kinetochore proteins, required for chromosome segregation. Basic helix-loop-helix (bHLH) protein; forms homodimer to bind E-box consensus sequence CACGTG present at MET	+

	gene promoters and centromere DNA element I (CDEI); affects nucleosome positioning at this motif; associates with other transcription factors such as Met4 and Isw1 to mediate transcriptional activation or repression;	
GLN3	Transcriptional activator of genes regulated by nitrogen catabolite repression; localization and activity regulated by quality of nitrogen source and Ure2.	+
IXR1	Transcriptional repressor that regulates hypoxic genes during normoxia; involved in the aerobic repression of genes such as <i>COX5b</i> , <i>TIR1</i> , and <i>HEM13</i> .	+++
NGG1	Transcriptional regulator involved in glucose repression of Gal4-regulated genes. Subunit of chromatin modifying histone acetyltransferase complexes; member of the ADA complex, the SAGA complex, and the SLIK complex.	++
OPI1	Transcriptional regulator of a variety of genes; its phosphorylation by protein kinase A stimulates Opi1 function in negative regulation of phospholipid biosynthetic genes; involved in telomere maintenance.	+++
RPH1	Transcription factor with JmjC domain-containing histone demethylase. Rph1 targets tri- and dimethylated H3K36 and associates with actively transcribed regions and promotes elongation. Rph1 acts as a repressor of autophagy-related genes in nutrient-replete conditions.	+
RPN4	Transcription factor that stimulates expression of proteasome encoding genes being regulated by the 26S proteasome in a negative feedback control mechanism; <i>RPN4</i> is transcriptionally regulated by various stress response.	+
SFL1	Transcriptional repressor and activator; involved in repression of flocculation-related genes, and activation of stress responsive genes; has direct role in <i>INO1</i> transcriptional memory; negatively regulated by cAMP-dependent protein kinase A subunit Tpk2.	++
SOK2	Transcription factor that negatively regulates pseudohyphal differentiation. Sok2 also plays a regulatory role in the cyclic AMP (cAMP)-dependent protein kinase (PKA) signal transduction pathway.	++
SFP1	Transcription factor that regulates ribosomal protein and biogenesis genes. Sfp1 also regulates response to	++

	nutrients and stress, G2/M transitions during mitotic cell cycle and DNA-damage response and modulates cell size.	
STB5	Transcription factor involved in the regulation multidrug resistance and oxidative stress response; forms a heterodimer with Pdr1; contains a Zn(II) ₂ Cys ₆ zinc finger domain that interacts with a pleiotropic drug resistance element <i>in vitro</i> .	++
UME6	Transcriptional regulator of early meiotic genes; involved in chromatin remodelling and transcriptional repression via DNA looping; binds URS1 upstream regulatory sequence, represses transcription by recruiting conserved histone deacetylase Rpd3 (through co-repressor Sin3) and chromatin-remodelling factor Isw2; couples metabolic responses to nutritional cues with initiation and progression of meiosis.	++

Transporters

Gene	Function	Susceptibility to methanol
AGP2	General amino acid permease with broad substrate specificity. Can also transport carnitine.	++
FEN2	Plasma membrane H ⁺ -pantothenate symporter.	+++
MCH4	Probable transporter. Does not act in the transport of monocarboxylic acids across the plasma membrane.	+
MCH5	Riboflavin transporter involved in riboflavin (vitamin B ₂) uptake. monocarboxylic acids across the plasma membrane.	+++
MUP1	High affinity methionine permease that is also involved in cysteine uptake.	++
PET8	S-adenosyl-L-methionine transport.	+
SPF1	Mediates manganese transport into the endoplasmic reticulum. The ATPase activity is required for cellular manganese homeostasis.	+++
TPN1	Thiamine-regulated, high affinity import carrier of pyridoxine, pyridoxal and pyridoxamine.	++

<i>VMR1</i>	ATP-binding cassette (ABC) family member involved in multiple drug resistance and metal sensitivity.	+
Unknown function		
Gene	Function	Susceptibility to methanol
<i>AIM22</i>	Putative lipoate-protein ligase.	++
<i>AIM26</i>	Protein of unknown function.	+++
<i>DIA1</i>	Protein of unknown function; involved in invasive and pseudohyphal growth.	++
<i>EMI1</i>	Non-essential protein of unknown function; required for transcriptional induction of the early meiotic-specific transcription factor <i>IME1</i> , also required for sporulation.	+
<i>ERD1</i>	Predicted membrane protein required for luminal ER protein retention.	+
<i>FSH3</i>	Putative serine hydrolase.	+
<i>FYV1</i>	Dubious open reading frame; unlikely to encode a functional protein.	+
<i>ILM1</i>	Protein of unknown function; may be involved in mitochondrial DNA maintenance; required for slowed DNA synthesis-induced filamentous growth.	+++
<i>IRC13</i>	Putative protein of unknown function.	+
<i>MCT1</i>	Predicted malonyl-CoA:ACP transferase.	+
<i>NRP1</i>	Putative RNA binding protein of unknown function.	++
<i>OPI8</i>	Dubious open reading frame; unlikely to encode a functional protein,	++
<i>OPI9</i>	Dubious open reading frame; unlikely to encode a functional protein	+++
<i>RBK1</i>	Putative ribokinase.	++
<i>RRG9</i>	Protein of unknown function.	+
<i>SWS2</i>	Putative mitochondrial ribosomal protein of the small subunit.	+
<i>TAN1</i>	Putative tRNA acetyltransferase;	+++
<i>VPS61</i>	Dubious open reading frame; unlikely to encode a functional protein.	**
<i>VPS63</i>	Putative protein of unknown function.	+++
<i>VPS65</i>	Dubious open reading frame; unlikely to encode a functional protein.	+++

YBL083C	Dubious open reading frame; unlikely to encode a functional protein.	++
YBL094C	Dubious open reading frame; unlikely to encode a functional protein.	+++
YBR085C-A	Protein of unknown function.	+
YBR225W	Putative protein of unknown function.	+
YBR226C	Dubious open reading frame; unlikely to encode a functional protein.	++
YCR025C	Putative protein of unknown function.	++
YDL062W	Dubious open reading frame; unlikely to encode a functional protein.	++
YDL199C	Putative transporter; member of the sugar porter family.	++
YDR008C	Dubious open reading frame; unlikely to encode a functional protein.	++
YDR203W	Dubious open reading frame; unlikely to encode a functional protein.	++
YDR230W	Dubious open reading frame; unlikely to encode a functional protein.	++
YDR417C	Dubious open reading frame; unlikely to encode a functional protein.	+
YDR431W	Dubious open reading frame; unlikely to encode a functional protein.	+
YER156C	Putative protein of unknown function.	+
YGL007C-A	Putative protein of unknown function	+++
YGL149W	Putative protein of unknown function.	+
YGL235W	Putative protein of unknown function.	++
YGR011W	Dubious open reading frame; unlikely to encode a functional protein.	++
YGR064W	Dubious open reading frame; unlikely to encode a functional protein.	++
YGR182C	Dubious open reading frame; unlikely to encode a functional protein.	+++
YHL005C	Putative protein of unknown function.	+
YIM2	Dubious open reading frame; unlikely to encode a functional protein.	+
YJL120W	Dubious open reading frame; unlikely to encode a functional protein.	++
YJR011C	Putative protein of unknown function.	++

YJR120W	Protein of unknown function.	+
YLR111W	Dubious open reading frame; unlikely to encode a functional protein.	++
YLR202C	Dubious open reading frame; unlikely to encode a functional protein.	++
YLR235C	Dubious open reading frame; unlikely to encode a functional protein,	++
YLR269C	Dubious open reading frame; unlikely to encode a functional protein.	+++
YLR366W	Dubious open reading frame; unlikely to encode a functional protein.	+
YML009W-B	Dubious open reading frame; unlikely to encode a functional protein.	++
YML012C-A	Dubious open reading frame; unlikely to encode a functional protein.	++
YMR031W-A	Dubious open reading frame; unlikely to encode a functional protein,	+++
YMR075C-A	Dubious open reading frame; unlikely to encode a functional protein.	++
YNL140C	Protein of unknown function.	+
YNL165W	Putative protein of unknown function.	+
YNL319W	Dubious open reading frame; unlikely to encode a functional protein.	++
YNR005C	Dubious open reading frame; unlikely to encode a functional protein.	++
YOR139C	Dubious open reading frame; unlikely to encode a functional protein.	++
YOR199W	Dubious open reading frame; unlikely to encode a functional protein.	+

Table S1. 2- List of genes whose expression increases *S. cerevisiae* tolerance to 5.5%(v/v) ethanol based on the screening of the Euroscarf deletion mutant collection; the elimination of the indicated genes increases yeast susceptibility to ethanol. Biological functions are based on the information available in SGD (www.yeastgenome.org). The symbols '+++', '++' and '+' correspond to phenotypes as shown in Figure 2.1.

Autophagy		
Gene	Function	Susceptibility level
ATG10	Conserved E2-like conjugating enzyme; mediates formation of the Atg12-Atg5 conjugate, which is a critical step in autophagy.	+
ATG11	Adapter protein for pexophagy and the Cvt targeting pathway; directs receptor-bound cargo to the phagophore assembly site (PAS) for packaging into vesicles; required for recruiting other proteins to the PAS; recruits Dnm1p to facilitate fission of mitochondria that are destined for removal by mitophagy.	++
ATG17	Scaffold protein responsible for phagophore assembly site organization; regulatory subunit of an autophagy-specific complex that includes Atg1 and Atg13; stimulates Atg1 kinase activity.	+
ATG2	Peripheral membrane protein required for autophagic vesicle formation; also required for vesicle formation during pexophagy and the cytoplasm-to-vacuole targeting (Cvt) pathway; involved in Atg9p cycling between the phagophore assembly site and mitochondria; contains an APT1 domain that binds phosphatidylinositol-3-phosphate; essential for cell cycle progression from G2/M to G1 under nitrogen starvation; forms cytoplasmic foci upon DNA replication stress.	+
ATG20	Sorting nexin family member; required for the cytoplasm-to-vacuole targeting (Cvt) pathway and for endosomal sorting; has a Phox homology domain that binds phosphatidylinositol-3-phosphate; interacts with Snx4; potential Cdc28 substrate.	+++
ATG4	Conserved cysteine protease required for autophagy; cleaves Atg8p to a form required for autophagosome and Cvt vesicle generation.	+
MEH1	Component of the EGO and GSE complexes; EGO is involved in the regulation of microautophagy and GSE is required for proper sorting of amino acid permease Gap1.	+
Carbohydrate metabolism		
Gene	Function	Susceptibility level
ADH3	Mitochondrial alcohol dehydrogenase isozyme III; involved in the shuttling of mitochondrial NADH to the cytosol under anaerobic conditions and ethanol production.	++
ARO1	Pentafunctional arom protein; catalyzes steps 2 through 6 in the biosynthesis of chorismate, which is a precursor to aromatic amino acids.	+

ARO2	Bifunctional chorismate synthase and flavin reductase; catalyzes the conversion of 5-enolpyruvylshikimate 3-phosphate (EPSP) to form chorismate, which is a precursor to aromatic amino acids; protein abundance increases in response to DNA replication stress.	++
ARO7	Chorismate mutase; catalyzes the conversion of chorismate to prephenate to initiate the tyrosine/phenylalanine-specific branch of aromatic amino acid biosynthesis.	+++
BNA1	3-hydroxyanthranilic acid dioxygenase; required for the <i>de novo</i> biosynthesis of NAD from tryptophan via kynurenine; expression regulated by Hst1.	++
FUM1	Fumarase; converts fumaric acid to L-malic acid in the TCA cycle; cytosolic and mitochondrial distribution determined by the N-terminal targeting sequence, protein conformation, and status of glyoxylate shunt; phosphorylated in mitochondria.	++
GCN5	Catalytic subunit of ADA and SAGA histone acetyltransferase complexes; modifies N-terminal lysines on histones H2B and H3; acetylates Rsc4p, a subunit of the RSC chromatin-remodeling complex, altering replication stress tolerance; relocates to the cytosol in response to hypoxia; mutant displays reduced transcription elongation in the G-less-based run-on (GLRO).	++
GPH1	Glycogen phosphorylase required for the mobilization of glycogen; non-essential; regulated by cyclic AMP-mediated phosphorylation; phosphorylation by Cdc28 may coordinately regulate carbohydrate metabolism and the cell cycle; expression is regulated by stress-response elements and by the HOG MAP kinase pathway.	++
KGD2	Dihydrolipoyl transsuccinylase; component of the mitochondrial alpha-ketoglutarate dehydrogenase complex, which catalyzes the oxidative decarboxylation of alpha-ketoglutarate to succinyl-CoA in the TCA cycle.	+
MET7	Folypolyglutamate synthetase; catalyzes extension of the glutamate chains of the folate coenzymes, required for methionine synthesis and for maintenance of mitochondrial DNA.	+
PCL7	Pho85p cyclin of the Pho80 subfamily; forms a functional kinase complex with Pho85 which phosphorylates Mmr1 and is regulated by Pho81; involved in glycogen metabolism, expression is cell-cycle regulated; <i>PCL7</i> has a paralog, <i>PCL6</i> , that arose from the whole genome duplication.	+
PDC1	Major of three pyruvate decarboxylase isozymes; key enzyme in alcoholic fermentation; decarboxylates pyruvate to acetaldehyde; involved in amino acid catabolism.	+
PRS3	5-phospho-ribosyl-1(alpha)-pyrophosphate synthetase; synthesizes PRPP, which is required for nucleotide, histidine, and tryptophan biosynthesis; one of five related enzymes, which are active as heteromultimeric complexes.	+++
REG1	Regulatory subunit of type 1 protein phosphatase Glc7; involved in negative regulation of glucose-repressible genes; involved in regulation of the nucleocytoplasmic shuttling of Hxk2; <i>REG1</i> has a paralog, <i>REG2</i> , that arose from the whole genome duplication.	+++

REG2	Regulatory subunit of the Glc7 type-1 protein phosphatase; involved with Reg1, Glc7, and Snf1 in regulation of glucose-repressible genes.	+
RIB4	Lumazine synthase (DMRL synthase); catalyzes synthesis of immediate precursor to riboflavin; DMRL synthase stands for 6,7-dimethyl-8-ribityllumazine synthase.	+++

Cell cycle

Gene	Function	Susceptibility level
CIK1	Kinesin-associated protein; required for both karyogamy and mitotic spindle organization, interacts stably and specifically with Kar3 and may function to target this kinesin to a specific cellular role; locus encodes a long and short transcript with differing functions; <i>CIK1</i> has a paralog, <i>VIK1</i> , that arose from the whole genome duplication.	+++
CLN1	G1 cyclin involved in regulation of the cell cycle; activates Cdc28 kinase to promote the G1 to S phase transition; late G1 specific expression depends on transcription factor complexes, MBF (Swi-Mbp1) and SBF (Swi6-Swi4).	+
HOS4	Subunit of the Set3 complex; complex is a meiotic-specific repressor of sporulation specific genes that contains deacetylase activity.	+
IRC19	Protein of unknown function; <i>YLL033W</i> is not an essential gene but mutant is defective in spore formation; null mutant displays increased levels of spontaneous Rad52 foci.	++
SPO22	Meiosis-specific protein essential for chromosome synapsis; involved in completion of nuclear divisions during meiosis.	+

Cell wall function

Gene	Function	Susceptibility level
CHS1	Chitin synthase I; requires activation from zymogenic form in order to catalyze the transfer of N-acetylglucosamine (GlcNAc) to chitin; required for repairing the chitin septum during cytokinesis; transcription activated by mating factor.	+++
CWH43	GPI lipid remodelase; responsible for introducing ceramides into GPI anchors having a C26:0 fatty acid in sn-2 of the glycerol moiety; can also use lyso-GPI protein anchors and various base resistant lipids as substrates.	+
FKS1	Catalytic subunit of 1,3-beta-D-glucan synthase; functionally redundant with alternate catalytic subunit Gsc2; binds to regulatory subunit Rho1p; involved in cell wall synthesis and maintenance; localizes to sites of cell wall remodeling.	+++
MNN11	Subunit of a Golgi mannosyltransferase complex; this complex also contains Anp1, Mnn9, Mnn10, and Hoc1, and mediates elongation of the polysaccharide mannan backbone; has homology to Mnn10.	+++

PUN1	Plasma membrane protein with a role in cell wall integrity; co-localizes with Sur7 in punctate membrane patches.	+
ROM2	Guanine nucleotide exchange factor (GEF) for Rho1 and Rho2; mutations are synthetically lethal with mutations in <i>rom1</i> , which also encodes a GEF; Rom2 localization to the bud surface is dependent on Ack1p; <i>ROM2</i> has a paralog, <i>ROM1</i> , that arose from the whole genome duplication.	+
ROT2	Glucosidase II catalytic subunit; required to trim the final glucose in N-linked glycans; required for normal cell wall synthesis; mutations in <i>rot2</i> suppress <i>tor2</i> mutations, and are synthetically lethal with <i>rot1</i> mutations.	++
SAG1	Alpha-agglutinin of alpha-cells; binds to Aga1 during agglutination, N-terminal half is homologous to the immunoglobulin superfamily and contains binding site for alpha-agglutinin, C-terminal half is highly glycosylated and contains GPI anchor.	++
SLG1	Sensor-transducer of the stress-activated PKC1-MPK1 kinase pathway; involved in maintenance of cell wall integrity; required for mitophagy; involved in organization of the actin cytoskeleton; secretory pathway <i>Wsc1</i> is required for the arrest of secretion response.	+++
SMI1	Protein involved in the regulation of cell wall synthesis; proposed to be involved in coordinating cell cycle progression with cell wall integrity.	++
YEH2	Steryl ester hydrolase; catalyzes sterol ester hydrolysis at the plasma membrane; involved in sterol metabolism; <i>YEH2</i> has a paralog, <i>YEH1</i> , that arose from the whole genome duplication.	++

Chromatin remodelling and transcriptional control

Gene	Function	Susceptibility level
ADA2	Transcription coactivator; component of the ADA and SAGA transcriptional adaptor/HAT (histone acetyltransferase) complexes.	++
APA1	AP4A phosphorylase; catalyzes phosphorolysis of dinucleoside oligophosphates, cleaving substrates' alpha/beta-anhydride bond and introducing Pi into the beta-position of the corresponding NDP formed.	+
ADO1	Adenosine kinase; required for the utilization of S-adenosylmethionine (AdoMet); may be involved in recycling adenosine produced through the methyl cycle.	+++
APT1	Adenine phosphoribosyltransferase; catalyzes the formation of AMP from adenine and 5-phosphoribosylpyrophosphate; involved in the salvage pathway of purine nucleotide biosynthesis; <i>APT1</i> has a paralog, <i>APT2</i> , that arose from the whole genome duplication.	++
BUD13	Subunit of the RES complex; RES complex is required for nuclear pre-mRNA retention and splicing; involved in bud-site selection; diploid mutants display a unipolar budding pattern instead of the wild-type bipolar pattern due to a specific defect in MATa1 pre-mRNA splicing which leads to haploid gene expression in diploids.	+++

<i>CBP2</i>	Required for splicing of the group I intron b15 of the COB pre-mRNA; nuclear-encoded mitochondrial protein that binds to the RNA to promote splicing; also involved in but not essential for splicing of the COB b12 intron and the intron in the 21S rRNA gene.	++
<i>CBS1</i>	Mitochondrial translational activator of the COB mRNA; membrane protein that interacts with translating ribosomes, acts on the COB mRNA 5'-untranslated leader.	+
<i>CBS2</i>	Mitochondrial translational activator of the COB mRNA; interacts with translating ribosomes, acts on the COB mRNA 5'-untranslated leader.	++
<i>CCR4</i>	Component of the <i>CCR4-NOT</i> transcriptional complex; <i>CCR4-NOT</i> is involved in regulation of gene expression; component of the major cytoplasmic deadenylase, which is involved in mRNA poly(A) tail shortening.	+
<i>CDC50</i>	Endosomal protein that interacts with phospholipid flippase Drs2; interaction with Cdc50 is essential for Drs2 catalytic activity; mutations affect cell polarity and polarized growth; similar to Lem3; <i>CDC50</i> has a paralog, <i>YNR048W</i> , that arose from the whole genome duplication.	+++
<i>COQ4</i>	Protein with a role in ubiquinone (Coenzyme Q) biosynthesis; possibly functioning in stabilization of Coq7; located on matrix face of mitochondrial inner membrane.	+
<i>COQ10</i>	Coenzyme Q (ubiquinone) binding protein; functions in the delivery of Q6 to its proper location for electron transport during respiration; START domain protein with homologs in bacteria and eukaryotes; respiratory growth defect of the null mutant is functionally complemented by human <i>COQ10A</i> .	++
<i>CSE2</i>	Subunit of the RNA polymerase II mediator complex; associates with core polymerase subunits to form the RNA polymerase II holoenzyme; component of the Middle domain of mediator; required for regulation of RNA polymerase II activity; relocalizes to the cytosol in response to hypoxia.	++
<i>DEP1</i>	Component of the Rpd3L histone deacetylase complex; required for diauxic shift-induced histone H2B deposition onto rDNA genes; transcriptional modulator involved in regulation of structural phospholipid biosynthesis genes and metabolically unrelated genes, as well as maintenance of telomeres, mating efficiency, and sporulation.	+
<i>DHH1</i>	Cytoplasmic DEAD-box helicase, stimulates mRNA decapping; coordinates distinct steps in mRNA function and decay, interacting with both decapping and deadenylase complexes; role in translational repression, mRNA decay, and possibly mRNA export; interacts and cooperates with Ngr1 to promote specific mRNA decay; ATP- and RNA-bound form promotes processing body (PB) assembly, while ATPase stimulation by Not1p promotes PB disassembly; forms cytoplasmic foci on replication stress.	+++

DST1	General transcription elongation factor TFIIIS; enables RNA polymerase II to read through blocks to elongation by stimulating cleavage of nascent transcripts stalled at transcription arrest sites; maintains RNAPII elongation activity on ribosomal protein genes during conditions of transcriptional stress.	+++
ELP3	Subunit of Elongator complex; Elongator is required for modification of wobble nucleosides in tRNA; exhibits histone acetyltransferase activity that is directed to histones H3 and H4; disruption confers resistance to <i>K. lactis</i> zymotoxin; human homolog <i>ELP3</i> can partially complement yeast <i>elp3</i> null mutant.	++
GTF1	Subunit of the trimeric GatFAB AmidoTransferase(AdT) complex; involved in the formation of Q-tRNA ^Q ; transposon insertion mutant is salt sensitive and null mutant has growth defects; non-tagged protein is detected in purified mitochondria.	++
HDA2	Subunit of the HDA1 histone deacetylase complex; possibly tetrameric trichostatin A-sensitive class II histone deacetylase complex contains Hda1p homodimer and an Hda2-Hda3 heterodimer; involved in telomere maintenance; relocalizes to the cytosol in response to hypoxia.	++
HIT1	Protein involved in C/D snoRNP assembly; regulates abundance of Rsa1p; required for growth at high temperature; similar to human <i>ZNHIT</i> .	++
HMI1	Mitochondrial inner membrane localized ATP-dependent DNA helicase; required for the maintenance of the mitochondrial genome; not required for mitochondrial transcription; has homology to <i>E. coli</i> helicase <i>uvrD</i> .	++
HMO1	Chromatin associated high mobility group (HMG) family member; involved in compacting, bending, bridging and looping DNA; rDNA-binding component that regulates transcription from RNA polymerase I promoters; regulates start site selection of ribosomal protein genes via RNA polymerase II promoters.	+++
HPR1	Subunit of <i>THO/TREX</i> complexes; this complex couple transcription elongation with mitotic recombination and with mRNA metabolism and export, subunit of an RNA Pol II complex; regulates lifespan; involved in telomere maintenance; similar to Top1.	+++
HTL1	Component of the RSC chromatin remodeling complex; RSC functions in transcriptional regulation and elongation, chromosome stability, and establishing sister chromatid cohesion; involved in telomere maintenance.	+++
HTZ1	Histone variant H2AZ; exchanged for histone H2A in nucleosomes by the SWR1 complex; involved in transcriptional regulation through prevention of the spread of silent heterochromatin; Htz1-containing nucleosomes facilitate RNA Pol II passage by affecting correct assembly and modification status of RNA Pol II elongation complexes and by favoring efficient nucleosome remodeling.	+++
IME4	mRNA N6-adenosine methyltransferase required for entry into meiosis; mediates N6-adenosine methylation of bulk mRNA during the induction of sporulation which includes the meiotic regulators <i>IME1</i> , <i>IME2</i> and <i>IME4</i> itself; repressed in haploids via production of antisense <i>IME4</i> transcripts.	+

IST3	Component of the U2 snRNP; required for the first catalytic step of splicing and for spliceosomal assembly; interacts with Rds3 and is required for Mer1p-activated splicing; diploid mutants have a specific defect in MATA1 pre-mRNA splicing which leads to haploid gene expression in diploids.	+
LEA1	Component of U2 snRNP complex; disruption causes reduced U2 snRNP levels; physically interacts with Msl1p; putative homolog of human U2A' snRNP protein.	+
LDB7	Component of the RSC chromatin remodeling complex; interacts with Rsc3, Rsc30, Npl6, and Htl1 to form a module important for a broad range of RSC functions.	+
MAF1	Highly conserved negative regulator of RNA polymerase III; involved in tRNA processing and stability; inhibits tRNA degradation via rapid tRNA decay (RTD) pathway; binds N-terminal domain of Rpc160 subunit of Pol III to prevent closed-complex formation; regulated by phosphorylation mediated by <i>TORC1</i> , protein kinase A, Sch9, casein kinase 2; localizes to cytoplasm during vegetative growth and translocates to nucleus and nucleolus under stress conditions.	+++
MED1	Subunit of the RNA polymerase II mediator complex; associates with core polymerase subunits to form the RNA polymerase II holoenzyme; essential for transcriptional regulation.	++
MFT1	Subunit of the THO complex; <i>THO</i> is a nuclear complex comprised of Hpr1, Mft1, Rlr1, and Thp2, that is involved in transcription elongation and mitotic recombination; involved in telomere maintenance.	+
MRF1	Mitochondrial translation release factor; involved in stop codon recognition and hydrolysis of the peptidyl-tRNA bond during mitochondrial translation; lack of <i>MRF1</i> causes mitochondrial genome instability.	+++
MSE1	Mitochondrial glutamyl-tRNA synthetase; predicted to be palmitoylated.	++
NPT1	Nicotinate phosphoribosyltransferase; acts in the salvage pathway of NAD ⁺ biosynthesis; required for silencing at rDNA and telomeres and has a role in silencing at mating-type <i>loci</i> .	+
NPL3	RNA-binding protein; promotes elongation, regulates termination, and carries poly(A) mRNA from nucleus to cytoplasm; represses translation initiation by binding eIF4G; required for pre-mRNA splicing; interacts with E3 ubiquitin ligase Bre1, linking histone ubiquitination to mRNA processing; may have role in telomere maintenance; dissociation from mRNAs promoted by Mtr10; phosphorylated by Sky1 in cytoplasm; protein abundance increases in response to DNA replication stress.	++
NRP1	Putative RNA binding protein of unknown function; localizes to stress granules induced by glucose deprivation; predicted to be involved in ribosome biogenesis.	++
PHO23	Component of the Rpd3L histone deacetylase complex; involved in transcriptional regulation of <i>PHO5</i> ; affects termination of snoRNAs and cryptic unstable transcripts (CUTs).	+

POP2	RNase of the DEDD superfamily; subunit of the Ccr4-Not complex that mediates 3' to 5' mRNA deadenylation.	++
REF2	RNA-binding protein; involved in the cleavage step of mRNA 3'-end formation prior to polyadenylation, and in snoRNA maturation; part of holo-CPF subcomplex APT, which associates with 3'-ends of snoRNA- and mRNA-encoding genes; putative regulatory subunit of type 1 protein phosphatase Glc7p, required for actomyosin ring formation, and for timely dephosphorylation and release of Bnr1p from the division site; relocalizes to the cytosol in response to hypoxia.	++
RXT2	Component of the histone deacetylase Rpd3L complex; possibly involved in cell fusion and invasive growth.	+
RXT3	Component of the Rpd3L histone deacetylase complex; involved in histone deacetylation.	+
RMI1	Subunit of the RecQ (Sgs1) - Topo III (Top3p) complex; stimulates superhelical relaxing, DNA catenation/decatenation and ssDNA binding activities of Top3; involved in response to DNA damage; functions in S phase-mediated cohesion establishment via a pathway involving the Ctf18-RFC complex and Mrc1; stimulates Top3 DNA catenation/decatenation activity; null mutants display increased rates of recombination and delayed S phase.	++
RPB9	RNA polymerase II subunit B12.6; contacts DNA; mutations affect transcription start site selection and fidelity of transcription.	+++
RRN10	Protein involved in promoting high level transcription of rDNA; subunit of UAF (upstream activation factor) for RNA polymerase I.	++
RRP6	Nuclear exosome exonuclease component; has 3'-5' exonuclease activity that is regulated by Lrp1; involved in RNA processing, maturation, surveillance, degradation, tethering, and export; role in sn/snoRNAs precursor degradation; forms a stable heterodimer with Lrp1; has similarity to <i>E. coli</i> RNase D and to human PM-Sc1 100 (EXOSC10).	++
RSC2	Component of the RSC chromatin remodeling complex; required for expression of mid-late sporulation-specific genes; involved in telomere maintenance; RSC2 has a paralogue, RSC1, that arose from the whole genome duplication.	+++
SHE2	RNA-binding protein that binds specific mRNAs and interacts with She3; part of the mRNA localization machinery that restricts accumulation of certain proteins to the bud.	+
SDS23	Protein involved in cell separation during budding; one of two <i>S. cerevisiae</i> homologs (Sds23p and Sds24p) of the <i>S. pombe</i> Sds23 protein, which is implicated in APC/cyclosome regulation; SDS23 has a paralogue, SDS24, that arose from the whole genome duplication.	+++
SGS1	RecQ family nucleolar DNA helicase; role in genome integrity maintenance, chromosome synapsis, meiotic joint molecule/crossover formation; stimulates activity of Top3; rapidly lost in response to rapamycin in Rrd1p-dependent manner; forms nuclear foci upon DNA replication stress; yeast SGS1 complements mutations in human homolog BLM implicated in Bloom syndrome; also similar to human	++

	WRN implicated in Werner syndrome; human BLM and WRN can each complement yeast null mutant.	
SIN3	Component of both the Rpd3S and Rpd3L histone deacetylase complexes; involved in transcriptional repression and activation of diverse processes, including mating-type switching and meiosis; involved in the maintenance of chromosomal integrity.	+
SRB2	Subunit of the RNA polymerase II mediator complex; associates with core polymerase subunits to form the RNA polymerase II holoenzyme; general transcription factor involved in telomere maintenance.	+++
SRB8	Subunit of the RNA polymerase II mediator complex; associates with core polymerase subunits to form the RNA polymerase II holoenzyme; essential for transcriptional regulation; involved in glucose repression.	++
SSN2	Subunit of the RNA polymerase II mediator complex; associates with core polymerase subunits to form the RNA polymerase II holoenzyme; required for stable association of Srb10-Srb11 kinase; essential for transcriptional regulation.	+++
SSN8	Cyclin-like component of the RNA polymerase II holoenzyme; involved in phosphorylation of the RNA polymerase II C-terminal domain; forms a kinase-cyclin pair in the RNAPII holoenzyme with Ssn3p; required for both entry into and execution of the meiotic program; involved in glucose repression and telomere maintenance; cyclin homolog 35% identical to human cyclin C.	+++
SSO2	Plasma membrane t-SNARE; involved in fusion of secretory vesicles at the plasma membrane; syntaxin homolog that is functionally redundant with Sso1; SSO2 has a paralog, SSO1, that arose from the whole genome duplication.	+
SWC5	Component of the SWR1 complex; complex exchanges histone variant H2AZ (Htz1) for chromatin-bound histone H2A; protein abundance increases in response to DNA replication stress; relocalizes to the cytosol in response to hypoxia.	++
TCD2	tRNA threonylcarbamoyladenosine dehydratase; required for the ct6A tRNA base modification, where an adenosine at position 37 is modified to form a cyclized active ester with an oxazolone ring; localized to the mitochondrial outer membrane; TCD2 has a paralog, TCD1, that arose from the whole genome duplication.	++
TDA5	Putative protein of unknown function; detected in highly purified mitochondria in high-throughput studies; proposed to be involved in resistance to mechlorethamine and streptozotocin.	++
THO2	Subunit of the THO complex; THO2 is required for efficient transcription elongation and involved in transcriptional elongation-associated recombination; required for LacZ RNA expression from certain plasmids.	+++

<i>THP3</i>	Protein that may have a role in transcription elongation; forms a complex with Csn12 that is recruited to transcribed genes; possibly involved in splicing based on pre-mRNA accumulation defect for many intron-containing genes.	++
<i>TOP1</i>	Topoisomerase I; nuclear enzyme that relieves torsional strain in DNA by cleaving and re-sealing the phosphodiester backbone; relaxes both positively and negatively supercoiled DNA; functions in replication, transcription, and recombination; role in processing ribonucleoside monophosphates in genomic DNA into irreversible single-strand breaks; enzymatic activity and interaction with Nsr1p are negatively regulated by polyphosphorylation.	++
<i>TOP3</i>	DNA Topoisomerase III; conserved protein that functions in a complex with Sgs1 and Rmi1 to relax single-stranded negatively-supercoiled DNA preferentially; DNA catenation/decatenation activity is stimulated by RPA and Sgs1-Top3-Rmi1; involved in telomere stability and regulation of mitotic recombination.	++
<i>TRM1</i>	tRNA methyltransferase; two forms of protein are made by alternative translation starts; localizes to both nucleus and mitochondrion to produce modified base N ² ,N ² -dimethylguanosine in tRNAs in both compartments; nuclear Trm1 is evenly distributed around inner nuclear membrane in WT, but mislocalizes as puncta near ER-nucleus junctions in spindle pole body (SPB) mutants; both Trm1 inner nuclear membrane targeting and maintenance depend upon SPB.	+++
<i>TRM10</i>	tRNA methyltransferase; methylates the N-1 position of guanine at position 9 in tRNAs; protein abundance increases in response to DNA replication stress; member of the SPOUT (SpoU-TrmD) methyltransferase family; human ortholog <i>TRMT10A</i> plays a role in the pathogenesis of microcephaly and early onset diabetes; an 18-mer originates from the <i>TRM10</i> locus; genetic analysis shows the 18-mer is the translation regulator.	++
<i>XRN1</i>	Evolutionarily-conserved 5'-3' exonuclease; component of cytoplasmic processing (P) bodies involved in mRNA decay; also enters the nucleus and positively regulates transcription initiation and elongation; plays a role in microtubule-mediated processes, filamentous growth, ribosomal RNA maturation, and telomere maintenance; activated by the scavenger decapping enzyme Dcs1.	+++
<i>YTA7</i>	Protein that localizes to chromatin; has a role in regulation of histone gene expression; has a bromodomain-like region that interacts with the N-terminal tail of histone H3, and an ATPase domain; relocalizes to the cytosol in response to hypoxia; potentially phosphorylated by Cdc28.	+
Cytoskeleton organization and morphogenesis		
Gene	Function	Susceptibility level
<i>ALF1</i>	Alpha-tubulin folding protein; similar to mammalian cofactor B; Alf1p-GFP localizes to cytoplasmic microtubules; required for the folding of alpha-tubulin and may play an additional role in microtubule maintenance.	+++

ARC18	Subunit of the ARP2/3 complex; <i>ARP2/3</i> is required for the motility and integrity of cortical actin patches.	++
ARP1	Actin-related protein of the dynactin complex; required for spindle orientation and nuclear migration; forms actin-like short filament composed of 9 or 10 Arp1 monomers.	++
AVO2	Component of a complex containing the Tor2pkinase and other proteins; complex may have a role in regulation of cell growth.	+++
BEM1	Protein containing SH3-domains; involved in establishing cell polarity and morphogenesis; functions as a scaffold protein for complexes that include Cdc24, Ste5, Ste20, and Rsr1.	+++
BEM2	Rho GTPase activating protein (RhoGAP); involved in the control of cytoskeleton organization and cellular morphogenesis; required for bud emergence.	++
BEM4	Protein involved in establishment of cell polarity and bud emergence; interacts with the Rho1p small GTP-binding protein and with the Rho-type GTPase Cdc42; involved in maintenance of proper telomere length.	+++
BUB3	Kinetochores checkpoint WD40 repeat protein; localizes to kinetochores during prophase and metaphase, delays anaphase in the presence of unattached kinetochores; forms complexes with Mad1-Bub1 and with Cdc20, binds Mad2 and Mad3; functions at kinetochores to activate APC/C-Cdc20 for normal mitotic progression.	++
KEL1	Protein required for proper cell fusion and cell morphology; forms a complex with Bud14 and Kel2 that regulates Bnr1 (formin) to affect actin cable assembly, cytokinesis, and polarized growth.	+
MDY2	Protein involved in inserting tail-anchored proteins into ER membranes; forms a complex with Get4; required for efficient mating; involved in shmoo formation and nuclear migration in the pre-zygote; associates with ribosomes.	++
MMR1	Phosphorylated protein of the mitochondrial outer membrane; localizes only to mitochondria of the bud; interacts with Myo2 to mediate mitochondrial distribution to buds; mRNA is targeted to the bud via the transport system involving She2.	+
NCL1	S-adenosyl-L-methionine-dependent tRNA: m5C-methyltransferase; methylates cytosine to m5C at several positions in tRNAs and intron-containing pre-tRNAs; increases proportion of tRNA ^{Leu} (CAA) with m5C at wobble position in response to hydrogen peroxide, causing selective translation of mRNA from genes enriched in TTG codon; loss of <i>NCL1</i> confers hypersensitivity to oxidative stress; similar to Nop2 and human proliferation associated nucleolar protein p120.	++
RTN1	Reticulon protein; involved in nuclear pore assembly and maintenance of tubular ER morphology.	+
RVS161	Amphiphysin-like lipid raft protein; N-BAR domain protein that interacts with Rvs167p and regulates polarization of the actin cytoskeleton, endocytosis, cell polarity, cell fusion and viability following starvation or osmotic stress.	+

SAC6	Fimbrin, actin-bundling protein; cooperates with Scp1 in organization and maintenance of the actin cytoskeleton; phosphorylated by Cdc28/Clb2 in metaphase on T103, to regulate conformation, and modulate actin filament binding affinity and actin cable dynamics; relocalizes from the plasma membrane to the cytoplasm upon DNA replication stress; human homologs <i>PLS3</i> and <i>LCP1</i> implicated in spinocerebellar ataxia type 2 (SCA2) can each complement yeast null mutant.	+++
SHS1	Component of the septin ring that is required for cytokinesis; present at the ends of rod-like septin hetero-oligomers; C-terminal extension is important for recruitment of Bni5 to the mother-bud neck, which in turn is required for Myo1 recruitment and cytokinesis; undergoes sumoylation and phosphorylation during mitosis; protein abundance increases in response to DNA replication stress.	+++
SLA1	Cytoskeletal protein binding protein; required for assembly of the cortical actin cytoskeleton; interacts with proteins regulating actin dynamics and proteins required for endocytosis; found in the nucleus and cell cortex; has 3 SH3 domains.	+++
SPC72	Gamma-tubulin small complex (gamma-TuSC) receptor; recruits the gamma-TuSC complex to the cytoplasmic side of the SPB, connecting nuclear microtubules to the SPB; involved in astral microtubule formation, stabilization, and with Stu2, anchoring astral MTs at the cytoplasmic face of the SPB, and regulating plus-end MT dynamics; regulated by Cdc5 kinase.	++
SSD1	Translational repressor with a role in polar growth and wall integrity; regulated by Cbk1 phosphorylation to effect bud-specific translational control and localization of specific mRNAs; interacts with TOR pathway components; contains a functional N-terminal nuclear localization sequence and nucleocytoplasmic shuttling appears to be critical to Ssd1 function.	++
VAC17	Phosphoprotein involved in vacuole inheritance; degraded in late M phase of the cell cycle; acts as a vacuole-specific receptor for myosin Myo2.	+
VRP1	Verprolin, proline-rich actin-associated protein; involved in cytoskeletal organization and cytokinesis; promotes actin nucleation and endocytosis; related to mammalian Wiskott-Aldrich syndrome protein (WASP)-interacting protein (WIP).	+++

DNA repair

Gene	Function	Susceptibility level
CTF3	Outer kinetochore protein that forms a complex with Mcm16 and Mcm22; may bind the kinetochore to spindle microtubules; required for the spindle assembly checkpoint; orthologous to human centromere constitutive-associated network (CCAN) subunit CENP-I and fission yeast <i>mis6</i> .	+

FZO1	Mitofusin; integral membrane protein involved in mitochondrial outer membrane tethering and fusion; role in mitochondrial genome maintenance; efficient tethering and degradation of Fzo1p requires an intact N-terminal GTPase domain; targeted for destruction by the ubiquitin ligase SCF-Mdm30p and the cytosolic ubiquitin-proteasome system.	+++
MET18	Component of cytosolic iron-sulfur protein assembly (CIA) machinery; acts at a late step of Fe-S cluster assembly; forms the CIA targeting complex with Cia1 and Cia2 that directs Fe-S cluster incorporation into a subset of proteins involved in methionine biosynthesis, DNA replication and repair, transcription, and telomere maintenance; ortholog of human <i>MMS19</i> .	+
MIP1	Mitochondrial DNA polymerase gamma; single subunit of mitochondrial DNA polymerase in yeast, in contrast to metazoan complex of catalytic and accessory subunits; polymorphic in yeast, petites occur more frequently in some lab strains; human ortholog <i>POLG</i> complements yeast <i>mip1</i> mutant; mutations in human <i>POLG</i> associated with Alpers-Huttenlocher syndrome (AHS), progressive external ophthalmoplegia (PEO), parkinsonism, other mitochondrial diseases.	++
MLH1	Protein required for mismatch repair in mitosis and meiosis; also required for crossing over during meiosis; forms a complex with Pms1 and Msh2-Msh3 during mismatch repair; human homolog is associated with hereditary non-polyposis colon cancer.	++
MTF1	Mitochondrial RNA polymerase specificity factor; has structural similarity to S-adenosylmethionine-dependent methyltransferases and functional similarity to bacterial sigma-factors; Mtf1 interacts with and stabilizes the Rpo41-promoter complex, enhancing DNA bending and melting to facilitate pre-initiation open complex formation.	++
MTF2	Mitochondrial protein that interacts with mitochondrial RNA polymerase; interacts with an N-terminal region of mitochondrial RNA polymerase (Rpo41) and couples RNA processing and translation to transcription.	+

Ion homeostasis

Gene	Function	Susceptibility level
FRE8	Protein with sequence similarity to iron/copper reductases; involved in iron homeostasis; deletion mutant has iron deficiency/accumulation growth defects.	+
ICE2	Integral ER membrane protein with type-III transmembrane domains; required for maintenance of ER zinc homeostasis; necessary for efficient targeting of Trm1 tRNA methyltransferase to inner nuclear membrane; mutations cause defects in cortical ER morphology in both the mother and daughter cells.	+++
LSO2	Protein with a potential role in response to iron deprivation; localizes to nucleus and cytoplasm, and nuclear localization is enhanced under iron-replete	++

	conditions; null mutant exhibits slow growth during iron deprivation.	
TRK1	Component of the Trk1-Trk2 potassium transport system; 180 kDa high affinity potassium transporter; phosphorylated <i>in vivo</i> and interacts physically with the phosphatase Ppz1, suggesting Trk1 activity is regulated by phosphorylation.	++
Internal pH homeostasis		
Gene	Function	Susceptibility level
VMA1	Subunit A of the V1 peripheral membrane domain of V-ATPase; protein precursor undergoes self-catalyzed splicing to yield the extein Tfp1 and the intein Vde (PI-Scel), which is a site-specific endonuclease; the V1 peripheral membrane domain of the vacuolar H ⁺ -ATPase (V-ATPase) has eight subunits; involved in methionine restriction extension of chronological lifespan in an autophagy-dependent manner.	+++
VMA10	Subunit G of the V1 peripheral membrane domain of V-ATPase; part of the electrogenic proton pump found throughout the endomembrane system; involved in vacuolar acidification; the V1 peripheral membrane domain of the vacuolar H ⁺ -ATPase (V-ATPase) has eight subunits.	+++
VMA13	Subunit H of the V1 peripheral membrane domain of V-ATPase; part of the electrogenic proton pump found throughout the endomembrane system; serves as an activator or a structural stabilizer of the V-ATPase; the V1 peripheral membrane domain of the vacuolar H ⁺ -ATPase (V-ATPase) has eight subunits.	+++
VMA16	Subunit c" of the vacuolar ATPase; v-ATPase functions in acidification of the vacuole; one of three proteolipid subunits of the V0 domain.	+++
VMA21	Integral membrane protein required for V-ATPase function; not an actual component of the vacuolar H ⁺ -ATPase (V-ATPase) complex; diverged ortholog of human XMEA (X-linked Myopathy with Excessive Autophagy); functions in the assembly of the V-ATPase; localized to the yeast endoplasmic reticulum.	+++
VMA5	Subunit C of the V1 peripheral membrane domain of V-ATPase; part of the electrogenic proton pump found throughout the endomembrane system; required for the V1 domain to assemble onto the vacuolar membrane; the V1 peripheral membrane domain of vacuolar H ⁺ -ATPase (V-ATPase) has eight subunits.	+++
VMA9	Vacuolar H ⁺ ATPase subunit e of the V-ATPase V0 subcomplex; essential for vacuolar acidification; interacts with the V-ATPase assembly factor Vma21p in the ER; involved in V0 biogenesis.	+++
VPH2	Integral membrane protein required for V-ATPase function; not an actual component of the vacuolar H ⁺ -ATPase (V-ATPase) complex; functions in the assembly of the V-ATPase; localized to the endoplasmic reticulum (ER); involved in methionine restriction extension of	++

chronological lifespan in an autophagy-dependent manner.

Intracellular trafficking

Gene	Function	Susceptibility level
ARL3	ARF-like small GTPase of the RAS superfamily; required for recruitment of Arl1, a GTPase that regulates membrane traffic, to the Golgi apparatus; NatC-catalyzed N-terminal acetylation regulates Golgi membrane association mediated by interaction with membrane receptor, Sys1; similar to ADP-ribosylation factor and orthologous to mammalian <i>ARFRP1</i> .	+
ARV1	Cortical ER protein; implicated in the membrane insertion of tail-anchored C-terminal single transmembrane domain proteins; may function in transport of glycosylphosphatidylinositol intermediates into the ER lumen; required for normal intracellular sterol distribution; human <i>ARV1</i> , required for normal cholesterol and bile acid homeostasis, can complement yeast <i>arv1</i> null mutant; human variant causing early onset epileptic encephalopathy is unable to rescue the yeast null.	++
AVL9	Conserved protein involved in exocytic transport from the Golgi; mutation is synthetically lethal with <i>apl2 vps1</i> double mutation; member of a protein superfamily with orthologs in diverse organisms.	+
CHS3	Chitin synthase III; catalyzes the transfer of N-acetylglucosamine (GlcNAc) to chitin; required for synthesis of the majority of cell wall chitin, the chitin ring during bud emergence, and spore wall chitosan; contains overlapping di-leucine and di-acidic signals that mediate, respectively, intracellular trafficking by AP-1 and trafficking to plasma membrane by exomer complex.	+
CHS5	Component of the exomer complex; the exomer which also contains Csh6p, Bch1p, Bch2p, and Bud7, is involved in the export of select proteins, such as chitin synthase Chs3p, from the Golgi to the plasma membrane.	+
DID2	Class E protein of the vacuolar protein-sorting (Vps) pathway; binds Vps4 and directs it to dissociate ESCRT-III complexes; forms a functional and physical complex with Ist1p; human ortholog may be altered in breast tumors.	++
DID4	Class E Vps protein of the ESCRT-III complex; required for sorting of integral membrane proteins into luminal vesicles of multivesicular bodies, and for delivery of newly synthesized vacuolar enzymes to the vacuole, involved in endocytosis.	++
DOA1	WD repeat protein required for ubiquitin-mediated protein degradation; ubiquitin binding cofactor that complexes with Cdc48; required for ribophagy; controls cellular ubiquitin concentration; promotes efficient NHEJ	+

	in postdiauxic/stationary phase; facilitates N-terminus-dependent proteolysis of centromeric histone H3 (Cse4) for faithful chromosome segregation.	
DOA4	Ubiquitin hydrolase; deubiquitinates intraluminal vesicle (ILVs) cargo proteins; required for recycling ubiquitin from proteasome-bound ubiquitinated intermediates, acts at the late endosome/prevacuolar compartment to recover ubiquitin from ubiquitinated membrane proteins destined for the vacuole; <i>DOA4</i> has a paralog, <i>UBP5</i> , that arose from the whole genome duplication.	+++
DRS2	Trans-golgi network aminophospholipid translocase (flippase); maintains membrane lipid asymmetry in post-Golgi secretory vesicles; contributes to clathrin-coated vesicle formation, endocytosis, protein trafficking between the Golgi and endosomal system and the cellular response to mating pheromone; autoinhibited by its C-terminal tail; localizes to the trans-Golgi network; mutations in human homolog <i>ATP8B1</i> result in liver disease.	++
END3	EH domain-containing protein involved in endocytosis; actin cytoskeletal organization and cell wall morphogenesis; forms a complex with Sla1 and Pan1.	+++
EPS1	ER protein with chaperone and co-chaperone activity; involved in retention of resident ER proteins; has a role in recognizing proteins targeted for ER-associated degradation (ERAD), member of the protein disulfide isomerase family.	++
FYV10	Subunit of GID complex; involved in proteasome-dependent catabolite inactivation of gluconeogenic enzymes FBpase, PEPCK, and c-MDH; forms dimer with Rmd5 that is then recruited to GID Complex by Gid8; contains a degenerate RING finger motif needed for GID complex ubiquitin ligase activity in vivo, as well as CTLH and CRA domains; plays role in anti-apoptosis; required for survival upon exposure to K1 killer toxin.	+
GCS1	ADP-ribosylation factor GTPase activating protein (ARF GAP); involved in ER-Golgi transport; required for prospore membrane formation; regulates phospholipase Spo14; shares functional similarity with Glo3; <i>GCS1</i> has a paralog, <i>SPS18</i> , that arose from the whole genome duplication.	+++
GET1	Subunit of the GET complex; involved in insertion of proteins into the ER membrane; required for the retrieval of HDEL proteins from the Golgi to the ER in an <i>ERD2</i> dependent fashion and for normal mitochondrial morphology and inheritance.	+
GTR2	Subunit of a TORC1-stimulating GTPase complex; subunit of the Gtr1-Gtr2 GTPase complex that stimulates TORC1 in response to amino acid stimulation; stimulates the GTPase activity of Gtr1p; negatively regulates the Ran/Tc4 GTPase cycle; activates transcription; tethered to the vacuolar membrane as part of the EGO complex (EGOC); required for sorting of Gap1p; activated by the the Lst4-Lst7 GAP complex; localizes to cytoplasm and to chromatin.	++
GYP1	Cis-golgi GTPase-activating protein (GAP) for yeast Rabs; the Rab family members are Ypt1 (<i>in vivo</i>) and for Ypt1, Sec4, Ypt7, and Ypt51 (<i>in vitro</i>); involved in vesicle docking and fusion.	++

<i>HSE1</i>	Subunit of the endosomal Vps27-Hse1 complex; complex is required for sorting of ubiquitinated membrane proteins into intraluminal vesicles prior to vacuolar degradation, as well as for recycling of Golgi proteins and formation of luminal membranes.	+++
<i>PKH2</i>	Serine/threonine protein kinase; involved in sphingolipid-mediated signaling pathway that controls endocytosis; activates Ypk1 and Ykr2, components of signaling cascade required for maintenance of cell wall integrity; contains a PH-like domain; redundant with Pkh1p; <i>PKH2</i> has a paralog, <i>PKH1</i> , that arose from the whole genome duplication.	++
<i>RAV1</i>	Subunit of RAVE complex (Rav1, Rav2, Skp1); the RAVE complex promotes assembly of the V-ATPase holoenzyme; required for transport between the early and late endosome/PVC and for localization of TGN membrane proteins; potential Cdc28 substrate.	++
<i>RAV2</i>	Subunit of RAVE complex (Rav1, Rav2, Skp1); the RAVE complex associates with the V1 domain of the vacuolar membrane (H ⁺)-ATPase (V-ATPase) and promotes assembly and reassembly of the holoenzyme.	++
<i>RER1</i>	Protein involved in retention of membrane proteins; including Sec12, in the ER; localized to Golgi.	+
<i>RGP1</i>	Subunit of a Golgi membrane exchange factor (Ric1-Rgp1); this complex catalyzes nucleotide exchange on Ypt6.	+++
<i>SEC22</i>	R-SNARE protein; assembles into SNARE complex with Bet1p, Bos1 and Sed5; cycles between the ER and Golgi complex; involved in anterograde and retrograde transport between the ER and Golgi.	+
<i>SEC28</i>	Epsilon-COP subunit of the coatomer; regulates retrograde Golgi-to-ER protein traffic; stabilizes Cop1, the alpha-COP and the coatomer complex; non-essential for cell growth; protein abundance increases in response to DNA replication stress.	++
<i>SEC66</i>	Non-essential subunit of Sec63 complex; with Sec61 complex, Kar2/BiP and Lhs1 forms a channel competent for SRP-dependent and post-translational SRP-independent protein targeting and import into the ER; other members are Sec63, Sec62, and Sec72.	+++
<i>SLM4</i>	Component of the EGO and GSE complexes; essential for integrity and function of EGO; EGO is involved in the regulation of microautophagy and GSE is required for proper sorting of amino acid permease Gap1; gene exhibits synthetic genetic interaction with <i>MSS4</i> .	++
<i>SLM5</i>	Mitochondrial asparaginyl-tRNA synthetase.	++
<i>SNF2</i>	Catalytic subunit of the SWI/SNF chromatin remodeling complex; involved in transcriptional regulation; contains DNA-stimulated ATPase activity; functions interdependently in transcriptional activation with Snf5p and Snf6p.	+
<i>SNF7</i>	One of four subunits of the ESCRT-III complex; involved in the sorting of transmembrane proteins into the multivesicular body (MVB) pathway; recruited from the cytoplasm to endosomal membranes; ESCRT-III stands for endosomal sorting complex required for transport III.	+++

SNF8	Component of the ESCRT-II complex; ESCRT-II is involved in ubiquitin-dependent sorting of proteins into the endosome; appears to be functionally related to <i>SNF7</i> ; involved in glucose derepression.	+++
STP22	Component of the ESCRT-I complex; ESCRT-I is involved in ubiquitin-dependent sorting of proteins into the endosome; prevents polyubiquitination of the arrestin-related protein Rim8p, thereby directing its monoubiquitination by Rsp5; homologous to the mouse and human Tsg101 tumor susceptibility gene; mutants exhibit a Class E Vps phenotype.	+++
TIM18	Component of the mitochondrial <i>TIM22</i> complex; involved in insertion of polytopic proteins into the inner membrane; may mediate assembly or stability of the complex.	++
TLG2	Syntaxin-like t-SNARE; forms a complex with Tlg1 and Vti1 and mediates fusion of endosome-derived vesicles with the late Golgi; required along with <i>VPS45</i> for an early step of the constitutive CVT pathway.	+
TRS33	Core component of TRAPP complexes I, II and IV; transport protein particle (TRAPP) complexes are related multimeric guanine nucleotide-exchange factor for the GTPase Ypt1, regulating ER-Golgi traffic (TRAPPI), intra-Golgi traffic (TRAPP II), endosome-Golgi traffic (TRAPP II and III) and autophagy (TRAPP III, and IV); proposed subunit of a novel complex, TRAPP IV, that may function redundantly with TRAPP III as a GEF that activates Ypt1 during autophagy.	++
TRS85	Component of transport protein particle (TRAPP) complex III; TRAPP III is a multimeric guanine nucleotide-exchange factor for the GTPase Ypt1, regulating endosome-Golgi traffic and required for membrane expansion during autophagy and the CVT pathway; directs Ypt1 to the PAS; late post-replication meiotic role.	++
VAM10	Protein involved in vacuole morphogenesis; acts at an early step of homotypic vacuole fusion that is required for vacuole tethering.	++
VAM3	Syntaxin-like vacuolar t-SNARE; functions with Vam7 in vacuolar protein trafficking; mediates docking/fusion of late transport intermediates with the vacuole; has an acidic di-leucine sorting signal and C-terminal transmembrane region.	++
VAM6	Guanine nucleotide exchange factor for the GTPase Gtr1; subunit of the HOPS endocytic tethering complex; vacuole membrane protein; functions as a Rab GTPase effector, interacting with both GTP- and GDP-bound conformations of Ypt7; facilitates tethering and promotes membrane fusion events at the late endosome and vacuole; required for both membrane and protein trafficking; component of vacuole-mitochondrion contacts (vCLAMPs) important for lipid transfer between organelles.	++
VPS1	Dynamamin-like GTPase required for vacuolar sorting; also involved in actin cytoskeleton organization, endocytosis, late Golgi-retention of some proteins, regulation of peroxisome biogenesis.	+++
VPS16	Subunit of the HOPS and the CORVET complexes; part of the Class C Vps complex essential for membrane	++

	docking and fusion at Golgi-to-endosome and endosome-to-vacuole protein transport stages.	
VPS17	Subunit of the membrane-associated retromer complex; essential for endosome-to-Golgi retrograde protein transport; peripheral membrane protein that assembles onto the membrane with Vps5 to promote vesicle formation; required for recruiting the retromer complex to the endosome membranes.	++
VPS21	Endosomal Rab family GTPase; required for endocytic transport and sorting of vacuolar hydrolases; required for endosomal localization of the CORVET complex; required with <i>YPT52</i> for MVB biogenesis and sorting; involved in autophagy and ionic stress tolerance; geranylgeranylation required for membrane association; protein abundance increases in response to DNA replication stress; mammalian Rab5 homolog; <i>VPS21</i> has a paralog, <i>YPT53</i> , that arose from the whole genome duplication.	++
VPS24	One of four subunits of the ESCRT-III complex; forms an endosomal sorting complex required for transport III (ESCRT-III) subcomplex with Did4; involved in the sorting of transmembrane proteins into the multivesicular body (MVB) pathway.	+++
VPS25	Component of the ESCRT-II complex; ESCRT-II is involved in ubiquitin-dependent sorting of proteins into the endosome.	++
VPS27	Endosomal protein that forms a complex with Hse1; required for recycling Golgi proteins, forming luminal membranes and sorting ubiquitinated proteins destined for degradation; has Ubiquitin Interaction Motifs which bind ubiquitin (Ubi4).	++
VPS28	Component of the ESCRT-I complex; complex is involved in ubiquitin-dependent sorting of proteins into the endosome; conserved C-terminal domain interacts with ESCRT-III subunit Vps20p; other members include Stp22, Srn2, Vps28, and Mvb12.	+++
VPS33	ATP-binding protein that is a subunit of the HOPS and CORVET complexes; essential for protein sorting, vesicle docking, and fusion at the vacuole; binds to SNARE domain.	+++
VPS36	Component of the ESCRT-II complex; contains the GLUE (GRAM Like Ubiquitin binding in EAP45) domain which is involved in interactions with ESCRT-I and ubiquitin-dependent sorting of proteins into the endosome; plays a role in the formation of mutant huntingtin (Htt) aggregates in yeast.	+++
VPS4	AAA-ATPase involved in multivesicular body (MVB) protein sorting; ATP-bound Vps4p localizes to endosomes and catalyzes ESCRT-III disassembly and membrane release; ATPase activity is activated by Vta1; regulates cellular sterol metabolism.	+

VPS41	Subunit of the HOPS endocytic tethering complex; vacuole membrane protein that functions as a Rab GTPase effector, interacting specifically with the GTP-bound conformation of Ypt7p, facilitating tethering, docking and promoting membrane fusion events at the late endosome and vacuole; required for both membrane and protein trafficking; Yck3-mediated phosphorylation regulates the organization of vacuolar fusion sites.	++
VPS5	Nexin-1 homolog; required for localizing membrane proteins from a prevacuolar/late endosomal compartment back to late Golgi; structural component of retromer membrane coat complex; forms a retromer subcomplex with Vps17; required for recruiting the retromer complex to the endosome membranes; <i>VPS5</i> has a paralog, <i>YKR078W</i> , that arose from the whole genome duplication.	++
VPS52	Component of the GARP (Golgi-associated retrograde protein) complex; GARP is required for the recycling of proteins from endosomes to the late Golgi, and for mitosis after DNA damage induced checkpoint arrest; involved in localization of actin and chitin; members of the GARP complex are Vps51-Vps52-Vps53-Vps54.	++
VPS61	Dubious open reading frame; unlikely to encode a functional protein, based on available experimental and comparative sequence data; not conserved in closely related <i>Saccharomyces</i> species; 4% of ORF overlaps the verified gene <i>RGP1</i> ; deletion causes a vacuolar protein sorting defect.	+++
VPS63	Putative protein of unknown function; not conserved in closely related <i>Saccharomyces</i> species; 98% of ORF overlaps the verified gene <i>YPT6</i> ; deletion causes a vacuolar protein sorting defect; decreased levels of protein in enolase deficient mutant.	+++
VPS74	Golgi phosphatidylinositol-4-kinase effector and PtdIns4P sensor; interacts with the cytosolic domains of cis and medial glycosyltransferases, and in the PtdIns4P-bound state mediates the targeting of these enzymes to the Golgi; interacts with the catalytic domain of Sac1, the major cellular PtdIns4P phosphatase, to direct dephosphorylation of the Golgi pool of PtdIns4P; tetramerization required for function; ortholog of human <i>GOLPH3/GPP34/GMx33</i> .	++
YPT6	Rab family GTPase; required for endosome-to-Golgi, intra-Golgi retrograde, and retrograde Golgi-to-ER transport; temporarily at the Golgi, dissociating into the cytosol on arrival of the late Golgi GTPase Ypt32; Golgi-localized form is GTP bound, while cytosolic form is GDP-bound; required for delivery of Atg9 to the phagophore assembly site during autophagy under heat stress, with Ypt6p for starvation induced autophagy and for the CVT pathway.	+++

Lipid synthesis

Gene	Function	Susceptibility level
------	----------	----------------------

ELO2	Fatty acid elongase, involved in sphingolipid biosynthesis; acts on fatty acids of up to 24 carbons in length; mutations have regulatory effects on 1,3-beta-glucan synthase, vacuolar ATPase, and the secretory pathway; <i>ELO2</i> has a paralog, <i>ELO1</i> , that arose from the whole genome duplication; lethality of the <i>elo2 elo3</i> double null mutation is functionally complemented by human <i>ELOVL1</i> and weakly complemented by human <i>ELOVL3</i> or <i>ELOV7</i> .	+++
ELO3	Elongase; involved in fatty acid and sphingolipid biosynthesis; synthesizes very long chain 20-26-carbon fatty acids from C18-CoA primers; involved in regulation of sphingolipid biosynthesis; lethality of the <i>elo2 elo3</i> double null mutation is functionally complemented by human <i>ELOVL1</i> and weakly complemented by human <i>ELOVL3</i> or <i>ELOV7</i> .	++
ERG2	C-8 sterol isomerase; catalyzes isomerization of delta-8 double bond to delta-7 position at an intermediate step in ergosterol biosynthesis; transcriptionally down-regulated when ergosterol is in excess.	+++
ERG24	C-14 sterol reductase; acts in ergosterol biosynthesis; mutants accumulate the abnormal sterol ignosterol (ergosta-8,14 dienol), and are viable under anaerobic growth conditions but inviable on rich medium under aerobic condition.	++
ERG28	Endoplasmic reticulum membrane protein; may facilitate protein-protein interactions between the Erg26 dehydrogenase and the Erg27p 3-ketoreductase and/or tether these enzymes to the ER, also interacts with Erg6.	+++
ERG3	C-5 sterol desaturase; glycoprotein that catalyzes the introduction of a C-5(6) double bond into episterol, a precursor in ergosterol biosynthesis; transcriptionally down-regulated when ergosterol is in excess; mutants are viable, but cannot grow on non-fermentable carbon sources; substrate of HRD ubiquitin ligase; mutation is functionally complemented by human <i>SC5D</i> .	++
ERG4	C-24(28) sterol reductase; catalyzes the final step in ergosterol biosynthesis; mutants are viable, but lack ergosterol.	+
ERG5	C-22 sterol desaturase; a cytochrome P450 enzyme that catalyzes the formation of the C-22(23) double bond in the sterol side chain in ergosterol biosynthesis; may be a target of azole antifungal drugs	+
ETR1	2-enoyl thioester reductase; member of the medium chain dehydrogenase/reductase family; localized to mitochondria, where it has a probable role in fatty acid synthesis; human MECR functionally complements the respiratory growth defect of the null mutant.	++
HTD2	Mitochondrial 3-hydroxyacyl-thioester dehydratase; involved in fatty acid biosynthesis, required for respiratory growth and for normal mitochondrial morphology.	++

KCS1	Inositol hexakisphosphate and inositol heptakisphosphate kinase; generation of high energy inositol pyrophosphates by Kcs1 is required for many processes such as vacuolar biogenesis, stress response, RNA polymerase I-mediated rRNA transcription and telomere maintenance; inositol hexakisphosphate is also known as IP6; inositol heptakisphosphate is also known as IP7.	+++
LAM1	Putative sterol transfer protein; localizes to puncta in the cortical ER; probable role in retrograde transport of sterols from the plasma membrane to the ER; one of six StART-like domain-containing proteins in yeast that may be involved in sterol transfer between intracellular membranes.	+
LIP5	Protein involved in biosynthesis of the coenzyme lipoic acid.	+
LOA1	Lysophosphatidic acid acyltransferase; involved in triacylglyceride homeostasis and lipid droplet formation; localized to lipid droplets and the ER; specificity for oleoyl-CoA.	+
PDX3	Pyridoxine (pyridoxamine) phosphate oxidase; has homologs in <i>E. coli</i> and <i>Myxococcus xanthus</i> ; transcription is under the general control of nitrogen metabolism.	+++
SAC1	Phosphatidylinositol phosphate (PtdInsP) phosphatase; involved in hydrolysis of PtdIns[4]P in the early and medial Golgi; regulated by interaction with Vps74p; ER localized transmembrane protein which cycles through the Golgi; involved in protein trafficking and processing, secretion, and cell wall maintenance; regulates sphingolipid biosynthesis through the modulation of PtdIns(4)P metabolism.	++
SPO7	Putative regulatory subunit of Nem1-Spo7 phosphatase holoenzyme; regulates nuclear growth by controlling phospholipid biosynthesis, required for normal nuclear envelope morphology, premeiotic replication, and sporulation.	+

Mitochondrial function

Gene	Function	Susceptibility level
AEP1	Protein required for expression of the mitochondrial <i>OLI1</i> gene; mitochondrial <i>OLI1</i> gene encodes subunit 9 of F1-F0 ATP synthase.	++
AIF1	Mitochondrial cell death effector; translocates to the nucleus in response to apoptotic stimuli, homolog of mammalian Apoptosis-Inducing Factor, putative reductase.	++
ATP1	Alpha subunit of the F1 sector of mitochondrial F1-F0 ATP synthase; which is a large, evolutionarily conserved enzyme complex required for ATP synthesis; F1 translationally regulates <i>ATP6</i> and <i>ATP8</i> expression to achieve a balanced output of ATP synthase genes encoded in nucleus and mitochondria; phosphorylated; N-terminally propionylated <i>in vivo</i> .	+++
ATP10	Assembly factor for the F0 sector of mitochondrial F1-F0 ATP synthase; mitochondrial inner membrane protein; interacts genetically with <i>ATP6</i> .	+++

ATP11	Molecular chaperone; required for the assembly of alpha and beta subunits into the F1 sector of mitochondrial F1-F0 ATP synthase; N-terminally propionylated <i>in vivo</i> .	++
ATP23	Putative metalloprotease of the mitochondrial inner membrane; required for processing of Atp6; has an additional role in assembly of the F0 sector of the F1-F0 ATP synthase complex; substrate of the Mia40p-Erv1p disulfide relay system, and folding is assisted by Mia40.	++
CEM1	Mitochondrial beta-keto-acyl synthase; possible role in fatty acid synthesis; required for mitochondrial respiration; human homolog <i>OXSM</i> can complement yeast <i>cem1</i> null mutant.	+++
COA3	Mitochondrial protein required for cytochrome c oxidase assembly; also involved in translational regulation of Cox1 and prevention of Cox1 aggregation before assembly; located in the mitochondrial inner membrane.	+++
COQ1	Hexaprenyl pyrophosphate synthetase; catalyzes the first step in ubiquinone (coenzyme Q) biosynthesis.	++
COQ3	O-methyltransferase; catalyzes two different O-methylation steps in ubiquinone (Coenzyme Q) biosynthesis; component of a mitochondrial ubiquinone-synthesizing complex; phosphoprotein.	+
COX5B	Subunit Vb of cytochrome c oxidase; cytochrome c oxidase is the terminal member of the mitochondrial inner membrane electron transport chain; Cox5B is predominantly expressed during anaerobic growth while its isoform Va (Cox5A) is expressed during aerobic growth.	+
COX13	Subunit VIa of cytochrome c oxidase; present in a subclass of cytochrome c oxidase complexes that may have a role in minimizing generation of reactive oxygen species; not essential for cytochrome c oxidase activity but may modulate activity in response to ATP	+
COX17	Copper metallochaperone that transfers copper to Sco1 and Cox11; eventual delivery to cytochrome c oxidase; contains twin cysteine-x9-cysteine motifs; interacts with the MICOS complex, and interaction is promoted by copper ions; human homolog <i>COX17</i> partially complements yeast null mutant.	++
COX18	Protein required for membrane insertion of C-terminus of Cox2; mitochondrial integral inner membrane protein; interacts genetically and physically with Mss2 and Pnt1; similar to <i>S. cerevisiae</i> Oxa1, <i>N. crassa</i> Oxa2, and <i>E. coli</i> YidC; respiratory defect of the null mutant is functionally complemented by human <i>COX18</i> carrying the N-terminal 54 amino acids of <i>S. cerevisiae</i> Cox18.	+++
COX19	Protein required for cytochrome c oxidase assembly; located in the cytosol and mitochondrial intermembrane space; putative copper metallochaperone that delivers copper to cytochrome c oxidase; contains twin cysteine-x9-cysteine motifs.	+
COX6	Subunit VI of cytochrome c oxidase (Complex IV); Complex IV is the terminal member of the mitochondrial inner membrane electron transport chain; expression is regulated by oxygen levels.	++

<i>FIS1</i>	Protein involved in mitochondrial fission and peroxisome abundance; may have a distinct role in tethering protein aggregates to mitochondria in order to retain them in the mother cell; required for localization of Dnm1 and Mdv1 during mitochondrial division; mediates ethanol-induced apoptosis and ethanol-induced mitochondrial fragmentation.	+
<i>FMC1</i>	Mitochondrial matrix protein; required for assembly or stability at high temperature of the F1 sector of mitochondrial F1-F0 ATP synthase; null mutant temperature sensitive growth on glycerol is suppressed by multicopy expression of Odc1.	+++
<i>GPD2</i>	NAD-dependent glycerol 3-phosphate dehydrogenase; expression is controlled by an oxygen-independent signaling pathway required to regulate metabolism under anoxic conditions; located in cytosol and mitochondria.	+
<i>GGC1</i>	Mitochondrial GTP/GDP transporter; essential for mitochondrial genome maintenance; has a role in mitochondrial iron transport; member of the mitochondrial carrier family.	+++
<i>MGM1</i>	Mitochondrial GTPase, present in complex with Ugo1p and Fzo1p; required for mitochondrial morphology, fusion, and genome maintenance; promotes membrane bending.	+
<i>MCX1</i>	Non-proteolytic ATPase of the AAA family; stimulates incorporation of the pyridoxal phosphate cofactor into Hem1p (5-aminolevulinic acid synthase).	+
<i>MDM10</i>	Subunit of both the ERMES and the SAM complex; component of ERMES complex which acts as a molecular tether between the mitochondria and the ER, necessary for efficient phospholipid exchange between organelles and for mitophagy; SAM/TOB complex component that functions in the assembly of outer membrane beta-barrel proteins; involved in mitochondrial inheritance and morphology; ERMES complex is often co-localized with peroxisomes and concentrated areas of pyruvate dehydrogenase.	+
<i>MDM12</i>	Mitochondrial outer membrane protein, ERMES complex subunit; required for transmission of mitochondria to daughter cells; required for mitophagy; may influence import and assembly of outer membrane beta-barrel proteins; ERMES complex is often co-localized with peroxisomes and with concentrated areas of pyruvate dehydrogenase.	++
<i>MDM20</i>	Non-catalytic subunit of the NatB N-terminal acetyltransferase; NatB catalyzes N-acetylation of proteins with specific N-terminal sequences; involved in mitochondrial inheritance and actin assembly.	++
<i>MDM34</i>	Mitochondrial component of the ERMES complex; links the ER to mitochondria and may promote inter-organellar calcium and phospholipid exchange as well as coordinating mitochondrial DNA replication and growth; required for mitophagy; ERMES complex is often co-localized with peroxisomes and with concentrated areas of pyruvate dehydrogenase.	++
<i>MEF2</i>	Mitochondrial elongation factor involved in translational elongation.	++

MHR1	Mitochondrial ribosomal protein of the large subunit; also involved in homologous recombination in mitochondria; required for recombination-dependent mtDNA partitioning; involved in stimulation of mitochondrial DNA replication in response to oxidative stress.	++
MRS1	Splicing protein; required for splicing of two mitochondrial group I introns (BI3 in COB and AI5beta in COX1); forms a splicing complex, containing four subunits of Mrs1 and two subunits of the BI3-encoded maturase, that binds to the BI3 RNA; <i>MRS1</i> has a paralog, <i>CCE1</i> , that arose from the whole genome duplication.	++
MSF1	Mitochondrial phenylalanyl-tRNA synthetase; active as a monomer, unlike the cytoplasmic subunit which is active as a dimer complexed to a beta subunit dimer; similar to the alpha subunit of <i>E. coli</i> phenylalanyl-tRNA synthetase.	+++
MSK1	Mitochondrial lysine-tRNA synthetase; required for import of both aminoacylated and deacylated forms of tRNA (Lys) into mitochondria and for aminoacylation of mitochondrially encoded tRNA (Lys).	+
NAM2	Mitochondrial leucyl-tRNA synthetase; also has direct role in splicing of several mitochondrial group I introns; indirectly required for mitochondrial genome maintenance; human homolog LARS2 can complement yeast null mutant and is implicated in Perrault syndrome.	++
OAR1	Mitochondrial 3-oxoacyl-[acyl-carrier-protein] reductase; may comprise a type II mitochondrial fatty acid synthase along with Mct1; human homolog <i>CBR4</i> complements yeast null mutant.	++
PET100	Chaperone that facilitates the assembly of cytochrome c oxidase; integral to the mitochondrial inner membrane; interacts with a subcomplex of subunits VII, VIIa, and VIII (Cox7, Cox9, and Cox8) but not with the holoenzyme.	++
PET117	Protein required for assembly of cytochrome c oxidase.	+
PET54	Mitochondrial inner membrane protein; binds to the 5' UTR of the COX3 mRNA to activate its translation together with Pet122 and Pet494p; also binds to the COX1 Group I intron AI5 beta to facilitate exon ligation during splicing.	++
PRX1	Mitochondrial peroxiredoxin with thioredoxin peroxidase activity; has a role in reduction of hydroperoxides; reactivation requires Trr2 and glutathione; induced during respiratory growth and oxidative stress; phosphorylated; protein abundance increases in response to DNA replication stress.	++
PSD1	Phosphatidylserine decarboxylase of the mitochondrial inner membrane; converts phosphatidylserine to phosphatidylethanolamine; regulates mitochondrial fusion and morphology by affecting lipid mixing in the mitochondrial membrane and by influencing the ratio of long to short forms of Mgm1p; partly exposed to the mitochondrial intermembrane space; autocatalytically processed.	++
RRG9	Protein of unknown function; null mutant lacks mitochondrial DNA and cannot grow on glycerol; the authentic, non-tagged protein is detected in highly purified mitochondria in high-throughput studies.	++

RSM23	Mitochondrial ribosomal protein of the small subunit; has similarity to mammalian apoptosis mediator proteins; null mutation prevents induction of apoptosis by overproduction of metacaspase Mca1.	+++
RSM24	Mitochondrial ribosomal protein of the small subunit.	+
RTC6	Protein involved in translation; mutants have defects in biogenesis of nuclear ribosomes; sequence similar to prokaryotic ribosomal protein L36, may be a mitochondrial ribosomal protein; protein abundance increases in response to DNA replication stress.	++
SCO1	Copper-binding protein of mitochondrial inner membrane; required for cytochrome c oxidase activity and respiration; may function to deliver copper to cytochrome c oxidase.	+
SCO2	Protein anchored to mitochondrial inner membrane; may have a redundant function with Sco1p in delivery of copper to cytochrome c oxidase.	+
SOV1	Mitochondrial protein of unknown function.	++
YTA12	Mitochondrial inner membrane m-AAA protease component; mediates degradation of misfolded or unassembled proteins; also required for correct assembly of mitochondrial enzyme complexes; overexpression of human <i>AFG3L2</i> complements respiratory defect of yeast <i>afg3 yta12</i> double null mutation, but overexpression of disease-associated <i>AFG3L2</i> variants does not; expression of both human <i>SPG7</i> (paraplegin) and <i>AFG3L2</i> complements yeast <i>yta12 afg3</i> double mutation.	+

Peroxisomal function

Gene	Function	Susceptibility level
PEX12	C3HC4-type RING-finger peroxin and E3 ubiquitin ligase; required for peroxisome biogenesis and peroxisomal matrix protein import.	+
PEX27	Peripheral peroxisomal membrane protein; involved in controlling peroxisome size and number.	+
PEX34	Protein that regulates peroxisome populations; peroxisomal integral membrane protein; interacts with Pex11p, Pex25p, and Pex27p to control both constitutive peroxisome division and peroxisome morphology and abundance during peroxisome proliferation.	+
PEX19	Chaperone and import receptor for newly-synthesized class I PMPs; binds peroxisomal membrane proteins (PMPs) in the cytoplasm and delivers them to the peroxisome for subsequent insertion into the peroxisomal membrane.	+
PEX22	Putative peroxisomal membrane protein; required for import of peroxisomal proteins.	+
PEX6	AAA-peroxin; heterodimerizes with AAA-peroxin Pex1 and participates in the recycling of peroxisomal signal receptor Pex5 from the peroxisomal membrane to the cytosol; mutations in human <i>PEX6</i> can lead to severe peroxisomal disorders and early death.	++

Protein modification

Gene	Function	Susceptibility level
<i>AIM22</i>	Putative lipoate-protein ligase; required along with Lip2 and Lip5 for lipoylation of Lat1 and Kgd2; similar to <i>E. coli</i> LplA; null mutant displays reduced frequency of mitochondrial genome loss.	++
<i>ARD1</i>	Subunit of protein N-terminal acetyltransferase NatA; NatA comprises Nat1, Ard1, Nat5; acetylates many proteins to influence telomeric silencing, cell cycle, heat-shock resistance, mating, sporulation, early stages of mitophagy; protein abundance increases under DNA replication stress.	+++
<i>BNI5</i>	Linker protein responsible for recruitment of myosin to the bud neck; interacts with the C-terminal extensions of septins Cdc11 and Shs1 and binds Myo1p to promote cytokinesis.	++
<i>BRE5</i>	Ubiquitin protease cofactor; forms deubiquitination complex with Ubp3 that coregulates anterograde and retrograde transport between the endoplasmic reticulum and Golgi compartments; null is sensitive to brefeldin A.	++
<i>CDC73</i>	Component of the Paf1 complex; binds to and modulates the activity of RNA polymerases I and II; required for expression of certain genes, modification of some histones, and telomere maintenance; involved in transcription elongation as demonstrated by the G-less-based run-on (GLRO) assay; protein abundance increases in response to DNA replication stress; human homolog, parafibromin, is a tumour suppressor linked to breast, renal and gastric cancer.	++
<i>CTK1</i>	Catalytic (alpha) subunit of C-terminal domain kinase I (CTDK-I); phosphorylates both RNA pol II subunit Rpo21 to affect transcription and pre-mRNA 3' end processing, and ribosomal protein Rps2 to increase translational fidelity; required for H3K36 trimethylation but not dimethylation by Set2; suggested stimulatory role in 80S formation during translation initiation.	+++
<i>DBF2</i>	Ser/Thr kinase involved in transcription and stress response; functions as part of a network of genes in exit from mitosis; localization is cell cycle regulated; activated by Cdc15 during the exit from mitosis; also plays a role in regulating the stability of <i>SWI5</i> and <i>CLB2</i> mRNAs; phosphorylates Chs2 to regulate primary septum formation and Hof1 to regulate cytokinesis.	+++
<i>EFM4</i>	Lysine methyltransferase; involved in the dimethylation of <i>eEF1A</i> (Tef1/Tef2) at lysine 316; sequence similarity to S-adenosylmethionine-dependent methyltransferases of the seven beta-strand family; role in vesicular transport.	+
<i>EFT2</i>	Elongation factor 2 (EF-2), also encoded by <i>EFT1</i> ; catalyzes ribosomal translocation during protein synthesis; contains diphthamide, the unique posttranslationally modified histidine residue specifically ADP-ribosylated by diphtheria toxin; <i>EFT2</i> has a paralog, <i>EFT1</i> , that arose from the whole genome duplication.	+

FES1	Hsp70 (Ssa1) nucleotide exchange factor; required for the release of misfolded proteins from the Hsp70 system to the Ub-proteasome machinery for destruction; cytosolic homolog of Si11, which is the nucleotide exchange factor for BiP (Kar2) in the endoplasmic reticulum; protein abundance increases in response to DNA replication stress.	+++
FPK1	Ser/Thr protein kinase; phosphorylates several aminophospholipid translocase family members, regulating phospholipid translocation and membrane asymmetry; phosphorylates and inhibits upstream inhibitory kinase, Ypk1; localizes to the cytoplasm, early endosome/TGN compartments and thplasma membrane.	+
GIM3	Subunit of the heterohexameric cochaperone prefoldin complex; prefoldin binds specifically to cytosolic chaperonin and transfers target proteins to it; prefoldin complex also localizes to chromatin of actively transcribed genes in the nucleus and facilitates transcriptional elongation.	++
HPM1	AdoMet-dependent methyltransferase; involved in a novel 3-methylhistidine modification of ribosomal protein Rpl3p; seven beta-strand MTase family member	+
KEX2	Kexin, a subtilisin-like protease (proprotein convertase); a calcium-dependent serine protease involved in the activation of proproteins of the secretory pathway.	+++
LIP2	Lipoyl ligase; involved in the modification of mitochondrial enzymes by the attachment of lipaic acid groups.	+
MCK1	Dual-specificity ser/thr and tyrosine protein kinase; roles in chromosome segregation, meiotic entry, genome stability, phosphorylation-dependent protein degradation (Rcn1 and Cdc6), inhibition of protein kinase A, transcriptional regulation, inhibition of RNA pol III, calcium stress and inhibition of Clb2-Cdc28 after nuclear division; <i>MCK1</i> has a paralog, <i>YGK3</i> , that arose from the whole genome duplication.	+
NAS2	Evolutionarily conserved 19S regulatory particle assembly-chaperone; involved in assembly of the base subcomplex of the 19S proteasomal regulatory particle (RP); non-essential gene; interacts with Rpn4; protein abundance increases in response to DNA replication stress; ortholog of human p27.	++
NAT1	Subunit of protein N-terminal acetyltransferase NatA; NatA comprised of Nat1, Ard1, and Nat5; N-terminally acetylates many proteins to influence multiple processes such as cell cycle progression, heat-shock resistance, mating, sporulation, telomeric silencing and early stages of mitophagy; orthologous to human <i>NAA15</i> ; expression of both human <i>NAA10</i> and <i>NAA15</i> functionally complements <i>ard1 nat1</i> double mutant although single mutations are not complemented by their orthologs.	+++
NAT3	Catalytic subunit of the NatB N-terminal acetyltransferase; NatB catalyzes acetylation of the amino-terminal methionine residues of all proteins beginning with Met-Asp or Met-Glu and of some proteins beginning with Met-Asn or Met-M.	+++
NAT4	N alpha-acetyl-transferase; involved in acetylation of the N-terminal residues of histones H4 and H2A.	+++

OST3	Gamma subunit of the oligosaccharyltransferase complex of the ER lumen; complex catalyzes asparagine-linked glycosylation of newly synthesized proteins.	+
OST4	Subunit of the oligosaccharyltransferase complex of the ER lumen; complex catalyzes protein asparagine-linked glycosylation; type I membrane protein required for incorporation of Ost3 or Ost6 into the OST complex.	+++
PMT1	Protein O-mannosyltransferase of the ER membrane; transfers mannose from dolichyl phosphate-D-mannose to protein serine and threonine residues.	+
PPM1	Carboxyl methyltransferase; methylates the C terminus of the protein phosphatase 2A catalytic subunit (Pph21 or Pph22), which is important for complex formation with regulatory subunits; required for methionine to inhibit autophagy and promote growth.	++
PPT2	Phosphopantetheine:protein transferase (PPTase); activates mitochondrial acyl carrier protein (Acp1) by phosphopantetheinylation.	++
PTK2	Serine/threonine protein kinase; involved in regulation of ion transport across plasma membrane; carboxyl terminus is essential for glucose-dependent Pma1 activation via phosphorylation of Pma1-Ser899.	++
RAM1	Beta subunit of the CAAX farnesyltransferase (FTase); this complex prenylates the a-factor mating pheromone and Ras proteins; required for the membrane localization of Ras proteins and a-factor; homolog of the mammalian FTase beta subunit.	+
SHR5	Palmitoyltransferase subunit; this complex adds a palmitoyl lipid moiety to heterolipidated substrates such as Ras1 and Ras2 through a thioester linkage; palmitoylation is required for Ras2 membrane localization; Palmitoyltransferase is composed of Shr5 and Erf.	+++
SWM1	Subunit of the anaphase-promoting complex (APC); APC is an E3 ubiquitin ligase that regulates the metaphase-anaphase transition and exit from mitosis; required for activation of the daughter-specific gene expression and spore wall maturation.	+++
TOS3	Protein kinase; related to and functionally redundant with Elm1 and Sak1p for the phosphorylation and activation of Snf1; functionally orthologous to <i>LKB1</i> , a mammalian kinase associated with Peutz-Jeghers cancer-susceptibility syndrome; <i>TOS3</i> has a paralog, <i>SAK1</i> , that arose from the whole genome duplication.	++
UBA4	E1-like protein that activates Urm1 before urmylation; also acts in thiolation of the wobble base of cytoplasmic tRNAs by adenylating and then thiolating Urm1; receives sulfur from Tum1.	++
UBI4	Ubiquitin; becomes conjugated to proteins, marking them for selective degradation via the ubiquitin-26S proteasome system.	+
UBP14	Ubiquitin-specific protease; specifically disassembles unanchored ubiquitin chains; involved in fructose-1,6-bisphosphatase (Fbp1) degradation	+
UBP6	Ubiquitin-specific protease; situated in the base subcomplex of the 26S proteasome, releases free	+

	ubiquitin from branched polyubiquitin chains <i>en bloc</i> , rather than from the distal tip of the chain.	
VMS1	Component of a Cdc48-complex involved in protein quality control; exhibits cytosolic and ER-membrane localization, with Cdc48p, during normal growth, and contributes to ER-associated degradation (ERAD) of specific substrates at a step after their ubiquitination; forms a mitochondrially-associated complex with Cdc48 and Npl4 under oxidative stress that is required for ubiquitin-mediated mitochondria-associated protein degradation (MAD); conserved in <i>C. elegans</i> and humans.	++
YME1	Catalytic subunit of i-AAA protease complex; complex is located in mitochondrial inner membrane; responsible for degradation of unfolded or misfolded mitochondrial gene products; serves as nonconventional translocation motor to pull PNPase into intermembrane space; also has role in intermembrane space protein folding; mutation causes elevated rate of mitochondrial turnover.	++

Protein synthesis

Gene	Function	Susceptibility level
HCR1	eIF3j component of translation initiation factor 3 (eIF3); dual function protein involved in translation initiation as a substoichiometric component (eIF3j) of eIF3; required for 20S pre-rRNA processing; required at post-transcriptional step for efficient retrotransposition; absence decreases Ty1 Gag:GFP protein levels.	+++
IFM1	Mitochondrial translation initiation factor.	++
MRP17	Mitochondrial ribosomal protein of the small subunit; <i>MRP17</i> exhibits genetic interactions with <i>PET122</i> , encoding a <i>COX3</i> -specific translational activator.	++
MRP7	Mitochondrial ribosomal protein of the large subunit.	++
MRPL13	Mitochondrial ribosomal protein of the large subunit; not essential for mitochondrial translation.	+
MRPL20	Mitochondrial ribosomal protein of the large subunit.	++
MRPL22	Mitochondrial ribosomal protein of the large subunit.	++
MRPL24	Mitochondrial ribosomal protein of the large subunit; two mitochondrial ribosomal proteins, <i>YmL14</i> and <i>YmL24</i> , have been assigned to the same gene.	+
MRPL36	Mitochondrial ribosomal protein of the large subunit; overproduction suppresses mutations in the <i>COX2</i> leader peptide-encoding region.	++
MRPL49	Mitochondrial ribosomal protein of the large subunit.	++
MRPS12	Mitochondrial protein; may interact with ribosomes based on co-purification experiments; similar to <i>E. coli</i> and human mitochondrial S12 ribosomal proteins.	++
MRX14	Putative mitochondrial ribosomal protein of the large subunit; similar to <i>E. coli</i> L34 ribosomal protein; required for respiratory growth, as are most mitochondrial ribosomal proteins; protein increases in abundance and	+

	relocalizes to the plasma membrane upon DNA replication stress.	
RML2	Mitochondrial ribosomal protein of the large subunit (L2); has similarity to <i>E. coli</i> L2 ribosomal protein; mutant allele (<i>fat21</i>) causes inability to utilize oleate, and induce oleic acid oxidation; may interfere with activity of the Adr1 transcription factor.	+++
RPB4	RNA polymerase II subunit B32; forms dissociable heterodimer with Rpb7; Rpb4/7 dissociates from RNAPII as Ser2 CTD phosphorylation increases; Rpb4/7 regulates cellular lifespan via mRNA decay process; involved in recruitment of 3'-end processing factors to transcribing RNAPII complex, export of mRNA to cytoplasm under stress conditions; also involved in translation initiation.	+++
RPL20B	Ribosomal 60S subunit protein L20B; homologous to mammalian ribosomal protein L18A, no bacterial homolog; <i>RPL20B</i> has a paralog, <i>RPL20A</i> , that arose from the whole genome duplication.	+++
RPL21A	Ribosomal 60S subunit protein L21A.	+
RPL21B	Ribosomal 60S subunit protein L21B; homologous to mammalian ribosomal protein L21, no bacterial homolog; <i>RPL21B</i> has a paralog, <i>RPL21A</i> , that arose from the whole genome duplication.	+
RPL39	Ribosomal 60S subunit protein L39; required for ribosome biogenesis; loss of both Rpl31p and Rpl39p confers lethality; also exhibits genetic interactions with <i>SIS1</i> and <i>PAB1</i> ; homologous to mammalian ribosomal protein L39, no bacterial homolog.	+++
RPL40A	Ubiquitin-ribosomal 60S subunit protein L40A fusion protein; cleaved to yield ubiquitin and ribosomal protein L40A; ubiquitin may facilitate assembly of the ribosomal protein into ribosomes; homologous to mammalian ribosomal protein L40, no bacterial homolog; <i>RPL40A</i> has a paralog, <i>RPL40B</i> , that arose from the whole genome duplication; relative distribution to the nucleus increases upon DNA replication stress.	+
RPL42B	Ribosomal 60S subunit protein L42B; required for propagation of the killer toxin-encoding M1 double-stranded RNA satellite of the L-A double-stranded RNA virus; homologous to mammalian ribosomal protein L36A, no bacterial homolog; <i>RPL42B</i> has a paralog, <i>RPL42A</i> .	++
RPP1A	Ribosomal stalk protein P1 alpha; involved in the interaction between translational elongation factors and the ribosome; free (non-ribosomal) P1 stimulates the phosphorylation of the <i>eIF2</i> alpha subunit (Sui2) by Gcn2; accumulation of P1 in the cytoplasm is regulated by phosphorylation and interaction with the P2 stalk component.	++
RPS10A	Protein component of the small (40S) ribosomal subunit; homologous to mammalian ribosomal protein S10, no bacterial homolog; <i>RPS10A</i> has a paralog, <i>RPS10B</i> , that arose from the whole genome duplication; mutations in the human homolog associated with Diamond-Blackfan anemia.	+

RPS11B	Protein component of the small (40S) ribosomal subunit; homologous to mammalian ribosomal protein S11 and bacterial S17; <i>RPS11B</i> has a paralog, <i>RPS11A</i> , that arose from the whole genome duplication.	+
RPS16A	Protein component of the small (40S) ribosomal subunit	+
RPS21A	Protein component of the small (40S) ribosomal subunit; homologous to mammalian ribosomal protein S21, no bacterial homolog.	+
RPS21B	Protein component of the small (40S) ribosomal subunit; homologous to mammalian ribosomal protein S21, no bacterial homolog; <i>RPS21B</i> has a paralog, <i>RPS21A</i> , that arose from the whole genome duplication.	++
RPS24A	Protein component of the small (40S) ribosomal subunit; homologous to mammalian ribosomal protein S24, no bacterial homolog; <i>RPS24A</i> has a paralog, <i>RPS24B</i> , that arose from the whole genome duplication.	+
RPS27B	Protein component of the small (40S) ribosomal subunit; homologous to mammalian ribosomal protein S27, no bacterial homolog; <i>RPS27B</i> has a paralog, <i>RPS27A</i> , that arose from the whole genome duplication.	+++
RPS6A	Protein component of the small (40S) ribosomal subunit; homologous to mammalian ribosomal protein S6, no bacterial homolog; phosphorylated on S233 by Ypk3 in a TORC1-dependent manner, and on S232 in a TORC1/2-dependent manner by Ypk1/2/3; <i>RPS6A</i> has a paralog, <i>RPS6B</i> , that arose from the whole genome duplication.	++
RPS6B	Protein component of the small (40S) ribosomal subunit;	+
RSM19	Mitochondrial ribosomal protein of the small subunit; has similarity to <i>E. coli</i> S19 ribosomal protein.	++
RSM26	Mitochondrial ribosomal protein of the small subunit.	+
SEM1	19S proteasome regulatory particle lid subcomplex component; role in Ub-dependent proteolysis and proteasome stability; involved in TREX-2 mediated mRNA export, and in the prevention of transcription-associated genome instability; ubiquitinated by Nedd4-like E3-ligase, Rsp5; human ortholog <i>DSS1</i> , a <i>BRCA1</i> binding protein implicated in cancer, complements the yeast null; drives trinucleotide repeat expansion; protein abundance increases in response to DNA replication stress.	+
TIF3	Translation initiation factor eIF-4B; contains an RNA recognition motif and binds to single-stranded RNA; has RNA annealing activity; interacts with Rps20 at the head of the 40S ribosomal subunit and alters the structure of the mRNA entry channel.	++
TIF4631	Translation initiation factor <i>eIF4G</i> ; subunit of the mRNA cap-binding protein complex (eIF4F) that also contains eIF4E (Cdc33); interacts with Pab1 and with eIF4A (Tif1).	+

Response to stress

Gene	Function	Susceptibility level
------	----------	----------------------

CCS1	Copper chaperone for superoxide dismutase Sod1; involved in oxidative stress protection; Met-X-Cys-X2-Cys motif within N-terminus is involved in insertion of copper into Sod1 under conditions of copper deprivation; required for regulation of yeast copper genes in response to DNA-damaging agents; protein abundance increases in response to DNA replication stress; human homolog CCS can complement yeast <i>ccs1</i> null mutant.	++
MXR2	Methionine-R-sulfoxide reductase; involved in the response to oxidative stress; protects iron-sulfur clusters from oxidative inactivation along with <i>MXR1</i> .	+
SYM1	Protein required for ethanol metabolism; induced by heat shock and localized to the inner mitochondrial membrane; homologous to mammalian peroxisomal membrane protein Mpv17; human homolog MPV17 is implicated in hepatocerebral mtDNA depletion syndromes (MDDS), and complements yeast null mutant.	+
WHI2	Protein required for full activation of the general stress response; required with binding partner Psr1, possibly through Msn2 dephosphorylation; regulates growth during the diauxic shift.	+
WHI5	Repressor of G1 transcription; binds to SCB binding factor (SBF) at SCB target promoters in early G1.	+

Signal transduction

Gene	Function	Susceptibility level
GPB2	Multistep regulator of cAMP-PKA signaling; inhibits PKA downstream of Gpa2 and Cyr1, thereby increasing cAMP dependency; inhibits Ras activity through direct interactions with Ira1/2.	+
IRS4	EH domain-containing protein; involved in regulating phosphatidylinositol 4,5-bisphosphate levels and autophagy; Irs4 and Tax4 bind and activate the PtdIns phosphatase Inp51; Irs4 and Tax4 are involved in localizing Atg17 to the PAS; <i>IRS4</i> has a paralog.	++
NBP2	Protein involved in the HOG (high osmolarity glycerol) pathway; negatively regulates Hog1 by recruitment of phosphatase Ptc1 the Pbs2-Hog1 complex; interacts with Bck1 and down regulates the cell wall integrity pathway; found in the nucleus and cytoplasm, contains an SH3 domain and a Ptc1 binding domain (PBM).	++
PDE2	High-affinity cyclic AMP phosphodiesterase; component of the cAMP-dependent protein kinase signaling system, protects the cell from extracellular cAMP	+
RAS2	GTP-binding protein; regulates nitrogen starvation response, sporulation, and filamentous growth; farnesylation and palmitoylation required for activity and localization to plasma membrane; homolog of mammalian Ras proto-oncogenes; <i>RAS2</i> has a paralog, <i>RAS1</i> , that arose from the whole genome duplication.	+++
REI1	Cytoplasmic pre-60S factor; required for the correct recycling of shuttling factors Alb1, Arx1 and Tif6 at the end of the ribosomal large subunit biogenesis; involved in bud growth in the mitotic signaling network.	++

SIP1	Alternate beta-subunit of the Snf1 kinase complex; may confer substrate specificity; vacuolar protein containing KIS (Kinase-Interacting Sequence) and ASC (Association with Snf1 kinase Complex) domains involved in protein interaction	+
SNF1	AMP-activated S/T protein kinase; forms a complex with Snf4 and members of the Sip1/Sip2/Gal83 family; required for transcription of glucose-repressed genes, thermotolerance, sporulation, and peroxisome biogenesis; regulates nucleocytoplasmic shuttling of Hxk2; regulates filamentous growth and acts as a non-canonical GEF, activating Arf3 during invasive growth; SUMOylation by Mms21 inhibits its function and targets Snf1 for destruction via the Slx5-Slx8 Ub ligase.	++
STE50	Adaptor protein for various signaling pathways; involved in mating response, invasive/filamentous growth, osmotolerance.	+
TUS1	Guanine nucleotide exchange factor (GEF) that modulates Rho1 activity; involved in the cell integrity signaling pathway; interacts with Rgl1; localization of Tus1 to the bud neck is regulated by Rgl1; multicopy suppressor of <i>tor2</i> mutation and <i>ypk1 ypk2</i> double mutation; potential Cdc28 substrate.	++

Transcription factors

Gene	Function	Susceptibility level
CBF1	Basic helix-loop-helix (bHLH) protein; forms homodimer to bind E-box consensus sequence CACGTG present at <i>MET</i> gene promoters and centromere DNA element I (CDEI); affects nucleosome positioning at this motif; associates with other transcription factors such as Met4 and Isw1 to mediate transcriptional activation or repression; associates with kinetochore proteins, required for chromosome segregation; protein abundance increases in response to DNA replication stress.	++
HAP5	Subunit of the Hap2/3/4/5 CCAAT-binding complex; complex is heme-activated and glucose repressed; complex is a transcriptional activator and global regulator of respiratory gene expression.	+
MGA2	ER membrane protein involved in regulation of <i>OLE1</i> transcription; inactive ER form dimerizes and one subunit is then activated by ubiquitin/proteasome-dependent processing followed by nuclear targeting; <i>MGA2</i> has a paralog, <i>SPT23</i> , that arose from the whole genome duplication.	++
OAF1	Oleate-activated transcription factor; subunit of a heterodimeric complex with Pip2, which binds to oleate-response elements (ORE) in the promoter of genes involved in beta-oxidation of fatty acids, peroxisome organization and biogenesis, activating transcription in the presence of oleate.	+
RPN4	Transcription factor that stimulates expression of proteasome genes; Rpn4 levels are in turn regulated by the 26S proteasome in a negative feedback control mechanism; RPN4 is transcriptionally regulated by various stress responses; relative distribution to the nucleus increases upon DNA replication stress.	+++

<i>RSF2</i>	Zinc-finger protein; involved in transcriptional control of both nuclear and mitochondrial genes, many of which specify products required for glycerol-based growth, respiration.	+
<i>SFL1</i>	Transcriptional repressor and activator; involved in repression of flocculation-related genes, and activation of stress responsive genes; has direct role in <i>INO1</i> transcriptional memory; negatively regulated by cAMP-dependent protein kinase A subunit Tpk2; premature stop codon (C1430T, Q477-stop) in SK1 background is linked to the aggressively invasive phenotype of SK1 relative to BY4741 (S288C).	++
<i>SFP1</i>	Regulates transcription of ribosomal protein and biogenesis genes; regulates response to nutrients and stress, G2/M transitions during mitotic cell cycle and DNA-damage response and modulates cell size; regulated by TORC1 and Mrs6; sequence of zinc finger, ChIP localization data, and protein-binding microarray (PBM) data, and computational analyses suggest it binds DNA directly at highly active RP genes and indirectly through Rap1 at others; can form the [ISP+] prion.	+++
<i>STP1</i>	Transcription factor; contains a N-terminal regulatory motif (RI) that acts as a cytoplasmic retention determinant and as an Asi dependent degron in the nucleus; undergoes proteolytic processing by SPS (Ssy1-Ptr3-Ssy5)-sensor component Ssy5 in response to extracellular amino acids; activates transcription of amino acid permease genes and may have a role in tRNA processing.	+
<i>SWI6</i>	Transcription cofactor; forms complexes with Swi4 and Mbp1 to regulate transcription at the G1/S transition; involved in meiotic gene expression; also binds Stb1 to regulate transcription at START; cell wall stress induces phosphorylation by Mpk1, which regulates Swi6 localization; required for the unfolded protein response, independently of its known transcriptional coactivators.	++
<i>TUP1</i>	General repressor of transcription; forms complex with Cyc8, involved in the establishment of repressive chromatin structure through interactions with histones H3 and H4.	+
<i>UME6</i>	Rpd3L histone deacetylase complex subunit; key transcriptional regulator of early meiotic genes; involved in chromatin remodeling and transcriptional repression via DNA looping; binds <i>URS1</i> upstream regulatory sequence, represses transcription by recruiting conserved histone deacetylase Rpd3 (through co-repressor Sin3) and chromatin-remodeling factor Isw2; couples metabolic responses to nutritional cues with initiation and progression of meiosis.	+++
<i>UPC2</i>	Sterol regulatory element binding protein; induces sterol biosynthetic genes, upon sterol depletion; acts as a sterol sensor, binding ergosterol in sterol rich conditions.	+
<i>URE2</i>	Nitrogen catabolite repression transcriptional regulator; inhibits <i>GLN3</i> transcription in good nitrogen source; role in sequestering Gln3 and Gat1 to the cytoplasm; has glutathione peroxidase activity and can mutate to acquire GST activity; self-assembly under limited nitrogen conditions creates [<i>URE3</i>] prion and releases catabolite repression.	+

Transporters

Gene	Function	Susceptibility level
------	----------	----------------------

DAL5	Allantoate permease; ureidosuccinate permease; also transports dipeptides, though with lower affinity than for allantoate and ureidosuccinate; expression is constitutive but sensitive to nitrogen catabolite repression.	+
FPS1	Aquaglyceroporin, plasma membrane channel; involved in efflux of glycerol and xylitol, and in uptake of acetic acid, arsenite, and antimonite; key factor in maintaining redox balance by mediating passive diffusion of glycerol; phosphorylated by Hog1 MAPK under acetate stress; deletion improves xylose fermentation; regulated by Rgc1 and Ask10, which are regulated by Hog1p phosphorylation under osmotic stress; phosphorylation by Ypk1 required to maintain an open state.	+++
MME1	Transporter of the mitochondrial inner membrane that exports magnesium; involved in mitochondrial Mg ²⁺ homeostasis; has similarity to human mitochondrial ATP-Mg/Pi carriers.	++
NHA1	Na ⁺ /H ⁺ antiporter; involved in sodium and potassium efflux through the plasma membrane; required for alkali cation tolerance at acidic pH.	+
OPT2	Oligopeptide transporter; localized to peroxisomes and affects glutathione redox homeostasis; also localizes to the plasma membrane (PM) and to the late Golgi, and has a role in maintenance of lipid asymmetry between the inner and outer leaflets of the PM; member of the OPT family, with potential orthologs in <i>S. pombe</i> and <i>C. albicans</i> ; also plays a role in formation of mature vacuoles and in polarized cell growth.	+
SPF1	P-type ATPase, ion transporter of the ER membrane; required to maintain normal lipid composition of intracellular compartments and proper targeting of mitochondrial outer membrane tail-anchored proteins; involved in ER function and Ca ²⁺ homeostasis; required for regulating Hmg2 degradation; confers sensitivity to a killer toxin (SMKT) produced by <i>Pichia farinosa</i> KK1.	+++
TPN1	Plasma membrane pyridoxine (vitamin B6) transporter; member of the purine-cytosine permease subfamily within the major facilitator superfamily; proton symporter with similarity to Fcy21, Fcy2, and Fcy22.	++
TPO1	Polyamine transporter of the major facilitator superfamily; member of the 12-spanner drug:H(+) antiporter <i>DHA1</i> family; recognizes spermine, putrescine, and spermidine; catalyzes uptake of polyamines at alkaline pH and excretion at acidic pH; during oxidative stress exports spermine, spermidine from the cell, which controls timing of expression of stress-responsive genes; phosphorylation enhances activity and sorting to the plasma membrane.	+
YIA6	Mitochondrial NAD ⁺ transporter; involved in the transport of NAD ⁺ into the mitochondria (see also <i>YEA6</i>); member of the mitochondrial carrier subfamily; disputed role as a pyruvate transporter; has putative mouse and human orthologs; <i>YIA6</i> has a paralogue, <i>YEA6</i> , that arose from the whole genome duplication.	++

Unknown function

Gene	Function	Susceptibility level
AIM4	Protein proposed to be associated with the nuclear pore complex; null mutant is viable, displays elevated frequency of mitochondrial genome loss and is sensitive to freeze-thaw stress.	+

API2	Putative protein of unknown function; conserved among <i>S. cerevisiae</i> strains; not conserved in closely related <i>Saccharomyces</i> species; 26% of ORF overlaps the dubious ORF YDR524C-A	+
BIL1	Protein that binds Bud6 and has a role in actin cable assembly; involved in the Bnr1p-dependent pathway of cable assembly; localizes to bud tip and bud neck.	++
BUD26	Dubious open reading frame; unlikely to encode a functional protein, based on available experimental and comparative sequence data; not conserved in closely related <i>Saccharomyces</i> species; 1% of ORF overlaps the verified gene SNU56.	+
HGH1	Nonessential protein of unknown function.	++
IRC13	Putative protein of unknown function; conserved across <i>S. cerevisiae</i> strains.	+
JIP4	Protein of unknown function; previously annotated as two separate ORFs, YDR474C and YDR475C, which were merged as a result of corrections to the systematic reference sequence.	+
MRP8	Protein of unknown function; undergoes sumoylation; transcription induced under cell wall stress; protein levels are reduced under anaerobic conditions.	+
OPI10	Protein with a possible role in phospholipid biosynthesis; null mutant displays an inositol-excreting phenotype that is suppressed by exogenous choline; protein abundance increases in response to DNA replication stress.	++
OPI7	Dubious open reading frame; unlikely to encode a functional protein.	+
OPI9	Dubious open reading frame; unlikely to encode a functional protein.	+++
PAL1	Protein of unknown function thought to be involved in endocytosis.	+
RGL1	Regulator of Rho1p signaling, cofactor of Tus1; required for the localization of Tus1 during all phases of cytokinesis; green fluorescent protein (GFP)-fusion protein localizes to the bud neck and cytoplasm; null mutant is viable and exhibits growth defect on a non-fermentable (respiratory) carbon source.	++
RMD8	Cytosolic protein required for sporulation.	+
RRG1	Protein of unknown function; required for vacuolar acidification and mitochondrial genome maintenance; the authentic, non-tagged protein is detected in highly purified mitochondria in high-throughput studies.	+
SRP40	Nucleolar serine-rich protein; role in preribosome assembly or transport; may function as a chaperone of small nucleolar ribonucleoprotein particles (snoRNPs).	+
TPH3	Putative protein of unknown function; GFP-fusion protein localizes to the cytoplasm; contains two adjacent PH-like domains; conserved in closely related <i>Saccharomyces</i> species.	+
TVP15	Integral membrane protein; localized to late Golgi vesicles along with the v-SNARE Tlg2.	+
YAR029W	Member of <i>DUP240</i> gene family but contains no transmembrane domains; green fluorescent protein (GFP)-fusion protein localizes to the cytoplasm in a punctate pattern.	+
YBL071C-B	Putative protein of unknown function.	++

YBL094C	Dubious open reading frame; unlikely to encode a functional protein.	+
YBL100C	Dubious open reading frame; unlikely to encode a functional protein.	+++
YCL007C	Dubious open reading frame; unlikely to encode a functional protein.	+++
YCL026C	Deleted ORF; does not encode a protein.	+
YDR008C	Dubious open reading frame; unlikely to encode a functional protein.	+++
YDR203W	Dubious open reading frame; unlikely to encode a functional protein.	+
YDR442W	Dubious open reading frame; unlikely to encode a functional protein.	+++
YDR524C-B	Putative protein of unknown function.	++
YDR524W-C	Putative protein of unknown function.	++
YGL024W	Dubious open reading frame; unlikely to encode a functional protein.	+
YGL218W	Dubious open reading frame; unlikely to encode a functional protein.	++
YGR079W	Putative protein of unknown function.	+
YHR175W-A	Putative protein of unknown function.	++
YIL028W	Dubious open reading frame; unlikely to encode a functional protein.	++
YIL029C	Putative protein of unknown function.	++
YIL077C	Putative protein of unknown function.	+
YIL092W	Putative protein of unknown function.	+
YIL141W	Dubious open reading frame; unlikely to encode a functional protein.	+
YJR011C	Putative protein of unknown function.	+++
YJR114W	Dubious open reading frame; unlikely to encode a functional protein.	++
YKL118W	Dubious open reading frame; unlikely to encode a functional protein.	++
YKR004C-A	Merged open reading frame; does not encode a discreet protein; YKR004C-A was originally annotated as an independent ORF.	+
YLR202C	Dubious open reading frame; unlikely to encode a functional protein.	++
YLR235C	Dubious open reading frame; unlikely to encode a functional protein.	++
YLR264C-A	Putative protein of unknown function.	+
YLR297W	Protein of unknown function; green fluorescent protein (GFP)-fusion protein localizes to the vacuole.	+
YLR358C	Protein of unknown function.	+++
YLR407W	Putative protein of unknown function.	++
YMR001C-A	Putative protein of unknown function.	+

YNL190W	Hydrophilin essential in desiccation-rehydration process; cell wall protein; contains a putative GPI-attachment site.	++
YNL193W	Putative protein of unknown function.	+
YNL194C	Integral membrane protein; required for sporulation and plasma membrane sphingolipid content; similar to <i>SUR7</i> ; GFP-fusion protein is induced in response to the DNA-damaging agent MMS; GFP-fusion protein is more abundant at MCCs (membrane compartment occupied by Can1) in the presence of glycerol and oleate; <i>YNL194C</i> has a paralog, <i>FMP45</i> , that arose from the whole genome duplication.	+
YOL050C	Dubious open reading frame; unlikely to encode a functional protein.	+
YOL107W	Putative protein of unknown function; green fluorescent protein (GFP)-fusion protein localizes to the cytoplasm and colocalizes in a punctate pattern with the early Golgi/COPI vesicles; <i>YOL107W</i> is not an essential protein.	++
YOR082C	Dubious open reading frame; unlikely to encode a functional protein.	+
YOR139C	Dubious open reading frame; unlikely to encode a functional protein.	++
YPL205C	Hypothetical protein; deletion of locus affects telomere length.	+